

# **53rd American Solar Energy Society National Solar Conference 2024 (SOLAR 2024)**

Connecting Technology and Policy

Washington, DC, USA  
20-23 May 2024

**Editors:**

**Kat Friedrich  
Carly Rixham**

Print ISBN: 979-8-3313-0908-4  
eISBN: 979-8-3313-0907-7

**Printed from e-media with permission by:**

Curran Associates, Inc.  
57 Morehouse Lane  
Red Hook, NY 12571



**Some format issues inherent in the e-media version may also appear in this print version.**

Copyright© (2024) by American Solar Energy Society  
All rights reserved.

Printed with permission by Curran Associates, Inc. (2024)

For permission requests, please contact American Solar Energy Society  
at the address below.

American Solar Energy Society  
2525 Arapahoe Ave, Ste E4-253  
Boulder, Colorado 80302  
USA

Phone: (303) 443-3130

[info@ases.org](mailto:info@ases.org)

**Additional copies of this publication are available from:**

Curran Associates, Inc.  
57 Morehouse Lane  
Red Hook, NY 12571 USA  
Phone: 845-758-0400  
Fax: 845-758-2633  
Email: [curran@proceedings.com](mailto:curran@proceedings.com)  
Web: [www.proceedings.com](http://www.proceedings.com)

Kat Friedrich  
Carly Rixham  
Editors

Proceedings of the 53rd American Solar  
Energy Society National Solar  
Conference 2024  
Connecting Technology and Policy

## Editors

Kat Friedrich  
American Solar Energy Society  
Boulder, CO, USA

Carly Rixham  
American Solar Energy Society  
Boulder, CO, USA

Print ISBN: 979-8-3313-0908-4

eISBN: 979-8-3313-0907-7

© American Solar Energy Society 2024

This work is subject to copyright. All rights are solely and exclusively licensed by the Publisher, whether the whole or part of the material is concerned, specifically the rights of translation, reprinting, reuse of illustrations, recitation, broadcasting, reproduction on microfilms or in any other physical way, and transmission or information storage and retrieval, electronic adaptation, computer software, or by similar or dissimilar methodology now known or hereafter developed. The use of general descriptive names, registered names, trademarks, service marks, etc. in this publication does not imply, even in the absence of a specific statement, that such names are exempt from the relevant protective laws and regulations and therefore free for general use. The publisher, the authors, and the editors are safe to assume that the advice and information in this book are believed to be true and accurate at the date of publication. Neither the publisher nor the authors or the editors give a warranty, expressed or implied, with respect to the material contained herein or for any errors or omissions that may have been made. The publisher remains neutral with regard to jurisdictional claims in published maps and institutional affiliations.

Published by Curran Associates, Inc.



# TABLE OF CONTENTS

## **TRACK 1: TECHNOLOGY INNOVATIONS AND LIFE CYCLES (APPLICATIONS OF PV AND SOLAR THERMAL, LIFE CYCLES AND IMPACTS)**

|  |     |
|--|-----|
| Solar Synergy: Unifying PV Energy and Smart Home Solutions.....  | 4   |
| <i>Boris Budagyan</i>  |     |
| Productive Uses of Renewable Energy (PURE) for Uganda.....   | 20  |
| <i>Robert Foster</i>   |     |
| Solar Thermal Collectors and Multi-Source Heat Pump Systems.....   | 34  |
| <i>Gaylord Olson</i>   |     |
| An Approach Characterizing the Performance Degradation of a 140 kW Solar Panel in WV.....                                      | 49  |
| <i>R. Subnom</i>   |     |
| Analyzing Optimal Renewable Energy Portfolio for Electricity Generation in Arizona and Texas with Lowest Carbon Emissions..... | 61  |
| <i>Rahim Khoie</i>   |     |
| A Study of Carbon Emissions and Energy Consumption of Solar Power Generation in Phoenix, Arizona.....                          | 75  |
| <i>Rahim Khoie</i>   |     |
| Optimizing a Foldable Solar Cooker with Enhanced Thermal Properties for Humanitarian and Refugee Camp Deployment.....          | 88  |
| <i>Tariku Demissie</i>   |     |
| Modeling and Production Performance Analysis of a Campus 5 MW Solar Installation in the California San Joaquin Valley.....     | 93  |
| <i>David Mueller</i>   |     |
| Beyond the Surface: Environmental Depth of Photovoltaic Recycling Methods.....   | 100 |
| <i>Asli Birturk</i>  |     |

## **TRACK 2: GRIDS AND SOLAR COMMUNITIES (SMART GRIDS FROM NANO TO MICRO)**

|   |     |
|---|-----|
| Predicting Weather-Dependent Energy Savings for Low-Income Residential Buildings for Specific Upgrades with Limited Data..... | 112 |
| <i>Phillip Clayton</i>  |     |
| Renewables in Recent and Future Heat Waves.....   | 118 |
| <i>Nir Krakauer</i>   |     |
| Experimental Study of Ambient Dusts and Installment Orientations Effects on Solar Panel Efficiency.....                       | 127 |
| <i>Xiuhua Si</i>  |     |

**TRACK 3: NET ZERO ENERGY BUILDINGS, PASSIVE HEATING AND COOLING  
(DECARBONIZING THE BUILDING SECTOR)**

Enhancing Building Performance with Solar Heating Reflective Coatings: Impacts on Thermal and Electrical Efficiency ..... 142  
*Yizhou Yang*

Solar Energy Potential and Integration in Alabama Residential Buildings: A Photovoltaic System Feasibility Study ..... 154  
*Yizhou Yang*

Exploring the Impact of Spatial Factors on Circadian Daylight Distribution..... 167  
*Neda Ghaeili*

Team SHUNYA: Harnessing Solar Power and Circularity in Urban Housing - A Student-Built Net Zero Home Case Study..... 179  
*Ali Khan*

Designing High-Performance Buildings with a Focus on Equity: A U.S. Department of Energy Solar Decathlon Case Study ..... 191  
*Nea Maloo*

Early Experiences with a High-Elevation Off-Grid Solar Residence in Colorado ..... 203  
*Dave Renné*

Evaluation of Retrofit Passive Solar Heating for Emergencies ..... 216  
*Martin Smallen*

Thermal Comfort in Hot, Humid Weather in a Dome-Shaped Building ..... 228  
*Roya Taheri*

Energy and Economic Analysis of Combined Use of Phase Change Material with Insulation in Residential Buildings..... 244  
*Prabhat Sharma*

**TRACK 4: EDUCATION AND TRAINING (EDUCATING & ENGAGING  
STAKEHOLDERS)**

Integrating Energy Technology and Policy: A New Graduate-Level Course ..... 255  
*Kristin Field*

Mobilizing to Support Large-Scale Solar and Storage Goals ..... 258  
*Jill Cliburn*

**TRACK 5: POLICY, LEGISLATION, ECONOMICS, AND FINANCE (EQUITABLE  
ENERGY OWNERSHIP AND ACCESS — POLICY, REGULATION, AND INVESTMENT)**

To What Extent Are the United States and Nigeria Able to Balance Economic Growth Against Emission Reduction Goals?..... 271  
*Bolu Ayankoji*

What Is the Future of Photovoltaics in the Electrification of Africa?..... 285  
*Moses Bass*

Firm-Dispatchable Power and Its Requirement in a Power System Based on Variable Generation..... 294  
*Stephen Clark*

Policy and Data Needs for Increased Grid Reliability and Energy Equity ..... 308  
*Clifford Ho*

Maximizing DPV Hosting Capacity with Regional Firm VRE Power..... 319  
*Marc Perez*

The Practical Implementation of Distributed Solar CHP With Thermal and EV Battery Storage for  
Schools ..... 329  
*Steven Smiley*

Comparative Analysis of Building Envelope Performance across Income Levels for Enhancing  
Thermal Resilience during Heatwaves ..... 342  
*Suman Paneru*

Review of Sustainable Urban Planning and Design Policy Interventions for Heatwave Management  
in Urban Environments..... 358  
*Huijin Zhang*

Navigating South Africa’s Energy Crisis: Advancing Toward a Solar-Powered Future..... 371  
*Akua Debrah*

**Author Index**

**Solar Synergy: Unifying PV Energy and Smart Home Solutions**

Boris Budagyan

Adapses Inc.

5638 Via Romano Dr., Apt. F, Charlotte, NC 28270

## Abstract

Optimizing energy efficiency through the synergy of solar photovoltaic (PV) and smart home technologies involves integrating essential smart home devices with a solar PV system that encompasses both a battery bank and a connection to the grid. This approach aims to reduce energy expenses by efficiently managing energy resources in two primary operational modes: normal power operation and power disruption mode. During normal power operations, when solar PV energy and grid electricity are available, smart home devices such as thermostats, lights, and smart plugs work in tandem to optimize energy usage. Their goal is to ensure that a sufficient portion of PV-generated electricity is directed to the batteries for charging. By doing so during nighttime, overcast days and high-demand periods, the system can minimize reliance on grid electricity, resulting in cost savings on the energy bill. During power disruptions or outages, the solar PV system and battery backup solutions step in to provide uninterrupted electricity to critical smart home components to ensure the continued safety and protection of the household. Simultaneously, smart home devices like smart thermostats, smart lights, and smart plugs play a crucial role in minimizing energy consumption. Their efforts aim to extend the battery charge and improve its overall lifespan, reducing expenses associated with the installation of more costly battery banks. In essence, the synergy between smart home technology and solar PV systems offers not only energy cost savings during normal operations but also enhanced resilience and cost-effectiveness during power disruptions.

Keywords: solar PV, solar storage, hybrid solar PV, smart home, smart thermostat, energy efficiency, energy cost savings, energy bill reduction

## **Solar Synergy: Unifying PV Energy and Smart Home Solutions**

The integration of solar PV and smart home solutions marks a significant step toward energy-efficient living by revolutionizing how we generate and consume energy. Solar PV systems have emerged as a prominent solution, harnessing the power of the sun to generate electricity. Recent advancements in solar PV technology such as high-efficiency solar cells and panels, high-efficiency inverters, solar backup batteries, and software have significantly improved energy efficiency. According to EcoFlow estimates, a 7.15-kWh solar array will fully cover the electricity bill for a household with below 965 kWh average usage or save approximately \$125 a month (EcoFlow, 2023).

With consistent technological improvements, hybrid solar PV systems with backup storage have emerged as a promising solution. These systems, which are grid-connected with battery storage, serve multiple purposes: providing backup power during grid outages, optimizing electricity costs through energy shifting, and increasing the self-consumption of solar energy (Solar Technologies, 2022). However, challenges such as high battery costs and limited lifespan need to be addressed to make these systems more accessible to homeowners, a goal that can be potentially achieved through effective management of energy consumption.

The concept of smart homes has gained momentum in recent years, offering homeowners greater control, convenience, and efficiency in energy management. Installing smart thermostats alone can yield significant savings, with approximately 12% saved on heating and 15% saved on cooling, translating to about \$140 annually (Smart Energy, 2023). Efficient home energy management complements hybrid solar PV by enabling the installation of smaller backup batteries, prolonging their lifespan and thus decreasing overall costs.

Furthermore, integrating smart home systems with hybrid solar PV addresses vulnerabilities in smart home functionality, particularly during outages. With an uninterrupted power supply from hybrid solar PV batteries, smart homes become robust energy efficiency, security, and hazard prevention solutions, operating continuously.

In our study, we highlight the benefits of integrating solar PV systems and smart home technologies with a comprehensive overview of their combined benefits and operational modes. Benefits include reduced energy consumption and environmental impact, reduced energy bills, prolonged solar battery lifetime, decreased cost of the solar PV installation, shortened payback time, and uninterrupted smart home functionality for house security, safety, and energy efficiency.

### **Constructing a Case Study: Exploring the Integration of Solar PV and Smart Home Systems**

To demonstrate the benefits of integrated solar PV and smart home systems we utilized a cutting-edge hybrid solar PV system alongside essential smart home devices in a typical property located in Charlotte, NC.

### *The Hybrid Solar PV System*

Our cutting-edge solar PV system harnesses the latest in solar storage technology, consolidating charge controllers, batteries, and inverters into a single, innovative solution. These systems are ideal for off-grid and hybrid solar PV setups and can be seamlessly integrated with smart home solutions. For our demonstration, we selected The SunPower Equinox Home Solar System paired with the SunPower SunVault™ Storage backup battery (SunPower, 2024b). Renowned for its efficiency (22.6%) and integrated design (Fig.1), this system minimizes roof space requirements and is available nationwide (SolarReviews, 2024).

### *Essentials of the Smart Home Systems*

Our smart home devices address four key aspects of homeowner life (Fig. 2): enhancing energy efficiency and cost savings, bolstering security against intrusions, safeguarding against hazards like fires and floods, and enhancing overall comfort and convenience (Adapses, 2024). These devices can be seamlessly integrated with solar PV systems, optimizing solar energy use, enhancing battery management, and prolonging the lifespan of the PV systems.

### *The Property*

Our featured property is an average-sized home in Charlotte, NC managed by Duke Energy utility company with an average electricity cost of 13 cents per kWh and a fixed-rate plan. The property is a typical two-story, 2,000-square-foot house with a southern-facing roof area of about 700 square feet oriented at an azimuth of 230 degrees with a typical pitch of 18.5 degrees. With an average monthly energy consumption of 1,200 kWh, totaling 14,400 kWh annually, this property is positioned at a latitude of 35 degrees. It receives an average of 5.04 Peak Sun Hours (PSH) per day (NREL, 2024).

## **Building an Integrated Solar PV and Smart Home System**

### *Sizing a Solar PV System*

Solar PV system sizing involves employing a standardized formula to determine its appropriate size (Adapses, 2024). This formula calculates the Solar PV System Size in kWh by dividing the Daily Energy Consumption by the product of the % Roof Performance and Peak Sun Hours (PSH). The % Roof Performance is derived from the formula:

*%Roof Performance*

$$= 100\% - (Your\ Altitude - Roof's\ Tilt) \div 3 + (Your\ Azimuth - 180) \div 6$$

Considering factors such as property size, roof efficiency, and location, the estimated ideal size for this property's solar PV system is 8 kW. Employing SunPower Maxeon 3 series 400 W SPR-MAX3-400 solar panels, the system requires 20 solar panels and 2

SunVault (13 kWh) battery banks, each with a maximum usable energy of 12 kWh, to support 8 hours of backup operation (SunPower, 2024a).

This configuration, featuring two batteries, efficiently reduces electricity costs during winter nights when heating is active and summer days when cooling systems are in use. However, it's essential to acknowledge that the actual performance of our 8 kW solar PV systems may be reduced by approximately 14% due to derating factors, solar panel operating temperature, inverter efficiency, and others (NREL, 2024).

According to the NREL calculator, the actual yearly AC output of our 8 kW solar PV system will be about 10,974 kWh, resulting in a 76% reduction in energy usage from the grid and an economic benefit of \$1,427 per year. Nonetheless, this significant reduction entails a substantial upfront cost due to SunPower's high-efficiency equipment, which, even after a 30% federal rebate, averages \$21,000 including installation, with a payback time of approximately 15 years (\$21,000/\$1,427) (MarketWatch Guides, 2024).

While we deliberately selected this high-end, expensive solution to showcase the potential impact of a smart home system on energy efficiency and savings, it's worth noting that more affordable solar PV systems are available on the market, with payback times ranging between six and 11 years.

### *Selecting Energy-Efficient Smart Home Devices*

Choosing the correct energy-efficient smart home devices can significantly enhance household energy management. These devices, namely smart thermostats, smart lights, and smart plugs, form the cornerstone of energy-saving in smart home systems.

In our project, we opted for the Google Smart Learning Thermostat, renowned for its ability to save an average of 2000 kWh annually (EnergyEarth, 2024). By intelligently adjusting heating and cooling settings based on seasonal demands and occupancy patterns, this thermostat ensures efficient energy use. Moreover, its AI-driven functionality adapts to homeowners' habits, further minimizing energy consumption.

Our selection for smart plugs was the TOPGREENER Smart Mini Wi-Fi Plug with Energy Monitoring. This plug not only powers down connected appliances when not in use or when the house is vacant but also provides real-time energy consumption data. This enables homeowners to remotely manage power usage, potentially saving up to 1000 kWh annually (Oakter, 2024).

For the home's lighting system, we selected Philips Hue Smart Bulbs, which are recognized for their reliability and energy-efficient LED technology. With up to 80% energy savings compared to traditional lighting, smart lights significantly reduce electricity consumption. On average, households can save around 1500 kWh per year by transitioning to LED lighting, which typically accounts for 15% of total electricity usage (Energy.gov, 2024).

Collectively implementing these three smart home devices can save approximately 4500 kWh of energy annually, resulting in savings of \$585 per year. While these



devices slightly consume energy and initial investment ranges from \$300 to \$500, depending on available utility rebate programs, the long-term benefits far outweigh the upfront costs.

It is worth noting that it is essential to ensure investing in reliable devices and software to avoid common problems and pitfalls associated with smart home automation specifically when a vendor goes out of business and discontinues support. Essential tips and strategies for creating a reliable smart home are described in detail on the website Adapses.com (Adapses.com, 2024).

### **Maximizing Energy Efficiency: Integrating Solar PV and Smart Home Systems**

Table 1 presents a breakdown of monthly energy usage derived from a typical Duke Energy utility bill for this house type, alongside monthly average sunlight hours (PSH) for the region, the calculated AC output generated by a Solar PV system of 8-kW capacity, and the simulated Smart Home energy savings (NREL, 2024).

For the smart home system simulation, we employed conservative estimates for smart plugs (500 kWh/year) and smart lights (1000 kWh/year) providing 3% and 7% monthly energy savings, respectively. For the smart thermostat, energy savings amount to 20% during the months it is in use, or 14% (2000 kWh) annually. According to this data, the Solar PV system produces 10,974 kWh, resulting in 76% annual savings.

However, during winter, the energy savings are only 39% due to reduced solar exposure on panels, with an average PSH of approximately 3.63. Moreover, winter places increased strain on the battery backup system due to reduced daylight hours and frequent power outages, while household energy usage rises for heating and lighting purposes. As a result, smart thermostats and smart lights become pivotal in enhancing energy efficiency during the winter months, working in tandem with solar power to bolster savings.

In contrast, summer experiences peak solar PV output, while cooling becomes the primary energy draw. Here, the smart thermostat regulates consumption, ensuring ample energy reserves for battery backup during high-demand periods, cloudy days, and outages.

Figure 3 demonstrates the combined benefits of solar PV and smart home systems based on the data presented in Table 1. Typical monthly energy consumption from the Duke Energy bill is represented in grey, while calculated output from Solar PV and simulated savings from smart home devices are highlighted in orange and blue, respectively. During winter, smart home devices nearly double the savings from the solar PV system, adding another 29%, primarily from the smart thermostat and smart lighting, covering 68% of energy demand. In other seasons, the integrated smart home and solar PV systems meet household energy needs entirely, with surplus electricity available for sale back to the grid, offering additional benefits.

The notable result from the incorporation of the smart home system is a total energy reduction of 14,740 kWh (3,500 kWh from smart home plus 10,974 kWh from solar PV)

equating to \$1,882 in annual savings and effectively trimming the payback period from 15 years down to 11 ( $\$21,000/\$1,882$ ). Our study underscores the pivotal role of reducing the years required for return on investment through smart home integration and accurately managing its functionality. Furthermore, coupling this with increasingly accessible solar PV solutions can yield even more remarkable outcomes.

The benefits from the integration of these two systems, however, extend beyond simply summing the benefits of each. Instead, it provides homeowners with a unified, mutually beneficial solution, elevating both energy efficiency and home safety to new levels.

### **Unifying PV Energy and Smart Home Solutions**

Integrating the essential smart home devices with the hybrid solar PV system that encompasses both a battery bank and a connection to the grid (Fig. 4) will synergize mutually beneficial effects in two primary operational modes: normal power operation and power disruption mode.

#### *Normal Power Operation*

During normal power operations, when solar PV energy and grid electricity are available, smart home devices such as thermostats, lights, and smart plugs collaborate to optimize energy consumption. Their objective is to prioritize directing a sufficient portion of PV-generated electricity toward battery charging. This strategy minimizes reliance on grid electricity during night hours, overcast days, and peak-demand periods, reducing energy costs. This optimization is particularly advantageous when operating under a time-of-use (TOU) billing schedule, effectively cutting expenses during high-demand periods.

#### *Power Disruption or Outages*

During power disruptions or outages, the solar PV system and battery backup solutions seamlessly supply uninterrupted electricity to critical smart home components, including security cameras, video doorbells, smart lights, smart thermostats, flood and fire protection devices, and essential appliances. This ensures ongoing safety and protection for the household.

In such situations, smart home devices such as smart thermostats, smart lights, and smart plugs play a vital role in minimizing energy consumption. Their combined efforts aim to prolong the battery charge and enhance its overall lifespan, thereby reducing expenses related to installing more expensive battery banks and maintenance costs.

Many solar batteries, like SunPower's SunVault Storage, come with a 10-year limited warranty, typically within the payback period. This implies that after paying off the solar PV system, homeowners might need to invest in replacing the battery storage. By intelligently monitoring energy usage from the backup battery system with smart home devices, one can extend their lifespan, minimizing additional expenses associated with the solar PV system.

Furthermore, because the Smart Home system reduces energy consumption by approximately 24% annually, it becomes feasible to downsize the backup storage from two to one SunVault battery, further reducing upfront costs and shortening the payback period.

In our demonstration of integrated solar PV systems, we used one of the more expensive solutions to showcase the impact of smart home technology on energy efficiency and cost reduction. However, there are more affordable solar PV systems and longer-lasting backup batteries available for integration with smart home setups, offering homeowners even greater benefits.

### **Conclusion**

By integrating smart home technology with a solar PV system, we enhance home energy efficiency concurrently with the PV system installation, reducing energy waste by 24%. Advantages of the integrated solar PV with backup storage solution and smart home system include reduced energy consumption and environmental impact; reduced energy bills; prolonged solar battery lifetime; decreased cost of the solar PV installation; shortened payback time; and uninterrupted smart home functionality for house security, safety, and energy efficiency. These benefits become increasingly significant amid ongoing utility rate inflation. Opting for integration of the smart home systems with solar PV offers a dependable solution to mitigate reliance on the grid and mitigate the impact of frequent outages, especially during stormy seasons.

### **Conflict of Interest**

The author has no conflicts of interest to disclose.

## References

- Adapses. (2024). *Creating an affordable and reliable smart home in 2024. Essential tips and strategies.* <https://adapses.com/how-to-get-an-affordable-and-reliable-smart-home/>
- Adapses. (2024). *Smart some solutions.* <https://adapses.com/smart-home-solutions/>
- EcoFlow. (2023, March 16). *How much so solar panels save on average electricity bills?* <https://blog.ecoflow.com/us/how-much-solar-panels-save-on-electricity-bill/>
- EnergyEarth. (2024). *Thermostats savings calculations.* <https://www.energyearth.com/product/calculatesavings/nest-3rd-generation>
- Energy.gov. (2024). *Lighting choices to save you money.* <https://www.energy.gov/energysaver/lighting-choices-save-you-money>
- MarketWatch Guides (2024). *SunPower: Reviews, Services and Costs (2024).* <https://www.marketwatch.com/guides/solar/sunpower-reviews/>
- NREL (2024). *PVWatts calculator.* <https://pwwatts.nrel.gov/pwwatts.php>
- Oakter (2024). *Do smart plugs really save energy?* <https://oakter.com/smart-plugs-save-energy/>
- SolarReviews (2024, January 19). *Best solar panels 2024.* <https://www.solarreviews.com/solar-panel-reviews>
- Solar Technologies (2022, November 30). *What is a hybrid solar system?* <https://solartechnologies.com/what-is-a-hybrid-solar-system/>
- Smart Energy (2023). *Is a smart thermostat a worthwhile investment for your home?* <https://whatissmartenergy.org/featured-article/is-a-smart-thermostat-a-worthwhile-investment-for-your-home>

SunPower (2024a). *Calculate energy savings with SunPower.*

<https://us.sunpower.com/home-solar/residential-solar-power-calculator>

SunPower (2024b). *Install home solar panels with SunPower.*

<https://us.sunpower.com/home-solar>

**Table 1**

*Monthly household energy consumption and energy savings from solar PV and smart home systems. Solar irradiation and solar PV AC output are derived from the NREL PVWatts® Calculator (NREL, 2034).*

| Month     | Household Energy Consumption kWh | Solar Irradiation (PSH) kWh/m <sup>2</sup> /day | Solar PV AC Output kWh | Smart Home Energy Savings kWh |
|-----------|----------------------------------|---|------------------------|-------------------------------|
| January   | 2,101                            | 3.47  | 693                    | 603                           |
| February  | 1,472                            | 4.26  | 753                    | 435                           |
| March     | 675                              | 4.81  | 925                    | 88                            |
| April     | 860                              | 5.68  | 1,022                  | 101                           |
| May       | 953                              | 6.58  | 1,191                  | 108                           |
| June      | 1,200                            | 6.64  | 1,137                  | 362                           |
| July      | 964                              | 6.46  | 1,135                  | 299                           |
| August    | 833                              | 5.88  | 1,039                  | 264                           |
| September | 655                              | 5.45  | 954                    | 87                            |
| October   | 1,187                            | 4.43  | 824                    | 124                           |
| November  | 1,291                            | 3.78  | 705                    | 386                           |
| December  | 2,249                            | 3.01  | 596                    | 642                           |
| Annual    | 14,400                           | 5.04  | 10,974                 | 3500                          |

### SunPower Solar PV with a Backup Battery Storage Solution

*Fig. 1. SunPower's complete solar PV solution has high-efficiency solar panels, backup battery storage, and inverters with the control system and software (SunPower, 2024).*



## Essential Smart Home Devices

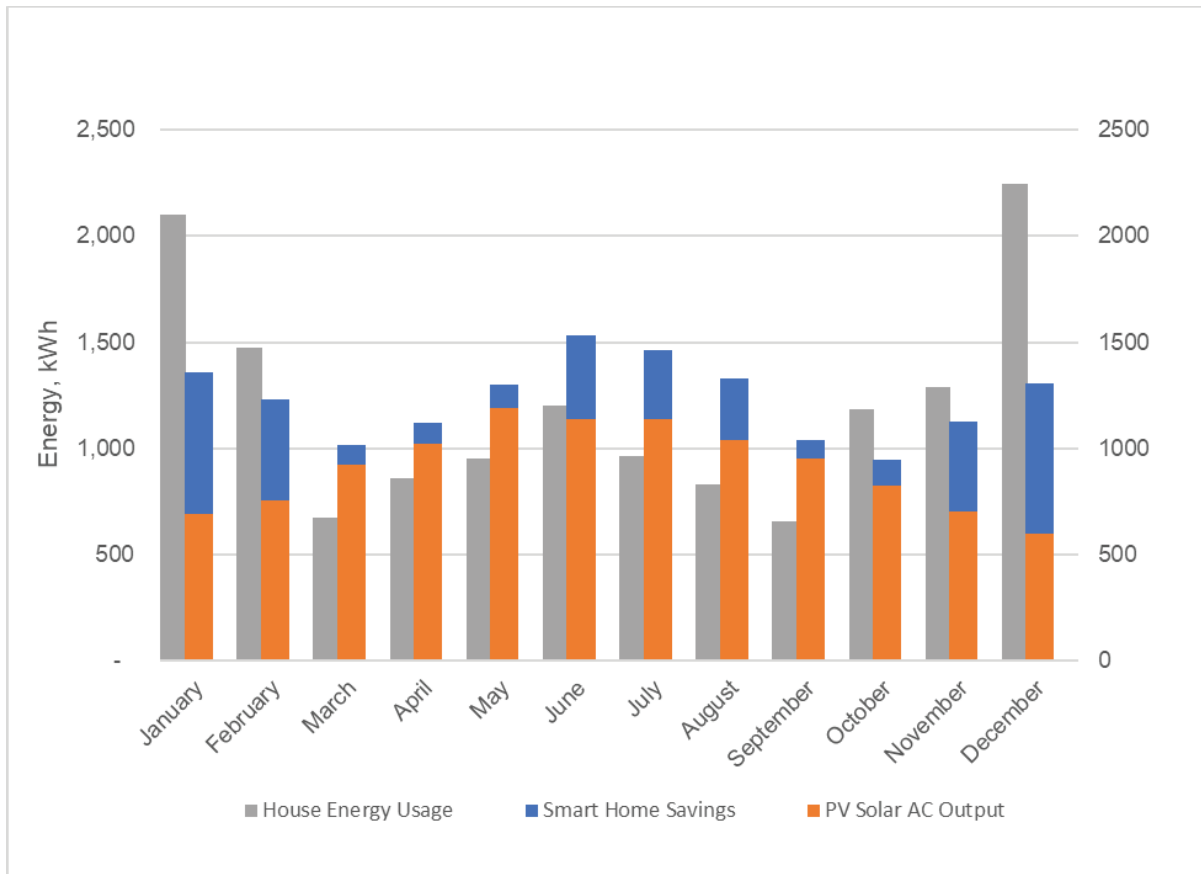
Fig. 2. Essential smart home devices provide energy efficiency, security, and hazard prevention (Adapses, 2024).





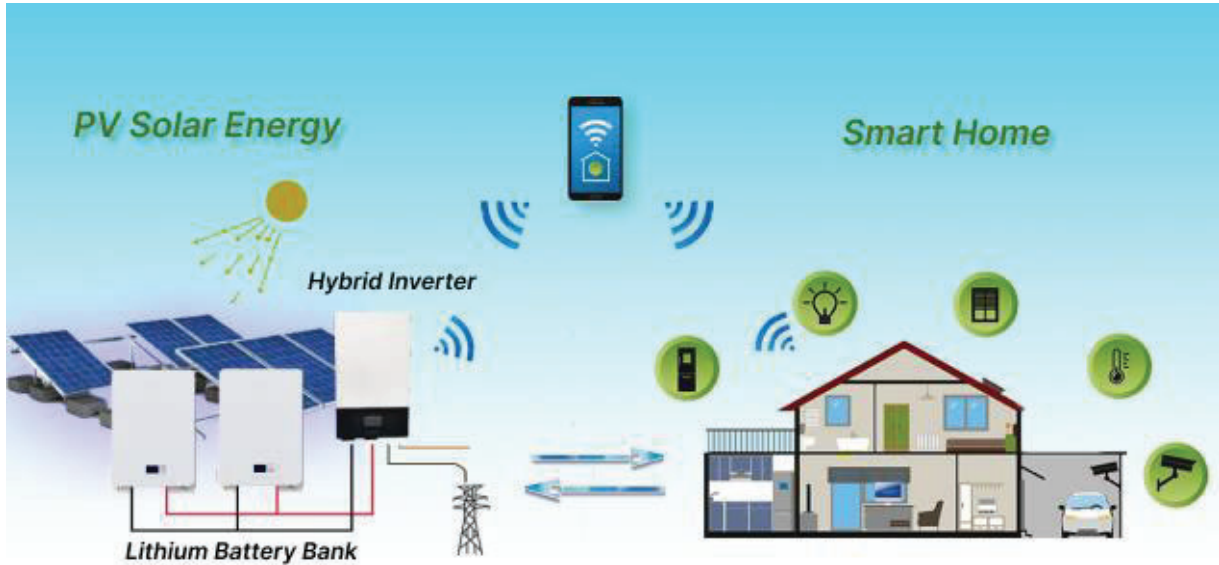
### Integrated Smart Home and Solar PV Energy Savings

Fig. 3. Monthly energy savings accrue from solar PV output and smart home savings vs. house energy consumption.



### Integrated Solar PV and Smart Home Solution

Fig. 4. The synergy of integration of a smart home system with a hybrid solar PV solution.



**This page intentionally left blank.**

**Productive Uses of Renewable Energy (Pure)  
for Uganda**

Robert Foster  
Assistant Professor  
College of Engineering  
New Mexico State University

Ismail Muyinda  
Assistant National Coordinator  
National Renewable Energy Platform  
Ministry of Energy and Mineral Development  
Government of Uganda

## Abstract

**Productive** uses of renewable energy (PURE) technologies are mature, economical, and offer practical solutions that meet the needs of off-grid regions across the globe. Solar photovoltaics (PV) in particular are a mature, reliable, and economically practical solution for both on and off-grid PURE applications such as water pumping for irrigation, flour milling, milk chilling, and cold storage. Solar thermal technologies are practical for crop drying and process heat for agroprocessing. Access to affordable clean energy especially for rural communities is not only economically feasible but also a social justice issue. This paper discusses Productive Uses of Renewable Energy (PURE) impacts in Uganda for rural communities using solar water pumping, solar mini-grids, solar chilling, and solar crop drying.

### 1. **Keywords: photovoltaics, solar energy, water pumping, mini-grids, chilling, milling, food preservation, Uganda**

**Introduction**  
We coined the brand Productive Uses of Renewable Energy (PURE) technologies to extend the original PUE concept to indicate further use of clean energy sources such as solar, wind, geothermal, and hydropower to meet local energy needs for economic development. PURE technologies are clean and affordable and often the most economical way to energize processes for locations that otherwise do not have access to conventional energy options such as the national power grid. PURE technologies use local energy that in turn helps create local jobs and community economic growth.

The U.S. Department of Agriculture Foreign Agricultural Service (USDA FAR), the Uganda Solar Energy Association (USEA) and the Government of Uganda (GoU) have helped lead in the application of PURE technologies in the country. Solar through direct applications or mini-grids is a well-developed, mature, and more economical alternative to grid expansion and diesel generators, especially in rural Uganda. There is often an excellent match between seasonal solar resources and seasonal energy needs. When it is dry and sunny, the needs for water and chilling increase along with the available solar energy to power them. USEA has been working with GoU on a number of PURE projects and activities, including developing a roadmap for PURE promotion in Uganda, as well as a national market assessment (GoU, 2023).

## 2. **Uganda Energy Landscape**

Only 28% of Ugandans are connected to the national power grid and they are mainly in urban areas; this is one of the lowest grid-connection rates in all of Africa. Only about 2% of the total Uganda energy consumption is from electricity. The total installed grid generation capacity is about 1,400 MW, with a peak demand of about 650 MW. Hydropower remains the nation's leading power source, representing 80 percent of total electrical generating capacity (IEA, 2023).

Biomass accounts for 90% of the energy used in the country, with about 90% of Ugandans reliant on fuel woods for cooking and heating. The National Environment Management Authority estimates that about 2.6% of Uganda's forests are cut down annually for firewood, charcoal, and agriculture, and that the country will be completely deforested in another ~25 years if there is no usage change (GoU, 2023).

The Uganda Ministry of Energy and Mineral Development (MEMD) is responsible for overall national energy policy direction and guidance. MEMD recently updated its 20-year-old energy policy in 2023. For the first time ever, the MEMD-updated energy policy specifically calls for the use of productive uses of energy with an emphasis on renewable energy (GoU, 2023). PURE promotes local economic development using clean energy solutions that offer greater energy security, local jobs, and energy independence.

### 3. Solar Water Pumping

Solar water pumps (SWP) are one of the earliest PURE technologies, providing water for crops, livestock, and community water supply. SWP system costs have declined significantly over the past decade to < \$3 per peak watt (with pump) installed today. SWPs are about five times cheaper to operate than traditional diesel pumps, and less than half the cost of electric pumps powered by the conventional power grid. One of the authors of this paper has installed AC SWPs in Mexico that have operated for 25+ years with little maintenance besides an inverter replacement after about 15 years. NMSU was one of the first three U.S. Department of Energy PV experimental stations in the nation. It has early Block 5 PV modules installed on its facilities in 1981 that are still operational at about 60 percent of name plate rating.



Fig. 1. The USDA farmer training by Green Powered Technology uses a portable solar water pump system with a folding array mounted on bicycle wheels for transportation. It was for crop irrigation that was shared between several farmers at the Rugendabara Coop in western Uganda in August 2022. It uses the world's only surface helical rotor pump, developed by Ennos. (Credit: Robert Foster)

In western Uganda, the USDA FAS partnered with Green Powered Technology, Solar Now, and Clean Energy Enthusiasts to introduce a new and innovative portable SWP with wheels that allows several farmers to share the same pump for irrigation that is wheeled from field to field as needed. This Sunlight SWP is an innovative high-quality surface ½ HP helical rotor pump from Ennos with a maximum total dynamic head of 40 m. This is the only surface helical rotor pump available anywhere. The expected lifetime for the DC pump is 10+ years. The Ugandan farmers irrigate maize, rice, bananas, and other crops.



Fig. 2. The world's only helical rotor surface pump is the Ennos Sunlight, used in PURE projects sponsored by USDA FAS in western Uganda. (Credit: Robert Foster)

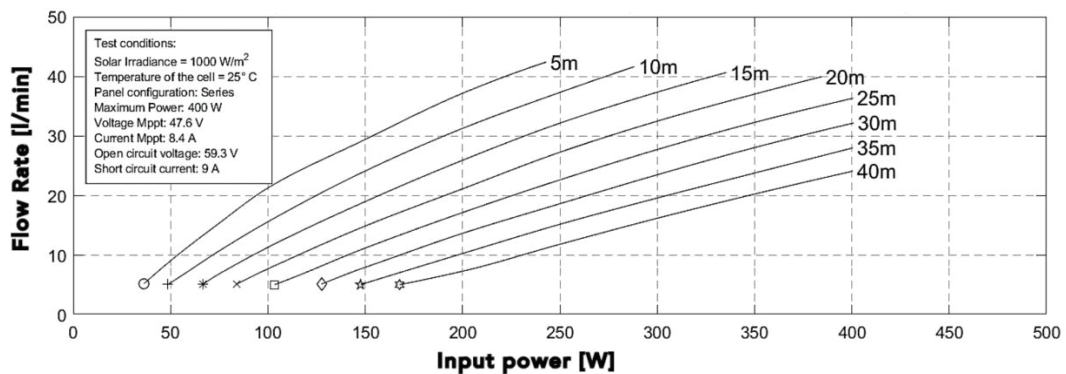


Fig. 3. Ennos Sunlight 1/2 HP pump curves. (Courtesy of ENNOS)

Micropower and low-power SWP systems provide affordable water even for smallholder farmers, by pumping throughout the entire day. The smallest SWPs have over 40 years of experience in commercial applications (e.g., Grundfos, Dankoff, Lorentz) and show the most technology diversity. They use displacement pumps and DC motors. The low-power range brings in greater use of centrifugal pumps and AC motors. The medium and high-power ranges use conventional centrifugal pumps with AC motors. The following figure summarizes how the various SWP mechanisms fit the full range of water lift and flow that is found throughout Uganda.



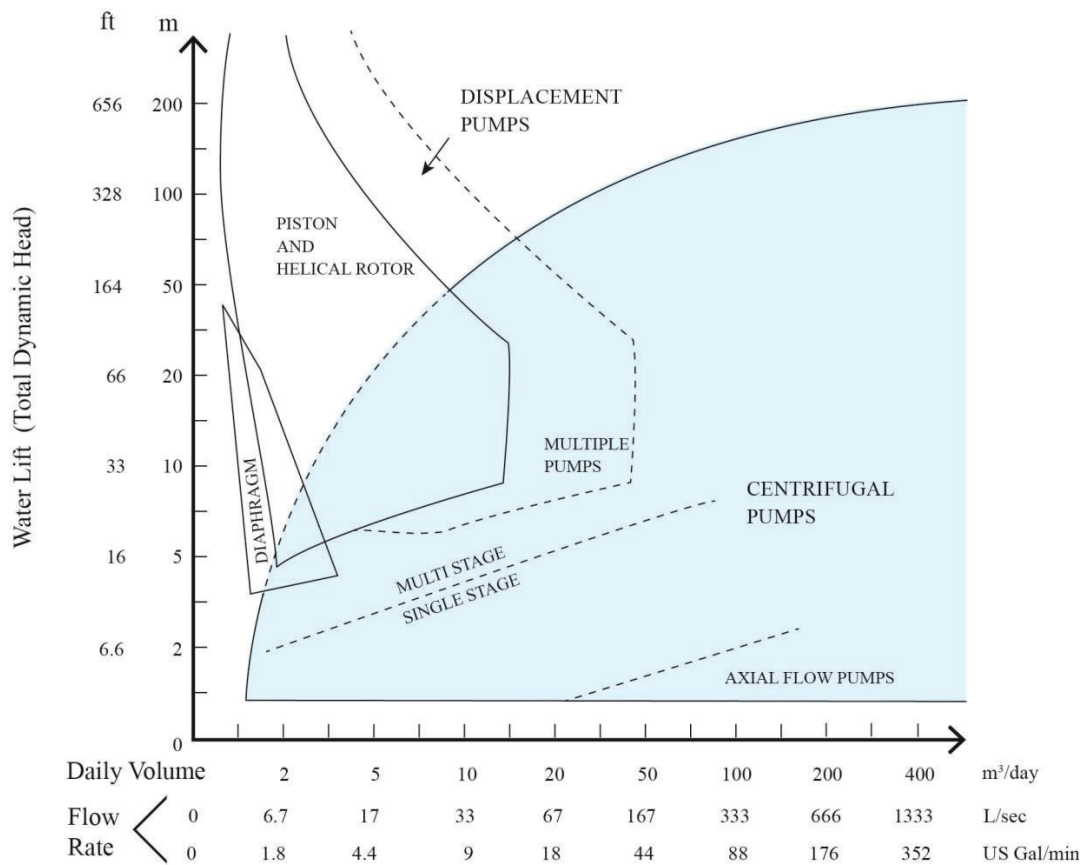


Fig. 4. Pump mechanisms in relation to vertical lift and water requirements. (Dankoff & Foster, 2022)

#### 4. Solar Chilling and Cold Storage

Direct-drive solar refrigeration technology was introduced to western Uganda in 2022 as part of the USDA FAR PURE in support of the Power Africa program. The direct-drive refrigerator uses no batteries that use thermal phase change material (ice) energy storage.

The technology was originally developed in support of NASA’s future planetary mission’s refrigeration requirements, and later commercialized for vaccine battery-free refrigeration by SunDanzer and subsequently approved by the World Health Organization (WHO).

This is accomplished by integrating water as a phase-change material into a well-insulated refrigerator cabinet and by developing a microprocessor-based control system that allows direct connection of a PV panel to a fixed or variable speed DC compressor. By storing ice in the walls of the refrigerator, it eliminates the need for electrochemical energy storage.

The solar refrigerator uses a vapor compression cooling cycle with an integral thermal storage liner, PV modules, and a controller. The direct-drive solar refrigerator used in Uganda employs a variable-speed dc compressor. By storing ice in the walls of the refrigerator, it eliminates the need for battery storage. Ice never wears out and it provides sufficient energy storage to cool 40 L of milk overnight or other products. Pilot units were placed in Katairwe village near Kyegegwa area in western Uganda.



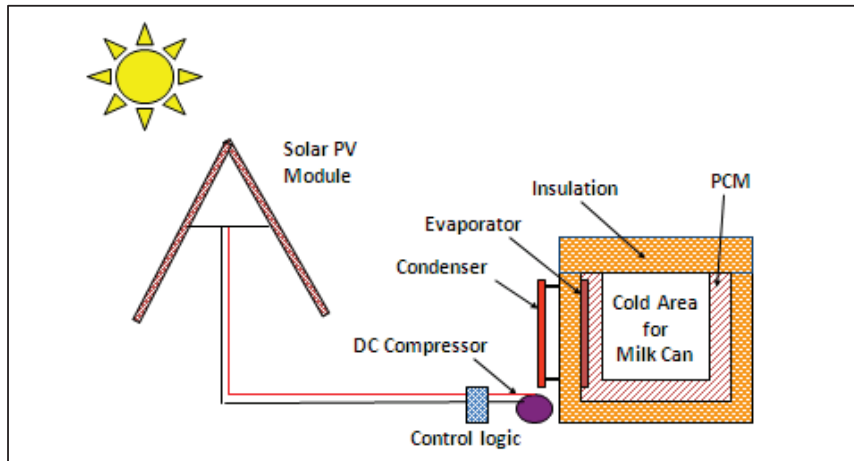


Fig. 5. Solar direct drive refrigerator with DC compressor and E-W “fixed tracking” array. (Foster, 2017)

A unique innovation of the SunDanzer direct-drive solar chillers is the east-west “fixed tracking” array alignment of the photovoltaic array to optimize compressor run time instead of maximizing energy generation. This enables the direct-drive photovoltaic refrigerator (PVR) DC compressors to run longer by starting up earlier in the day and running longer in the afternoon than a traditional equatorial facing array would and thus lengthen daily chilling time. Tests at New Mexico State University found that the battery-free phase-change thermal storage (ice) system enables the PVR to stay cool for up to a week of cloudy weather.

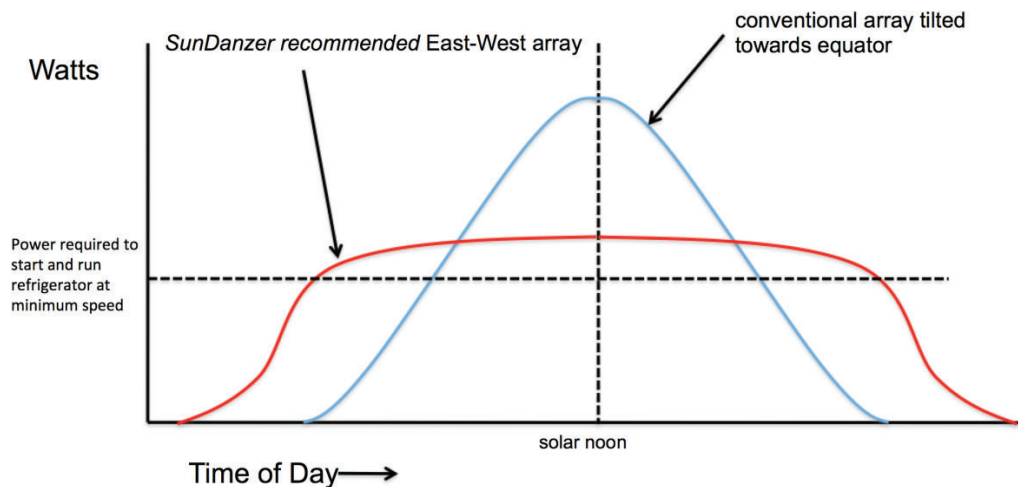


Fig. 6. A fixed E-W tracking array was designed to maximize compressor run time rather than maximum energy capture. (Foster, 2017).



Fig. 7. A PVR Fixed E-W tracking array was installed in Katairwe village for a local convenience store that sells milk, meat, and cold drinks. (Credit: Robert Foster)

In order to maximize heat transfer, the PVR can also incorporate brine bags that do not freeze at  $0^{\circ}\text{C}$ . They are placed around the milk cans to increase heat transfer rates and cool milk quickly. Milk has some natural substances referred to as the lactoperoxidase system, that has both bacteriostatic and bactericidal effects against some milk spoilage microflora.

This natural system is effective and able to preserve the milk from microbial spoilage for about the first three hours after milking. Bacteriological growth is further retarded when milk temperatures fall to about  $10^{\circ}\text{C}$  and stops at  $4^{\circ}\text{C}$ . The PVR chills 25 liters of milk down to  $10^{\circ}\text{C}$  in a couple of hours, and the milk temperature in the morning is about  $4^{\circ}\text{C}$  as shown in Fig. 9.

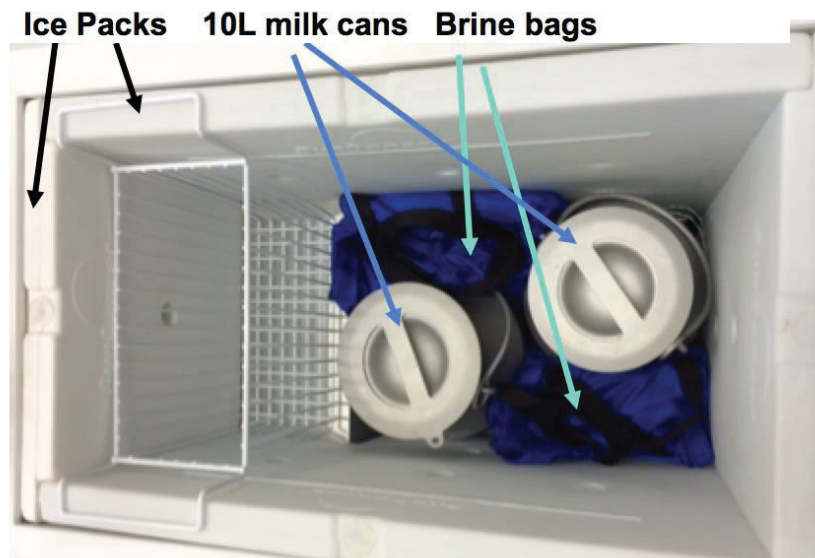


Fig. 8. The project used thermal ice storage and brine bags to chill evening milk. (Credit: Robert Foster)

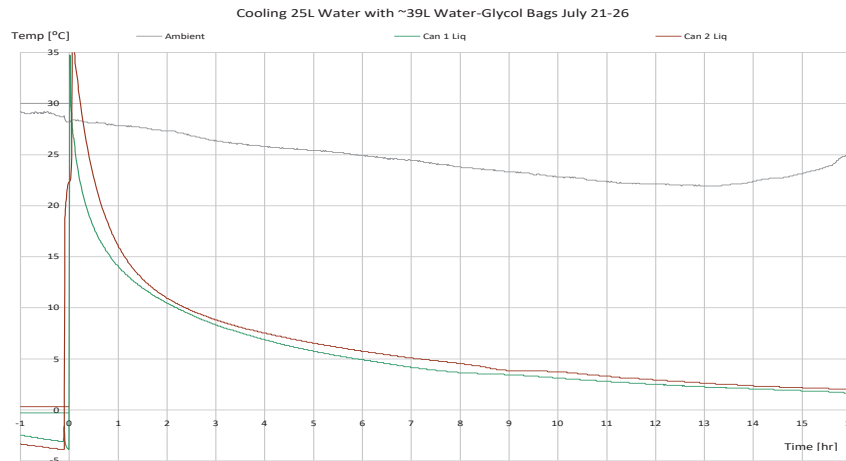


Fig. 9. Solar milk-chilling test results for 40-liter milk cans. Bacteriological growth in milk largely becomes inactive below 7°C. There is about a 4-hour window before significant bacterial growth starts in milk. The PVR unit successfully meets this threshold. (Foster 2017).

The SunDanzer direct drive PVR can chill 25 liters of evening milk to 40°C overnight. Figure 10 shows the daily milk cooling cycle for milk temperature is repeatedly cooled to 5°C by early morning. Note that the farmer places the empty milk can outside in sunlight for drying after cleaning representing the daily peak outdoor temperature of 30+°C.

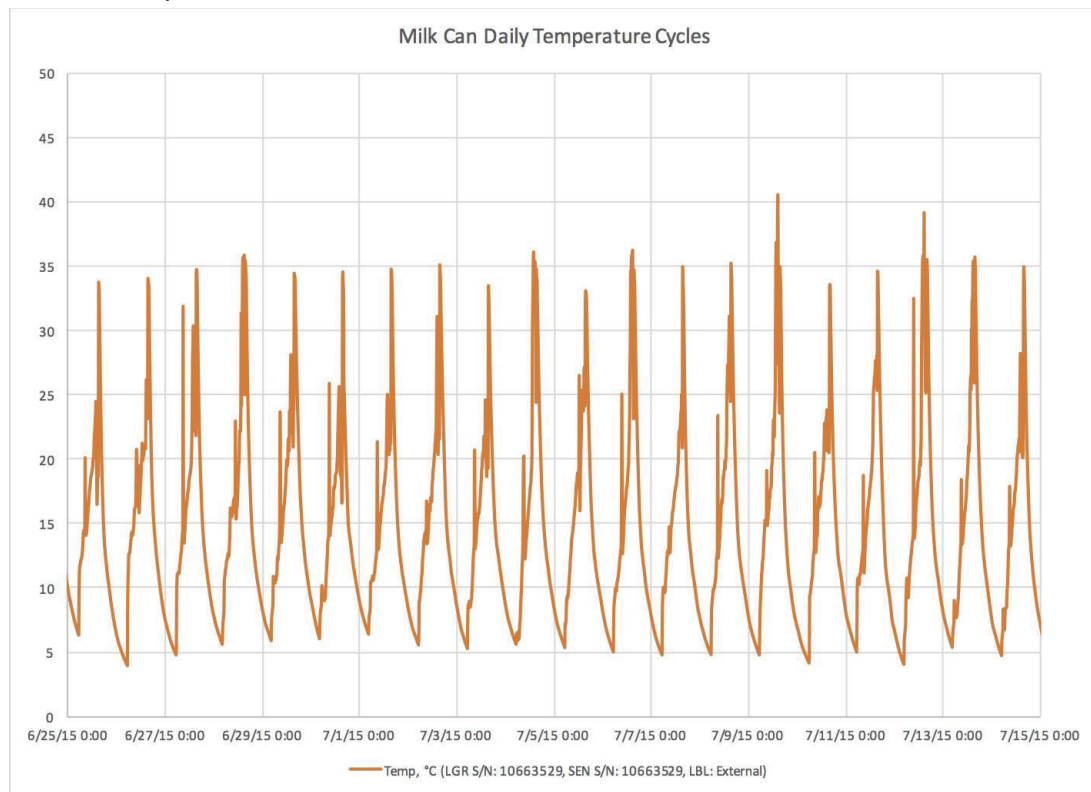


Fig. 10. Daily milk can temperatures show daily cooling cycles on a smallholder dairy farm. The farmers clean out the can daily and put it outside in the sun to dry during the day. (Foster, 2017)



Fig. 11. Local Katairwe farmers during a USDA-sponsored PURE training event inspected a direct-drive PV refrigerator (PVR) with thermal storage used by a store to preserve meat and chill milk and drinks. (Credit: Robert Foster)

The PVRs are also equipped with two 5V USB charging ports installed on the refrigeration units so the users can charge cell phones, flashlights, or other devices as needed. These ports are sometimes rented out by the owners for a small fee to neighbors to charge cell phones.

## 5. Solar Mini-Grids for Uganda

Mini-grids are independent small to medium-scale electricity generation systems serving a fixed customer base via a stand-alone electrical distribution grid. Mini-grids can fill the gap where the national grid cannot provide coverage for 70 percent of Ugandans without power. Mini-grids can supply reliable 24/7 electricity to villages where grid extension is unaffordable or impractical.

The Uganda electric grid of the future will become more decentralized and reliable using mini-grids to power electrical loads. There are about 50 mini-grids currently operating in Uganda, the majority of which use hydropower. But increasingly new solar mini-grids are under development to expand beyond hydropower regions. The Government of Uganda is promoting private investment for mini-grids in Uganda.

In 2023 the German bank KfW granted 35 million Euro to MEMD to install ~6 MWp of mini-grids in Uganda with construction starting in 2024. The Beyond the Grid Fund for Africa has recently signed agreements in 2024 to develop Uganda solar mini-grids, as well as direct-drive solar-powered refrigerators with ice storage.

### 5.1 Mbaata Mini-Grid for Cold Storage, Milling, Hair Salon, and Theater

The Mbaata 25 kWp solar mini-grid in western Uganda was installed in late 2022 by a UK developer. It provides power via three 8 kW SunSynk Inverters and WECO



battery energy storage system. The mini-grid powers a milling machine, metal workshop, hair salon, and a small theater. Most importantly, it provides for a cold room chilled by two LG split room air conditioners with a cooling capacity of 6.4 kW each using dozens of cold water containers for cold storage in the insulated cold room to keep horticultural and other crops cool before shipping. This allows farmers to have options to achieve better pricing for their products since they are in a better position to negotiate with vendors.



Fig. 12. The Mbaata 25-kWp rooftop solar mini-grid powers a cold room, a milling machine, a hair salon, a metalworking workshop, and a small movie theater. (Credit: Robert Foster)



Fig. 13. A state-of-the-art Mbaata solar mini-grid control room consists of 3 SunSynk inverters (3-phase AC) and WECS lithium-based batteries. (Credit: Robert Foster)



Fig. 14. The Mbaata solar mini-grid powers this milling machine used for cassava flour. The author [Which author?] left all his surgical masks behind so the operators will not breathe in fine cassava particulates. (Credit: Robert Foster)

## 5.2 Katarwe Mini-Grid for Bulk Chilled Milk Storage and Village Loads

The Kyegegwa Rural Electricity Cooperative Society Limited (KRECS) solar mini-grid serves the Katarwe community. KRECS partnered with NRECA International and USAID Power Africa to develop a solar mini-grid to provide PURE electricity. It developed a state-of-the-art solar mini-grid to power community needs for residences and businesses, including a milk-bulking station for the dairy farmers. These efforts have helped stimulate socioeconomic well-being while promoting environmental conservation. The mini-grid system was installed by NRECA and KRECS in late 2022. This is a 56-kWp solar mini-grid with a 5-kWh battery bank and a backup diesel-powered generator rated at 50 KVA. It is a 3-phase distribution system connected within a 4-km radius that serves 176 households and small stores, as well as four medium-scale commercial users comprised of two dairies with milk bulking stations, one coffee factory, and one telecommunications mast.



Fig. 15. The Katarwe village 56-kWp solar mini-grid was installed by NRECA in 2022 for USAID Power Africa and operated by the local KRECS utility. This system provides 3-phase power to 176 households, several small stores, two dairies, a coffee factory, and a telcom mast. (Credit: Robert Foster)

## 6. Acknowledgments

The USDA FAS-sponsored Uganda Productive Uses of Energy Project (2022) is a component of the USAID Power Africa program. Technical assistance was provided by Green Powered Technology, based in Arlington, Virginia, in collaboration with Clean Energy Enthusiasts and the Uganda Solar Energy Association, both based in Kampala. The project built upon USAID Feed the Future programming in the Kasese and Kyegegwa Districts of western Uganda.

## 7. Conclusions

The USDA FAS Productive Uses of Energy project successfully introduced new and innovative sustainable PURE technologies to western Uganda. This included portable solar-powered surface helical rotor pumps (Ennos), which supply water for irrigation, livestock, and community water supply. Farmer ROI is only a couple of years through increased crop production from irrigation. The new portable design allowed the ROI benefits to be shared between several farmers. The USDA project also introduced direct-drive solar refrigeration with ice storage (SunDanzer) eliminating the need for batteries. Solar chillers help farmers and stores to preserve fresh milk and crops. Payback is less than two years. There are over 5 million smallholder dairy farmers in East Africa who can benefit from solar chilling technologies.

## Conflict of Interest

There is no conflict of interest. The authors are not employed by any of the companies stated.

## References

- Dankoff, W. Foster, R., Cota, A., & Lespin, E.. Advances in solar powered water pumping providing for energy resiliency and social equity. *Solar 2022*, Albuquerque, New Mexico, pp. 24-35.
- Foster, R., Jensen, B., Dugdill, B., Knight, B., Faraj, A., Mwove, J. K., and Hadley, W. (2017). *Direct drive photovoltaic milk chilling experience in Kenya*. IEEE Photovoltaic Specialists Conference 44: Washington D.C.
- GoU. (2023). *Energy policy for Uganda 2023*. Government of Uganda, Ministry of Energy and Mineral Development..
- IEA. (2023). *Uganda 2023: energy policy review*. International Energy Agency.





**Gap in pagination due to formatting issues.**

**Pages 32-33**

**Solar Thermal Collectors and Multi-Source Heat Pump Systems**

Gaylord Olson<sup>1</sup>

Yao Yu<sup>2</sup>

Xiaou Hu<sup>2</sup>

Abhishek Dangol<sup>2</sup>

<sup>1</sup>Temple University, Mech. Engr. Advisory Committee,  
Philadelphia, PA

<sup>2</sup>North Dakota State University  
Fargo, ND

## Abstract

Combining one or more types of solar thermal collectors in a hybrid or multi-source heat pump system offers a potentially more cost-effective method for heating buildings compared to traditional approaches. This means a lower total cost of ownership. The initial cost of the system can be lower than a conventional ground source heat pump system because of a significantly smaller total ground loop (less borehole drilling), and the electricity use can be relatively low because the ground loop (or loops) will provide better efficiency than any air source heat pump. Even the recent “cold climate” heat pumps will never compare with a ground loop when the air temperature is either below freezing or above 100°F. The laws of physics do not allow high efficiency for any air source system at those temperatures, but a ground loop gives high efficiency at any outdoor air temperature.

Keywords: solar thermal collectors, multi-source heat pump, energy efficiency, cost-effective

## Introduction

The combination of Solar Thermal Collectors (STCs) with multi-source heat pump systems has paved the way for energy-efficient and cost-effective heating and cooling solutions. This use of a hybrid system has helped channel the use of renewable energy, yielding significant reductions in both operational costs and greenhouse gas emissions.

Former studies have explored the performance and benefits of integrating STCs with heat pump systems. A variety of multi-source system designs were presented by Olson and Yu with seasonal storage and optimized solar/air collection systems (Olson & Yu, 2016; Olson & Yu, 2017). These works highlight the potential for significant energy savings and improved system efficiency.

Additionally, research by Emmi et al. and Kjellson et al., using the TRNSYS simulation program to evaluate various system configurations, highlighted the benefits of using multi-source systems, such as optimized system performance along with reduced electricity demand by integrating ground-source heat pumps with solar collectors (Emmi et al., 2016; Kjellsson et al., 2010).

A study by Chen et al. proposed a hybrid ground source heat pump system and integrated it with concentrated photovoltaic thermal (CPC-PVT) solar collectors. This hybrid system exhibited higher primary energy ratios (a measure of the system's efficiency in converting primary energy into useful outputs and exergy efficiency versus the conventional system, highlighting the benefits of combining geothermal and solar resources for performance enhancement (Chen et al., 2019).

In another study conducted by Han et al., a multi-source hybrid heat pump system (MSHPHS) was simulated to be located in the cold region of Harbin, China. By using solar, geothermal, and air energy, the MSHPHS maintained a high coefficient of performance (COP) of 3.06 and showed a higher energy efficiency of 29.84% compared

to a standard ground-source heat pump system. This showed the effectiveness of integrating STCs and multi-source heat pump systems (Han et al., 2017).

There are different types of STCs that can be useful for multi-source heat pump systems, as listed below:

1. Glazed flat plate collectors: Primarily used for domestic heating for decades, these collectors are most effective at temperatures up to 200°F. They are not useful for cooling the types of systems described here because the glazing panel is intended to prevent convection cooling of the absorber plate.
2. Unglazed flat plate collectors (also known as polymer flat plate collectors): These are cost-effective and versatile since there is no glazing. They are suitable for both heating and cooling applications. They are used especially in swimming pool heating and have much lower output temperature than the glazed collectors. For the cooling application, they collect cold from both cold air convection and also radiative cooling into a clear, cold sky.
3. Photovoltaic Thermal (PVT) collectors: These devices are considered to be dual-use products, since they produce both electricity and hot water from sunlight. What most people do not realize is that these devices can be made into triple-use products when they are part of a multi-source heat pump system for electricity generation and the production of hot or cold water. These can be made in both glazed and unglazed versions; however, the unglazed type is most widespread. In this case, they are useful for electricity generation, hot water production and also cold-water production (when the sun is not out and the air temperature is low). It is possible that the useful life of a PVT panel might be longer than that of a plastic unglazed pool solar collector since the solid PV layer on the top of the panel gives protection to the pipes and other material used for hot or cold-water collection below the PV layer.
4. Evacuated Tube Collectors: Evacuated tube collectors with vacuum insulation inside multiple glass tubes are highly efficient at higher temperatures and are less influenced by the external weather conditions, but are less useful for collecting cold, i.e., heat removal. They can attain higher temperatures when combined with curved reflectors for sunlight concentration.

The objective of this paper is to evaluate the design, performance and energy-efficiency potential of a newly-developed multi-source heat pump system equipped with various sources, such as ground, air, and/or solar. It examines the design optimization and configurations using numerical simulations in the TRNSYS environment (TRNSYS 18). This study also compares multiple cases (operation modes) with conventional systems to quantify efficiency and energy savings. It highlights the potential of the multi-source system developed, demonstrating its potential as a sustainable and cost-effective solution for residential heating and cooling.

### **Multi-Source Heat Pump Systems**

In recent years, there have been improvements and simplifications in the multi-source system designs, reducing the number of pumps and valves needed to accomplish full

functionality. Perhaps the simplest form of a multi-source system (but not with full functionality) is one that has two sources and allows a selection of one or the other to connect to a water source heat pump. Fig. 1 shows three versions of this.

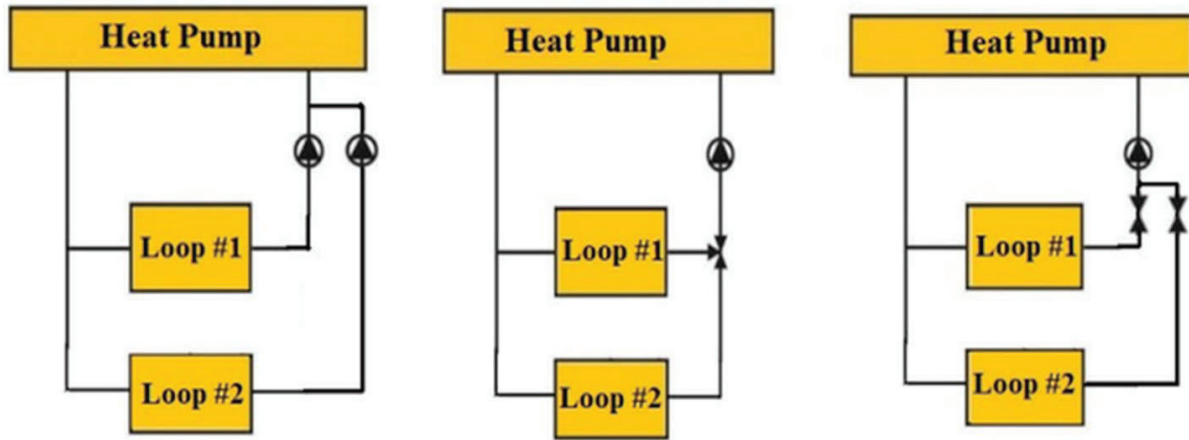


Fig. 1. Dual Source Heat Pump Configurations

Note that Fig. 1 also allows a mode which has source water from both sources simultaneously (parallel mode). By including one more pump or one more valve, there could be three optional sources rather than just two. There are also many sources to choose from beyond STCs:

1. Ground loop (either borehole or trench)
2. Cooling tower (evaporative or dry)
3. Open loop from a conventional water well
4. Surface water (lake, pond, or river)

Certainly, many other sources beyond those above are also possible.

If the system has just a single ground loop, the addition of a second source such as a STC allows what might be called a preconditioning mode. With this mode, the ground around the loop can be either preheated or precooled to gain an improvement in heat pump efficiency at some future time. For example, in the summer and/or fall of the year, a STC can circulate very hot water through the ground loop pipes in preparation for the upcoming winter. This technique has been widely used and can sometimes convert a failing ground loop system from total failure into a long-term success.

A simple example of a single-loop system with preconditioning is shown in Fig. 2.

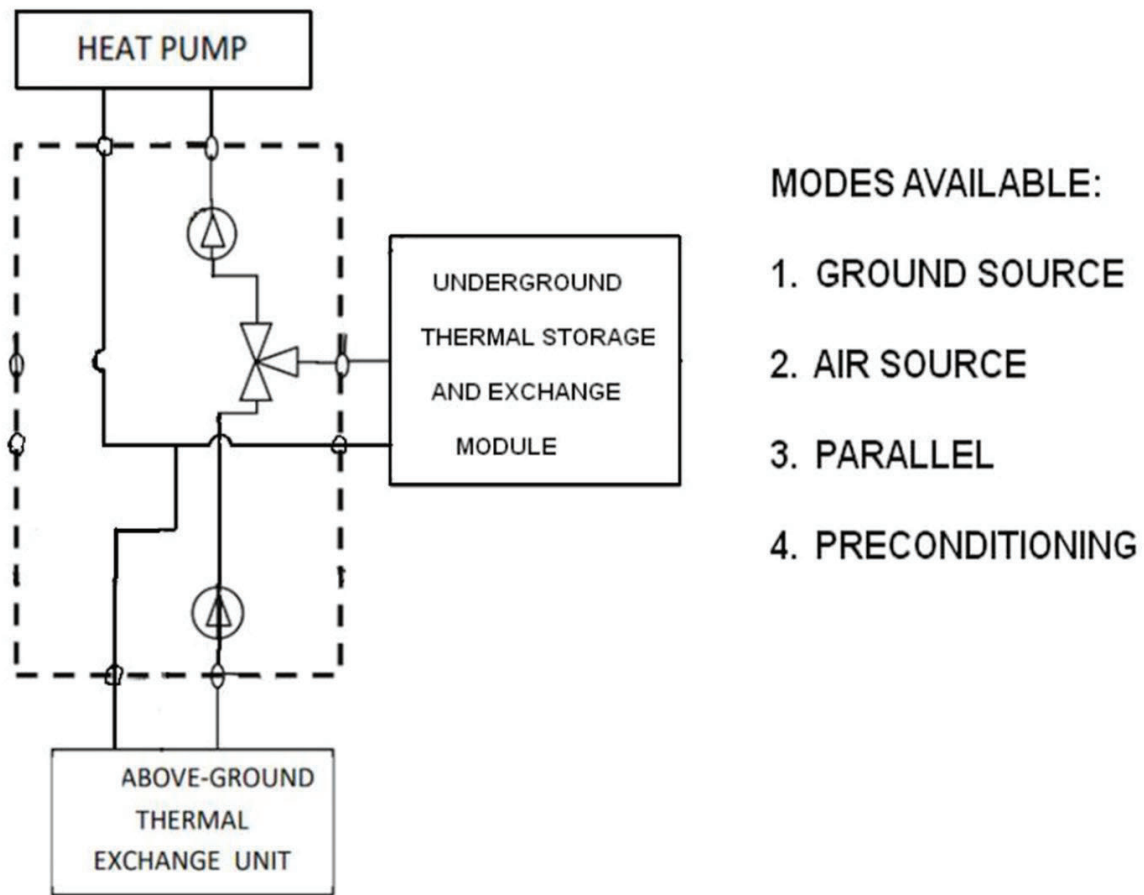


Fig. 2. Single ground loop system with preconditioning

Numerical simulations have been conducted to evaluate the energy-saving potential of the system depicted in Fig. 2. These simulations were performed in the TRNSYS environment (TRNSYS 18) for a heat pump system incorporating underground regions, STCs, and a buffer tank as illustrated in Fig. 3. The system is designed to provide heating and cooling for a single-family house (Fig. 4) located in Bismarck, North Dakota. Details about the house and the system are presented in Table 1 and Table 2.

The operational strategies for this system are categorized into four control modes, as shown in Fig. 5. Based on these modes, three specific cases were analyzed in this study:

- Case 1: Alternates the heating source for the heat pump between the underground loop and the solar buffer tank (Modes 1 & 2).
- Case 2: Builds on the setup of Case 1 by also enabling simultaneous use of both the underground loop and the solar buffer tank, splitting the flow equally (Mode 3) when both sources are advantageous.

- Case 3: Extends the functionality of Case 2 to include charging the underground region using the solar buffer tank (preconditioning – Mode 4) when space heating is not required.

The performance of these cases was compared to a baseline scenario, where a conventional air source heat pump system is used for heating and cooling in the target building, as depicted in Fig. 4.

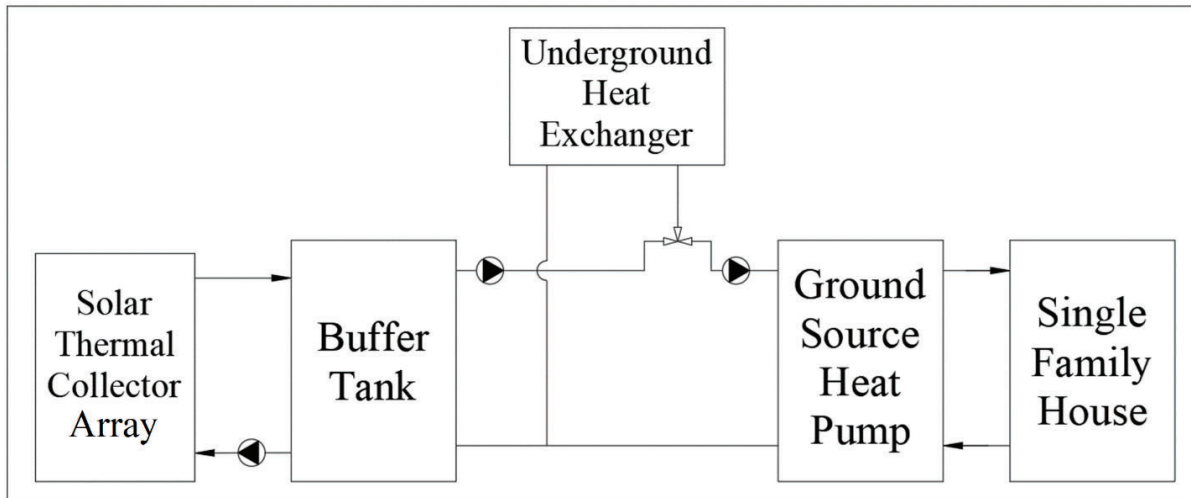


Fig. 3. Single ground loop system with solar collectors for simulations

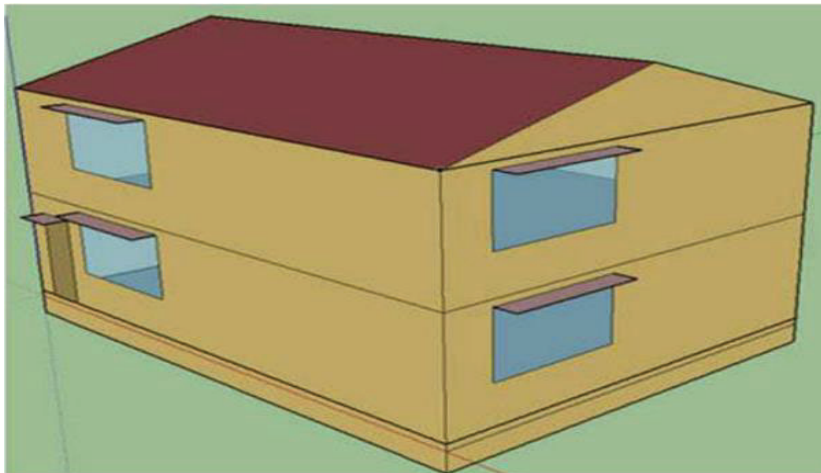


Fig. 4. Single-family house for simulations

Table 1. Building Information

|                  |                     |
|------------------|---------------------|
| Building Type    | Single-Family House |
| Number of Floors | 2                   |

|  |       |
|--|-------|
| Building Total Area [m <sup>2</sup> ]    | 334.5 |
| Total Conditioned Area [m <sup>2</sup> ] | 223.1 |
| Window-Wall Ratio                        | 14.1% |
| Gross Roof Area [m <sup>2</sup> ]        | 219.8 |

Table 2. System Information

|  |                      |
|--|----------------------|
| Borehole Type                                | Vertical Closed Loop |
| Number of Boreholes                          | 4                    |
| Borehole Depth [m]                           | 61                   |
| Borehole Separation Distance [m]             | 6.1                  |
| Number of Heat Pump Units                    | Water-to-Air HP: 1   |
| HP Air Flow Rate [L/s]                       | 774.0                |
| HP Water Flow Rate [L/s]                     | 0.76                 |
| HP Rated Heating Capacity [W]                | 11517.7              |
| HP Rated Heating COP                         | 3.4                  |
| HP Rated Cooling Capacity [W]                | 14184.6              |
| HP Rated Cooling COP                         | 4.8                  |
| HP Rated Fan Power [W]                       | 560                  |
| Solar Thermal Collector (STC) Dimensions [m] | 2.44 × 1.22          |
| Total Number of Evacuated Tube STCs          | 2                    |
| Buffer Tank Size [L]                         | 302.8                |



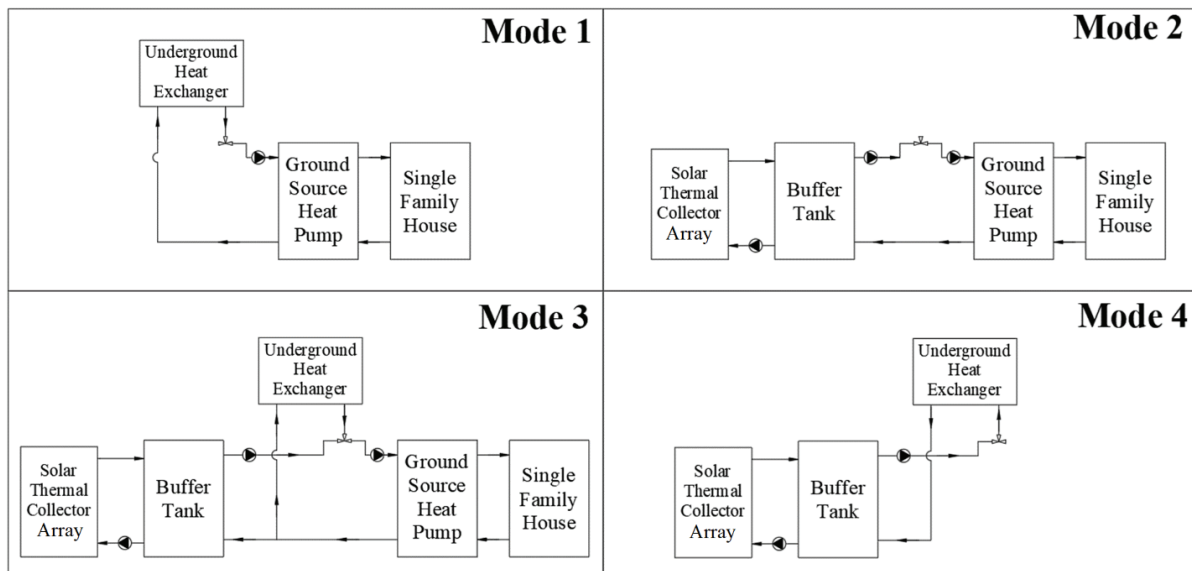


Fig. 5. Diagrams of different operation modes

Fig. 6 displays the monthly averaged heating Coefficient of Performance (COP) for the different cases. The data reveal that higher heating COPs are achieved during the winter months when using the hybrid heat pump system rather than the baseline system, which relies on an air source. Notably, Case 3 exhibits lower heating COPs than Cases 1 and 2 during summer. This reduction is primarily due to the heat stored in the buffer tank being transferred to the underground regions for preconditioning, leaving less available for space heating. Moreover, due to the limited number of boreholes and the small size of the underground regions, a significant portion of this heat is lost through the edges and top of the ground. Consequently, there is no notable improvement in heating COPs after summer, as illustrated in Fig. 6. A higher winter temperature requires different parameters for borehole spacing, solar collection area, and tank size. An even higher temperature will be obtained after 5 or 10 years of use.

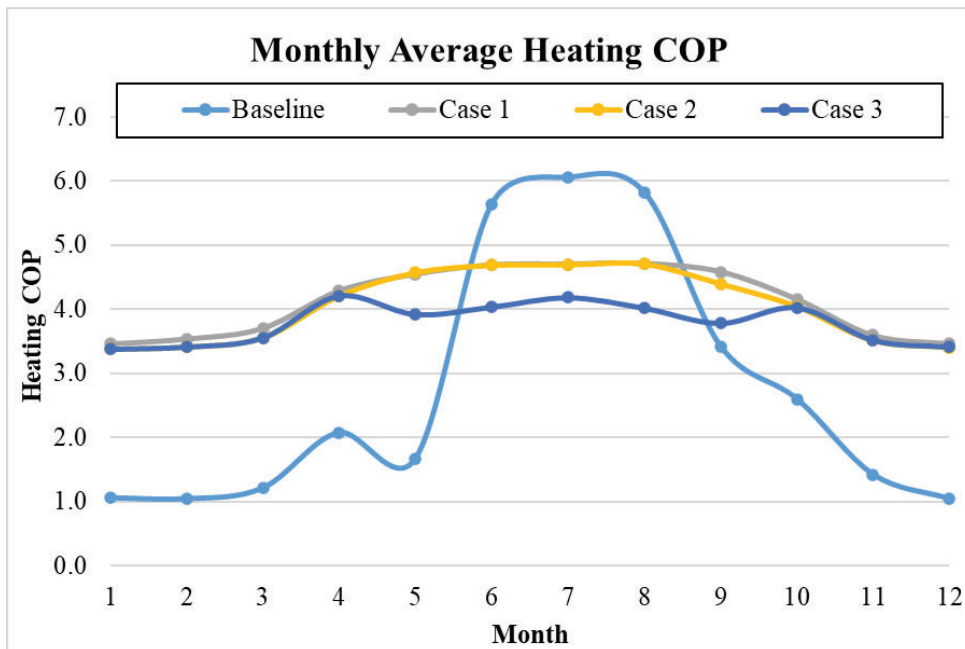


Fig. 6. Monthly average heating COP

Fig. 7 illustrates the monthly energy usage of the heat pump system across various cases. As indicated, Cases 1, 2, and 3 demonstrate significant energy savings compared to the baseline system. The annual energy savings for these cases is approximately 60%, highlighting the energy-saving potential of the hybrid heat pump system over a conventional air source heat pump system in cold climates.

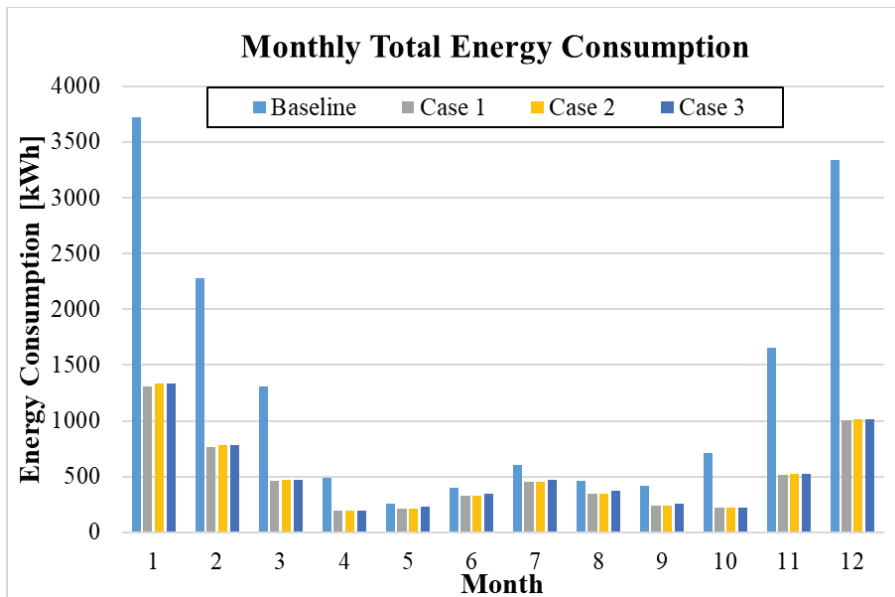


Fig. 7. Monthly energy consumption

For a new system design, there might be two somewhat separated ground loops rather than just one. In this case, it is possible to have preconditioning such that one region underground is warmer than the deep earth temperature in the winter and the other region is colder than the deep earth temperature in the summer. Geothermal heat pump proponents generally claim that their systems are the most efficient heating and cooling systems in the world because of a very stable temperature from the deep earth. With two ground loops and preconditioning, it is possible to have source temperatures even better than stable by providing more desirable temperatures for heating or cooling from the two distinct underground regions. A dual-loop system with preconditioning is shown in Fig. 8.

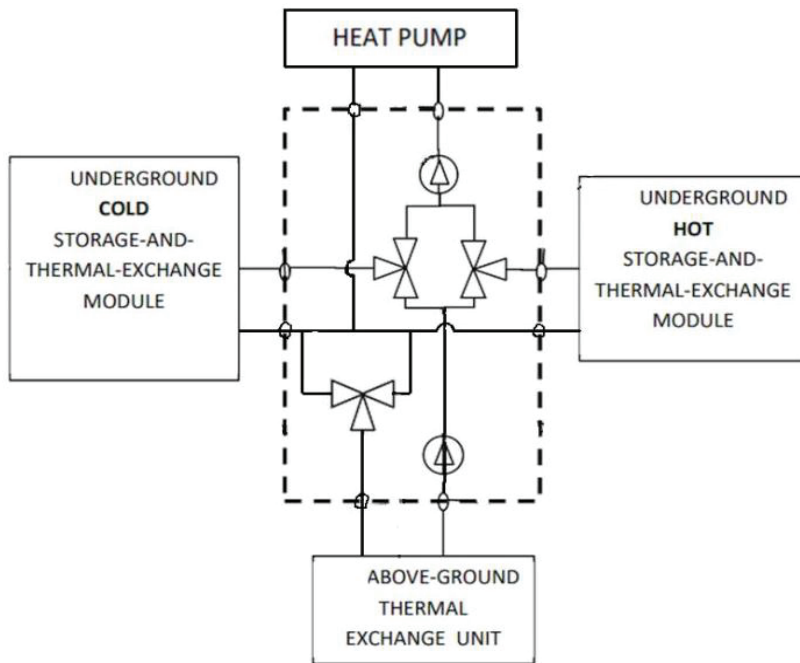


Fig. 8. Multi-source system with two ground loops (Olson & Yu, 2020).

A more complete description of the block diagram of Fig. 8 can be found in U.S. Patent 11105568. It is assumed that the system will have multiple temperature sensors and computer control to automatically change valve settings and pump speeds to give the optimum result for long-term efficiency in operation (optimum heating and cooling and minimum electricity use). Here are the most essential operating modes based on outdoor air temperature, assuming that there is a significant need for both heating and cooling over a full year:

1. At very low air temperatures, the system preconditions by transferring cold from the ambient air to the underground cold region, while simultaneously utilizing the hot region for space heating via the heat pump.

2. When the temperature from the aboveground unit (e.g., STCs) is close to the hot region temperature, the heat pump may use water from both sources simultaneously (parallel mode).

3. When the aboveground unit has a temperature higher than either of the underground regions and there is a need for heating, the heat pump source water will be from the aboveground unit.

There are also three modes similar to those above for cooling where, at the highest air temperatures, there is preconditioning into the underground hot region while the cold region provides cold water for the heat pump. If this water temperature is lower than 50°F, the heat pump might be used in a bypass or economizer mode for cooling so that power for a compressor is not needed and system efficiency will be very high.

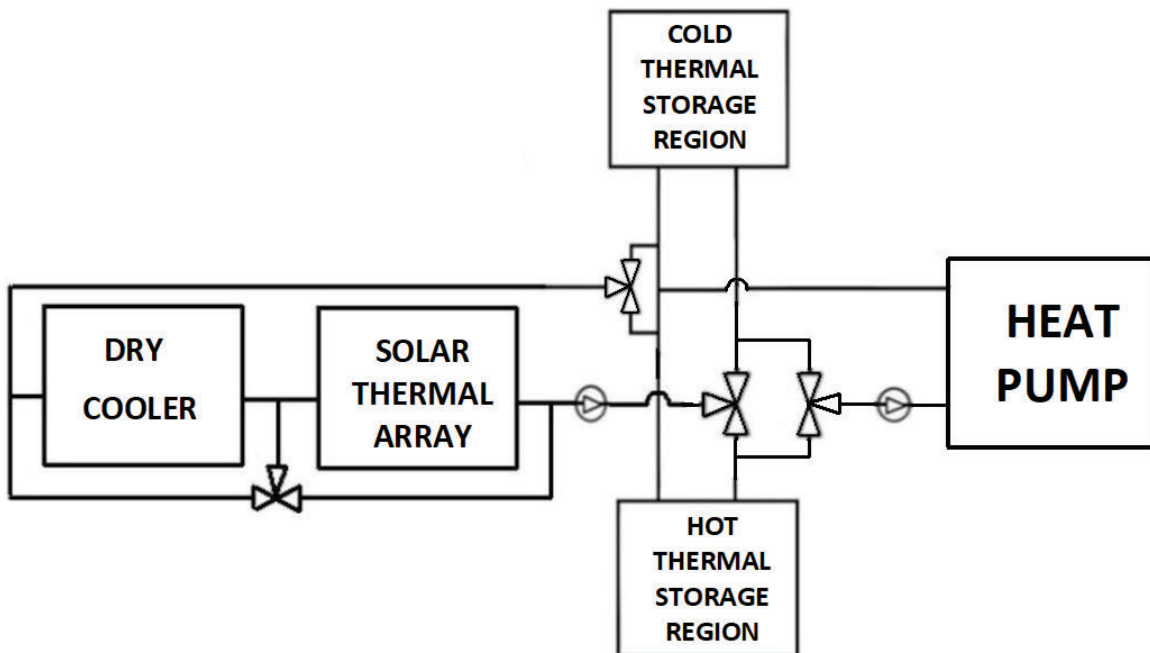


Fig. 9. Multi-source system with higher-temperature solar thermal collection

The system of Fig. 8 is well suited for any climate region. However, for a cold-climate region, there is another option that uses one additional three-way valve but can take advantage of higher-temperature versions of STCs. This configuration is shown in Fig. 9.

Although Fig. 9 shows the use of a dry cooler, this could just as well be an array of unglazed solar or PVT collector types. The solar thermal array in Fig. 9 could be a glazed flat-plate type or any of the vacuum-insulated types. For collection of heat on a sunny but cold day, the leftmost valve can bypass water around the dry cooler, and for preconditioning with very cold air, the solar thermal array can be bypassed.

Although all of the block diagrams above show the use of just a single heat pump, this could instead be multiple heat pumps and/or water-cooled chillers. For thermal energy networks, where natural gas pipes are being replaced with continuous-flow water pipes, it is possible that the systems above could be more cost-effective than the exclusive use of borehole heat exchangers, which is the current practice.

If there is a need for underground seasonal thermal storage (six months) and on a large enough scale, the best model in North America is at Drake Landing Solar Community in Canada (Drake Landing Solar Community).

The Drake Landing borehole array is designed specifically for thermal storage, not geexchange. Here are some differences:

1. The spacing between boreholes is 7 feet, which is about 1/3 that of conventional geexchange systems.
2. The borehole depth is 115 feet, which is about 1/5 of the typical geexchange depth.
3. The water-circulation path is designed for the hottest region to be always at the center, not at the perimeter.

This design allows for the seasonal thermal efficiency to be as high as 50 percent (ratio of thermal output to thermal input). Widely spaced boreholes will never be close to that efficiency.

The water used for thermal transfer at Drake Landing can have a temperature as high as 175°F, which requires the use of PEX pipe rather than the more common HDPE type. If even higher temperatures are desired, a special version of PEX might be considered that allows temperatures in the 230°F range (trade name Pexgol).

For many solar thermal applications, a buffer water tank is used to allow for an optimization of flow rate and temperature from the (highly intermittent) solar collector output to the underground storage or the end-use equipment (heat pumps or fan coils). The Drake Landing system uses two buffer tanks for this purpose.

### **Conclusion**

In conclusion, using STCs in multi-source heat pump systems can significantly improve building heating and cooling efficiencies. By using various types of collectors like glazed and unglazed flat plates, PVT systems, and evacuated tubes, these hybrid systems can effectively harness solar energy and optimize thermal storage for both heating and cooling. The flexibility in design and the ability to adapt to different climate conditions make these systems versatile. This approach not only significantly improves energy efficiency but also contributes to reducing greenhouse gas emissions, aligning with environmental sustainability goals. The future of building climate control could see a shift towards these innovative, multi-source systems, leveraging renewable energy sources to create more cost-effective, efficient, and environmentally friendly solutions.

**Conflict of Interest**

There are no conflicts of interest regarding the publication of this paper.

## References

- Chen, Y., Wang, J., Ma, C., & Shi, G. (2019). Multicriteria performance investigations of a hybrid ground source heat pump system integrated with concentrated photovoltaic thermal solar collectors. *Energy Conversion and Management*, 197, 111862. <https://doi.org/10.1016/J.ENCONMAN.2019.111862>
- Drake Landing Solar Community. Retrieved February 28, 2024, from <https://www.dlsc.ca/>
- Emmi, G., Tisato, C., Zarrella, A., & De Carli, M. (2016). Multi-source heat pump coupled with a photovoltaic thermal (PVT) hybrid solar collectors technology: a case study in residential application. *International Journal of Energy Production and Management*, 1(4), 382–392. <https://doi.org/10.2495/EQ-V1-N4-382-392>
- Han, Z., Qu, L., Ma, X., Song, X., & Ma, C. (2017). Simulation of a multi-source hybrid heat pump system with seasonal thermal storage in cold regions. *Applied Thermal Engineering*, 116, 292–302. <https://doi.org/10.1016/J.APPLTHERMALENG.2017.01.057>
- Kjellsson, E., Hellström, G., & Perers, B. (2010). Optimization of systems with the combination of ground-source heat pump and solar collectors in dwellings. *Energy*, 35(6), 2667–2673. <https://doi.org/10.1016/J.ENERGY.2009.04.011>
- Olson, G., & Yu, Y. (2016). *Solar thermal collection with seasonal storage*. <http://www.seasonalstoragetech.com/papers/ASES%20Paper%20-%20Final%20June%202030.pdf>
- Olson, G., & Yu, Y. (2017). *Optimized design of solar/air collection and storage systems for HVAC*. <http://www.sstusa.net/papers/Optimized%20Design%20of%20Solar%20or%20Air%20Collection%20and%20Storage%20Systems%20for%20%20HVAC.pdf>



Olson, G., & Yu, Y. (2020). *New ways to combine solar thermal with geothermal*.

<https://doi.org/10.18086/solar.2020.01.06>

TRNSYS 18. Retrieved February 28, 2024, from <https://www.trnsys.com/>

**An Approach Characterizing the Performance Degradation of a 140 kW Solar Panel in WV**

R. Subnom<sup>1\*</sup>  
B. Gopalakrishnan<sup>1</sup>  
S. Qiu<sup>1</sup>  
D. Johnson<sup>1</sup>  
H. Li<sup>1</sup>

<sup>1</sup>West Virginia University, Morgantown, West Virginia

[\\*rs00081@mix.wvu.edu](mailto:rs00081@mix.wvu.edu)

## Abstract

The research presents a methodology for evaluating the degradation of a 140-kW photovoltaic (PV) solar panel system's performance in Morgantown, WV. It assumes that panel's productivity depends on the solar energy received and the panel efficiency. To account for daily energy variations, daily electricity production was corrected to the average of the theoretical solar energy received in that month. The maximum of the corrected daily production data was considered the best performance of that month. These monthly best performances were averaged to represent the panel's yearly performance and used to assess the performance degradation. The results show that the yearly average performance of this panel decreased by 2.28% from 2013 to 2016 and then the degradation is 0.17% from 2017 to 2023. This methodology is also based on the assumption that there is at least one sunny day each month, which may not always be correct but is likely to occur.

Keywords: PV module, performance degradation, weather, electricity generation

## Introduction

In recent decades, renewable energy sources such as solar, wind, hydropower, and geothermal energy have rapidly been improved and deployed in response to global warming. Solar is largely unintrusive, and unlike the other main renewable sources, it can be feasibly installed at smaller non-industrial scales (Sobri et al., 2018).

Typically, a standard PV module has an optimal efficiency of about 10% to 23%, with the rest of the solar energy being either reflected to the environment or converted into heat (Musthafa, 2014). Environmental parameters responsible for the declining performance of a PV module are solar radiation, dust, soiling, atmospheric temperature, wind velocity, shading, precipitation, and humidity. The presence of dust in the air can decrease PV efficiency by up to 60% (Santhakumari & Sagar, 2019). Natural or artificial shades lower the power output of PV panels. High relative humidity leads to the accumulation of minuscule water droplets and water vapor on solar panels. This reduces the amount of solar radiation reaching the solar panel, lowering electricity production. Additionally, PV construction factors, installation factors, operation, and maintenance also affect the degradation rate of solar panel yearly performance (Hasan et al., 2022). There are numerous failure modes triggered by different environmental factors, including module delamination, hotspot failure, corrosion, glass breakage, anti-reflection coating (ARC) damage, electro-migration in the contact layers and interconnect, discoloration, and others (Kumar & Kumar, 2017).

The degradation rate of solar panels can be examined each year by experimentally measuring the efficiency of solar panels, which is a time-consuming process. A comprehensive 10-year analysis of the degradation rates of PV systems at six different sites, three located within the United Kingdom and three in Australia, was evaluated

using a year-on-year (YOY) degradation technique by Dhimish et al. (Dhimish & Alrashidi, 2020). The research team found that the PV system in the UK displayed degradation rates ranging from 1.05% to 1.16% per year. On the other hand, their counterparts in Australia found higher degradation rates within the range of 1.35% to 1.46% per year.

The energy loss and performance degradation of a 200-kW roof-integrated crystalline PV system installed at IRB Complex-5, Chandigarh, India was studied by the Kumar research group using the PVsyst simulation tool (Kumar et al., 2019). The estimated degradation rate of the PV system would lie between 0.6 and 5% per year under local weather conditions. The yearly capacity factor, performance ratio, and energy losses are 16.72%, 77.27%, and 26.5%, respectively.

Another study showed that the thin-film PV technology exhibits a significantly lower yearly degradation rate, nearly 0.1% compared to polycrystalline technology within the range of 0.67% to 0.83% after 2.5 years of outdoor exposure (Dag & Buker, 2020).

In a degradation study conducted in the semi-arid climate on a 1-MW PV system for four years, the system efficiency and performance ratio were found to be 11% and 76.46%, respectively (Kumar & Malvoni, 2019).

Sangpongsanont et al. examined the degradation rate of 16 poly-Si PV modules in outdoor conditions for 15 years in Thailand (Sangpongsanont et al., 2020). The average degradation rate was found to be 1.47%/year.

Kazem et al. published a literature on the aging measurements of a grid-tied 1.4-kW solar PV plant located in Oman for a period of seven months (Kazem et al., 2020). They reported that aging decreased the system efficiency by 6.3% and the production rate to 5.9%. In a 1-MWp solar PV power plant in Andhra Pradesh, India, Navothna et al. investigated the performance, degradation rate, and power and energy losses (Navothna & Thotakura, 2022). There are several forecasting methods that can predict the performance degradation rate of PV solar panel performance. Most forecasting techniques use artificial neural network and deep neural network models (Ahmed et al., 2020).

Finally, the references in the existing literature describing degradation analysis in the United States are very limited. In this study, a new methodology is proposed for estimating the performance degradation rate of an existing solar array installed at Mountain Line Transit Authority (MLTA), located in Morgantown, WV. The research team used this solar power plant project to examine the average solar power plant performance degradation rate.

However, as years of data on solar panel performance and radiant solar energy received is required to evaluate degradation in the performance of solar panels, it is

## Performance Degradation of a 140-kW Solar Panel

impossible to calculate the efficiency of a solar panel at a given time unless data on how much solar energy reached the panel at this time is available.

### System Description

The 140-kW PV solar panel system was installed and commissioned on June 12, 2012. MLTA was awarded \$1.1 million to fund a solar power plant project in 2010. The PV modules are situated in 39°6 N and 79.8° W. A 140-kW solar panel array consisting of 572-piece 245-W polycrystalline PV modules was installed on the roof of MLTA's Morgantown maintenance and administrative facility. One 135-kW inverter is used in the system to convert the DC power input from the PV array to AC power. The datalogger collects the real-time performance information from the inverter and sends this information via internet to the performance monitoring software. The system tilt angle is 12.0 degrees and azimuth angle is 210 degrees.

### System Performance

While a general trend over the year can be observed from month to month, the amount of energy generated each day varies substantially due to dramatic variations in local weather conditions. Solar extraterrestrial radiation reaching the top of the atmosphere for each year is calculated using an online calculator provided by Santa Clara University (Calculation of Extraterrestrial Solar Radiation). The online calculator uses Eq. 1 from Duffie and Beckman to calculate the solar extraterrestrial radiation (Duffie & Beckman, 2013). Daily extraterrestrial radiation on a horizontal surface in the absence of the atmosphere,  $H$  in a particular location can be calculated by:

$$(1) H = \frac{24 \times 3600 G_{sc}}{\pi} \left( 1 + 0.033 \cos \frac{360n}{365} \right) x \left( \cos \phi \cos \delta \sin \omega + \frac{\pi \omega}{180} \sin \phi \sin \delta \right)$$

$G_{sc}$  is the solar constant, 1,367 W/m<sup>2</sup>,  $\omega$  is the sunset hour angle in degrees,  $\phi$  is the latitude of the location,  $\delta$  is the solar declination angle, and  $n$  is the  $n^{\text{th}}$  day of the year. We can also use the following equations for this calculation:

$$\text{Solar declination angle, } \delta = 23.45 \sin\left(360 \frac{284+n}{365}\right)$$

$$\text{Sunset hour angle, } \omega = \cos^{-1}[-\tan(\delta)\tan(\phi)]$$

The daily power production and solar irradiation of the study location from January 2023 to December 2023 are presented in Figure 1.

## Performance Degradation of a 140-kW Solar Panel

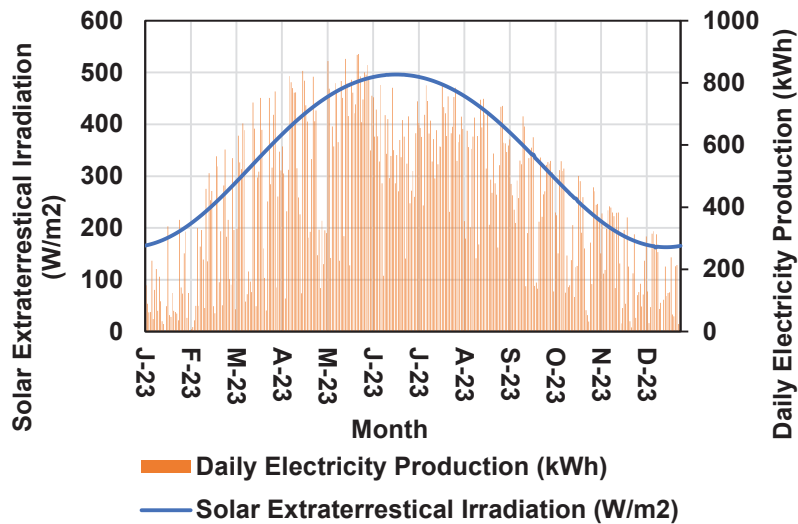


Fig. 1. Daily electricity production and solar extraterrestrial irradiation

Figure 2 shows the yearly production of electricity from 2012 to 2023. This solar power plant was installed in June 2012, so the yearly production data of this system in 2012 was low. As shown in Figure 2, the electricity produced in 2020–2023 was much higher than that in 2018 and 2019. The yearly electricity production cannot be used as a criterion for evaluating the degradation of solar panel performance.

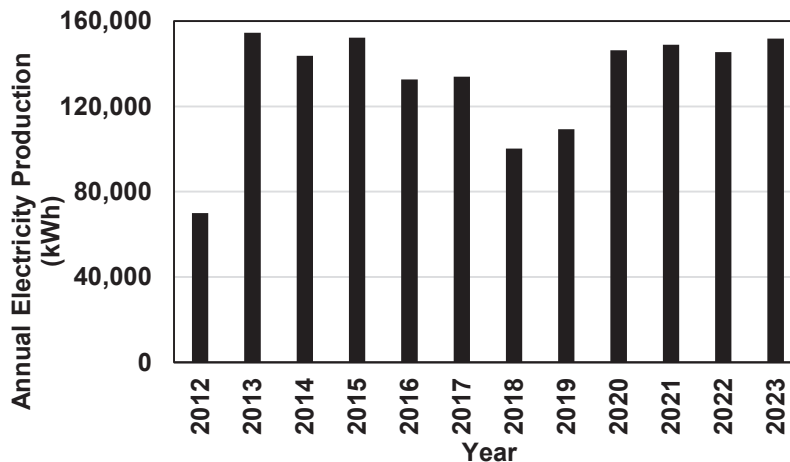


Fig. 2. Annual electricity produced from 2013 to 2023

Figure 3 shows the variation of the maximum daily electricity produced in each month of 2022, 2020, 2018, 2016, 2014, and 2012. The highest maximum electricity production was observed in July 2012 (in the 1<sup>st</sup> year). However, the maximum daily production data did not always decrease with additional years of service. For example, the maximum daily electricity produced in May 2016 is 4.14% lower in average than in May

## Performance Degradation of a 140-kW Solar Panel

2018, May 2020, and May 2022. The maximum daily electricity production in October 2018 is 5.22% lower in average than October 2020 and 2022.

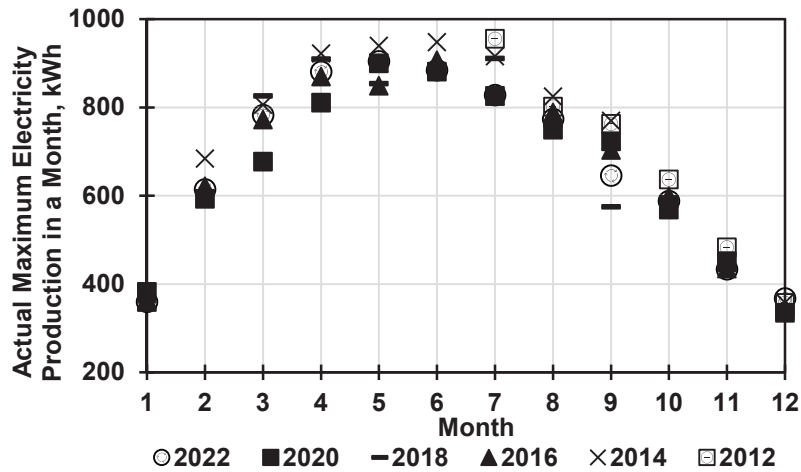


Fig. 3. Actual maximum daily electricity production in each month in 2022, 2020, 2018, 2016, 2014 and 2012

Figure 4 shows the maximum daily solar power production in each month of 2012–2023. This figure shows that there is no firm trend in degradation of power production capacity in each year from 2012–2023.

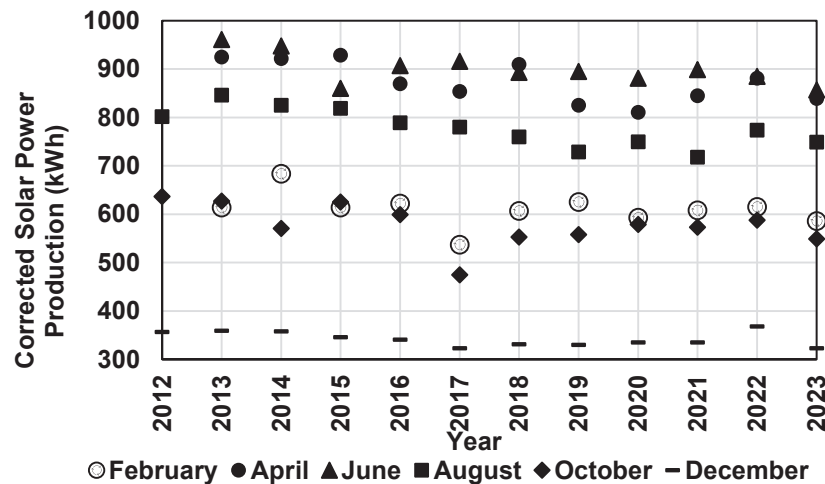


Fig. 4. The maximum actual daily production observed in specific months from 2012–2023

It is concluded that solar panel performance degradation cannot be evaluated using the actual solar panel production data without considering weather contributions. This gives us the opportunity to develop a new methodology to characterize the degradation of solar panel performance using solar panel production data.



## Methodology

This research developed a methodology to assess the degradation of solar panel performance with time using the daily solar panel productivity data. This methodology assumes that electricity produced by a solar panel is affected by the solar panel efficiency and the solar energy received.

This method also assumes that there is at least one perfectly sunny day each month on which the daily electricity produced is the maximum possible electricity produced in that day. However, the amount of solar energy received each day in a month is different, so that affects the electricity production. The difference in electricity production can be corrected using a standard reference such as average extraterrestrial irradiance each month. In this research, the power produced each day of a month is corrected using the average irradiance energy received monthly as a reference. This is defined as correction-factor-corrected electricity production  $E_{i, corrected}$ , calculated using the following equation:

$$E_{i, corrected} = \frac{E_{i, actual} \times I_{Average}}{I_i}$$

Where,  $E_{i, actual}$ , Actual electricity produced in  $i^{\text{th}}$  day of the month, kWh

$I_{Average}$ , Average daily irradiation in the month,  $\frac{W}{m^2}$

$I_i$ , Extraterrestrial irradiation on the  $i^{\text{th}}$  day,  $\frac{W}{m^2}$

## Results and Discussion

Figure 5 shows the actual and corrected daily electricity produced using the average irradiation received in October 2022. The maximum actual daily electricity production is 588 kWh, which was observed on October 9<sup>th</sup>, 2022.

The corrected electricity produced on October 9<sup>th</sup> was 549 kWh. In comparison, the maximum corrected daily production observed was 571 kWh, which was observed on October 20<sup>th</sup>, 2022. The actual electricity produced on October 20<sup>th</sup> was 546 kWh, which was lower than the actual electricity of 588 kWh observed on October 9<sup>th</sup>. The day with the maximum corrected power production observed may not be the same day on which the maximum actual production was observed.

## Performance Degradation of a 140-kW Solar Panel

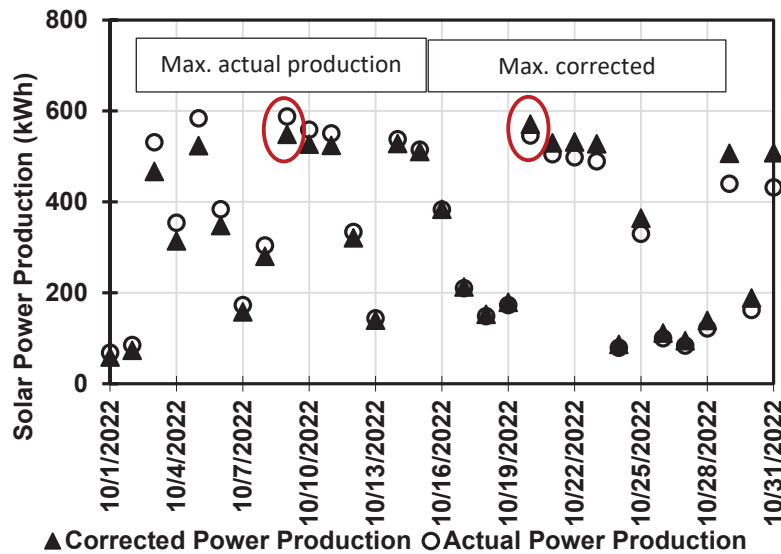


Fig. 5. The actual and corrected daily electricity produced in October 2022

Figure 6 shows the average of the maximum corrected daily production in each month from 2013 to 2023. The solar panel performance represented by the average of the maximum corrected daily production in each month was found to decrease rapidly from 2013 to 2016. The averages of the maximum corrected daily production observed in 2013 and 2016 were 706 kWh and 659 kWh respectively. The average yearly degradation from 2013 to 2016 was 2.28%. In comparison, the degradation of the averaged maximum corrected daily production in each year observed from 2016 to 2023 was very mild (0.17%). The average of the averaged maximum corrected daily production observed in each month from 2017 to 2023 was 658.8 kWh, which was comparable to the 659 kWh observed in 2016.

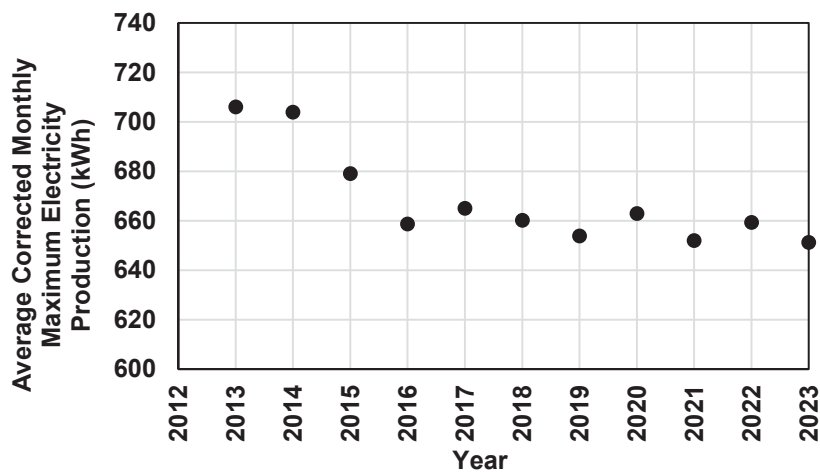


Fig. 6. The average of the maximum corrected daily production in each month from 2013 to 2023

### Conclusion

This research developed a methodology assessing the degradation of solar panel performance using daily electricity production data. The performance of the solar panel was evaluated by examining the maximum corrected daily electricity production data using the average of the irradiation of that month as a reference. The average of the maximum corrected daily production data found in each month of a year was used to represent the best performance of the solar panel in that year and used to assess the degradation rate of this solar panel array. This method was applied to assess the performance degradation of a 140-kW solar panel array installed in Morgantown, WV. The key findings are the following:

- Neither the actual yearly production nor the monthly electricity production of this solar panel array can be used to assess its degradation due to the significant variation in weather from year to year.
- From 2013 to 2016, the average yearly degradation of this solar panel system is 2.28%. In comparison, the average yearly degradation of this panel from 2017 to 2023 was comparatively mild (0.17%).

It should be noted that this methodology can only be applied to solar panels installed in areas where air quality is relatively stable. In the future, the effect of ambient temperature on solar panel performance should also be evaluated. The research team will continue to work on this methodology and further improve it to make it more accurate and viable.

## References

Ahmed, R., Sreeram, V., Mishra, Y., & Arif, M. D. (2020). A review and evaluation of the state-of-the-art in PV solar power forecasting: Techniques and optimization.

*Renewable and Sustainable Energy Reviews*, 124, 109792.

<https://doi.org/10.1016/j.rser.2020.109792>

*Calculation of extraterrestrial solar radiation*. Retrieved February 22, 2024, from

[https://www.engr.scu.edu/~emaurer/tools/calc\\_solar\\_cqi.pl](https://www.engr.scu.edu/~emaurer/tools/calc_solar_cqi.pl)

Dag, H. I., & Buker, M. S. (2020). Performance evaluation and degradation assessment of crystalline silicon based photovoltaic rooftop technologies under outdoor conditions. *Renewable Energy*, 156, 1292–1300.

<https://doi.org/10.1016/j.renene.2019.11.141>

Dhimish, M., & Alrashidi, A. (2020). Photovoltaic degradation rate affected by different weather conditions: A case study based on PV systems in the UK and Australia.

*Electronics*, 9(4), 650. <https://doi.org/10.3390/electronics9040650>

Duffie, J. A., & William A. Beckman. (2013). *Solar engineering of thermal processes* (4th ed.). John Wiley & Sons.

Hasan, K., Yousuf, S. B., Tushar, M. S. H. K., Das, B. K., Das, P., & Islam, M. S. (2022). Effects of different environmental and operational factors on the PV performance: A comprehensive review. *Energy Science & Engineering*, 10(2), 656–675.

<https://doi.org/10.1002/ese3.1043>

Kazem, H. A., Chaichan, M. T., Al-Waeli, A. H. A., & Sopian, K. (2020). Evaluation of aging and performance of grid-connected photovoltaic system northern Oman: Seven years' experimental study. *Solar Energy*, 207, 1247–1258.

<https://doi.org/10.1016/j.solener.2020.07.061>

Kumar, M., & Kumar, A. (2017). Performance assessment and degradation analysis of solar photovoltaic technologies: A review. *Renewable and Sustainable Energy Reviews*, 78, 554–587. <https://doi.org/10.1016/j.rser.2017.04.083>

Kumar, N. M., Gupta, R. P., Mathew, M., Jayakumar, A., & Singh, N. K. (2019). Performance, energy loss, and degradation prediction of roof-integrated crystalline solar PV system installed in Northern India. *Case Studies in Thermal Engineering*, 13, 100409. <https://doi.org/10.1016/j.csite.2019.100409>

Kumar, N. M., & Malvoni, M. (2019). A preliminary study of the degradation of large-scale c-Si photovoltaic system under four years of operation in semi-arid climates. *Results in Physics*, 12, 1395–1397. <https://doi.org/10.1016/j.rinp.2019.01.032>

Lillo-Sánchez, L., López-Lara, G., Vera-Medina, J., Pérez-Aparicio, E., & Lillo-Bravo, I. (2021). Degradation analysis of photovoltaic modules after operating for 22 years. A case study with comparisons. *Solar Energy*, 222, 84–94. <https://doi.org/10.1016/j.solener.2021.04.026>

Musthafa, M. M. (2014). *Enhancing photoelectric conversion efficiency of solar panel by water cooling*. 199–204.

## Performance Degradation of a 140-kW Solar Panel

Navothna, B., & Thotakura, S. (2022). Analysis on large-scale solar PV plant energy performance–loss–degradation in coastal climates of India. *Frontiers in Energy Research*, 10. <https://doi.org/10.3389/fenrg.2022.857948>

Santhakumari, M., & Sagar, N. (2019). A review of the environmental factors degrading the performance of silicon wafer-based photovoltaic modules: Failure detection methods and essential mitigation techniques. *Renewable and Sustainable Energy Reviews*, 110, 83–100. <https://doi.org/10.1016/j.rser.2019.04.024>

Sangpongsonont, Y., Chenvidhya, D., Chuangchote, S., & Kirtikara, K. (2020). Corrosion growth of solar cells in modules after 15 years of operation. *Solar Energy*, 205, 409–431. <https://doi.org/10.1016/j.solener.2020.05.016>

Sobri, S., Koohi-Kamali, S., & Rahim, N. A. (2018). Solar photovoltaic generation forecasting methods: A review. *Energy Conversion and Management*, 156, 459–497. <https://doi.org/10.1016/j.enconman.2017.11.019>

*West Virginia enters new energy era with completion of solar site*. Retrieved February 22, 2024, from <https://www.lootpress.com/west-virginia-enters-new-energy-era-with-completion-of-solar-site/>

**Analyzing Optimal Renewable Energy Portfolio for Electricity Generation in  
Arizona and Texas with Lowest Carbon Emissions**

Rahim Khoie<sup>1</sup>

Department of Electrical and Computer Engineering

University of the Pacific

Stockton, CA

<sup>1</sup>Correspondence: [rkhoie@pacific.edu](mailto:rkhoie@pacific.edu)



**Abstract**

In this paper, we present an optimization algorithm for determining the wind-solar portfolio for electricity generation with minimum emissions in two specific locations in the U.S., Texas and Arizona. Our model assumes a 1% annual increase in electricity demand as well as a 12% increase in the population over the next 25 years. The difference between the 2050 electricity demand and existing generation by nuclear, water, solar, and wind (which is currently being generated from fossil fuels) will be replaced by a solar-wind portfolio which will result in the lowest emissions. Our results show that Maricopa County will achieve its lowest emissions per capita in 2050, when its renewable electricity is produced with 100% solar and 0% wind, which will result in 402 kg CO<sub>2</sub>/person. Amarillo will be able to reduce its per capita emissions to as low as 277 kg CO<sub>2</sub>/person with a renewable portfolio consisting of 100% wind and 0% solar.

Keywords: emission intensity of solar power, emission intensity of wind power, optimization of electricity generation by wind and solar energies, lowest renewable emissions

### 1. Introduction

In 2022, the world consumed 25,530 billion kWh of electricity, of which 4,070 billion kWh (about 15.9%) was used in the United States (Statista 2023a; U.S. EIA 2023). It has been projected that by 2050, U.S. electricity consumption will reach 5,178 billion kWh which is about a 27% increase in the next 27 years, roughly 1% per year. In the next three decades, the world's electricity demand is expected to increase at a much higher rate of 3% per year (Enerdata 2023; Statista 2023b). Furthermore, it is estimated that about two thirds of the world's electricity generation in 2050 will be from nuclear and renewables, with solar and wind showing the highest levels of growth (IER 2023). Unfortunately, these projections still leave about a 30% share of coal and natural gas in the world's electricity portfolio in 2050.

The U.S. National Oceanic and Atmospheric Administration (NOAA) indicated in its 2022 report that while emission-reduction strategies are required in all energy sectors, there is a growing interest in removing greenhouse gases already in the atmosphere (NOAA 2022). The report identifies 11 removal strategies including several biological methods of removing carbon from the oceans and the atmosphere (NOAA 2023). The continued use of coal and natural gas in the world's electricity generation through 2050 – during the 25-year transition period – flies in the face of NOAA's recommendation for carbon removal. Furthermore, as the world transitions to a massive amount of electricity generation by solar power and wind power in the next 25 years, the issue of the carbon footprint of these two renewable sources becomes increasingly more important.

The United States has truly abundant solar and wind resources, as shown in Figures 1 and 2, respectively. However, there are great variations in the amounts of these resources from one location to another. While the Southwest of the U.S. enjoys significant solar irradiance (solar peak hours in 6 to 7 kWh/m<sup>2</sup>/day, the Northeast of the U.S. receives about 4 kWh/m<sup>2</sup>/day of sun energy. Similarly, while the sustained average wind speeds of 9 to 10 m/s (at 30 meters above the surface) are abundant in the U.S. Midwest region, the sustained wind speeds in the Southeast of the U.S. are in the range of 4 to 5 m/s and (NREL 2018; NREL 2023).

We previously investigated the emission intensity of wind power generation in one of the sweet spots of wind energy in the U.S., the panhandle of Texas (Khoie 2021). Our results showed that a 1.3-MW Nordex windmill operating in Amarillo, Texas produced 14.45 g CO<sub>2</sub>/kWh. More recently, we developed an LCA model for analyzing the emissions of solar power generation in one of the sweet spots of solar energy in the U.S., Phoenix, Arizona (Khoie, 2024a). The results of our model showed that the emission intensity (total emissions in g CO<sub>2</sub>/lifetime generation in kWh) of solar power

# Renewable Energy for Electricity Generation in Arizona and Texas

generation was 27.41, 36.37, and 40.88 g CO<sub>2</sub>/kWh depending on whether the solar panels are manufactured in the U.S., Europe, or China.

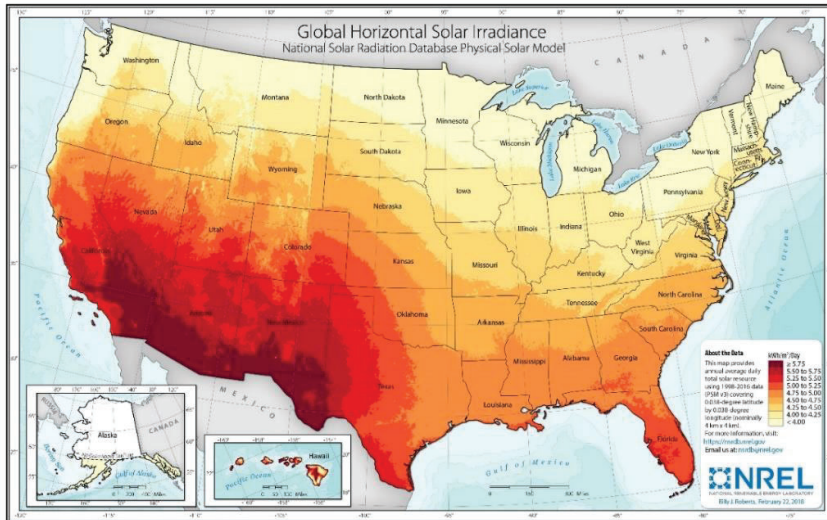


Fig. 1. The U.S. solar irradiance map (NREL 2018).

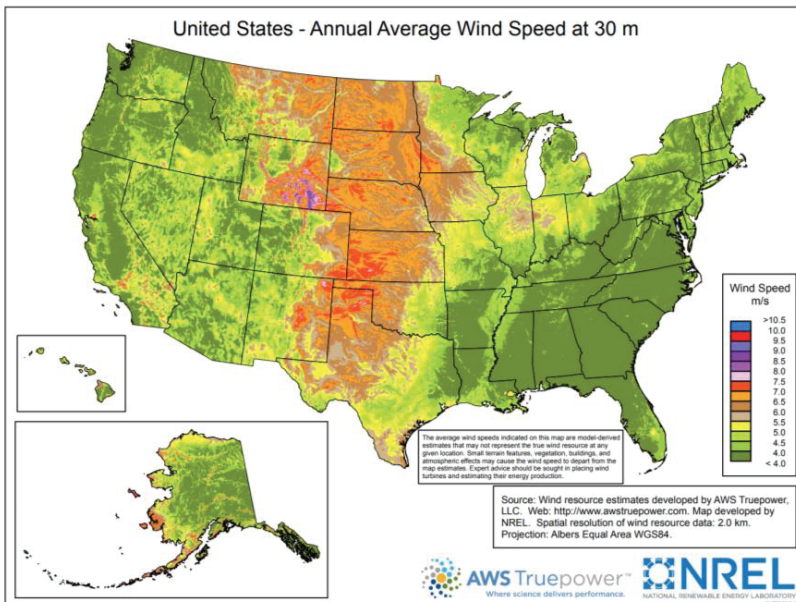


Fig. 2. The U.S. annual average wind speed at 30-meter elevation (U.S. EERE, 2024).

respectively. We have expanded our solar emissions model with additional details and the results are reported elsewhere (Khoie, 2024b).

## 2. Optimization Model

This paper aims to develop a model to produce strategies for the implementation of wind and solar power in various locations in the U.S. based on *local* variables as shown in Fig. 3 and as follows:

- (1) Determine the current and projected electricity need of the location.
- (2) Subtract the available existing renewable energy, nuclear energy, and hydropower.
- (3) Produce various solar-wind portfolios based on the amount of wind energy and solar irradiation available.
- (4) Determine the carbon emissions of each solar-wind portfolio using the emissions models we previously developed for solar and wind (Khoie, 2024b; Khoie, 2021).
- (5) Search for the optimal solar-wind portfolio for that location which results in lowest possible emissions.

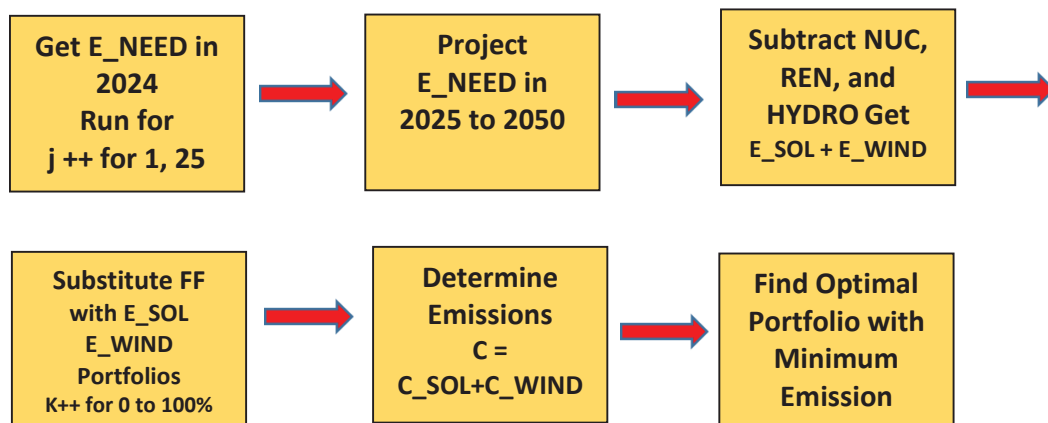


Fig. 3. Flow chart of the optimization model.

The optimal renewable electricity portfolio in 2050 is then determined as follows:

## Renewable Energy for Electricity Generation in Arizona and Texas

- Determine the population growth in 2050 by adding 12% to the current population (U.S. CBO, 2024):  $N_{pop-2050} = 1.12 * N_{pop-2024}$ .
- Start with current (2024) total annual generation and determine the electricity demand in 2050 by adding 1% per year:  $E_{total-gen-2050} = 1.25 * E_{total-gen-2024}$ .
- Determine the amount of current annual generation by renewables; add existing nuclear, water, solar, and wind generation from the total current generation:  
 $E_{renewable-gen-2024} = E_{nuclear-gen-2024} + E_{water-gen-2024} + E_{solar-gen-2024} + E_{wind-gen-2024}$ .
- Determine the amount of renewable generation needed in 2050; subtract the existing renewable generation from the total generation in 2050:  
 $E_{renewable-gen-2050} = E_{total-gen-2050} - E_{renewable-gen-2024}$ . This is the amount of renewable generation that is needed to be installed by 2050.
- Start with 0% solar and 100% wind combination and evaluate the emissions of the resulting renewable portfolio. Repeat this process 25 times, adding 4% solar while reducing wind by 4% each time.
- Determine the per capita emissions of each portfolio by dividing the total emissions of each portfolio (including the emissions of existing renewables in 2024) by the population in 2050:  $C_{per-capita-2050} = C_{total-2050}/N_{pop-2050}$
- Determine the portfolio that results in the lowest per capita emissions.

### 3. Results

The lifetime emissions of the 1.3-MW Nordex N-60 are 1,870 Mg CO<sub>2</sub>. With 161,808,798 kWh generated in its 25-year lifespan, the emission intensity of this windmill is 11.56 g CO<sub>2</sub>/kWh when operating in Amarillo, Texas (Khoie, 2021). However, this windmill has a significantly higher emission intensity of 77.59 g CO<sub>2</sub>/kWh when operating in Maricopa County due to a drop in average wind speed (from 9 m/s in Amarillo to 5.6 m/s in Maricopa). Using China’s electricity portfolio (which is close to those of Singapore’s, where the panels are made) the emission intensity of the REC Alpha Series 400-W panels (REC 2024) is 40.88 g CO<sub>2</sub>/kWh for Maricopa County, and 45.82 g CO<sub>2</sub>/kWh for Amarillo. The above data are tabulated in Table 1.

Table 1. Average wind speed and solar peak hours in Mariposa County, and Amarillo, along with emission intensities of wind, solar, and nuclear power generations in these locations

|   | Maricopa County, Arizona | Amarillo, Texas | Sources                           |
|---|--------------------------|-----------------|-----------------------------------|
| Average Wind Speed (m/s)                | 5.6                      | 9               | (U.S. EERE, 2024)<br>(NREL, 2023) |
| Wind Emissions (g CO <sub>2</sub> /kWh) | 77.59                    | 11.56           |                                   |

## Renewable Energy for Electricity Generation in Arizona and Texas

|   |       |       |             |
|---|-------|-------|-------------|
| Average Solar Peak Hours (kWh/m <sup>2</sup> /day)        | 6.5   | 5.8   | (NREL 2018) |
| China-Made Solar Panel Emissions (g CO <sub>2</sub> /kWh) | 40.88 | 45.82 |             |
| U.S.-Made Solar Panel Emissions (g CO <sub>2</sub> /kWh)  | 27.41 | 30.72 |             |
| Nuclear Emissions (g CO <sub>2</sub> /kWh)                | 12.0  | 12.0  | (WNA 2024)  |

With the emission intensities given in Table 1 and the current 2024 data on population, annual generation, fuel mix, and emissions of electricity generation from each fuel in Maricopa County and Amarillo, we run 25 simulations based on the algorithm described above. The results are shown in Fig. 4.

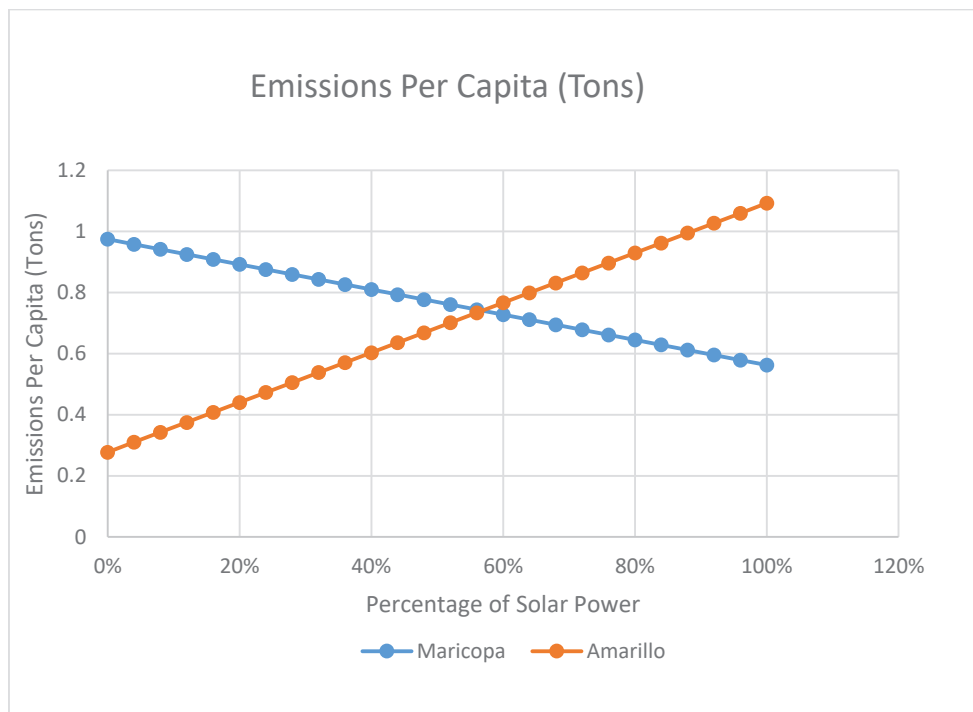


Fig. 4. The results of simulations for Maricopa County and Amarillo. The horizontal axis is the percentage of solar power in the portfolio.

Figure 4 shows that for Maricopa County, a 0% solar–100% wind portfolio results in 975 kg CO<sub>2</sub>/person/year, whereas a 100% solar–0% wind portfolio produces 563 kg CO<sub>2</sub>/person/year. This is because while solar peak hours in Maricopa County are 6.5

## Renewable Energy for Electricity Generation in Arizona and Texas

kWh/m<sup>2</sup>/day (near ideal condition), the average wind speed is only 5.6 m/s, which is rather low for the massive amount of wind power generation.

In contrast, for Amarillo, a 0% solar–100% wind portfolio has significantly less emissions, 277 kg CO<sub>2</sub>/person/year, compared to 1093 kg CO<sub>2</sub>/person/year for a 100% solar–0% wind portfolio. Again, this is because wind speed of 9 m/s makes Amarillo an ideal location for wind power generation.

It should be noted that although available solar peak hour in Amarillo is 5.8 kWh/m<sup>2</sup>/day which is much higher than many locations in the U.S., but there is no combination of solar-wind generation that will result in lower emissions than the 0% solar–100% wind combination.

Table 2 lists the details of the results of our optimization model for Maricopa County and Amarillo. In this table, we list the population, annual generation, and emissions for these two locations in the year 2050, and for comparison, we also list the 2024 data.

Table 2: Population, annual generation, and emissions of Maricopa County and Amarillo in the years 2024 (current portfolio including fossil fuels) and 2050 (optimal portfolio without fossil fuels)

|  | Maricopa County, Arizona in 2024 | Maricopa County, Arizona in 2050 | Amarillo Texas in 2024 | Amarillo Texas in 2050 |
|--|----------------------------------|----------------------------------|------------------------|------------------------|
| Population (12% increase by 2050) (U.S. CBO 2024)            | 4,950,000                        | 5,544,000                        | 202,000                | 226,240                |
| Total Annual Generation (GWh) (1% annual increase thru 2050) | 80,076                           | 100,896                          | 4,305                  | 5,424                  |
| Annual Generation Per Capita (kWh/person)                    | 16,176                           | 18,199                           | 21,287                 | 23,974                 |
| Annual Generation from Coal (GWh)                            | 0                                | 0                                | 3,490                  | 0                      |
| Annual Generation from Natural Gas (GWh)                     | 41,360                           | 0                                | 775                    | 0                      |
| Annual Generation from Other Fossil Fuels (GWh)              | 20                               | 0                                | 0                      | 0                      |
| Total Annual Generation from Fossil Fuels (GWh)              | 41,380                           | 0                                | 4,265                  | 0                      |
| Total Annual   | 18,220,000                       | 0                                | 3,984,560              | 0                      |



## Renewable Energy for Electricity Generation in Arizona and Texas

|   |            |           |           |        |
|---|------------|-----------|-----------|--------|
| Emissions from Fossil Fuels (Tons)                              |            |           |           |        |
| Annual Generation from Nuclear (GWh)                            | 34,510     | 34,510    | 0         | 0      |
| Annual Generation from Water (GWh)                              | 286        | 286       | 0         | 0      |
| Annual Generation from Wind (GWh)                               | 0          | 0         | 40        | 5,424  |
| Annual Generation from Solar (GWh)                              | 3,900      | 66,100    | 0         | 0      |
| Total Annual Generation from Renewables + Water + Nuclear (GWh) | 38,696     | 100,896   | 40        | 5,424  |
| Total Annual Emissions from Renewables + Water + Nuclear (Tons) | 576,984    | 3,119,710 | 462       | 62,705 |
| Total All Emissions (Tons)                                      | 18,796,984 | 3,119,710 | 3,985,022 | 62,705 |
| Annual Emissions Per Capita (Tons/person)                       | 3.80       | 0.563     | 19.73     | 0.277  |
| % Reduction in Per Capita Emissions                             |            | 85.2%     |           | 98.6%  |

The highlights of the results shown in Table 2 are:

- Amarillo, with 19.73 tons/person/year in 2024, has very high per capita emissions, due to its heavy reliance on coal power generation without any nuclear or hydropower generation and its minimal use of wind power (40 GWh of wind).
- Maricopa County, with 3.80 tons/person/year in 2024 has significantly lower per capita emissions in 2024 because of its reliance on nuclear power (34,510 GWh) and solar power (3,900 GWh).
- Amarillo’s optimal electricity portfolio in 2050 will be 100% wind power, which will result in per capita emissions of only 277 kg CO<sub>2</sub>/person/year. This is a significant drop (98.6%) in its emission from 2024 levels which is entirely due to the low emission intensity of wind in Amarillo, one of the sweet spots of wind energy in the U.S.
- Maricopa County’s optimal electricity in 2050 would be a mix of nuclear power (34,510 GWh) and solar power (66,100 GWh) which gives it 563 kg-CO<sub>2</sub>/person/year per capita in emissions. Although this would be a significant drop of 85.2% from its 2024 levels, it would remain much higher than that of



## Renewable Energy for Electricity Generation in Arizona and Texas

Amarillo. This is due to the relatively high emission intensity of solar power generation in Maricopa County although it is an ideal location for solar energy.

### 4. Conclusion

The choice of the two locations for this study, Maricopa County and Amarillo, was made based on their contrasting solar and wind potentials. This choice resulted in each location having either 100% solar or 100% wind as its optimal renewable portfolio. Our results show that electricity generation with lowest possible emissions requires consideration of (1) emission intensities of solar and wind power generation based on the fuel mix used at the manufacturing site, (2) emission intensities of solar and wind power at the generation site, and (3) the availability of solar and wind resources at the generation site. For Amarillo, Texas, a sweet spot for wind power generation, the lowest renewable emissions are achieved by using 100% wind power in its 2050 renewable electricity portfolio, whereas for Maricopa County, a sweet spot for solar power generation, 100% solar power results in lowest emissions. While these results were expected, our model establishes the validity of such expectations.

Another important takeaway from our results is that for locations with high percentages of solar power in their renewable electricity portfolios, solar panels that are made in the U.S. will have significantly lower emissions, as shown in Figure 5. Solar panels made in China have 563 kg/person emissions, while solar panels made in the U.S. produce 402 kg/person, a 29% decrease in per capita emissions.

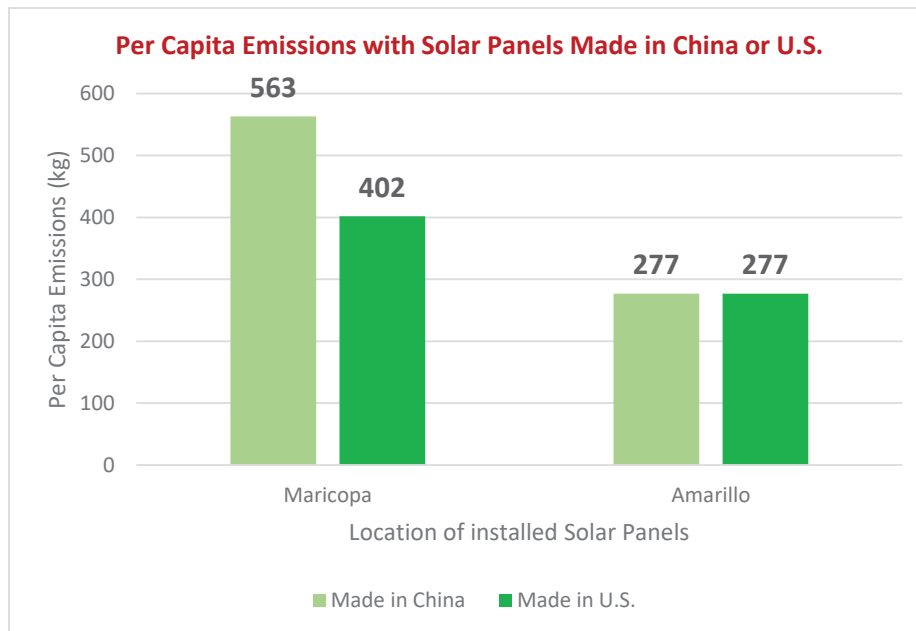


Fig. 5. For locations such as Maricopa County, Arizona, installing U.S. made solar panels reduces per capita emissions by 29 percent.

### *5. Limitations of Our Models and Future Refinements*

For limitations of our models for emission intensities of solar power generation see Khoie (2024a). For wind power generation see Khoie (2021). Additional limitations of the model presented here are:

- (1) The small difference in contribution of emissions due to land transportation of the solar panels to the two locations was ignored.
- (2) In calculating the population of each location in 2050, we used the 12% projected population growth of the U.S. and ignored local variations as well as possible migration among various locations (U.S. CBO, 2024).
- (3) Using a 1.3-MW windmill to power 260 homes (average of 5 kW per home) requires power distribution systems which will result not only in losses but also create additional emissions of the parts and components of the system. Our model does not take these into account.
- (4) The solar power generation used in our model is based on rooftop installation of 400-W panels. Studies have shown that the emissions can be reduced using utility-scale solar power generation.

Our future work will include incorporating the above in our emission models to more accurately determine the optimal portfolios for these and other locations throughout the U.S. (Khoie, 2024c).

### **Conflict of Interest**

This work was supported in part by grants from School of Engineering and Computer Science of the University of the Pacific through a research center; “Carbon Capture Center for Mitigating Climate Change Crisis ~ C<sup>3</sup>FMC<sup>3</sup>. We have not received any support, financial or otherwise, from any public or private organizations.

## References

Enerdata (2023). *Total electricity generation projections*.

<https://eneroutlook.enerdata.net/total-electricity-generation-projections.html>

IEA (2022). *Solar PV global supply chains*. <https://www.iea.org/reports/solar-pv-global-supply-chains/executive-summary>.

IER (2023). *EIA expects global energy consumption to increase through 2050*.

<https://www.instituteforenergyresearch.org/international-issues/eia-expects-global-energy-consumption-to-increase-through-2050/>

Khoie, R., Bose, A., & Saltsman, J. (2021). A study of carbon emissions and energy consumption of wind power generation in the panhandle of Texas. *Clean Technologies and Environmental Policy*, 23, pp. 653-667, 2021.

Khoie, R. & Mueller, D. (2024a). A study of carbon emissions and energy consumption of solar power generation in Phoenix, Arizona. Proceedings of the American Solar Energy Society 53<sup>rd</sup> National Solar Conference, Washington, DC.

Khoie, R., and Mueller, D. (2024b). A comprehensive study of carbon footprint of solar power generation from raw materials to operation and maintenance in various locations in the United States. To be submitted to *Clean Technology and Environmental Policy*.

Khoie, R. (2024c). Analyzing optimal renewable energy portfolio for electricity generation in the United States through 2050 with the lowest possible carbon

## Renewable Energy for Electricity Generation in Arizona and Texas

emissions. To be submitted to *Clean Technology and Environmental Policy*.

NOAA (2022). *Carbon dioxide removal as a tool to mitigate climate change*.

<https://www.noaa.gov/news-release/carbon-dioxide-removal-as-tool-to-mitigate-climate-change>

NOAA (2023). *NOAA carbon dioxide removal research*. <https://sciencecouncil.noaa.gov/cdr-strategy/>

Nordex (2020). *N60/1300KW*. <https://www.yumpu.com/en/www.nordex-online.com>

NREL (2018). *Geospatial data science*. <https://www.nrel.gov/gis/assets/images/solar-annual-ghi-2018-usa-scale-01.jpg>. Accessed May 2024.

NREL (2023). *Geospatial data science*. <https://www.nrel.gov/gis/assets/images/wtk-40m-2017-01.jpg>

REC (2024). *REC alpha pure series datasheet*.

[https://www.recgroup.com/sites/default/files/documents/ds\\_rec\\_alpha\\_pure\\_series\\_en\\_us.pdf?t=1709067961](https://www.recgroup.com/sites/default/files/documents/ds_rec_alpha_pure_series_en_us.pdf?t=1709067961)

Statista (2023a). *Net electricity consumption worldwide in select years from 1980 to 2022*. <https://www.statista.com/statistics/280704/world-power-consumption/>.

Statista (2023b). *Projected electricity use in the United States from 2022 to 2050*.

<https://www.statista.com/statistics/192872/total-electricity-use-in-the-us-since2009/#:~:text=Electricity%20use%20in%20the%20United,27%20percent%20C%20relative%20to%202022>.

## Renewable Energy for Electricity Generation in Arizona and Texas

- Statista (2023c). *Existing utility nameplate and net summer capacity in the United States in 2022, by energy source*. <https://www.statista.com/statistics/1012659/us-energy-capacity-by-source/>
- Statista (2023d). *Phoenix-Mesa-Chandler metro area population in the U.S. 2010-2021*. <https://www.statista.com/statistics/815239/phoenix-metro-area-population/>
- U.S. CBO (2024). *The demographic outlook: 2024 to 2054*. <https://www.cbo.gov/publication/59697>
- U.S. EERE (2024). *U.S. average annual wind speed at 30 meters*. <https://windexchange.energy.gov/maps-data/325>
- U.S. EIA (2023). *Electricity consumption in the United States was about 4 trillion kilowatt-hours (kWh) in 2022*. <https://www.eia.gov/energyexplained/electricity/use-of-electricity.php>
- WNA (2024). *Carbon dioxide emissions from electricity*. <https://world-nuclear.org/information-library/energy-and-the-environment/carbon-dioxide-emissions-from-electricity>

**A Study of Carbon Emissions and Energy Consumption of Solar Power Generation  
in Phoenix, Arizona**

Rahim Khoie<sup>1</sup>

David Mueller

Department of Electrical and Computer Engineering, University of the Pacific, Stockton,  
CA

[1rkhoie@pacific.edu](mailto:1rkhoie@pacific.edu)

### Abstract

The emissions of solar power generation have been extensively researched in the past three decades (NREL, 2021b). Meanwhile, the solar power generation (especially rooftop solar systems) in the U.S. and across the world has been rising, a trend that is expected to continue at a much faster rate in the next several decades. As this trend continues, the issue of carbon neutrality of solar power becomes even more important, especially because the catastrophic effects of climate change continue to intensify.

Our model has three components: (a) lifetime power generation model, (b) energy intensity model for a solar panel including manufacturing, transportation, installation, operation, and maintenance, and (c) emission model based on several factors including irradiation power density of the installation site, the fuel mixture used in various processes in manufacturing steps, and several other variables.

Our preliminary results show that a 400-W solar panel operating in Phoenix, Arizona takes an input energy of 1,423.34 kWh and produces 21,411.81 kWh in its 25-year operating life, which corresponds to an average annual generation of 856.47 kWh and an energy payback period of 1.66 years. Furthermore, the energy intensity of this panel is 66.47 Wh/kWh. More importantly, the emission intensity of this panel is either 27.41, 36.37, or 40.88 g-CO<sub>2</sub>/kWh depending on whether it is manufactured in the U.S., Europe, and China, respectively.

Keywords: Emission intensity, input energy, solar power generation, carbon footprint of photovoltaics, solar panel manufacturing

### Life Cycle Assessment (LCA) Model

We incorporated the energy input and emissions of 19 processes involved in the life cycle assessment (LCA) of solar panels. We partitioned these processes into three main components: (1) manufacturing, (2) transportation, and (3) installation at the consumer site, as shown in Fig. 1. Our LCA model has three components: (a) lifetime energy production model, (b) energy intensity model for a 400-W solar panel including raw material, manufacturing, transportation, installation, operation, and maintenance, and (c) emission model based on several factors including irradiation power density of the installation site, fuel mixture used in various processes in manufacturing steps, and several other variables.





Fig. 1. Overall model incorporating emissions from three main components.

### 1.1. Lifetime Energy Production Model:

The annual solar irradiation energy is given by Eq. 1:

$$E_{irr} = 365 * S_{ph} * A_p \quad Eq. (1)$$

where

$E_{irr}$  = annual irradiation energy received by the panel (kWh),

$S_{ph}$  = solar peak hours of the location (6.5 kWh/m<sup>2</sup>/day in Phoenix, AZ), and

$A_p$  = area of the panel (m<sup>2</sup>).

The area of the panel is given by Eq 2:

$$A_p = \frac{P_p}{A_{pd}} \quad Eq. (2)$$

where

$P_p$  = DC power rating of the panel (400 W in this model), and

$A_{pd}$  = panel area power density of REC Alpha Pure Series (216 W/m<sup>2</sup>) (REC, 2024).

The area of the 400 W is 1.85 m<sup>2</sup>. The generated DC electricity energy by the panel is given by Eq. 3:

$$E_{genDC} = \eta * E_{irr} \quad Eq. (3)$$

where

$E_{genDC}$  = annual DC electricity generated by the panel, (kWh) and

$\eta$  = net conversion efficiency of the panel (varies throughout the life of the panel).

The temperature and aging degradation of the panel are incorporated in the model as given by Eq 4:

$$\eta = \eta_0 [ a_{dc1} - (n_j - 1) a_{dc} ] \quad Eq. (4)$$

where

$\eta_0$  = conversion efficiency in year 0 (21.6%),



$n_j$  = number of years the panel has been in operation, (years  $j = 1$  to 25),

$a_{dc1}$  = aging degradation coefficient of the panel in year 1 (98%)

$a_{dc}$  = aging degradation coefficient of the panel in years 2 through 25 (-0.25%/year after year 1)

And finally, the annual AC electricity produced by the panel in years  $j = 1$  to 25 is given by Eq. 5:

$$E_{genACj} = \eta_{DCAC} * E_{genDC} \quad Eq. (5)$$

where

$E_{genACj}$  = annual AC electricity generated (kWh) in years  $j = 1$  to 25,

$\eta_{DCAC}$  = DC to AC inverter efficiency (95%),

The lifetime energy production will then be given by:

$$Lifetime\ Energy\ Produced = \left( \sum_{j=1}^{25} E_{genACj} \right) \quad Eq. (6)$$

## 1.2. Input Energy and Energy Intensity Model

Our model takes into account the contributions of 19 processes to the total energy required to manufacture, transport, install, and dispose of a 400-W solar panel. The required energy (also referred to as embodied energy) in the life cycle of the panel from starting raw materials to its final disposal is given by Eq. 7:

$$E = E_0 + E_1 + E_2 + E_3 + E_{BOM} + E_4 + E_5 + E_{AL} + E_{GL} + E_{BOP} + E_{BOS} \\ + E_{BOF} + E_{INV} + E_{TRANW} + E_{TRANL} + E_{INST} + E_{BOI} + E_{OPM} \\ + E_{DD} \quad Eq. (7)$$

where (all energy inputs are in kWh)

$E$  = total input energy of the 400-W system,

$E_0$  = input energy of metallurgical grade silicon (MG-Si, 9N),

$E_1$  = input energy of trichlorosilane (TCS, 11N),

$E_2$  = input energy of chemical vapor deposition (CVD),

$E_3$  = input energy of monocrystalline wafer (ingot formation, cropping, slicing, and cleaning),

$E_{BOM}$  = input energy of balance of materials (chemicals, mostly acids)

$E_4$  = input energy of cell conversion (n-type diffusion, emitter formation, silicon oxide, aluminum oxide, anti-reflective coating, ohmic contacts, fingers, and bus bars), (plus 7% for unusable rejects)

$E_5$  = input energy of panel assembly,

$E_{AL}$  = input energy of aluminum frame,

$E_{GL}$  = input energy of glass,

$E_{BOP}$  = input energy of balance of panel assembly (automatic loading of glass panels, soldering, pates, testing),

$E_{BOS}$  = input energy of balance of system (electrical components, panel wires and connectors)

$E_{BOF}$  = input energy of balance of finished product (preparation, packaging, storage)

$E_{INV}$  = input energy of inverter,

$E_{TRANW}$  = input energy of transportation (over water) of the system to the U.S.,

$E_{TRANL}$  = input energy of transportation (over land) to the system to installation site,

$E_{INST}$  = input energy of installation (site preparation, tools),

$E_{BOI}$  = input energy of balance of installation (wires, junction boxes, connectors),

$E_{OPM}$  = input energy of operation and maintenance, and

$E_{DD}$  = input energy of decommissioning and disposal.

The numerical values of the above input energies are calculated based on the data published by a large number of researchers, most notably at the National Renewable Energy Laboratory (NREL). The original data and the values calculated for a 400-W system are given in Tables 1, 2, and 3. The sources for the raw data shown in these tables are (NREL, 2019 a, b, c, d) (NREL, 2021a) and others. For a complete list of references for raw data used in our model, see (Khoie et. al. 2024).

Table 1: Energy input of 6 processes in the fabrication of wafers used in a 400-W solar panel. The panel consists of 66 wafers (132 half-cut), each with a 17 g weight.

| Major Process | Symbol    | Sub - Process                       | Raw data reported | Input energy kWh/wafer | Input energy for 400-W panel (kWh) |
|---------------|-----------|-------------------------------------|-------------------|------------------------|------------------------------------|
| A) MG-Si      | $E_0$     | Metal Grade Silicon Purity 8N to 9N | 1250 MJ/kg        | 5.9                    | <b>389.33</b>                      |
|               | Total (A) |                                     |                   |                        |                                    |
| B) Wafer      | $E_1$     | Trichlorosilane (TCS) 11N           | 15 kWh/kg         | 0.255                  | 16.83                              |

Solar Power Generation in Phoenix

|  |                  |                         |              |      |               |
|--|------------------|-------------------------|--------------|------|---------------|
|  | $E_2$            | Siemens CVD             | 30<br>kwh/kg | 0.51 | 33.66         |
|  | $E_3$            | Ingot                   |              | 0.76 | 49.50         |
|  | $E_{BOM}$        | Balance of materials    |              | 1.04 | 67.04         |
|  | $E_4$            | Cell conversion (+7%)   |              | 0.28 | 18.48         |
|  | <b>Total (B)</b> | <b>Wafer Production</b> |              |      | <b>185.51</b> |

Table 2: Energy input of 7 processes in the manufacturing of a 400-W solar panel using 66 wafers.

| Major Process    | Symbol                          | Sub - Process                                    | Raw data reported | Input energy kWh /panel | Input energy of 400-W panel (kWh) |
|------------------|---------------------------------|--|-------------------|-------------------------|-----------------------------------|
| C) Panel         | $E_5$                           | Panel assembly                                   |                   | 0.42                    | 27.72                             |
|                  | $E_{AL}$                        | Aluminum frame                                   | 17<br>kWh/kg      | 2.05<br>kg/panel        | 34.85                             |
|                  | $E_{GL}$                        | Glass layers                                     | 1.7<br>kWh/kg     | 16.4<br>kg/panel        | 27.88                             |
|                  | <b>Total (C)</b>                | <b>Panel Production</b>                          |                   |                         | <b>90.45</b>                      |
|                  | <b>Total (B+C)</b>              | <b>Wafers and Panel</b>                          |                   |                         | <b>275.96</b>                     |
|                  | $E_{BOP}$<br><b>Total (BOP)</b> | Balance of electrical energy of wafers and panel | 19% of (B+C)      |                         | <b>52.43</b>                      |
| D) Inverter      | $E_{INV}$<br><b>Total (D)</b>   | Inverter   | 59 % of (B+C)     |                         | <b>193.75</b>                     |
| <b>E) System</b> | <b>Total (E)</b>                | <b>Sum of (A+B+C+BOP+D)</b>                      |                   |                         | <b>911.73</b>                     |

## Solar Power Generation in Phoenix

|                           |              |                          |            |  |                |
|---------------------------|--------------|--------------------------|------------|--|----------------|
| <b>F) BOS</b>             | $E_{BOS}$    | Balance of system        | 10% of (E) |  | 91.17          |
| G) Ready to ship          | $E_{BOF}$    | Packaging, storage, etc. | 5% of (E)  |  | 45.59          |
| <b>H) Out the factory</b> | <b>Total</b> |                          |            |  | <b>1048.49</b> |

Table 3. Energy input of the remaining six processes, including transportation of a 400-W panel to the installation site, installation, operation, and maintenance, decommissioning and disposition.

| Major Process                | Symbol       | Sub - Process                         | Raw data reported         | Input energy of a 400-W panel kWh |
|------------------------------|--------------|---------------------------------------|---------------------------|-----------------------------------|
| I) Shipping                  | $E_{TRANW}$  | Transportation over water (12,000 km) | 10 gCO <sub>2</sub> /Tkm  | 4.81                              |
|                              | $E_{TRANL}$  | Transportation over land (600 km)     | 100 gCO <sub>2</sub> /Tkm | 3.07                              |
| J) Installation              | $E_{INST}$   | System Installation                   | 2.5% of (H)               | 26.21                             |
|                              | $E_{BOI}$    | Balance of Installation               | 2.5% of (H)               | 26.21                             |
| K) Operation and Maintenance | $E_{OPM}$    | Inverter                              | 20% of (H)                | 209.69                            |
| L) Disposal                  | $E_{DD}$     | Decommissioning and disposal          | 10% of (H)                | 104.85                            |
| Total LCA                    | <b>Total</b> | <b>Sum of (H thru L)</b>              |                           | <b>1423.34</b>                    |

### 1.3. Emissions Intensity Model

The energy supply in the manufacturing, installation, operation, and decommissioning of a solar panel is 80% electricity, and most of the remaining 20% is non-electricity sources, which are mostly natural gas (IEA, 2022). To accurately model the emissions of a solar panel, one must consider each and every one of the 19 processes (in Eq. 7)

and determine the fuel mixes used in these processes, a task that is extremely involved. A more reasonable approach is to separate the processes into three groups: (1) the processes that require mostly electricity energy, ( $E_{ELEC-INTENSE}$ ), (2) the processes that use mostly non-electricity energy sources ( $E_{NON-ELEC-INTENSE}$ ) and (3) the transportation processes ( $E_{TRANS}$ ). These three groups of energy sources are given by Eqs. 8, 9, and 10, respectively:

$$= E_1 + E_2 + E_3 + E_4 + E_5 + E_{BOP} + E_{BOS} + E_{BOF} + E_{INV} + E_{INST} + E_{BOI} + E_{OPM} + E_{DD} \quad Eq. (8)$$

$$E_{NON-ELEC-INTENSE} = E_0 + E_{BOM} + E_{AL} + E_{GL} \quad Eq. (9)$$

$$E_{TRANS} = E_{TRANW} + E_{TRANL} \quad Eq. (10)$$

The resulting emissions are then calculated using Eq. 9:

$$C_{O_2} = E_{ELEC-INTENSE} * C_{ELEC-INTENSE} + E_{NON-ELEC-INTENSE} * C_{NON-ELEC-INTENSE} + E_{TRANS} * C_{TRANS} \quad Eq. (9)$$

where (all energy inputs are in kWh)

$C_{O_2}$  = total emissions (g-CO<sub>2</sub>),

$E_{ELEC-INTENSE}$  = total energy of processes that are electricity intensive (kWh),

$C_{ELEC-INTENSE}$  = emissions coefficient of  $E_{ELEC-INTENSE}$  energy (g-CO<sub>2</sub>/kWh),

$E_{NON-ELEC-INTENSE}$  = total energy of processes that are non-electricity-intensive (kWh),

$C_{NON-ELEC-INTENSE}$  = emissions coefficient of  $E_{NON-ELEC-INTENSE}$  energy (g-CO<sub>2</sub>/kWh),

$E_{TRANS}$  = total transportation energy (kWh),

$C_{TRANS}$  = emissions coefficient of transportation energy (g-CO<sub>2</sub>/kWh),

The worldwide energy used in the manufacturing, installation, operation and decommissioning of a solar panel ( $E_{ELEC-INTENSE}$ ) is 80% electricity with the remaining 20% non-electricity sources mainly natural gas (IEA 2022). The  $E_{NON-ELEC-INTENSE}$  energy sources, vary from one process to another, but are very close to 50% electricity and 50% natural gas. For  $E_{TRANS}$  the transportation fuels are heavy fuel oil (HFO) for cargo ships and gasoline for trucks.

We simulated the emission intensity of the 400W solar panel for various scenarios including panels that are made in the U.S., Europe, China, based on the fuel mix used in these regions for electricity generation as tabulated in Table 4.

Table 4. Fuel mixes used in electricity generation in the U.S., Europe, and China. For comparison, the average values of the world are also listed. Other sources are nuclear, hydro, and renewables.

## Solar Power Generation in Phoenix

|               | U.S.                                 | Europe     | China           | World                     |
|---------------|--------------------------------------|------------|-----------------|---------------------------|
| Coal %        | 19.5                                 | 13.1       | 63.0            | 35.7                      |
| Oil %         | 0.5                                  | 30.5       | 1.0             | 3.0                       |
| Natural Gas % | 39.9                                 | 26.7       | 3.0             | 22.5                      |
| Other %       | 40.1                                 | 29.7       | 33.0            | 38.8                      |
| Sum %         | 100%                                 | 100%       | 100%            | 100%                      |
| Source        | (U.S. EIA 2023a)<br>(U.S. EIA 2023b) | (IEA 2021) | (U.S. EIA 2021) | (OWID 2020)<br>(IEA 2019) |

Using the information provided by the U.S. Energy Information agency (U.S. EIA, 2023c) the U.S. electricity generation emission coefficients of coal, natural gas, and petroleum are 1044 g CO<sub>2</sub>/kWh, 440 g CO<sub>2</sub>/kWh, and 1080 g CO<sub>2</sub>/kWh, respectively. The average emission coefficient for all sources other than the above (nuclear, hydro, and renewables) is about 25 g CO<sub>2</sub>/kWh (U.S. EIA, 2023c).

## 2. Results

The sweet spot of the U.S. for solar electricity generation is its Southwest region. We chose the Phoenix area as it is home to 4.95 million people (Statista, 2023). The Phoenix area has a 6.5 kWh/m<sup>2</sup>/day solar peak hour resulting in 21,411.81 kWh of AC electricity over 25 years of operation from the 400-W solar panel which amounts to an average annual production of 856.47 kWh. With 1423.34 kWh of input energy (Table 3), the panel's energy payback is 1.66 years. The energy intensity of this panel is 1,423.34 kWh/21,411.81 kWh, which is 66.47 Wh/kWh.

The input energies of the three groups of processes add up to 1,423,34 kWh as shown in Table 5, of which 976.56 kWh is electricity (mostly used in manufacturing processes), 438.90 kWh from natural gas (mostly used in the production of metal-grade silicon, aluminum frame and glass), and 7.88 kWh from oil used in transportation.

Table 5: Input energy of the three groups of processes,  $E_{ELEC-INTENSE}$ ,  $E_{NON-ELEC-INTENSE}$ , and  $E_{TRANS}$ . All numbers are in kWh.

| Process Group   | Electricity | Natural Gas | Oil  | Total of Group |
|---|-------------|-------------|------|----------------|
| $E_{ELEC-INTENSE}$<br>Electricity-Intense Group         | 716.88      | 179.22      | 0.00 | 896.10         |
| $E_{NON-ELEC-INTENSE}$<br>Non-Electricity-Intense Group | 259.68      | 259.68      | 0.00 | 519.35         |

## Solar Power Generation in Phoenix

|                                     |        |        |      |                |
|-------------------------------------|--------|--------|------|----------------|
| $E_{TRANS}$<br>Transportation Group | 0.00   | 0.00   | 7.88 | 7.88           |
| Total (kWh)                         | 976.56 | 438.90 | 7.88 | <b>1423.34</b> |

The total electricity of 976.56 kWh is produced from four different sources (fuel mixes) consisting of coal, oil, natural gas, and other sources which include, nuclear, hydro, and renewables including wind and solar. Table 6 shows the contribution of each source to the total electricity based on fuel mixes used in the U.S., Europe, and China. The resulting emissions for electricity used in the processes are shown in Table 7.

Table 6. Amount of electricity generated from each of four fuel types in the U.S., Europe, and China. All numbers are in kWh.

| Sources of Electricity Generation | U.S.   | Europe | China  |
|-----------------------------------|--------|--------|--------|
| Electricity from Coal             | 190.43 | 127.93 | 615.23 |
| Electricity from Oil              | 4.88   | 297.85 | 9.77   |
| Electricity from Natural Gas      | 389.65 | 260.74 | 29.30  |
| Electricity from Other Sources    | 391.60 | 290.04 | 322.26 |

Table 7. Emissions of electricity from each fuel type used in the U.S., Europe, and China.

| Emissions                                       | U.S.    | Europe  | China   |
|---|---------|---------|---------|
| Electricity from Coal (g CO <sub>2</sub> )      | 198,808 | 133,558 | 642,303 |
| Electricity from Oil (g CO <sub>2</sub> )       | 5,273   | 321,679 | 10,547  |
| Electricity from NG (g CO <sub>2</sub> )        | 171,445 | 114,726 | 12,891  |
| Electricity from other (g CO <sub>2</sub> )     | 9,790   | 7,251   | 8,057   |
| Total Electricity Emission (g CO <sub>2</sub> ) | 385,316 | 577,214 | 673,797 |

Adding all emissions from all sources, (shown in Table 8), the total emissions of a 400-W panels are 586,941 g CO<sub>2</sub> and 778,839 g CO<sub>2</sub>, if it is manufactured in the U.S. or Europe, respectively. However, the same panel, cradle to grave, produces 875,422 g-CO<sub>2</sub> if it is made in China. With a lifetime electricity generation of 21,411.81 kWh, this 400-W panel has carbon emission intensity of 27.41, 36.37, and 40.88 g CO<sub>2</sub>/kWh if it is made in the U.S., Europe, or China, respectively.

Table 8: Total emissions from various sources used in the U.S., Europe, and China.

| Emissions  | U.S.         | Europe       | China        |
|--|--------------|--------------|--------------|
| Total Electricity (g CO <sub>2</sub> )               | 385,316      | 577,214      | 673,797      |
| Total Natural Gas (g CO <sub>2</sub> )               | 193,115      | 193,115      | 193,115      |
| Total Oil (g CO <sub>2</sub> )                       | 8,510        | 8,510        | 8,510        |
| Total All groups (g CO <sub>2</sub> )                | 586,941      | 778,839      | 875,422      |
| <b>Emission Intensity<br/>(g CO<sub>2</sub>/kWh)</b> | <b>27.41</b> | <b>36.37</b> | <b>40.88</b> |

### 3. Conclusion

A 400-W solar panel operating in one of the sweet spots of solar power generation in the U.S., namely Phoenix, Arizona, takes an input energy of 1,423.34 kWh and produces 21,411.81 kWh in its 25-year operating life. The energy intensity of this panel is therefore 66.47 Wh/kWh ( $=1,423.34 \text{ kWh}/21,411.81 \text{ kWh}$ ) and with an average annual production of 856.47 ( $=21,411.81 \text{ kWh}/25 \text{ year}$ ), it takes 1.66 years ( $=1,423.34 \text{ kWh}/856.47 \text{ kWh per year}$ ) to give its input energy back.

Finally, the emission intensity of this panel (total emissions in g CO<sub>2</sub>/lifetime generation in kWh) is 27.41, 36.37, and 40.88 g CO<sub>2</sub>/kWh depending on whether it is manufactured in the U.S., Europe, or China, respectively. Our results, for both energy intensity and emission intensity, while well within the range of harmonized results reported by NREL (2021a), are on the lower side of the scale. These underestimations have two main reasons: (1) the solar panel studied here (as are most rooftop panels available in the market today) are now about 7% more efficient ( $\sim 21\%$  in 2024) than they were then ( $\sim 14\%$  in 2012), and (2) recent advances in manufacturing of solar panels have resulted in lower input energy of various processes.

### Conflict of Interest

This work was supported in part by grants from School of Engineering and Computer Science of the University of the Pacific through a research center; “Carbon Capture Center for Mitigating Climate Change Crisis ~ C<sup>3</sup>FMC<sup>3</sup>. We have not received any support financial or otherwise from any public or private organizations.



## References

- IEA (2019). *World energy balances overview*. [https://www.iea.org/reports/world-energy-balances-overview/world](https://www.iea.org/reports/world-energy-balances-overview/world-balances-overview/world)
- IEA (2021). *Energy system of Europe*. <https://www.iea.org/regions/europe>
- IEA (2022). *Solar PV global supply chains*. <https://www.iea.org/reports/solar-pv-global-supply-chains/executive-summary>.
- Khoie, R., & Mueller, D. (2024). *A comprehensive study of carbon footprint of solar power generation from raw materials to operation and maintenance in various locations in the United States*.
- NREL (2019a). *Crystalline silicon photovoltaic module manufacturing costs and sustainable pricing: 1H 2018 benchmark and cost reduction road map*. <https://www.nrel.gov/docs/fy19osti/72134.pdf>.
- NREL (2019b). *Cost modeling of PV technologies*. <https://www.nrel.gov/news/video/cost-modeling-pv-technologies-text.html>.
- NREL (2019c). *PV and storage system cost*. <https://www.nrel.gov/news/video/cost-modeling-pv-technologies-text.html>
- NREL (2019d). *Levelized cost of electricity*. <https://www.nrel.gov/news/video/cost-modeling-pv-technologies-text.html>
- NREL (2021a). *Life cycle assessment harmonization*. <https://www.nrel.gov/analysis/life-cycle-assessment.html>.

## Solar Power Generation in Phoenix

NREL (2021b). *Life cycle greenhouse gas emissions from electricity generation: update.*

<https://www.nrel.gov/docs/fy21osti/80580.pdf>.

OWID (2020). *Our World in Data: electricity mix.* <https://ourworldindata.org/electricity->

[mix](https://ourworldindata.org/electricity-mix).

REC (2024). *REC alpha pure series datasheet.*

[https://www.recgroup.com/sites/default/files/documents/ds\\_rec\\_alpha\\_pure\\_series\\_en\\_us.pdf?t=1709067961](https://www.recgroup.com/sites/default/files/documents/ds_rec_alpha_pure_series_en_us.pdf?t=1709067961).

Statista (2023). *Phoenix-Mesa-Chandler metro area population in the U.S. 2010-2021.*

<https://www.statista.com/statistics/815239/phoenix-metro-area-population/>.

U.S. EIA (2021). *China.* <https://www.eia.gov/international/analysis/country/CHN>.

[Accessed March 2024](#).

U.S. EIA (2023a). *Electricity in the United States.*

<https://www.eia.gov/energyexplained/electricity/electricity-in-the-us.php>.

U.S. EIA (2023b). *What is U.S. electricity generation by energy source?.*

<https://www.eia.gov/tools/faqs/faq.php?id=427&t=3>.

U.S. EIA (2023c). *How much carbon dioxide is produced per kilowatt-hour of U.S.*

*electricity generation?*

<https://www.eia.gov/tools/faqs/faq.php?id=74&t=11#:~:text=In%202022%2C%20total%20annual%20U.S.,billion%20short%20tons%E2%80%94of%20carbon>.

**Optimizing a Foldable Solar Cooker with Enhanced Thermal Properties for Humanitarian and Refugee Camp Deployment**

Tariku Negash Demissie <sup>a, \*</sup>

Sebastiano Tomassetti <sup>a</sup>

Claudia Paciarotti <sup>a</sup>

Matteo Muccioli <sup>b</sup>

Giovanni Di Nicola <sup>a, c</sup>

<sup>a</sup> Marche Polytechnic University, Department of Industrial Engineering and Mathematical Sciences, Ancona, Italy

<sup>b</sup> Studio MUMA, Rimini, Italy

<sup>c</sup> Construction Technologies Institute, National Research Council (ITC-CNR), Padova, Italy

### Extended Abstract

Humanitarian and refugee camps generally rely on inefficient and unsustainable cooking methods for preparing food and boiling water, such as intensive use of firewood. Due to this, the communities are contributing to deforestation and suffering health issues from inhaling the smoke (Demissie et al., 2024; Lahn & Grafham 2015). It is crucial to shift toward sustainable and efficient cooking technologies to resolve these problems. Providing clean and easy-to-use cooking systems should be seen as a humanitarian need, allowing organizations to meet their responsibilities effectively. Solar cookers offer an efficient and environmentally friendly alternative that can prevent these harmful effects on health and the environment. They play a central role in decreasing reliance on firewood and fossil fuels, reducing smoke exposure, and improving the well-being of camp residents.

In previous works by Regattieri (2016) and Mahavar et al. (2012), which also include a paper presented by Demissie et al. (2024), the potential benefits of solar cookers in humanitarian contexts have been emphasized.

In particular, a foldable solar cooker that ensured advancements over existing solar cookers was proposed in the previous study (Demissie et al., 2024). However, some issues remain concerning its thermal performance, portability, and usability. This study seeks to overcome these drawbacks by presenting an improved prototype with enhanced thermal performance and complete portability. By integrating features such as black coating inside the cooking chamber, cork insulation, and a fully foldable and lockable design, the improved solar cooker offers a practical solution for extensive deployment in humanitarian settings.

Indoor lab tests without load were carried out on the original and improved prototypes shown in Figures 1 and 2, using a metal halide solar simulator (Colarossi et al., 2021). The simulator produced a constant irradiance of about  $850 \text{ W/m}^2$  during the tests. The room and stagnation temperatures were recorded with T-type thermocouples and a Pico-Technology TC-08 datalogger. The effectiveness of both prototypes was determined by calculating the first figure of merit ( $F_1$ ). As shown in Figure 3, the upgraded prototype achieved a stagnation temperature of  $144.63^\circ\text{C}$  compared to  $109.44^\circ\text{C}$  for the original prototype. Consequently,  $F_1$  of the original and improved prototypes were  $0.1$  and  $0.14^\circ\text{C m}^2/\text{W}$ , respectively. These results highlight a performance improvement due to design enhancements.

The improved prototype boasts upgrades also over the design of the original solar cooker. Unlike the original prototype, the enhanced solar cooker has reflectors supported by ropes without requiring external components, as shown in the open configuration depicted in Figure 2a. As evident in Figure 2b, all components, including reflector panels, glass mirrors, and corks, can be conveniently stored inside the unit due to its design. This compact design ensures transportability and a secure locking mechanism while relocating the device from one place to another.

## Foldable Solar Cooker for Humanitarian and Refugee Camp Deployment



Fig. 1. Original foldable solar cooker

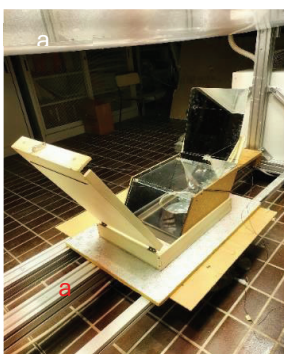


Fig. 2. Improved prototype: a) open configuration and b) closed configuration

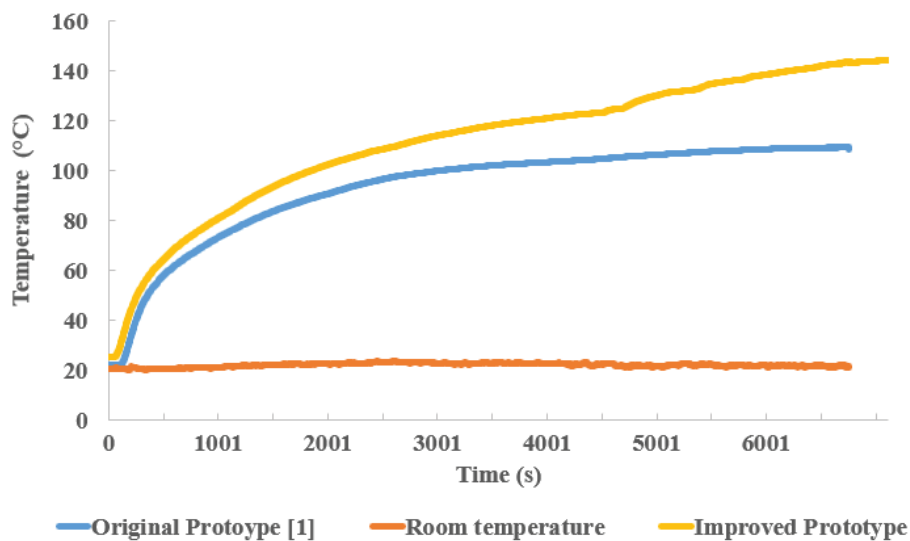


Fig. 3. Stagnation temperature of prototypes tested without load and at a constant irradiance of  $850 \text{ W/m}^2$ .

Keywords: Solar cooker, humanitarian camps

**Conflict of Interest**

The authors declare the following financial interests/personal relationships which may be considered as potential competing interests: Matteo Muccioli, Claudia Paciarotti, and Giovanni Di Nicola have a patent for a Removable, Resealable and Transportable Box-Type Solar Oven.

## References

- Colarossi, D., Tagliolini, E., Principi, P., & Fioretti, R. (2021). Design and validation of an adjustable large-scale solar simulator. *Applied Sciences*, 11(4), 1964.
- Demissie, T. N., Tomassetti, S., Paciarotti, C., Muccioli, M., Di Nicola, G., & Ruivo, C. R. (2024). Experimental characterization of a foldable solar cooker with a trapezoidal cooking chamber and adjustable reflectors. *Energy for Sustainable Development*, 79, 101409.
- Lahn, G., & Grafham, O. (2015). Heat, light and power for refugees: saving lives, reducing costs. *Chatham House Report*.
- Mahavar, S., Sengar, N., Rajawat, P., Verma, M., & Dashora, P. (2012). Design development and performance studies of a novel single-family solar cooker. *Renewable Energy*, 47, 67–76. <https://doi.org/10.1016/j.renene.2012.04.013>
- Regattieri, A., Piana, F., Bortolini, M., Gamberi, M., & Ferrari, E. (2016). Innovative portable solar cooker using the packaging waste of humanitarian supplies. *Renewable and Sustainable Energy Reviews*, 57, 319–326. <https://doi.org/10.1016/j>

**Modeling and Production Performance Analysis of a Campus 5MW Solar Installation in  
the California San Joaquin Valley**

David Mueller  
Harki Notra



### Abstract

A production analysis of a utility-scale solar system is presented in this paper. This system is installed as parking lot shade structures with a 7° tilt on a small urban university campus. It is comprised of 12,780 panels arranged in 45 arrays over eight locations for a total of 5.35 megawatts DC of capacity. The arrays have different orientations with most in a south-southeast (162° azimuth) and a west-southwest (252° azimuth) orientation. Theoretical system performance was determined using a variety of models available in the open-source pvlib python package (Anderson, 2023; Holmgren, 2018) and compared to a simple irradiance-based effective efficiency model. The theoretical performance is validated using onsite weather and solar irradiance measurements. Comparisons of theoretical, measured, and system performance characteristics are presented in this paper. Knowing real system performance comparisons to projected performance is an important component of closing the loop to improve system modeling and design.

### Introduction

In May 2022, the University of the Pacific commissioned a 5.35 MW (DC) photovoltaic power system, with specifications as shown in Table 1. The system was designed to meet approximately 30% of the campus' energy generation needs, making the system the largest in on-campus generation among private universities at the time of installation. In this work, we present a preliminary analysis of the system by modeling one of the subsystems – the arrays of parking Lot 4, also specified in Table 1. In this modeling, the clear-sky daily production is compared to the actual production of the subsystem during a summer day, June 21, 2023 (summer solstice), and a winter day, December 16, 2023 (the nearest clear day to winter solstice).

To comply with California Public Utilities Code for Renewable Energy Self-Generation Bill Credit Transfer (RES-BCT), the system's AC output was derated to 4.06 MW from 4.44 kW (Baird, 2008). This was accomplished by derating the inverters to a maximum output of 36.6 kW each. This effectively increases the system's overload ratio and creates many days of significant clipping. Inverter overloading is a common practice to maximize a systems output over the course of a year. It can be calculated by:

$$\text{Overload Ratio} = \frac{\text{Array Power [W]}}{\text{Inverter Power [W]}}$$

Clipping occurs when the power generated by an array exceeds the power capacity of the inverter. When a system is designed with an overload, this often occurs on peak summer days.

Table 1. University of the Pacific's PV system parameters.

| Item           | Total System | Lot 4 (Canopy 1) | Lot 4 (Canopy 2) | Lot 4 (Canopy 3) |
|----------------|--------------|------------------|------------------|------------------|
| No. of Modules | 12780        | 444              | 444              | 504              |

## Solar Installation in the San Joaquin Valley

|                         |                           |      |      |      |
|-------------------------|---------------------------|------|------|------|
| <b>No. of Inverters</b> | 111                       | 4    | 4    | 4    |
| <b>Strings/Inverter</b> | n/a                       | 18.5 | 18.5 | 18   |
| <b>Azimuth</b>          | varies                    |      | 162° |      |
| <b>Tilt</b>             |                           |      | 7°   |      |
| <b>Overload Ratio</b>   | 1.25 (avg)                | 1.18 | 1.18 | 1.34 |
| <b>Module Ratings</b>   | 415/425 W                 |      | 425W |      |
| <b>Inverter Ratings</b> | 40 kW (derated to 36.6kW) |      |      |      |

### Methods

Two different models were used to predict the system output – a simple irradiance-based effective efficiency model (IBEEM) and the standard models in pvlib python package (Anderson, 2023; Holmgren, 2018). The simple IBEEM model is now described.

The AC power output is given as:

$$P_{AC} = \begin{cases} \lambda \cdot P_{DC} \\ P_{AC,max} \end{cases}$$

$\lambda$  is the nominal conversion efficiency of the inverters. If the AC power calculated using conversion efficiency exceeds the maximum power rating of the inverter, the inverter is saturated and the output power is capped.

The DC power is predicted by multiplying the measured plane of array (POA) irradiance,  $G_{irr}$  [W/m<sup>2</sup>], the system's effective efficiency,  $\eta_{eff}$ , the single module panel area,  $A_p$  [m<sup>2</sup>], and the number of modules,  $N_M$ :

$$P_{DC} = \eta_{eff} \cdot G_{irr} \cdot A_p \cdot N_M$$

The effective efficiency considers the power-based age and temperature effects, as described in the module datasheet. Effective efficiency is calculated by:

$$\eta_{eff} = \eta_0 [1 + (T_{BOM} - 25)\gamma] [\alpha_0 + (t - 1)\alpha_p]$$

$\eta_0$  is the module conversion efficiency,  $T$  is the back-of-module temperature,  $\gamma$  is the temperature degradation coefficient,  $\alpha_0$  is the year 1 degradation,  $t$  is the module/system age, and  $\alpha_p$  is the power degradation coefficient.

Data for this model is provided by the on-site solar resource monitoring equipment shown in Figure 1. The solar resource monitoring equipment consists of three EKO MS-80 Class A pyranometers arranged in two plane-of-array orientations (162° and 252° at 7° tilt) and a global horizontal orientation; a back-of-module temperature sensor; and

weather sensors for temperature, humidity, barometric pressure, wind speed and direction.



Fig. 1. Solar irradiance and weather monitoring station co-located in University of the Pacific's parking lot 4.

The pvlib python modeling parameters are summarized in Table 2. As described in Table 1, the Lot 4 arrays create three shade canopies and are connected to 12 inverters. The size of two of the canopies is identical. To compute the total production of the Lot 4 sub-system, the single array outputs are multiplied by the corresponding number of inverters:

$$P_{AC,total} = 8P_{AC0} + 4P_{AC1}$$

$P_{AC0}$  is the AC power produced by an array of 18.5 modules x 6 strings connected to an inverter, and  $P_{AC1}$  is the AC power produced by an array of 18 modules x 7 strings connected to an inverter.

Table 2. pvlib-python modeling parameters for the Lot 4 sub-system array.

| Parameter/Method  | Value   |
|-------------------|---------|
| Latitude          | 37.98   |
| Longitude         | -121.31 |
| Time Zone         | GMT+8   |
| Surface Tilt      | 7       |
| Azimuth           | 162     |
| Modules Database  | CEC     |
| Inverter Database | CEC     |
| Mounting          | Fixed   |

## Solar Installation in the San Joaquin Valley

|                    |                                   |
|--------------------|-----------------------------------|
| Temperature Models | sapm,<br>open rack<br>glass/glass |
| Shading            | 0                                 |
| AOI Model          | physical                          |
| Spectral Model     | no loss                           |
| GHI/DNI/DHI        | clearsky                          |

### Results

Both the IBEEM and pvlib python models require irradiance data to predict the system production. To verify the summer (July 1) and winter (Dec 16) days are clear-sky days, the predicted clear-sky (from pvlib python) and measured global (GHI) and plane-of-array (POA) irradiance were compared for two days that represent typical near-peak summer and winter. Results show excellent agreement as shown in Figure 2.

#### Measured and Modeled Irradiance Summer/Winter

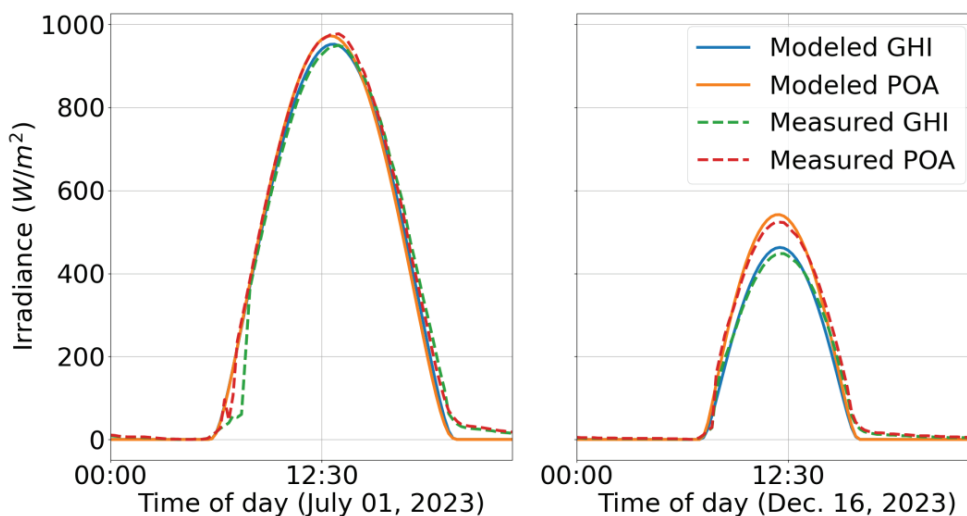


Fig. 2. GHI and POA clear-sky irradiance.

Figure 3 shows the predicted from both IBEEM and pvlib and the actual measured AC power production numbers for the parking lot 4 subsystem arrays.

## Measured and Modeled Production Summer/Winter

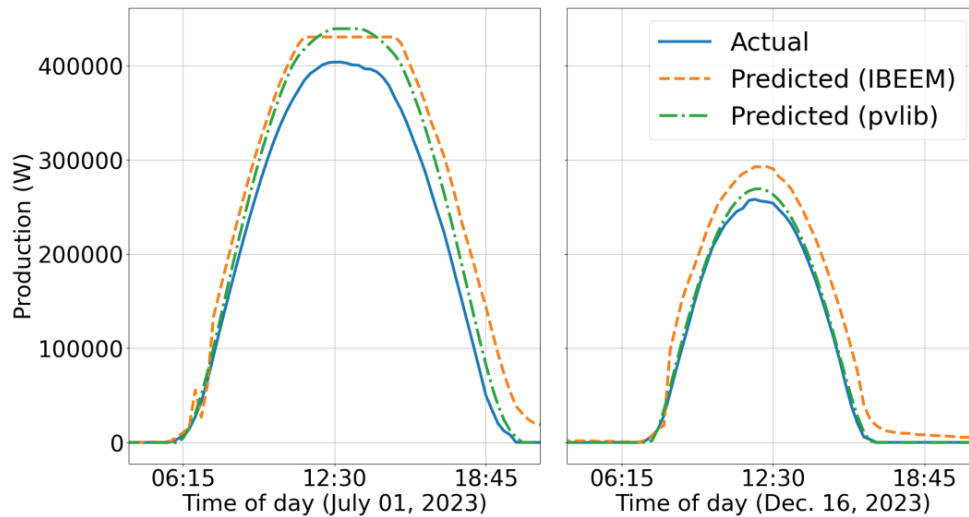


Fig. 3. Predicted and Actual Lot 4 System Production.

For the winter day, the pvlib model has excellent agreement with the actual production, with a slight overestimation during the peak of the day. This overestimation agrees with the slightly less-than-ideal irradiance conditions during peak day as shown in Fig. 2. For the summer day, the pvlib model overestimates the production significantly. For both predictions, show the system output clipping due to the inverter capacity. The actual production also indicates inverter clipping, but at a lower level than expected. This is likely due to both models not being able to fully account for the inverter efficiency reductions due to the heating effects of having to dissipate the excess energy.

### Conclusions

In this work, the production of a set of arrays, representing a subsystem, was analyzed and modeled for a 5.35-MW (DC) campus system set up as parking canopy shade structures. Since this system has inverters that are artificially capped at a lower power level to comply with non-utility production limits, these inverters are subject to additional stress to dissipate this extra power. This presents some unique circumstances that will require additional modeling considerations to accurately represent the actual system production. While the pvlib model was acceptably accurate for the winter modeling, where no inverter clipping was present, the model was not as accurate during the summer day. Future work will focus on determining how this overloading can be modeled and how this affects the long-term durability of the inverters.

### Conflict of Interest

This work was supported by a strategic investment grant from the School of Engineering and Computer Science at the University of the Pacific. System-level information and data were kindly provided by the Office of Sustainability at the University of the Pacific.

## References

Anderson, K., Hansen, C., Holmgren, W., Jensen, A., Mikofski, M., & Driesse, A. Pvlb python: 2023 project update. *Journal of Open Source Software*, 8(92), 5994, (2023). <https://doi.org/10.21105/joss.05994>

Holmgren, W. F., Hansen, C. W., & Mikofski, M. A. (2018.) Pvlb python: a Python package for modeling solar energy systems. *Journal of Open Source Software*, 3(29), 884. <https://doi.org/10.21105/joss.00884>

Laird. (2008). AB-2466. Bill Text - AB-2466 Local government renewable energy self-generation program. Retrieved from [https://leginfo.legislature.ca.gov/faces/billTextClient.xhtml?bill\\_id=200720080AB2466](https://leginfo.legislature.ca.gov/faces/billTextClient.xhtml?bill_id=200720080AB2466)

**Beyond the Surface: Environmental Depth of Photovoltaic Recycling Methods**

Asli Birturk<sup>1,2\*</sup>

Betul Aksoy<sup>2</sup>

Melih Soner Celiktaş<sup>2</sup>

<sup>1</sup>Columbia University, Center for Life Cycle Analysis, Department of Earth and  
Environmental Engineering, New York, NY

<sup>2</sup>Ege University, Solar Energy Institute, Izmir, Turkey

## Abstract

This study delved into the Life Cycle Assessment (LCA) literature review findings regarding photovoltaic (PV) recycling methodologies. LCAs' boundaries significantly influence environmental impact categories such as functional units, electricity consumption, material flows. Regardless of system scale functional unit values of literature studies are given to compare different system boundaries. This paper highlights PV module types and LCA tools, noting thermal methods in both c-Si and CdTe PV technologies yield lower environmental impacts than chemical and mechanical approaches. Additionally, a delamination process was conducted and LCA results were analyzed at the laboratory scale using hexane. The delamination success is 99%. Notably, recycling significantly diminishes environmental footprints compared to landfilling, with a fraction of Global Warming Potential (GWP) values.

Keywords: Global Warming Potential (GWP), photovoltaic recycling, Life Cycle Assessment (LCA), environmental Impact, sustainability

## Introduction

The increasing diversity in photovoltaic (PV) panel technologies, along with widespread efforts to enhance existing technologies in terms of efficiency, durability, power, and other technical specifications, has raised concerns about the environmental sustainability of solar energy production (Ghosh & Yadav, 2021; Smith et al., 2021).

PV modules play a significant role in promoting renewable energy and reducing the use of fossil fuels. Additionally, the management of end-of-life modules and the formulation of necessary policies are crucial factors for ensuring the sustainability of evolving technologies (Ghosh & Yadav, 2021). Therefore, research is being conducted on PV module recycling methods and their environmental impacts, especially after their average 30-year lifespan or in case of premature failures. Environmental impact categories considered by LCA studies offer quantitative assessment opportunities in this context. Generally, SimaPro, GaBi, and OpenLCA tools stand out in research (Dias et al., 2021; Klugmann-Radziemska & Kuczyńska-Łażewska, 2020; Lim et al., 2022a).

A report published by the IEA and IRENA states that by the year 2050, the world will face 78 million tons of PV-module waste. Making measures obligatory through legal regulations by countries will ensure the regulation of increasing waste management problems in the future (IRENA and IEA, 2016). European Union countries have served as role models for other countries in terms of setting collection and recycling targets for PV modules. Although comprehensive legislation is yet to be established, the inclusion of PV recycling in the EU's Waste Electrical and Electronic Equipment (WEEE) Directive is seen as a pioneering step. The directive limits recycling responsibility to panel manufacturers (Chowdhury et al., 2020; Council of the European Union, 2019).

In the United States, there is no comprehensive PV recycling regulation covering all states (Urbina, 2022). However, California has issued a regulation (Senate Bill 489) stating that PV module waste is included in universal waste management (Chowdhury et al., 2020; State of California, 2015). Senate Bill 5939, published by the state of Washington, discusses tax incentives for recycling renewable energy production



technologies and the collection of modules. It is noted that reusing materials obtained from the recycling of PV modules requires less cost than directly using raw materials and can potentially provide economic returns to countries where recycling is practiced (Washington State, 2019). However, factors such as waste collection, transportation to recycling facilities, and the economic and political structures of countries result in varying levels of economic return. Therefore, there is a need for LCA and feasibility studies to be diversified through country-specific research.

### Literature Review on LCA of PV Recycling

This study delved into the LCA results of PV recycling methods, with a focus on environmental-impact categories. The boundaries of LCAs, including functional units (given in Table 1), electricity consumption, material inputs and outputs, directly influence the environmental impact assessment (Table 1). Irrespective of whether recycling research is conducted at the laboratory or industrial scale, functional unit values serve as a crucial reference. Furthermore, the study outlines PV module types and specifies the LCA tools used.

Ravikumar et al., (2020) compared two scenarios for PV module recycling, highlighting combination methods as environmentally preferable due to lower impacts in various categories. Deng, Dias, Lunardi, and Ji (2021) developed a chemical process for recycling silver from silicon plates and solar panels, assessing environmental impact categories such as ecotoxicity and climate change. Singh, Powar, and Dhar (2023) analyzed the LCA of framed c-Si and frameless CdTe modules, emphasizing the environmental benefits of recycling materials from end-of-life panels. The FRELP recycling technology, referenced in multiple studies, especially for c-Si modules, achieves nearly 100% recycling efficiency and is discussed along with its environmental impacts and transportation logistics (Ganesan & Valderrama, 2022; Dias et al., 2021; Latunussa, Ardente, Blengini, & Mancini, 2016; Mathur, Singh, & Sutherland, 2020a).

Table 1. Classification of GWP Results of PV Recycling Methods

| No | Reference                | Scale       | Method(s)   | PV Type | GWP (kgCO <sub>2</sub> eq) | Database                                      | Functional Unit  |
|----|--------------------------|-------------|---|---------|----------------------------|---|------------------|
| 1  | (Ravikumar et al., 2020) | Lab scale   | Chemical, Thermal, and Mechanical (Probe sonicator, bath sonication)                        | CdTe    | 4.70E+00                   | SimaPro Ecoinvent                             | 1 m <sup>2</sup> |
| 2  | (Deng et al., 2021)      | Lab scale   | Mechanical, Chemical (Alkaline, KOH etching, HNO <sub>3</sub> leaching, and electrowinning) | c-Si    | -1.60E+00                  | OpenLCA Ecoinvent 3.2 ReCiPe2016 Midpoint (H) | 1000 g           |
| 3  | (Latunussa et al., 2016) | Large Scale | Chemical, Thermal, and Mechanical (Electrolysis, acid leaching, incineration)               | c-Si    | 3.70E+02                   | SimaPro                                       | 1000 kg          |

Photovoltaic Recycling Methods

|   |  |                     |  |                                     |                       |         |  |
|---|--|---------------------|--|-------------------------------------|-----------------------|---------|--|
| 4 | (Mathur, Singh, & Sutherland, 2020a)             | Large Scale         | Chemical, Thermal, and Mechanical (Incineration, electrolysis)                   | c-Si                                | 2.75E+03              | SimaPro | 1 ton  |
| 5 | (Singh et al., 2023)                             | Lab Scale           | Chemical, Thermal, and Mechanical (Burning, chemical solvent)                    | c-Si and CdTe                       | 4.14E-01 and 5.29E-01 | SimaPro | 1 kg   |
| 6 | (Ansanelli, Fiorentino, Tammaro, & Zucaro, 2021) | Large Scale         | Mechanical, Chemical, and Thermal Methods  | c-Si                                | 3.36                  | SimaPro | 24 tons                                      |
| 7 | (Oteng, Zuo, & Sharifi 2023)                     | Large Scale         | Mechanical, Chemical, and Thermal Methods (Incineration, leaching, electrolysis) | Conventional Mono c-Si              | 1 E+05                | SimaPro | 1000 kg                                      |
|   |  |                     |  | Policy Option A Mono c-Si           | -298.64               |         |  |
|   |  |                     |  | Policy Option B Mono c-Si           | -1 E+06               |         |  |
| 8 | (Ganesan & Valderram, 2022)                      | Lab and Large Scale | Mechanical (Cutting)   | Centralized bulk recycling (c-Si)   | -3021                 | OpenLCA | 1 ton  |
|   |  |                     | Mechanical (Cutting)   | Decentralized bulk recycling (c-Si) | -3040                 |         |  |
|   |  |                     | Mechanical, Chemical, and Thermal Methods (Incineration, leaching, electrolysis) | High-Value Recycling (FRELP) (c-Si) | -3539                 |         |  |
| 9 | (Lim et al., 2022b)                              | Lab and Large Scale | Mechanical, Chemical, and Thermal Methods (Incineration, leaching, electrolysis) | c-Si                                | 25                    | GaBi    | 1000 waste panels, each with 400 mm × 200 mm |

### Experimental PV Delamination Method

Tembo et al. used both acidified and non-acidified hexane for the recovery of PV modules. The PV sample was exposed to hexane at 25°C for 24 hours, resulting in a delamination rate of 66%. Brenes et al. in 2023, observed that when samples were exposed to hexane at 55°C for 30 minutes, the EVA layer swelled slightly, but the c-Si wafer was not delaminated from the EVA layers.

In this study, c-Si sample was placed in an Erlenmeyer flask containing 100 ml of hexane as the solvent, and the flask was covered with aluminum foil to prevent vapor escape. The experiment was conducted in a shaking incubator at 150 rpm for 24 hours. After 24 hours of exposure to hexane, the sample was filtered, and the separated parts were cleansed of the chemical. The details of the experimental study are provided in Table 2.

Table 2. Combination of Chemical and Thermal PV Delamination Method at Lab-Scale

| Parameter            | Value                         |
|----------------------|-------------------------------|
| Chemical             | Hexane                        |
| Chemical Amount      | 100 ml                        |
| PV Sample Weight     | 6.280 g                       |
| Temperature          | 58°C                          |
| Duration             | 24 hours                      |
| Energy Consumption   | 3.618 kWh                     |
| Separated Glass      | 5.061 g                       |
| Glass Separation     | Observed                      |
| Front EVA Separation | Observed                      |
| c-Si Wafer           | Not separated from back EVA   |
| Back EVA             | Not separated from c-Si Wafer |
| Backsheet Separation | Observed                      |

### Results and Discussion

In this experimental study, the laminated glass and front EVA layer were easily separated from each other. The c-Si wafer remained laminated to the back EVA layer (Figure 1). Under these experimental conditions, the recovery of the glass, front EVA, and backsheet layers from the c-Si wafer was achieved (Table 3). Therefore, considering the remaining laminated back EVA weighing 0.287 g, the delamination success rate over the total mass of 6.28 g was 99%.

Table 3. Mass Distribution of the PV Sample after Delamination

| Solution | Chemical Quantity (ml) | PV Quantity (g) | Energy Consumption (kWh) | Glass (g) | EVA(s) (g) | c-Si Layer (g) | Backsheet (g) |
|----------|------------------------|-----------------|--------------------------|-----------|------------|----------------|---------------|
| Hexane   | 100                    | 6,280           | 3,618                    | 5,061     | 0.574      | 0.52           | 0.125         |

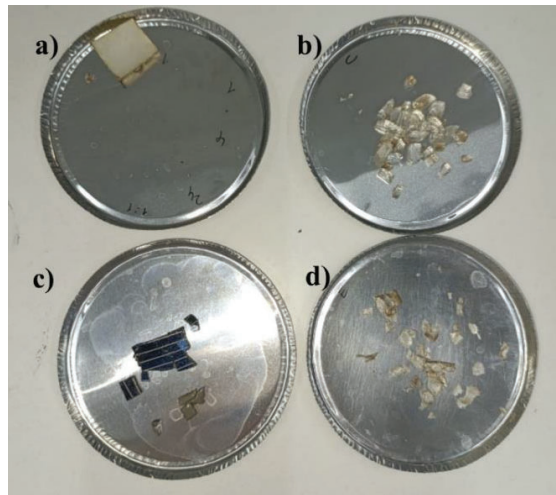


Fig. 1. A PV sample that has been exposed to hexane at 58°C for 24 hours a) Backsheet b) Glass c) c-Si Wafer + Back EVA d) Front EVA

Considering the 10 studies listed in Table 1, the chemical solvents and energy consumption employed in the delamination methods for the recycling of CdTe and c-Si modules directly influence the LCA results. It is understood that CdTe modules entail a lesser environmental impact compared to c-Si modules from similar chemical applications.

In this study's assessment, the use of strong chemical hexane resulted (compared to other landfilling parameters, EVA and PET) in higher environmental impact in categories such as terrestrial acidification, terrestrial ecotoxicity, and land use comparing to other categories given in Table 4. The prolonged 24-hour processing time to increase the success of delamination has led to high environmental impact in categories such as stratospheric ozone depletion, land use, mineral resource scarcity, and water consumption. The significant reduction in environmental impact resulting from the recycling of solar glass and multi-Si wafers is particularly notable in categories such as global warming potential, terrestrial acidification, stratospheric ozone depletion, ozone formation, and human health.

Table 4. LCA results of the Experimental Delamination Method

| Impact category   | Landfilling |          |          | Emission<br>Electricity | Recovery       |                   | Total    |
|---|-------------|----------|----------|-------------------------|----------------|-------------------|----------|
|   | EVA         | PET      | Hexane   |                         | Solar<br>glass | Multi-Si<br>wafer |          |
| Global warming<br>(kg CO <sub>2</sub> eq)                   | 2.56E-07    | 2.71E-08 | 1.05E-05 | 2.59E-04                | -6.84E-07      | -7.36E-06         | 2.62E-04 |
| Stratospheric<br>ozone depletion<br>(kg CFC11 eq)           | 6.62E-09    | 9.18E-10 | 3.01E-07 | 9.80E-06                | -8.16E-09      | -3.00E-07         | 9.80E-06 |
| Ozone formation,<br>Human health<br>(kg NO <sub>x</sub> eq) | 1.95E-07    | 2.31E-08 | 1.59E-05 | 2.44E-04                | -1.08E-06      | -6.28E-06         | 2.53E-04 |
| Terrestrial<br>acidification<br>(kg SO <sub>2</sub> eq)     | 1.13E-07    | 1.31E-08 | 6.08E-06 | 2.20E-04                | -8.62E-07      | -4.29E-06         | 2.21E-04 |
| Freshwater<br>eutrophication<br>(kg P eq)                   | 2.30E-07    | 1.28E-08 | 2.11E-05 | 3.43E-04                | -1.50E-07      | -4.79E-06         | 3.59E-04 |
| Marine<br>eutrophication<br>(kg N eq)                       | 7.59E-09    | 3.52E-09 | 3.34E-07 | 1.29E-06                | -1.71E-08      | -4.77E-07         | 1.14E-06 |
| Terrestrial<br>ecotoxicity<br>(kg 1,4-DCB)                  | 9.20E-07    | 1.36E-07 | 5.76E-05 | 3.30E-04                | -1.62E-06      | -4.90E-05         | 3.38E-04 |
| Freshwater<br>ecotoxicity<br>(kg 1,4-DCB)                   | 7.31E-08    | 1.14E-08 | 2.86E-06 | 2.27E-05                | -1.12E-07      | -1.84E-06         | 2.37E-05 |
| Land use<br>(m <sup>2</sup> a crop eq)                      | 8.03E-09    | 1.00E-09 | 4.94E-07 | 5.24E-06                | -2.23E-08      | -2.56E-07         | 5.46E-06 |
| Mineral resource<br>scarcity<br>(kg Cu eq)                  | 5.12E-11    | 4.81E-12 | 2.61E-09 | 8.91E-09                | -1.07E-10      | -5.54E-10         | 1.09E-08 |
| Water<br>consumption<br>(m <sup>3</sup> )                   | 5.22E-08    | 3.26E-09 | 3.44E-06 | 7.53E-05                | -1.12E-07      | -9.37E-06         | 6.93E-05 |

The environmental impact of recycling is significantly lower than landfilling, as explained through the Global Warming Potential (GWP) value in the study by (Lim et al., 2022b). While landfilling has an environmental GWP impact of 121 kg CO<sub>2</sub>-eq, the impact of recycling is nearly one-fifth of this value. Mathur et al., (2020b) report positive environmental benefits in the recovery of Al, Cu, and Ag metals across all impact categories such as Ozone depletion, Global warming potential, Acidification, Eutrophication, Carcinogenics, Non-carcinogenics, and Ecotoxicity excluding ozone depletion.

## Conclusion

In conclusion, this research underscored the critical role of LCA in evaluating PV recycling methods. It elucidated the varied environmental impacts associated with different recycling techniques and PV module types, emphasizing the necessity of maximizing environmental benefits through material reuse. Thermal methods emerge as more environmentally benign compared to chemical and mechanical approaches. Metal recovery processes present challenges due to their ozone-depleting potential, contrasting with the relatively lower impact of mechanical disassembly. Notably, recycling markedly reduces environmental burdens compared to landfilling, as specifically shown by Global Warming Potential (GWP) values. Insights from long-term studies, particularly regarding CdTe PV technology, elucidate emission patterns and address concerns about cadmium leakage. Moving forward, holistic approaches to PV recycling that consider lifecycle impacts and material flows will be instrumental in fostering sustainable energy practices and mitigating environmental footprints.

## Authorship Statement

Asli Birtürk: Conceptualization, Methodology, Investigation, Visualization, Writing – Original draft, Formal Analysis

Betul Aksoy: Conceptualization, Methodology, Formal Analysis, Investigation, Validation

Melih Soner Celiktas: Conceptualization, Project Administration, Supervision, Methodology, Review, Editing

## Conflict of Interest

The authors declare that they have no known competing financial interests or personal relationships that could have appeared to influence the work reported in this paper.

The authors would like to thank Ege University Scientific Research Projects Coordination Unit for project support (Project number: 29603), Turkish Scientific and Technological Council for financial support of ARDEB project (Project number: 121Y515) and both for the national and international doctoral scholarships to Asli Birtürk under the framework of BIDEB 2211-C (Grant number: 1649B032203727) and BIDEB 2214-A (Grant number: 1059B142300626). Special thanks to the American Solar Energy Society for the JEDI (Justice, Equity, Diversity, and Inclusion) conference scholarship (ASES SOLAR 2024) received by Asli Birtürk. We would also like to express our gratitude to everyone in the past who provided us with these opportunities for our research.

## References

- Ansanelli, G., Fiorentino, G., Tammaro, M., & Zucaro, A. (2021). A life cycle assessment of a recovery process from end-of-life photovoltaic panels. *Applied Energy*, 290(March), 116727. <https://doi.org/10.1016/j.apenergy.2021.116727>
- Chowdhury, M. S., Rahman, K. S., Chowdhury, T., Nuthammachot, N., Techato, K., Akhtaruzzaman, M., Tiong S. K., Sopian K, and Amin, N. (2020). An overview of solar photovoltaic panels' end-of-life material recycling. *Energy Strategy Reviews*, 27, 100431. <https://doi.org/10.1016/j.esr.2019.100431>
- Council of the European Union. (2019). Directive 2011/7/EU on waste electrical and electronic equipment (WEEE). *Official Journal of the European Union*, 38–71. <https://doi.org/10.5040/9781782258674.0030>
- Deng, R., Dias, P. R., Lunardi, M. M., & Ji, J. (2021). A sustainable chemical process to recycle end-of-life silicon solar cells. *Green Chemistry*, 23(24), 10157–10167. <https://doi.org/10.1039/d1gc02263f>
- Dias, P., Schmidt, L., Monteiro Lunardi, M., Chang, N. L., Spier, G., Corkish, R., & Veit, H. (2021). Comprehensive recycling of silicon photovoltaic modules incorporating organic solvent delamination – technical, environmental and economic analyses. *Resources, Conservation and Recycling*, 165, 105241. <https://doi.org/10.1016/j.resconrec.2020.105241>
- Ganesan, K., & Valderrama, C. (2022). Anticipatory life cycle analysis framework for sustainable management of end-of-life crystalline silicon photovoltaic panels. *Energy*, 245. <https://doi.org/10.1016/j.energy.2022.123207>



Ghosh, S., & Yadav, R. (2021). Future of photovoltaic technologies: A comprehensive review. *Sustainable Energy Technologies and Assessments*, 47, 101410.

<https://doi.org/10.1016/j.seta.2021.101410>

IRENA and IEA. (2016). End-of-life management: solar photovoltaic panels. In *International Renewable Energy Agency and the International Energy Agency Photovoltaic Power Systems*. Retrieved from

[http://www.irena.org/DocumentDownloads/Publications/IRENA IEAPVPS End-of-](http://www.irena.org/DocumentDownloads/Publications/IRENA_IEAPVPS_End-of-)

Klugmann-Radziemska, E., & Kuczyńska-Łażewska, A. (2020). The use of recycled semiconductor material in crystalline silicon photovoltaic modules production - A life cycle assessment of environmental impacts. *Solar Energy Materials and Solar Cells*, 205. <https://doi.org/10.1016/j.solmat.2019.110259>

Latunussa, C. E. L., Ardente, F., Blengini, G. A., & Mancini, L. (2016). Life Cycle Assessment of an innovative recycling process for crystalline silicon photovoltaic panels. *Solar Energy Materials and Solar Cells*, 156, 101–111.

<https://doi.org/10.1016/j.solmat.2016.03.020>

Lim, M. S. W., He, D., Tiong, J. S. M., Hanson, S., Yang, T. C. K., Tiong, T. J., Pan G. T., Chong, S. (2022a). Experimental, economic and life cycle assessments of recycling end-of-life monocrystalline silicon photovoltaic modules. *Journal of Cleaner Production*, 340, 130796. <https://doi.org/10.1016/j.jclepro.2022.130796>

Mathur, N., Singh, S., & Sutherland, J. W. (2020a). Promoting a circular economy in the solar photovoltaic industry using life cycle symbiosis. *Resources, Conservation and Recycling*, 155, 104649. <https://doi.org/10.1016/j.resconrec.2019.104649>



- Oteng, D., Zuo, J., & Sharifi, E. (2023). An evaluation of the impact framework for product stewardship on end-of-life solar photovoltaic modules: An environmental lifecycle assessment. *Journal of Cleaner Production*, 411, 137357. <https://doi.org/10.1016/j.jclepro.2023.137357>
- Ravikumar, D., Seager, T., Sinha, P., Fraser, M. P., Reed, S., Harmon, E., & Power, A. (2020). Environmentally improved CdTe photovoltaic recycling through novel technologies and facility location strategies. *Progress in Photovoltaics: Research and Applications*, 28(9), 887–898. <https://doi.org/10.1002/pip.3279>
- Singh, S., Powar, S., & Dhar, A. (2023). End of life management of crystalline silicon and cadmium telluride photovoltaic modules utilising life cycle assessment. *Resources, Conservation and Recycling*, 197, 107097. <https://doi.org/10.1016/j.resconrec.2023.107097>
- Singh, J. K. D., Molinari, G., Bui, J., Soltani, B., Rajarathnam, G. P., & Abbas, A. (2021). Life cycle analysis of disposed and recycled end-of-life photovoltaic panels in Australia. *Sustainability (Switzerland)*, 13(19), 1–16. <https://doi.org/10.3390/su131911025>
- Smith, B. L., Woodhouse, M., Horowitz, K. A. W., Silverman, T. J., Zuboy, J., & Margolis, R. M. (2021). *Photovoltaic (PV) module technologies: 2020 benchmark costs and technology evolution framework results*. Golden, CO: National Renewable Energy Laboratory. NREL/TP-7A40-78173
- State of California. (2015). *489 State of California, Hazardous Waste (Vol. 8)*. Retrieved from <https://legiscan.com/CA/text/SB489/id/1259603/California-2015-SB489->

[Amended.html](#)

Urbina, A. (2022). Standardization and regulations for PV technologies. *Green Energy and Technology*, 249–266. [https://doi.org/10.1007/978-3-030-91771-5\\_11](https://doi.org/10.1007/978-3-030-91771-5_11)

Washington State. (2019). Senate Bill 5939. *Angewandte Chemie International Edition*, 6(11), 951–952, 2. Retrieved from [https://lawfilesexternal.leg.wa.gov/biennium/2017-18/Pdf/Bills/Session Laws/Senate/5939-S.sl.pdf](https://lawfilesexternal.leg.wa.gov/biennium/2017-18/Pdf/Bills/Session%20Laws/Senate/5939-S.sl.pdf)

**Predicting Weather-Dependent Energy Savings for Low-Income Residential  
Buildings for Specific Upgrades with Limited Data**

Phillip Clayton

## Abstract

Energy efficiency in low-income residential buildings offers significant potential for reducing both carbon emissions and energy costs. This study develops a machine learning-based methodology to predict weather-dependent energy savings in low-income homes, utilizing limited building data. Leveraging detailed simulations from the National Renewable Energy Laboratory (NREL) and applying a nearest-neighbor approach, the model estimates potential energy savings for natural gas heating, electric heating, and electric cooling based on specific building modifications. A two-step clustering process refines predictions by removing outliers and improving accuracy. Results highlight that this approach is particularly effective for high-consumption buildings, which are often found in low-income areas. Additionally, a Python-based graphical user interface (GUI) enables both professionals and the public to easily access the results to make informed decisions about energy-saving improvements. This methodology provides targeted insights for utilities and city planners to prioritize energy-reduction initiatives, with significant implications for enhancing sustainability and supporting vulnerable communities.

Keywords: energy savings, machine learning, low-income households, energy efficiency, building upgrades

## Introduction

The pathway to sustainability is multifaceted, with one of the most effective strategies being the reduction of energy demand. While large-scale deployment of renewable energy is crucial, reducing energy consumption in existing buildings, particularly in low-income residential areas, offers significant potential for achieving carbon reduction at a lower cost. This study employs machine learning techniques to predict weather-dependent energy savings for low-income residential buildings based on specific upgrades, using limited building data.

The primary objective of this study is to develop a methodology that uses machine learning models to estimate potential energy savings for natural gas heating, electric heating, and electric cooling through various building modifications. By leveraging detailed energy profiles from the National Renewable Energy Laboratory (NREL) and comparing them with actual building data from Cincinnati, Ohio, the study aims to provide reliable savings estimates with minimal data input.

## Literature Review

Despite the widespread availability of energy modeling tools, there is a gap in the literature regarding tools that integrate machine learning with publicly available data to provide specific upgrade recommendations for low-income households. This study aims to address this gap by using a nearest-neighbor approach to estimate energy savings with minimal data requirements.

## Weather-Dependent Energy Savings for Low-Income Residential Buildings

Amasyali and El-Gohary (2018) reviewed the application of data-driven techniques in energy-consumption prediction, highlighting the strengths and limitations of machine learning models in building energy modeling. Their work underscores the potential of machine learning in capturing complex patterns in energy use, which this study leverages by focusing on the data constraints of low-income households (Amasyali & El-Gohary, 2018).

Ensemble machine learning models combine multiple learning algorithms to improve predictive performance compared to using a single model. This approach allows for more accurate energy savings predictions by aggregating the strengths of different algorithms. In the context of energy efficiency, Doukas (2023) demonstrates that ensemble models capture diverse patterns of energy consumption across buildings, which can be particularly beneficial when applied to data with varying characteristics. The lessons from Doukas' work are reflected in this study's focus on low-income households, where minimal data inputs are required, making the models accessible and practical for implementation at scale (Doukas, 2023).

Hu et al. (2022) discussed the use of k-nearest neighbor estimation in functional nonparametric regression models. K-nearest neighbor estimation is a nonparametric method used for classification and regression. The method identifies the k closest training examples in the data space and uses their values to predict the target variable for a new instance. Although the research of Hu et al. (2022) is centered on functional data analysis, it supports the theoretical foundation of this study's approach to energy savings estimation in residential buildings (Hu, Wang, Liu, & Yu, 2022).

Hallinan et al. (2011) conducted a multivariate analysis of energy consumption that provides a basis for understanding complex energy-use patterns in residential buildings. This study builds on their findings by applying advanced machine learning techniques to predict energy savings with limited data inputs (Hallinan et al., 2011).

Building on these foundational studies, this research employs a nearest-neighbor approach to provide specific and actionable upgrade recommendations for low-income households. By leveraging publicly available data and advanced machine learning techniques, this approach aims to fill a significant gap in the existing literature on energy efficiency and building energy modeling.

### Methods

#### Data and Model Development

Data from the National Renewable Energy Laboratory (NREL), encompassing 550,000 simulated buildings, approximately 21,000 of which were located in Ohio, were used for model development. These simulations included detailed information on residential energy use and building characteristics. Machine learning models were developed using H2O Flow, an open-source machine learning platform for building predictive models. These models focused on predicting energy consumption based on features such as

## Weather-Dependent Energy Savings for Low-Income Residential Buildings

attic insulation, wall insulation, infiltration, HVAC efficiency, and heating setpoint adjustments.

### **Prediction Methodology**

The methodology involves comparing actual building data from Cincinnati with NREL's simulated data through a nearest-neighbor approach. For each building, the 10 most similar simulated buildings are identified based on criteria such as area, natural gas heating, electric heating, and electric cooling. Mean savings are calculated for these 10 nearest neighbors.

### **Variability and Clustering**

To address variability in savings estimates, the coefficient of variation (CoV) is used as a measure of reliability. When CoV exceeds 0.2, indicating significant variability, clustering is applied to refine the predictions. Clustering groups the nearest neighbors into subgroups with similar values. In this research, the most common result was to have one cluster of zero values and one cluster of non-zero values. Clustering can be a good way of removing outliers. Often in this analysis, it would determine if the prevalent value is zero or not. If the larger cluster is all zeros, then the mean savings is concluded to be zero. If not, then the smaller cluster is removed to prevent them from skewing the data. This two-step clustering process enhances the accuracy of energy savings predictions.

## **Results**

The analysis demonstrated a notable inverse relationship between mean savings and CoV, particularly in buildings with high energy consumption. This indicates that the approach is particularly effective in identifying significant energy-saving opportunities in low-income, high-consumption homes. A Python-based graphical user interface (GUI) was developed to enable address-specific energy savings queries, providing a prioritized list of potential upgrades based on estimated mean savings and their associated CoV.

## **Discussion**

Low-income households often reside in older, less-efficient buildings, leading to disproportionately high energy costs relative to their income. Targeting these households for energy efficiency improvements can provide substantial benefits, both in terms of cost savings and quality of life. While financial constraints may hinder their ability to implement these upgrades without assistance, this study's findings can guide policymakers and utility companies in designing targeted support programs. By prioritizing high-consumption buildings, the methodology ensures that interventions are both impactful and cost-effective, helping to bridge the gap between energy efficiency and affordability. The methodology developed in this study offers a scalable and cost-effective approach to identify and prioritize energy-saving interventions. By using limited data inputs, the approach overcomes the barrier of resource-intensive traditional audits, making it accessible and practical for broader use. Focusing on high-consumption

## Weather-Dependent Energy Savings for Low-Income Residential Buildings

buildings in low-income areas is essential, as these buildings often present the greatest opportunities for energy savings and carbon reduction.

### **Future Work**

The next steps involve validating the estimated savings against actual energy consumption data to refine the methodology further. This validation process is crucial to ensure the accuracy and applicability of the predictions in real-world scenarios. Additionally, expanding the model to include more diverse building types and regions could enhance its generalizability.

### **Conclusion**

This study presents a novel approach to predicting energy savings in low-income residential buildings using machine learning and limited building data. By focusing on high-consumption buildings, the methodology provides targeted insights that can help utilities and city planners prioritize energy reduction initiatives effectively. This approach not only enhances sustainability but also supports vulnerable communities in achieving greater energy efficiency.

### **Conflict of Interest**

The author declares no conflict of interest.

### References

- Amasyali, K., & El-Gohary, N. M. (2018). A review of data-driven building energy consumption prediction studies. *Renewable and Sustainable Energy Reviews*, 81, 1192-1205.
- Doukas, H. (2023). Estimating the energy savings of energy efficiency actions with ensemble machine learning models. *Applied Sciences*, 13(4), 2749.
- Hu, X., Wang, J., Liu, L., & Yu, K. (2022). K-nearest neighbor estimation of functional nonparametric regression model under NA samples. *Axioms*, 11(3), 102.
- Hallinan, K. P., et al. (2011). Multivariate analysis of energy consumption. *Energy and Buildings*, 43(10), 2822-2831.



**Renewables in Recent and Future Heat Waves**

Nir Y. Krakauer

Department of Civil Engineering, The City College of New York

Earth and Environmental Sciences, City University of New York Graduate Center, New  
York, NY

[nkrakauer@ccny.cuny.edu](mailto:nkrakauer@ccny.cuny.edu)

### **Abstract**

Summer temperature extremes, particularly when accompanied by high humidity, drive peaks in power demand that can strain or even lead to failure of power grids. Here, I use meteorological reanalysis products to show regions where solar and wind availability were positively correlated with heat during summer 2023 to identify the potential of renewable energy to meet demand peaks and support energy resilience during heat waves.

Keywords: heat waves, solar energy, wind energy, grid resilience, global warming

### **Introduction**

Resilience of the electric grid during climate extremes is of increasing concern. Intermittent renewable sources, mainly solar and wind, are an increasing contributor to our electricity supply, so their reliability under extreme conditions is critical. Xu et al. (2024) provide a recent overview of the potential of distributed renewables for climate resilience, particularly as related to power outages associated with tropical cyclones, and highlight the need to study the interdependent "risks from escalating climate extremes and large-scale renewable integration."

Heat waves rank as a leading climate disaster category, and one which is steadily worsening due to global warming. In 2023, the USA recorded its largest-ever number of billion-dollar weather and climate disasters (as compiled by the NOAA National Centers for Environmental Information). Of these, the costliest and most deadly was the Southern/ Midwestern summer drought and heat wave. Texas, along with the world, recorded its hottest year on record, and also set a new record for deaths attributable to heat.

The Electric Reliability Council of Texas (ERCOT), which manages electricity supply for most of the state, recorded by far its highest electricity demand on record that summer. This demand was met without major power outages with the help of rapidly rising solar-generating capacity, which generally provided 10-16% of peak-hour demand, along with surging battery capacity. As of 2023, Texas had the most wind generation capacity of any state, and the second-highest solar generation and battery storage capacities, behind California. Nevertheless, many brief price spikes occurred in the ERCOT real-time electricity market, suggesting the need for additional clean power along with better grid management to improve summer grid reliability and reduce customer costs.

To better understand the availability of solar and wind resources during heat waves at different locations, I extracted hourly weather data for June–September 2023 from the fifth-generation European atmospheric reanalysis (ERA5), a global product informed by

extensive station and satellite data along with a state-of-the-art weather-forecast model (Hersbach et al., 2018; ERA, 2024).

### **Temperature-Solar Correlation**

First, I examined the correlation between the daily mean surface (2m height) temperature and the daily mean surface downward short-wave radiation flux (Figure 1a). A positive correlation would mean that hot summer days tend to also be more sunny, providing an ample solar resource that can be tapped to meet peak power demands. These correlations were, in fact, strongly positive for most land areas, including the southern, western, and central U.S. generally.

Correlations were more weakly positive for much of the Northeast and upper Mississippi Basin and were negative for many ocean areas. Inspection of daily power demand and solar energy output by state from the U.S. Energy Information Administration's Hourly Grid Electric Monitor for the same period showed patterns consistent with these ERA5 results, with strongly positive correlations between power demand and solar production in California and Texas, but only weakly positive ones in New York.

### **Temperature-Wind Correlation**

I also computed correlations between daily mean temperature and 100-m height wind speed (the wind speed was averaged from hourly values as  $(\bar{v^3})^{1/3}$  to better represent the proportionality of wind power to windspeed cubed) (Figure 1b). This correlation was near zero over many land and ocean areas, but was strongly positive for a large region that included the Great Plains, Texas, and eastern Mexico, for which hot days also tended to be windy. Indeed, in Texas, wind power made important contributions to evening power generation on many of the hottest days of summer 2023.

### **Correlations with Humid Heat**

Peak power demand depends not only on temperatures but also on humidity levels, with air at higher wet bulb temperature (WBT) requiring more energy to cool (Guan et al., 2017). Therefore, I computed hourly WBT from ERA5 2-m temperature, 2-m dew point, and surface pressure fields, using formulas from Sadeghi et al. (2013). Correlations of daily mean WBT with solar and wind resources, shown in Figure 2, tended to be less positive than those for temperature, but were still positive in Texas.

### **Discussion**

While preliminary (and needing to be confirmed by looking at more years and station data), these findings support the potential of solar and wind deployment, along with storage, to mitigate the impact of demand peaks during heat waves on grid reliability. This positive impact on resilience could be quantified for individual power grids, such as ERCOT, in more detailed follow-up modeling studies.

To comprehensively assess challenges to energy resilience during heat waves, a variety of other challenges and opportunities for grid resilience also need to be considered. Heavy air pollution, much of which is due to burning fossil fuels, reduces the solar resource substantially (Yang et al., 2022). Further, smoke from massive wildfires, which covered large parts of eastern North America for much of summer 2023, reduces solar generation, although also likely reducing the intensity of heatwaves in affected areas (Gilletly et al., 2023).

Contrarily, the recent implementation of low-sulfur fuel standards for global shipping has presumably increased solar resource availability, particularly close to shipping lanes, even while contributing to the acceleration of global warming (Ji et al., 2020). The ability of reanalysis products such as ERA5 to fully capture air pollution and smoke distribution as they impact solar resources needs to be validated. There are also other natural hazards whose co-occurrence with heatwaves should be prepared for.

Tropical cyclones can cause widespread destruction of power generation and transmission facilities, leaving people vulnerable to subsequent heatwaves (Matthews et al, 2019; Feng et al., 2020). Hailstorms, floods, and droughts are also increasingly likely to co-occur with heat waves and stress power grids by damaging generation and transmission facilities (Su et al., 2020; Stone et al., 2021; Yin et al., 2022; Gu et al., 2022). Resilient design of energy systems could include a diversity of sources and storage mediums as well as an emphasis on distributed generation (such as household-scale solar generation and neighborhood microgrids) and capacity for grid-independent operation during emergencies (Abdin et al., 2019; Bracken et al., 2023; Remund et al., 2023).

### **Conclusion**

In summary, recent operator experiences and meteorological data support the potential of renewable energy sources to provide power generation during heat waves. Additional work is needed to integrate renewables with power storage and transmission infrastructure for resilience during increasingly frequent and intense climate extremes.

### **Conflict of Interest**

The author declares that he has no conflicts of interest.

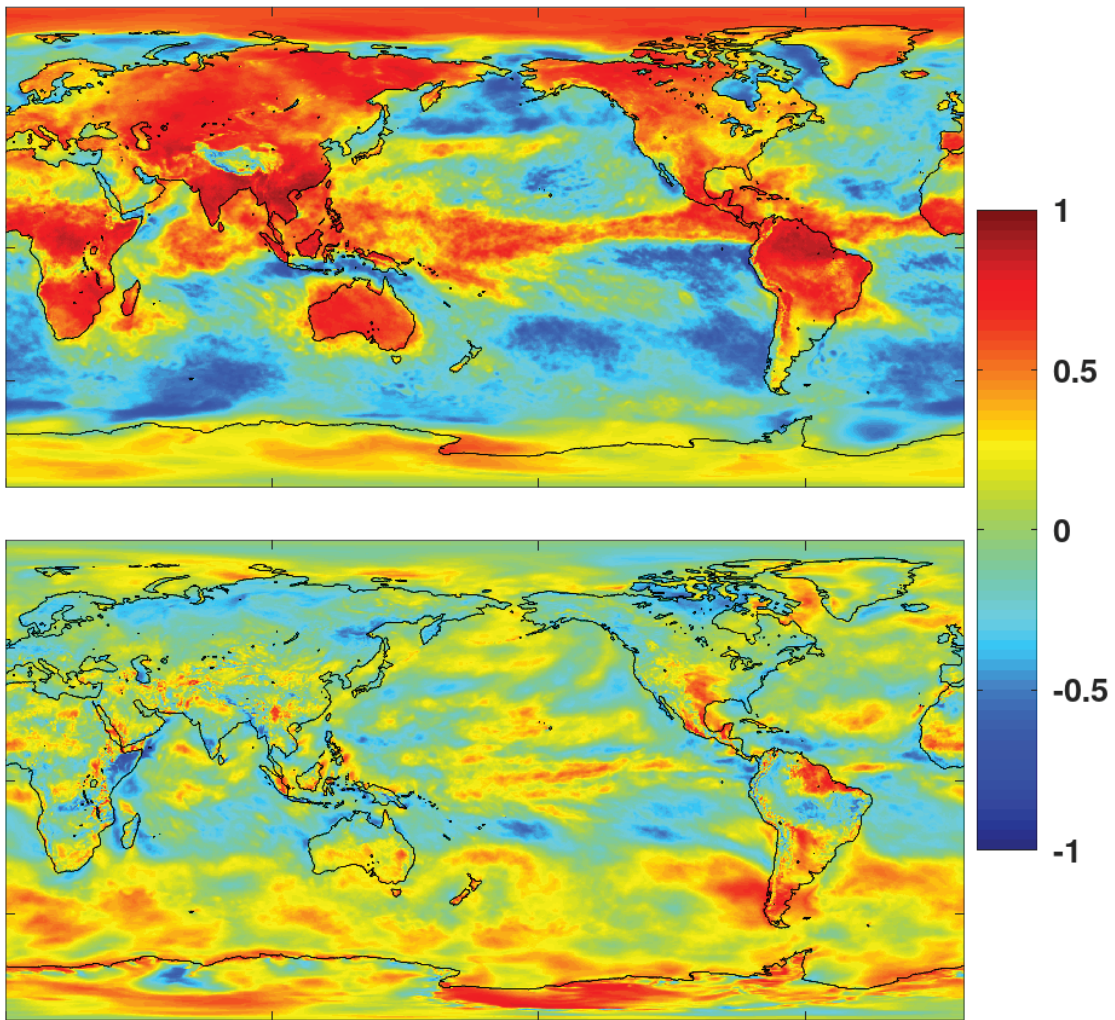


**Figure 1.** Correlation with daily-mean temperature for June-September 2023 of daily-mean (a [top]) solar irradiance and (b [bottom]) wind speed. Positive correlations generally indicate that hot days were likely to feature above-average solar and/or wind resources.



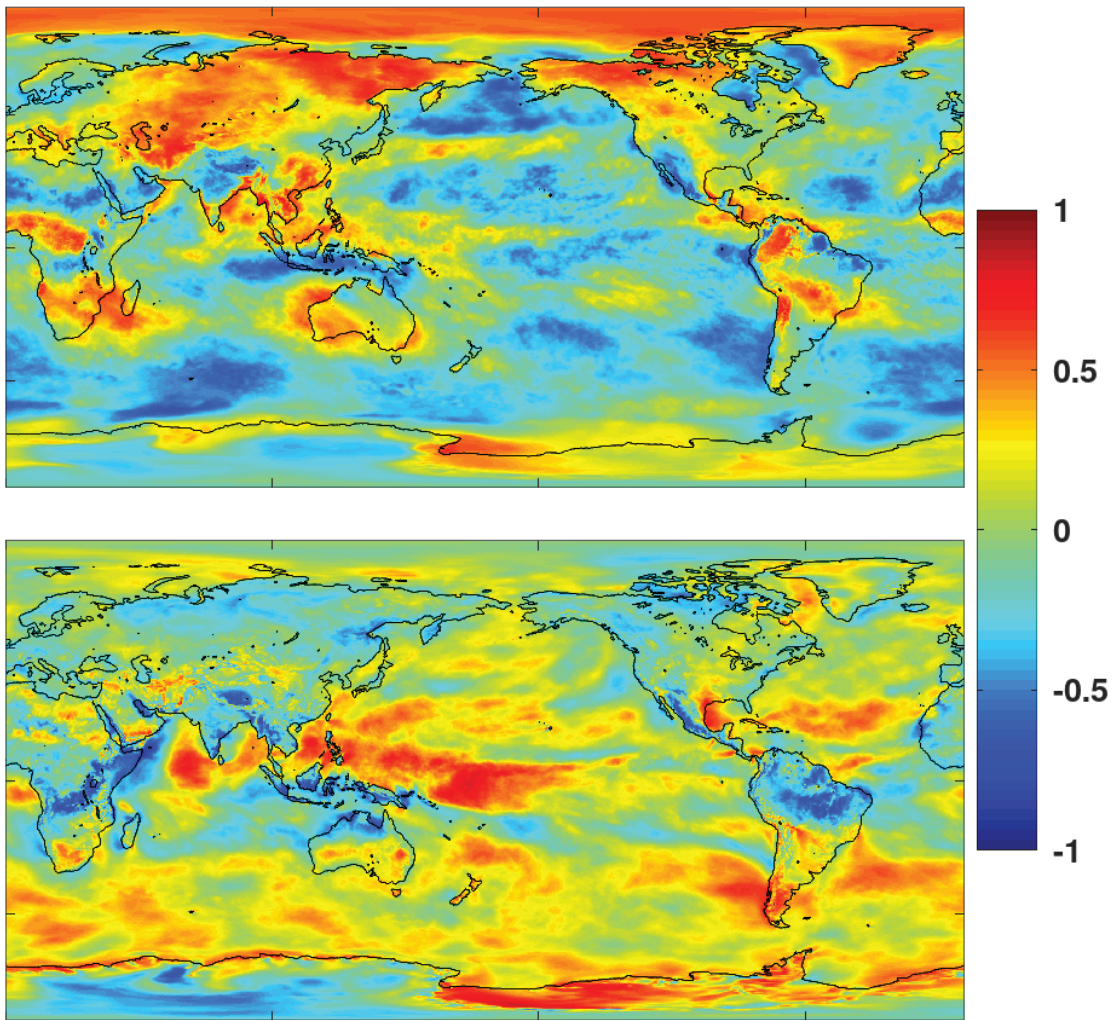


**Figure 2.** Same as Figure 1, but for daily-mean wet-bulb temperature instead of (dry-bulb) temperature.

**References**

- Abdin, A. F., Fang, Y.-P., & Zio, E. (2019). A modeling and optimization framework for power systems design with operational flexibility and resilience against extreme heat waves and drought events. *Renewable and Sustainable Energy Reviews*, 112, 706–719. <https://doi.org/10.1016/j.rser.2019.06.006>
- Bracken, C., Voisin, N., Burleyson, C. D., Campbell, A. M., Hou, Z. J., & Broman, D. (2023). Standardized benchmark of historical compound wind and solar energy droughts across the Continental United States. *Renewable Energy*, 119550. <https://doi.org/10.1016/j.renene.2023.119550>
- Feng, K., Min, O., & Lin, N. (2020). Hurricane-blackout-heatwave compound hazard risk and resilience in a changing climate. *arXiv*, 2012. <http://arxiv.org/abs/2012.04452v1>
- Gilletly, S. D., Jackson, N. D., & Staid, A. (2023). Evaluating the impact of wildfire smoke on solar photovoltaic production. *Applied Energy*, 348, 121303. <https://doi.org/10.1016/j.apenergy.2023.121303>
- Gu, L., Chen, J., Yin, J., Slater, L. J., Wang, H.-M., Guo, Q., Feng, M., Qin, H., & Zhao, T. (2022). Global increases in compound flood-hot extreme hazards under climate warming. *Geophysical Research Letters*, 49(8). <https://doi.org/10.1029/2022gl097726>
- Guan, H., Beecham, S., Xu, H., & Ingleton, G. (2017). Incorporating residual temperature and specific humidity in predicting weather-dependent warm-season

electricity consumption. *Environmental Research Letters*, 12(2), 24021.

<https://doi.org/10.1088/1748-9326/aa57a9>

Hersbach, H., de Rosnay, P., Bell, B., Schepers, D., Simmons, A., Soci, C., Abdalla, S., Alonso-Balmaseda, M., Balsamo, G., Bechtold, P., Berrisford, P., Bidlot, J.-R., de Boissésou, E., Bonavita, M., Browne, P., Buizza, R., Dahlgren, P., Dee, D., Dragani, R., et al. (2018). *Operational global reanalysis: progress, future directions and synergies with NWP* (No. 27). ECMWF.

<https://doi.org/10.21957/tkic6g3wm>

Ji, J. S. (2020). The IMO 2020 sulphur cap: a step forward for planetary health? *The Lancet Planetary Health*, 4(2), e46–e47. [https://doi.org/10.1016/s2542-5196\(20\)30002-4](https://doi.org/10.1016/s2542-5196(20)30002-4)

Matthews, T., Wilby, R. L., & Murphy, C. (2019). An emerging tropical cyclone–deadly heat compound hazard. *Nature Climate Change*, 9(8), 602–606.

<https://doi.org/10.1038/s41558-019-0525-6>

Remund, J., Perez, R., Perez, M., Pierro, M., & Yang, D. (2023). Firm photovoltaic power generation: overview and economic outlook. *Solar RRL*, 7(23).

<https://doi.org/10.1002/solr.202300497>

Sadeghi, S.-H., Peters, T. R., Cobos, D. R., Loescher, H. W., & Campbell, C. S. (2013). Direct calculation of thermodynamic wet-bulb temperature as a function of pressure and elevation. *Journal of Atmospheric and Oceanic Technology*, 30(8), 1757–1765. <https://doi.org/10.1175/JTECH-D-12-00191.1>



Stone, B., Mallen, E., Rajput, M., Gronlund, C. J., Broadbent, A. M., Krayenhoff, E. S., Augenbroe, G., O'Neill, M. S., & Georgescu, M. (2021). Compound climate and infrastructure events: how electrical grid failure alters heat wave risk. *Environmental Science & Technology*, 55(10), 6957–6964.

<https://doi.org/10.1021/acs.est.1c00024>

Su, Y., Kern, J. D., Reed, P. M., & Characklis, G. W. (2020). Compound hydrometeorological extremes across multiple timescales drive volatility in California electricity market prices and emissions. *Applied Energy*, 276, 115541.

<https://doi.org/10.1016/j.apenergy.2020.115541>

Xu, L., Feng, K., Lin, N., Perera, A. T. D., Poor, H. V., Xie, L., Ji, C., Sun, X. A., Guo, Q., & O'Malley, M. (2024). Resilience of renewable power systems under climate risks. *Nature Reviews Electrical Engineering*, 1(1), 53–66.

<https://doi.org/10.1038/s44287-023-00003-8>

Yang, L., Gao, X., Li, Z., & Jia, D. (2022). Quantitative effects of air pollution on regional daily global and diffuse solar radiation under clear sky conditions. *Energy Reports*, 8, 1935–1948. <https://doi.org/10.1016/j.egy.2021.12.081>

Yin, J., Slater, L., Gu, L., Liao, Z., Guo, S., & Gentile, P. (2022). Global increases in lethal compound heat stress: hydrological drought hazards under climate change. *Geophysical Research Letters*, 49(18).

<https://doi.org/10.1029/2022gl100880>

**Experimental Study of Ambient Dusts and Installment Orientations Effects on  
Solar Panel Efficiency**

Xiuhua Si <sup>1</sup>  
Annabelle Jin <sup>1</sup>  
James Dai <sup>1</sup>  
Jinxiang Xi <sup>2</sup>

<sup>1</sup> Department of Aerospace, Industrial, and Mechanical Engineering, California Baptist  
University, Riverside, CA

<sup>2</sup> Department of Biomedical Engineering, University of Massachusetts, Lowell, MA

## Abstract

Most solar panels are stationary without cleaning systems. However, solar panels' power-generating efficiency can be significantly impacted by sunlight intensity and dusts. To remedy this, one method is to maximize the panel's light-catching ability and the other is to keep the panel clean. We systematically studied solar panel efficiency with a panel aligned in different directions relative to the sunlight. We also investigated the dusts' effects by measuring the power output under controlled dust coverages. The results showed that solar panel efficiency can increase by 40% if the panel can follow the sun. Dust deposition can reduce efficiency by 75%. Information on ambient dust concentrations was collected at different locations in southern California, including a house roof, an agriculture field, a highway side, and a cattle ranch. The correlation between the solar panel efficiency and dust coverage was developed to estimate the solar farm performance under various dust coverages.

Keywords: solar panel, dust coverage, installation angle

## 1. Introduction

The escalating threat of global warming has emerged as a paramount concern for our planet. Governments worldwide are united in their concerted efforts to decelerate the pace of this phenomenon, striving to bequeath a verdant and sustainable earth to future generations. A crucial step in this endeavor lies in transitioning away from our reliance on fossil fuels as the primary energy source and embracing renewable and clean alternatives. These alternatives encompass a diverse array of options, including solar, wind, hydroelectric, geothermal, ocean, and bioenergy sources, each offering a promising path toward a greener and more sustainable future (Aberle et al., 2011; Ang et al., 2022; Jamalabadi and Xi 2023; Paraschiv and Paraschiv 2023).

The key milestone in the exponential growth of solar and wind energy is illustrated in Fig. 1a (Jaeger 2021). In 2000, Germany established renewable energy legislation, and in 2009, the U.S. and China made major stimulus investments in renewable energy (Zhang et al., 2014). After that, new solar and wind energy annual installations matched fossil fuels for the first time. Solar PV became cost-competitive with fossil fuel power and the Paris Agreement was established in 2015 (Skjærseth et al., 2021). In 2021, renewable energy become cheaper than existing coal power for the first time. Figure 1b shows the growth of the renewable energy share, which grew from around 20% in 2001 to 82% in 2020 (Benny 2024). Among the renewable energy sources, wind power and solar PV wave are the two main ones that have been applied. The U.S. has a goal that the renewable generation will reach 44%–45% of U.S. electricity by 2050. In 2008, solar energy was only a very small portion of the total renewable energy. Since then, solar energy has been gradually growing, with the goal that by 2050, 44%–45% of the renewable energy will be solar power (Jones-Albertus 2021).

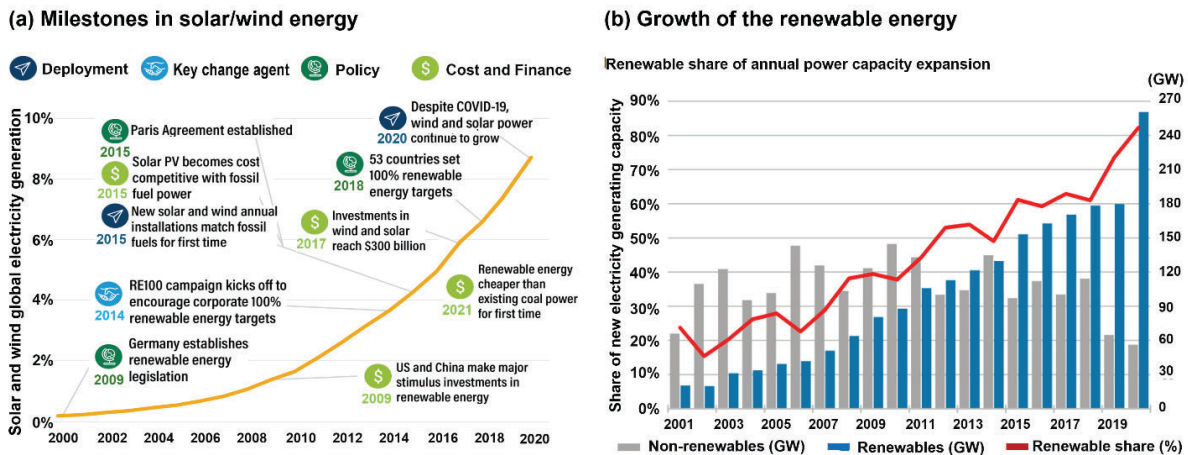


Fig. 1. (a) Key milestones in the exponential growth of solar and wind energy (adapted from Jaeger (2021)) and (b) Renewable share of annual power capacity expansion (adapted from Benny (2024)).

Solar power becomes an important player in future power supply. Different factors can affect solar panel power generation efficiency. The first concern is the degradation of the solar panel with time. However, previous studies showed that solar panel degradation after 25 years was less than 20%, which is small when compared with the degradation rate of other sources of power generation such as the traditional fossil fuel power plant, which needs periodic repair and maintenance (Aghaei et al., 2022; Noman et al., 2022; Olczak 2023; Zhang et al., 2021). Even with this degradation, the same panel after 25 years is still expected to generate 80% of the designed power capacity.

The second factor affecting solar efficiency is the solar panel’s orientation relative to the sunshine (Mamun et al., 2022; Prunier et al., 2023; Sharma et al., 2020). Figure 2 shows the simulated energy production of one kilowatt of solar PV capacity in Los Angeles, California.

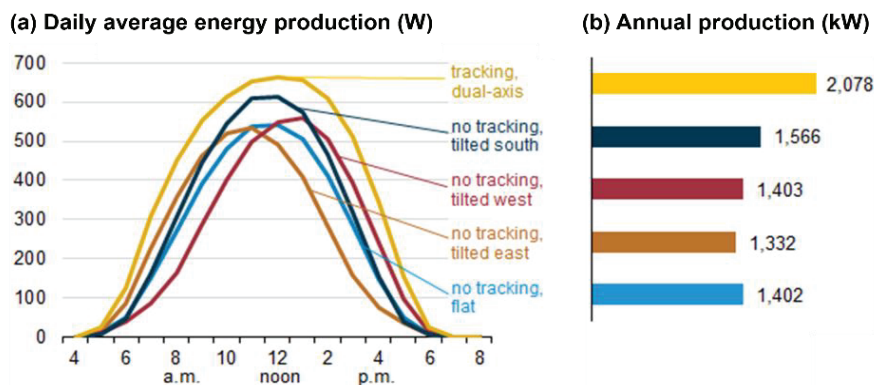


Fig. 2. (a) Average energy production in a day (W) and (b) Annual energy production (KW) (adapted from Zawaydeh 2015).

In Fig. 2, the solar panel with sunlight tracking generates the highest power, which is about 650 watts (Zawaydeh, 2015). By comparison, a solar panel with no tracking tilted south generates 50 watts less power, whereas a panel with no tracking that is flat generates 150 watts less power. Note that no tracking flat, no tracking tilted east, and no tracking tilted west generate approximately similar amounts of power (Fig. 2b). Within a year, the annual energy production of the same panel tracking sunlight generates 30% or more power than no tracking flat or no tracking tilted south/east/west.

Overall, multiple factors exist affecting solar panel power generation efficiency: wind speed, ambient temperature, solar intensity, dust accumulation, shading, soiling and panel orientation. Among these factors, dust deposition and panel face orientation toward the sunshine can be readily changed. The objective of this study is to better understand the dust deposition and panel orientation effects on solar panel power generation. Specific aims include:

- (1) To systematically study the factors affecting the power-generating efficiency of the solar panel with different orientations and dust accumulations
- (2) To quantify the effects of ambient dust on solar panel efficiency
- (3) To propose strategies to optimize the power-generation efficiency of the solar panel

## 2. Method and Materials

An HP-866B anemometer (HoldPeak Inc.) was used to measure the wind speed (Fig. 3a). An electric fan was used to simulate wind (Fig. 3b). A VPC300 particle counter from ExTech Instruments was used to mirror the number of particles in the air at different locations (Fig. 3c). The particle counter has six channels, measuring the number of particles with diameters of 0.3, 0.5, 1.0, 2.5, 5.0, and 10.0  $\mu\text{m}$ , respectively. A 2 $\times$ 2-ft solar panel from Dokio made from monocrystalline silicon was used to test the power output under various scenarios (Fig. 3d). Different types of dust particles were considered, including the natural dust deposited on the panel surface, dirt dust, and flour powder.



Fig. 3. Experimental methods and instruments: (a) anemometer, (b) electric fan, (c) particle counter, and (d) solar panel. (Photo credit: Xiuhua Si.)

## 3. Results

### 3.1 Dust coverage area and dust particle color



Figure 4a shows two dust-covered solar panels. A thick layer of dust particles covered the entire area of the first solar panel. Beside dust particles, there were also kernels, leaves, and other types of debris accumulated on top of the second panel. Figure 4b shows three solar panels with different dust coverages in preparation for experimental tests. Dirt particles were evenly distributed on the first panel. The second panel was covered with flour powders to assess the color effects. The third panel was covered with a flour solution that was applied to the panel surface by a brush. Depending on the test condition, the coverage could be even or scattered, and one layer or multiple layers.

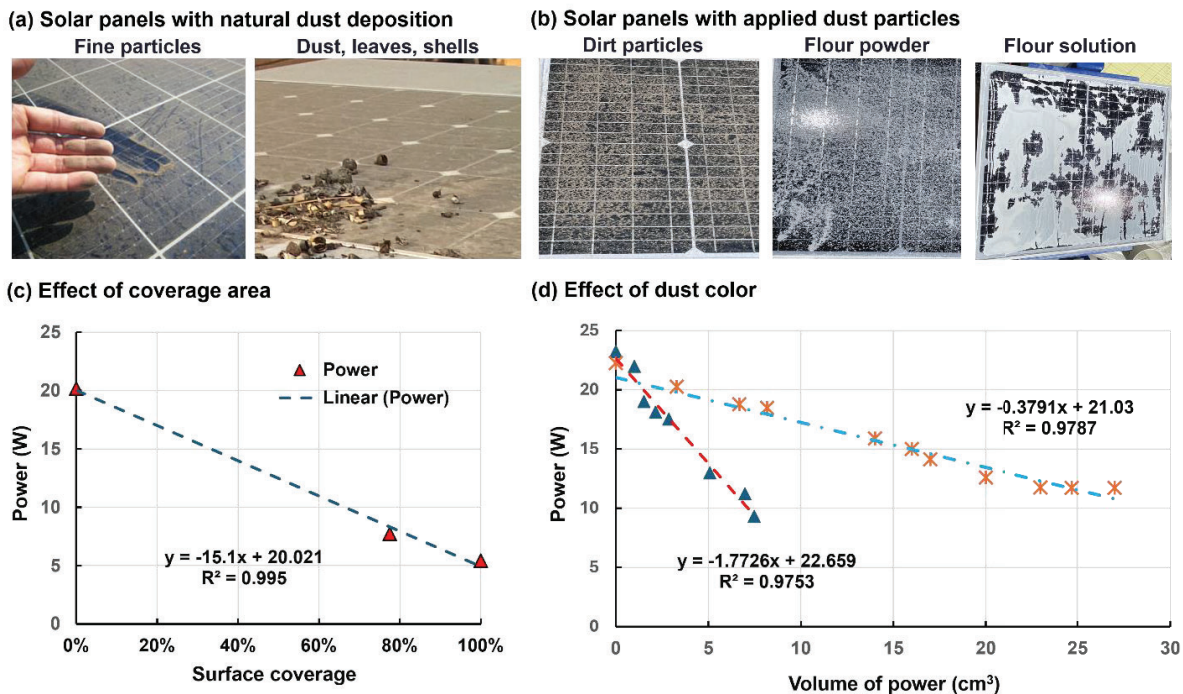


Fig. 4. Experimental results: (a) panels covered by scattered dust particles and fully covered by a thick layer of mud-like dusts, (b) experimental panels covered by different particles, (c) power output effects of surface area coverage, and (d) power output effects of scattered particles and colors of particles. (Photo credit: Xiuhua Si.)

We first compared solar panels fully covered and scatter-covered by dust. Flour powders were used to cover different regions of the solar panel. The power outputs by the solar panel were measured, as shown in Fig. 4c. Clearly, the more area was covered, the less power was generated. Power decreased linearly with increasing coverage. We also scattered different types of dusts on the panel surface. The more powder was scattered, the less power was generated.

The color of the dust was also found to affect the power generation of a solar panel. The lighter the dust color was, the smaller effect it had on the power generation. In Fig. 4d, the blue line (with the brown asterisk) represents the power generated by the panel covered with white powders. The red line (with the blue data symbols) represents the power generated by the panel covered with dirt dust (the brown color). Apparently, the

white powder has less of a negative effect on the power generation of the solar panel than the brown dust does.

### 3.2 Coverage Thickness Effect

We also simulated the situation when the solar panel was covered by a thicker layer of material, with different numbers of leaves scattered on the solar panel that was already covered by fine dust particles. It is clearly visible in Figure 5 that the more leaves were on the panel, the less power was generated, as demonstrated by the power output variation from Fig. 5a to Fig. 5c. The relatively large area of leaves and their irregular shapes form shade that can effectively block the sunshine reaching the PV panel.

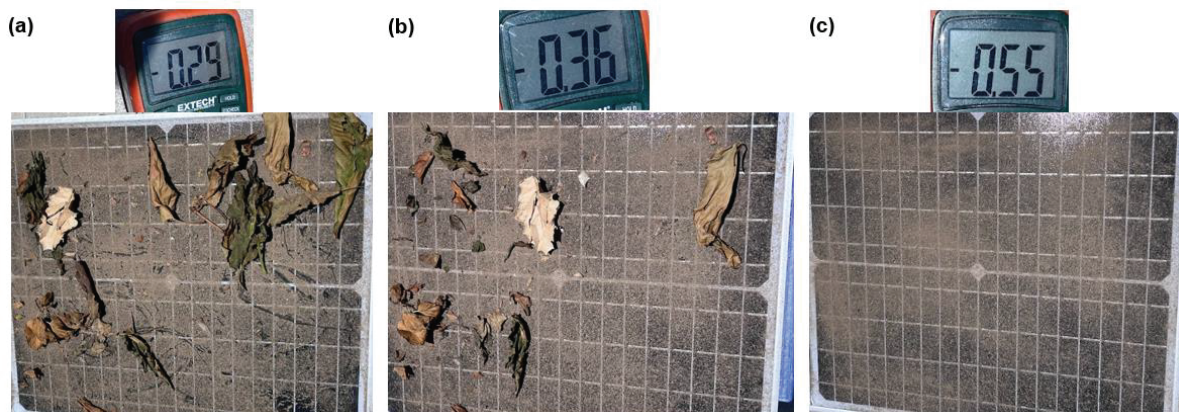


Figure 5. Coverage with dust and leaves: (a) 30% coverage with leaves, (b) 15% coverage with leaves, and (c) no leaves. (Photo credit: Xiuhua Si.)

When small raindrops fall on the solar panel covered with very fine dust particles, ring-shaped patterns form. More rain droplets or condensates can form liquid streams, leaving furrow-shaped patterns. In both conditions, dust coverages with varying thicknesses can form (Fig. 6a). As alluded to above, the thicker the dust coverage is, the less power will be generated.

For a partially covered solar panel, if the dust particles are more scattered, will it affect the total power generation? Figure 6b shows the power output with different amounts of dust particles. The number of particles did exert a noticeable effect on the power generation, but when compared with a fully covered panel, this effect is much smaller.

## Ambient Dusts and Installment Orientations Effects on Solar Panels

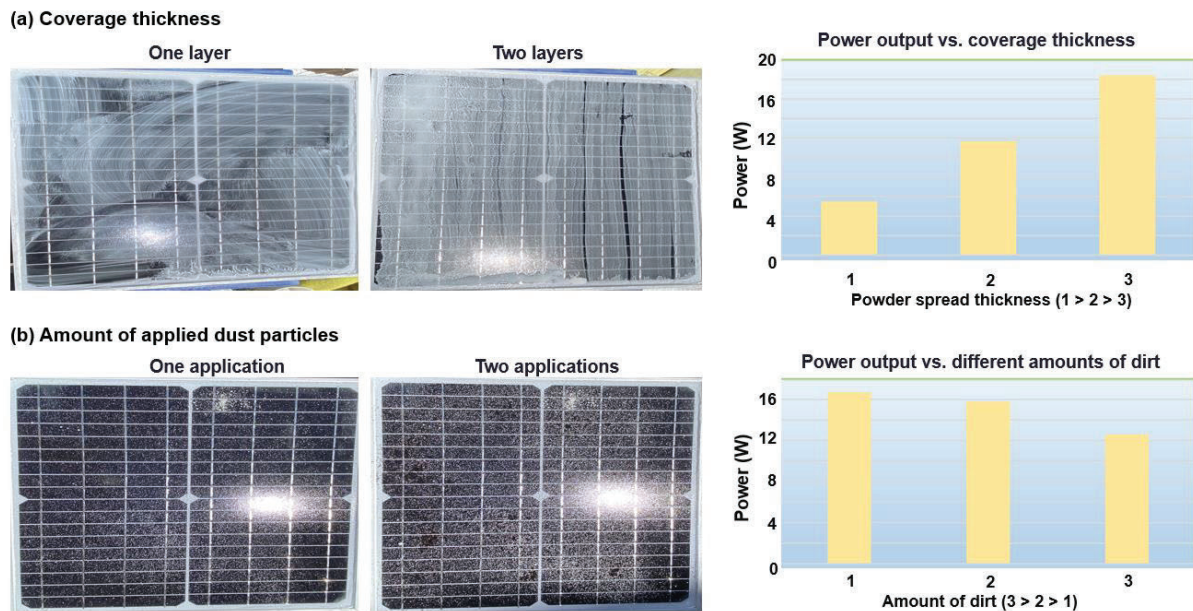


Fig. 6. Coverage layers and amounts of dust: (a) coverage thickness effect due to one layer or two layers of brushed flour solution 30% coverage with leaves, (b) effect of the amount of applied dust particles. (Photo credit: Xiuhua Si.)

### 3.3 Solar Panel Installation Angle Effect

Figure 7 shows photos of solar panels on top of the engineering building at California Baptist University that were installed in 2018. In the first photo (Fig. 7a), the panels were installed on top of the roof and parallel to the direction of the roof, facing south. Figure 7b shows the panels installed on slant frames, whose angle is almost straight up relative to the roof (Fig. 7b). The rightmost photo is a zoomed view of one of the panels in Fig. 7b. Compared with the panels in Fig. 7a, where there is a much smaller slope angle, far fewer dust particles are on the surface of the nearly straight-up panels in Fig. 7b.

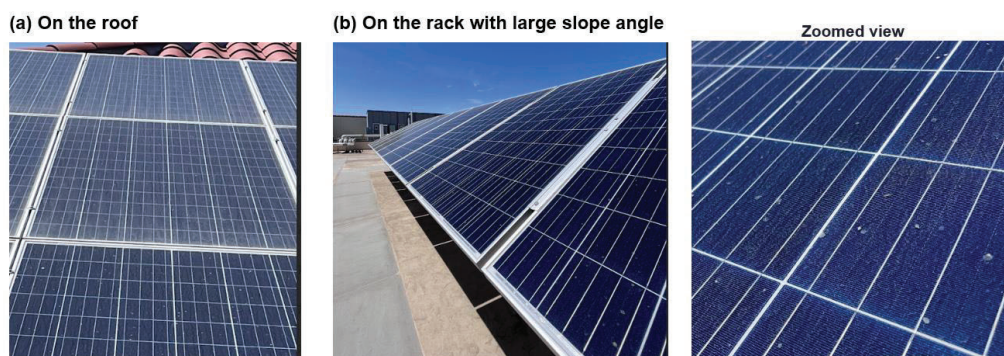


Fig. 7. Panel installation angle: (a) on the roof, and (b) on the rack with a large slope angle (Photo credit: Xiuhua Si.)



Figure 8 shows photos of the experimental solar panels with different amounts of dust particles on the surface. The power output decreases with increasing dust mass. Furthermore, this relationship is not strictly linear. This might be due to the fact that some particles pile up without spreading.



Fig. 8. Nonlinear panel output vs. applied dust amount (Photo credit: Xiuhua Si.)

### 3.3 Ambient Dust at Different Locations

It is crucial to know what kinds of dust aerosols are there and how many dust particles will be deposited on the solar panels. To research this question, we visited different solar farms in southern California. The first was in a parking lot in Riverside city suburb. The second was on top of a four-floor parking structure near a highway. The third was in a desert area. The fourth was on a mountainside (Fig. 9a). A particle counter was used to measure the particle-size distribution of the ambient air. Particles smaller than  $1.0\ \mu\text{m}$  can easily follow the airflow. If the ambient aerosol has more particles above  $1.0\ \mu\text{m}$ , the panels will be likely to collect more particles.

#### (a) Different locations



#### (b) Dust particle measurements

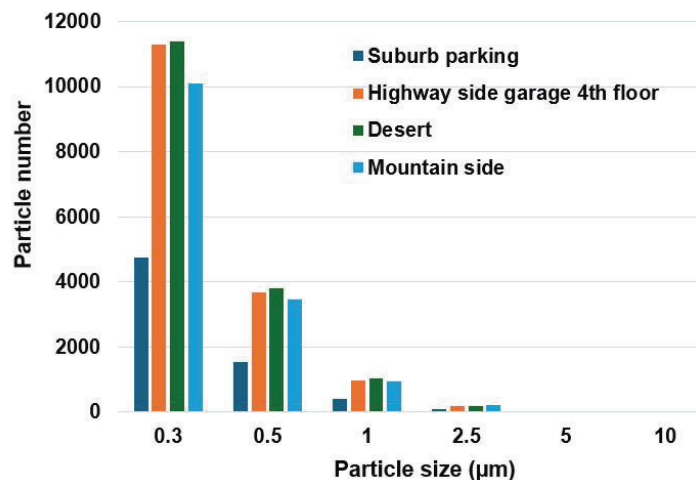


Fig. 9. Ambient dust measurements: (a) different locations, (b) particle count measurement (Photo credit: Xiuhua Si.)

## Ambient Dusts and Installment Orientations Effects on Solar Panels

Table 1. Dust size distribution at different locations

| PM ( $\mu\text{m}$ ) | Suburb parking | Highway side garage 4th floor | Desert | Mountain side |
|----------------------|----------------|-------------------------------|--------|---------------|
| 0.3                  | 4765           | 11290                         | 11386  | 10096         |
| 0.5                  | 1545           | 3682                          | 3791   | 3447          |
| 1.0                  | 389            | 979                           | 1031   | 941           |
| 2.5                  | 78             | 182                           | 197    | 205           |
| 5.0                  | 11             | 12                            | 19     | 26            |
| 10.0                 | 6              | 4                             | 11     | 9             |

As shown in Table 1 and Fig. 9b, the number of particles in the desert area is slightly larger than the number of particles on the mountainside and at the highway-side parking structure and much larger than that at the suburb parking. Especially for PM<sub>2.5</sub> (i.e., particulates  $\leq 2.5 \mu\text{m}$  in diameter), the number of particles in the desert, highway-side parking structure, and mountainside are more than twice that at the suburb parking. Based on these data, the frequency of panel dust cleaning can be calculated to ensure optimal power generation with minimized incurred cleaning costs.

Considering that the desert area is often windy, we used an electric fan to simulate the effect of wind speeds in the desert area on the measurement of the particle counter (Fig. 10a). As shown in Fig. 10b, the higher the wind speed is, the more particles are measured. Thus, in the desert area, knowledge of the average wind speed is needed to predict how often those panels need to be cleaned or washed.

(a) Setup with various wind speed



(b) Dust particle measurements

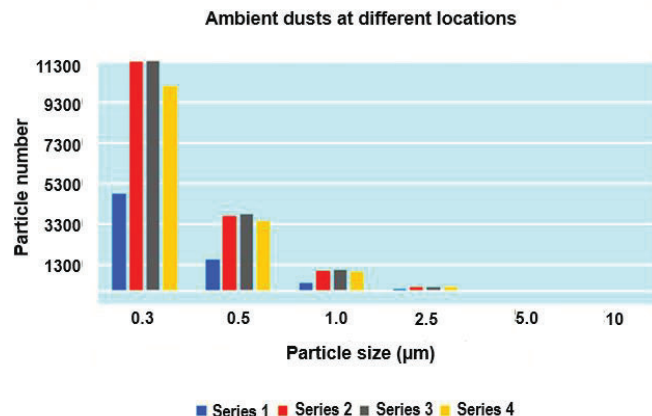


Figure 10. Ambient dust measurements: (a) different locations, (b) particle count measurement (Photo credit: Xiuhua Si.)

### 3.5 Panel Orientation Effects in Southern California

Figures 11a and 11b show the solar power output at three orientations on April 12, 2022 in the morning (9 am – noon) and afternoon (noon – 5:45 pm), respectively. The three orientations considered include: flat (or  $0^\circ$  angle toward the sun in Figs. 11a & 11b),  $20^\circ$

tilted from flat toward the sun, and 20° tilted from flat away from the sun. Measurements were taken every 30 minutes from 9:30 am to 5:45 pm.

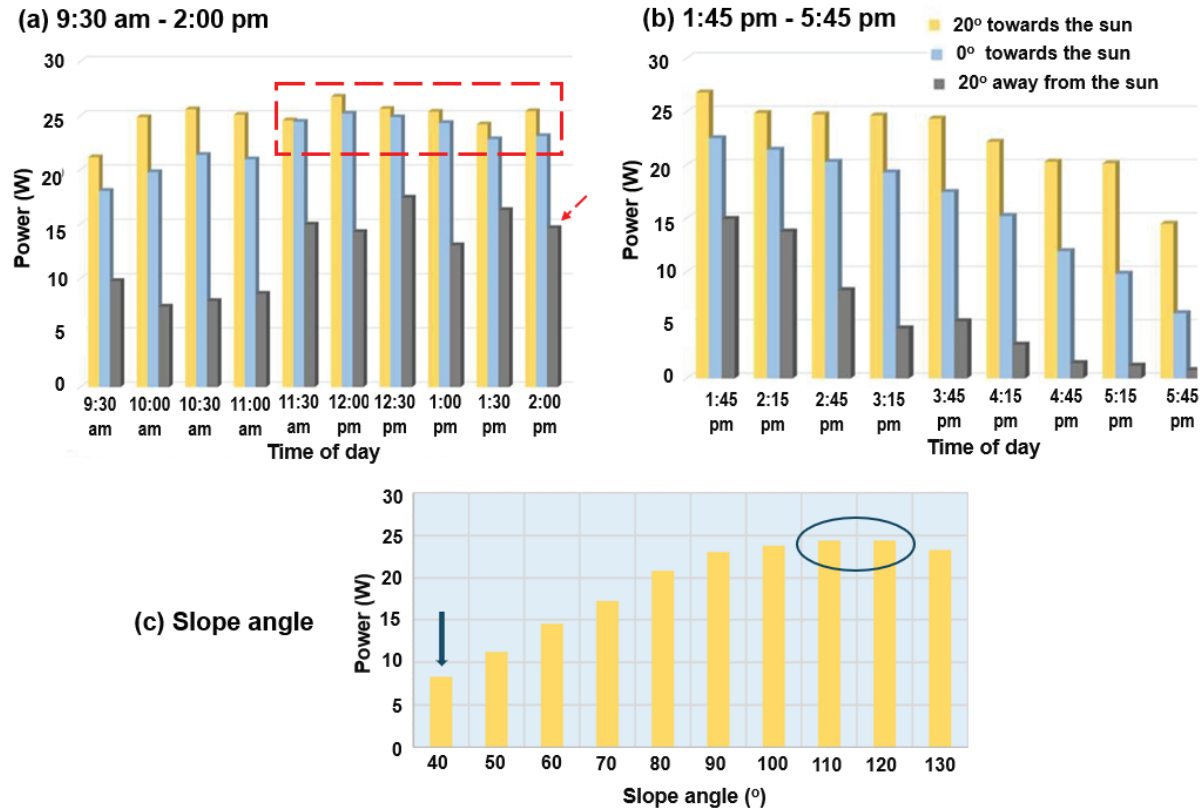


Fig. 11. Power output at three panel orientations: (a) 9:30 am – 2:00 pm; and (b) 1:45 pm – 5:45 pm; and (c) power output at different angles to the direction of the sunshine at 12:00 pm-1:00 pm.

Clearly, from 11:30 am to 2:00 pm, the flat panel and the panel tilted 20° toward the sun generated very similar amounts of power, as highlighted by the dashed rectangle in Fig. 11a. However, in the early morning or late afternoon, the panel tilted 20° toward the sun generated significantly more power, which was 20% more than the flat panel and 75% more than the panel at 20° away from the sun (Figs. 8a and 8b). This suggests the importance of the panel orientation, particularly in the early morning or late afternoon when the sunshine has large incidental angles.

To identify the optimal panel orientation, we gradually changed the panel orientation angles from flat (0°) toward the south to 40°, 50°, 60°, 70°, 80°, till 130° from noon to 2:30 pm. It is clearly observed that panels at an angle of 110° and 120° generate the highest power, while 40° generated the least, as indicated by the filled arrow in Fig. 11c. Moreover, the power output increased steadily from 40° to 100°.

#### 4. Conclusion

## Ambient Dusts and Installment Orientations Effects on Solar Panels

1. Panels standing in a more vertical direction will greatly reduce the deposition of dust.
2. A periodic cleaning schedule depending on the dust level of different locations will greatly enhance the power generation.
3. The average power output of the solar panel at 20° toward the sun is 40% more than that generated by the same panel at a flat position.
4. The power generated at the optimal angle can be three times more than that generated at the least effective direction.
5. The flat panel can generate up to 75% more power than the panel tilted 20° away from the sunshine.
6. A sun-following solar panel can significantly increase power generation. It is more significant than periodic cleaning in most of the desert areas where dust particles are scattered on the panel without fully covering it.
7. Power-generation reduction caused by coverage with different types of dirt is less significant compared with the power-generation reduction based on the orientation of the panel. The color of the dirt and the total area covered are both factors to be considered. Periodic cleaning of the panel will increase the power generation.

Several future studies are warranted. These include designing a programmed cleaning robot to automatically clean the panel periodically, with a frequency depending on average wind speeds, dust level, and rainy weather. A sun-following control device would be designed and installed on existing and future panels. Systematically studying the effects of temperature, solar insolation, shading, and humidity is necessary to identify the optimal use of solar power in different areas according to their specific climates and to provide advice to different local governments for renewable energy-development plans.

**Conflict of Interest**

The authors declare that they have no known competing financial interests or personal relationships that could have appeared to influence the work reported in this paper.

## References

- Aberle, D. R., Adams, A. M., Berg, C. D., Black, W. C., Clapp, J. D., Fagerstrom, R. M., Gareen, I. F., Gatsonis, C., Marcus, P. M., and Sicks, J. D. (2011.) Reduced lung-cancer mortality with low-dose computed tomographic screening. *New England Journal of Medicine*. 365(5), 395-409.
- Aghaei, M., Fairbrother, A., Gok, A., Ahmad, S., Kazim, S., Lobato, K., Oreski, G., Reinders, A., Schmitz, J., Theelen, M., Yilmaz, P., and Kettle, J. (2022.) Review of degradation and failure phenomena in photovoltaic modules. *Renewable and Sustainable Energy Reviews*. 159, 112160.
- Ang, T.-Z., Salem, M., Kamarol, M., Das, H. S., Nazari, M. A., and Prabakaran, N. (2022.) A comprehensive study of renewable energy sources: Classifications, challenges and suggestions. *Energy Strategy Reviews*. 43, 100939.
- Benny, J. (2024.) "Renewable energy growth sets new record in 2023 but more needed to hit 2030 target." *The National*, March 27, 2024, <https://www.thenationalnews.com/business/energy/2024/03/27/>.
- Jaeger, J. (2021). "Supercharging the renewables revolution." *World Resources Institute*, Sept. 23, 2021, <https://climatechampions.unfccc.int/supercharging-the-renewables-revolution/>.
- Jamalabadi, M.-Y.-A., and Xi, J. (2023.) Optimal design of porous media in solar vapor generators by carbon fiber bundles. *Frontiers in Heat and Mass Transfer*. 21(1), 65-79.



- Jones-Albertus, B. (2021.) "Solar Futures Study." U.S Department of Energy, <https://www.energy.gov/sites/default/files/2021-09/Solar%20Futures%20Study.pdf>.
- Mamun, M. A. A., Islam, M. M., Hasanuzzaman, M., and Selvaraj, J. (2022.) Effect of tilt angle on the performance and electrical parameters of a PV module: Comparative indoor and outdoor experimental investigation. *Energy and Built Environment*. 3(3), 278-290.
- Noman, M., Tu, S., Ahmad, S., Zafar, F. U., Khan, H. A., Rehman, S. U., Waqas, M., Khan, A. D., and Rehman, O. U. (2022.) Assessing the reliability and degradation of 10-35 years field-aged PV modules. *PLoS One*. 17(1), e0261066.
- Olczak, P. (2023.) Evaluation of degradation energy productivity of photovoltaic installations in long-term case study. *Applied Energy*. 343, 121109.
- Paraschiv, L. S., and Paraschiv, S. (2023.) Contribution of renewable energy (hydro, wind, solar and biomass) to decarbonization and transformation of the electricity generation sector for sustainable development. *Energy Reports*. 9, 535-544.
- Prunier, Y., Chuet, D., Nicolay, S., Hamon, G., and Darnon, M. (2023.) Optimization of photovoltaic panel tilt angle for short periods of time or multiple reorientations. *Energy Conversion and Management: X*. 20, 100417.
- Sharma, M. K., Kumar, D., Dhundhara, S., Gaur, D., and Verma, Y. P. (2020.) Optimal tilt angle determination for PV panels using real time data acquisition. *Global Challengs*. 4(8), 1900109.
- Skjærseth, J. B., Andresen, S., Bang, G., and Heggelund, G. M. (2021.) The Paris agreement and key actors' domestic climate policy mixes: comparative patterns.

*International Environmental Agreements: Politics, Law and Economics*. 21(1), 59-73.

Zawaydeh, S. (2015.) *Economic, environmental and social impacts of development of energy from sustainable resources – case study Jordan*. World Energy Engineering Congress, Orlando, Florida, pp. 1-20.

Zhang, J., Temmer, M., Gopalswamy, N., Malandraki, O., Nitta, N. V., Patsourakos, S., Shen, F., Vršnak, B., Wang, Y., Webb, D., Desai, M. I., Dissauer, K., Dresing, N., Dumbović, M., Feng, X., Heinemann, S. G., Laurenza, M., Lugaz, N., and Zhuang, B. (2021.) Earth-affecting solar transients: a review of progresses in solar cycle 24. *Progress in Earth and Planetary Science*. 8(1), 56.

Zhang, W., Yang, J., Sheng, P., Li, X., and Wang, X. (2014.) Potential cooperation in renewable energy between China and the United States of America. *Energy Policy*. 75, 403-409.



**Enhancing Building Performance with Solar Heating Reflective Coatings: Impacts on Thermal and Electrical Efficiency**

Yizhou Yang<sup>1</sup>

Qihua Duan<sup>1\*</sup>

<sup>1</sup>Department of Civil, Construction, and Environmental Engineering, University of Alabama, Tuscaloosa, USA

[\\*qduan@ua.edu](mailto:qduan@ua.edu)

# Enhancing Building Performance with Solar Heating Reflective Coatings

## Abstract

This paper reviews the use of solar heating reflective coatings on building envelopes, focusing on their ability to improve thermal and electrical performance. It examines their properties, application methods, and compatibility with different materials. The study highlights how these coatings reduce heat absorption, lower indoor temperatures, and decrease air conditioning reliance, with significant energy savings across diverse climates. It also explores the positive impact of coatings on photovoltaic system efficiency and their potential to reduce peak electricity demand. The review concludes by identifying future research needs, including long-term performance studies and innovative material exploration.

Keywords: building performance, building envelopes, solar heating reflective coatings, thermal performance, electrical performance

## 1. Introduction

Buildings are among the largest energy consumers, with heating, cooling, lighting, and electrical systems accounting for over one-third of global energy use. Nearly 40% of total global CO<sub>2</sub> emissions can be attributed to the construction and building sectors. The significant energy consumption by these structures highlights the need for energy-saving measures (Hamilton et al., 2020). Energy-efficient designs aim to reduce the reliance on fossil fuels, thereby lowering environmental impacts (Cheekatamarla et al., 2022). These designs incorporate features such as improved insulation, ventilation, air quality, temperature control, and natural lighting to optimize the building's energy performance.

By reducing heat loss or gain, energy-efficient buildings create more comfortable indoor environments while cutting energy usage and greenhouse gas emissions. In a world where climate change and resource depletion are critical concerns, focusing on energy efficiency in buildings is not just a preference but a necessity (Council, 2014; Khalvati et al., 2023; Wyon & Wargocki, 2013). Enhancing the performance of the building envelope — the physical barrier separating the conditioned interior of a building from the outdoor environment — is a key strategy to achieve these energy savings. One effective approach is the adoption of innovative materials like solar heating reflective coatings (SHRCs), which have emerged as a transformative solution (Zakaria et al., 2023).

SHRCs are applied to the exterior surfaces of buildings to reflect solar radiation. By reducing the amount of heat absorbed by the buildings, SHRCs lower cooling demands, enhance thermal comfort, and contribute to environmental sustainability (Zhang et al., 2017). This review paper will delve into the multifaceted benefits of SHRCs in improving the thermal and electrical performance of buildings. The objectives of this review are:

- 1) To analyze the effectiveness of SHRCs in reducing energy consumption and enhancing thermal comfort in buildings,
- 2) To evaluate how SHRCs influence the thermal dynamics of building envelopes by reflecting solar radiation and reducing heat gain,
- 3) To assess the impact of SHRCs on electrical systems, particularly in reducing energy consumption for cooling and their interaction with integrated photovoltaic (PV) systems, and
- 4) To identify gaps in the current research landscape and suggest directions for future studies, with a focus on long-term performance, scalability, and integration with other green building innovations.

## 2. Fundamentals of Solar Heating Reflective Coatings

Solar heating reflective coatings (SHRCs) have become a cornerstone in the effort to enhance building performance. These coatings act by reflecting a large portion of the solar radiation that would otherwise be absorbed by the building's surfaces, contributing to elevated indoor temperatures and the need for air conditioning.

### 2.1 Composition of SHRCs

The composition of SHRCs determines their ability to reflect solar radiation and reduce heat absorption. The key ingredients of these coatings are pigments, binders, additives, and solvents, each contributing to the performance and longevity of the coating (McQuown et al., 2021).

Pigments are the primary components responsible for the reflectivity of the coatings. Titanium dioxide (TiO<sub>2</sub>), a widely used pigment, is notable for its high reflectivity in the ultraviolet (UV) and visible light spectrum (Jenree et al., 2019; Shindy, 2016). Pigments can be tailored to meet aesthetic preferences without compromising on reflective properties, allowing for the creation of coatings that maintain high solar reflectance across a range of colors (Stuart-Fox et al., 2017). Binders ensure the adhesion of the coating to the substrate, providing elasticity and durability. Acrylics, silicones, and polyurethanes are the most commonly used binders in SHRCs due to their water resistance, flexibility, and suitability for different surfaces (Vicente et al., 2008; Zhou et al., 2017). Additives such as UV stabilizers, fungicides, and algacides enhance the durability of SHRCs. Fire retardants and infrared-reflective pigments are sometimes included to boost safety and reflectivity, respectively (Soumya et al., 2014). Solvents help dissolve or suspend the other ingredients, facilitating the application of the coating. Water-based solvents are environmentally friendly and popular for residential applications, while solvent-based coatings are used for more demanding environments due to their fast drying times.

Advances in nanotechnology have further improved SHRCs by incorporating nanomaterials that enhance reflectivity, durability, and self-cleaning properties. This makes SHRCs more resilient to environmental wear and more effective in reflecting solar radiation.

### 2.2 Types of SHRCs

SHRCs come in a variety of formulations, each suited to specific applications and environmental conditions. These include:

- 1) Acrylic-based coatings are known for their cost-effectiveness, durability, and reflectivity. They are suitable for a range of climates (Muradova et al., 2023).
- 2) Silicone-based coatings are prized for their excellent weather resistance, especially in humid environments. They adhere well to metal and concrete surfaces, making them ideal for high-humidity and water-exposed areas (Abd-Elnaiem et al., 2022).
- 3) Polyurethane-based coatings are used in industrial settings and high-traffic areas with superior resistance to physical and chemical wear, polyurethane coatings (Maiti et al., 2021).
- 4) Elastomeric coatings are highly flexible, elastomeric coatings. They are ideal for surfaces that experience thermal expansion and contraction. They are commonly used for waterproofing and reflecting heat from roofs and facades (Nguyen et al., 2020).
- 5) Ceramic-based coatings offer superior insulation and reflectivity by incorporating ceramic particles. They are often used in extreme temperature environments due to their ability to reflect heat and insulate against thermal gain (Murata & Nakatani, 2023).

## Enhancing Building Performance with Solar Heating Reflective Coatings

Each type of SHRC has unique benefits, and the choice of coating depends on the building's material, environmental exposure, and energy efficiency goals.

### *2.3 Properties of SHRCs*

SHRCs are designed with two primary physical properties: high solar reflectivity and high thermal emissivity. These properties enable SHRCs to reflect solar radiation effectively while releasing absorbed heat, thus reducing the need for air conditioning.

- 1) **Solar Reflectance:** SHRCs typically have a solar reflectance of 70% to 90%, meaning that they reflect the majority of solar radiation that strikes them. This helps keep building surfaces cool, reducing the amount of heat transferred indoors (Liu et al., 2022; Speroni et al., 2022).
- 2) **Thermal Emissivity:** SHRCs also have thermal emissivity values ranging from 0.1 to 0.5, allowing them to emit absorbed heat back into the atmosphere rather than retaining it. This is particularly beneficial at night when the surface releases accumulated heat, maintaining a stable indoor temperature (Middel et al., 2020; Zhu et al., 2020).

By reducing both direct and indirect heat gain, SHRCs play a crucial role in improving the thermal efficiency of buildings, especially in hot climates.

### *2.4. Thermal Performance Enhancement*

The thermal performance of SHRCs is crucial to their effectiveness in reducing energy consumption. By reflecting solar radiation and emitting absorbed heat, SHRCs can lower the surface temperatures of treated areas by as much as 30°C compared to untreated surfaces. This reduction in surface temperature translates to lower indoor temperatures, reducing the need for air conditioning during peak sunlight hours (Ashhar & Lim, 2023; Mahmoudi et al., 2022).

In addition to improving indoor comfort, SHRCs also enhance the energy efficiency of buildings by lowering cooling loads. Studies have shown that SHRCs can reduce energy consumption by 10% to 50%, depending on the building's design, location, and the type of coating used. These energy savings also lead to reduced greenhouse gas emissions, making SHRCs a valuable tool in promoting environmental sustainability (Athmani et al., 2022; Chen et al., 2022; Shapoval et al., 2022).

### *2.5 Electrical Performance Implications*

The use of SHRCs can also improve the electrical performance of buildings, particularly those with integrated PV systems (Choi & Choi, 2023). By reducing surface temperatures, SHRCs help lower the operating temperature of PV panels, thereby reducing efficiency losses caused by heat (Ekbatani et al., 2024; Hu et al., 2023). This leads to increased energy production and a longer lifespan for the PV system.

Furthermore, the cooling effect of SHRCs can reduce the need for air conditioning during hot periods, which often coincide with peak electricity demand. By lowering cooling loads, SHRCs help reduce stress on the electrical grid, potentially lowering energy costs and minimizing the risk of power outages.

## **3. Applications of Solar Heating Reflective Coatings**

## Enhancing Building Performance with Solar Heating Reflective Coatings

SHRCs can be applied to a wide range of building surfaces, including roofs, exterior walls, and glass windows. Each application requires careful consideration of the building's materials and architectural features to maximize the effectiveness of the coating.

### *3.1 Roof Application*

Roofs are particularly well-suited for SHRC application due to their direct exposure to sunlight. SHRCs can be applied to various roofing materials such as asphalt shingles, metal panels, and concrete tiles, reducing heat absorption and improving energy efficiency. For example, a commercial building in Phoenix, Arizona, experienced a 30°C reduction in roof surface temperature after applying SHRCs, leading to a 22% reduction in cooling energy consumption.

For example, a commercial office building in Phoenix, Arizona experienced a 30°C reduction in roof surface temperature and a 22% reduction in summer cooling energy consumption after applying white reflective SHRCs. Similarly, an industrial warehouse in Johannesburg, South Africa saw a 30% reduction in cooling energy consumption and improved worker comfort after SHRC application on its metal roof, potentially increasing productivity.

### *3.2 Exterior Wall Application*

SHRCs can also be applied to exterior walls, improving thermal insulation and reducing energy use. The application process involves cleaning and repairing the wall surface, applying a primer, and then applying multiple coats of the SHRC for even coverage. In Berlin, Germany, SHRCs applied to the walls of campus buildings reduced heating and cooling energy consumption by 15%, while in Singapore, combining SHRCs with green roof technology reduced air-conditioning energy consumption by 25%.

### *3.3 Glass and Fenestration*

Glass surfaces such as windows and skylights can also benefit from SHRCs, which control heat gain without significantly reducing natural light penetration. Transparent SHRCs were applied to the glass surfaces of a museum in Rome, Italy, reducing cooling loads by 20% while maintaining high levels of natural daylight.

## **4. Discussion**

### *4.1 Technical Challenges*

While SHRCs offer significant benefits, their application poses several technical challenges. Surface preparation is critical to ensure proper adhesion and performance, requiring meticulous cleaning and priming.

#### *4.1.1 Technical challenges in the application of SHRCs*

While SHRCs provide significant benefits, their application presents technical challenges that must be addressed to ensure optimal performance. Surface preparation is crucial, as improper cleaning, priming, or substrate selection can lead to reduced adhesion and performance over time. Older or weathered building materials may pose challenges during surface preparation, necessitating more intensive cleaning or specific primers to accommodate material degradation. Furthermore, achieving an even application of SHRCs is vital to ensuring consistent performance across the building envelope. Inconsistencies in coating thickness can result in uneven reflectivity, reduced thermal efficiency, and premature aging of the coating.

Environmental conditions during application also play a critical role in the performance of SHRCs. Variables such as temperature, humidity, and wind can influence the drying and curing

## Enhancing Building Performance with Solar Heating Reflective Coatings

process of the coating. High humidity levels may interfere with the adhesion process, leading to reduced durability, while extreme temperatures can affect the drying rate and bonding strength. Careful management of these conditions is necessary to ensure a proper application and a long-lasting coating that will deliver maximum thermal and electrical performance.

### *4.1.2 Technical challenges in the maintenance of SHRCs*

The maintenance of SHRCs also presents challenges, especially regarding the durability of the coatings in harsh environments. SHRCs can degrade over time due to UV exposure, thermal cycling, moisture, and airborne pollutants, reducing their solar reflectivity and thermal emissivity properties. Regular cleaning and periodic reapplication are required to restore their performance. However, cleaning SHRCs — especially on roofs or other difficult-to-access surfaces — can be labor-intensive and costly.

Repairs to damaged or worn areas must be conducted carefully to maintain the integrity of the surrounding coated areas. Moreover, the chemicals used in certain SHRCs or during maintenance may raise environmental and health concerns, particularly if they contain volatile organic compounds (VOCs). Ensuring that the coatings, cleaning agents, and solvents used are environmentally friendly is essential to minimizing the environmental impact of SHRCs while maintaining their effectiveness.

### *4.2 Current research gaps*

Despite the growing body of research on SHRCs, significant gaps remain in our understanding of their long-term performance, indoor air quality impact, and integration with other energy-saving technologies. While initial studies demonstrate the energy-saving potential of SHRCs, particularly in hot climates, there is a lack of comprehensive data on their performance in different climatic regions over extended periods. Research is needed to evaluate how SHRCs hold up over time in varying weather conditions, including areas with high humidity, cold winters, or frequent rainfall. Such studies would help determine the longevity and cost-effectiveness of SHRCs in diverse climates.

In addition to thermal performance, the impact of SHRCs on indoor air quality has not been fully explored. Because SHRCs reflect solar radiation and reduce heat gain, buildings may require less ventilation to cool indoor spaces. However, reduced air circulation could lead to the accumulation of indoor air pollutants. Further research is necessary to understand how SHRCs influence indoor environmental quality and whether additional measures, such as enhanced ventilation systems, are required to maintain healthy indoor air.

Moreover, the integration of SHRCs with other energy-saving technologies, such as green roofs, PV systems, and advanced insulation materials, remains underexplored. While the combination of SHRCs and PV systems has shown promise in increasing energy efficiency, more studies are needed to assess the synergies between SHRCs and other renewable energy technologies. For example, integrating SHRCs with green roofs could reduce heat gain while promoting biodiversity and stormwater management. Additionally, combining SHRCs with advanced insulation materials could further reduce the need for mechanical cooling, thereby enhancing the energy performance of buildings.

Comprehensive life cycle assessments (LCAs) are also required to evaluate the environmental footprint of SHRCs throughout their lifespans. Current research has primarily focused on the application and short-term benefits of SHRCs, with limited attention given to the energy and resource consumption during production, transportation, application, maintenance, and disposal. LCAs would provide a holistic understanding of SHRCs' environmental impact, helping policymakers, architects, and building owners make informed decisions about their use in sustainable building projects.



## Enhancing Building Performance with Solar Heating Reflective Coatings

Another research gap lies in the standardization of performance metrics for SHRCs. Currently, there are no universally accepted standards for measuring solar reflectance, thermal emissivity, durability, or environmental impact. Developing standardized test methods and evaluation criteria would enable more accurate comparisons between different SHRC products, guide manufacturers in product development, and inform consumers about the best options for their specific needs.

Finally, as climate change accelerates, it is essential to study the adaptability and resilience of SHRCs in the face of shifting weather patterns. Extreme weather events, such as heatwaves, storms, and prolonged droughts, are becoming more frequent, posing new challenges to building materials. SHRCs must be tested for their ability to withstand these extremes while continuing to provide effective thermal and electrical performance. Addressing these research gaps requires a multidisciplinary approach, combining insights from materials science, building physics, environmental science, and construction engineering. Furthermore, collaboration between academia, industry, and government agencies is crucial to developing the next generation of SHRCs that are both efficient and resilient.

### 5. Conclusion

Solar heating reflective coatings (SHRCs) represent a transformative technology for enhancing the thermal and electrical performance of buildings. By reflecting solar radiation and emitting absorbed heat, SHRCs reduce heat gain, lower cooling loads, and improve indoor thermal comfort. These benefits lead to significant energy savings, lower greenhouse gas emissions, and a reduced environmental footprint for buildings. As the global push for energy-efficient and sustainable buildings intensifies, SHRCs offer a promising solution to address the challenges of energy consumption and climate change in the built environment.

SHRCs leverage their properties of high solar reflectivity and thermal emissivity to create cooler building surfaces, reducing the amount of heat transferred into the interior. This, in turn, lowers the demand for mechanical cooling systems, cutting energy consumption and operational costs. In urban areas, where the heat island effect exacerbates heat buildup, the widespread adoption of SHRCs could lead to cooler microclimates, improving overall comfort for city residents and reducing the strain on municipal power grids. The electrical performance implications of SHRCs, particularly when integrated with PV systems, further enhance their value in sustainable building design. By reducing the operating temperature of PV panels, SHRCs minimize efficiency losses and extend the lifespan of the panels, contributing to increased renewable energy generation. The dual benefit of reducing energy consumption and boosting renewable energy production makes SHRCs an essential tool in the fight against climate change. However, for SHRCs to realize their full potential, several challenges must be addressed. The technical difficulties associated with surface preparation, application, and maintenance require careful attention to ensure consistent performance over time. Additionally, more research is needed to fill gaps in our understanding of SHRCs' long-term durability, their impact on indoor air quality, and their integration with other green building technologies. Standardized performance metrics and comprehensive life cycle assessments are critical to evaluating the environmental impact of SHRCs and guiding their widespread adoption in construction projects.

In conclusion, SHRCs offer a strategic approach to improving energy efficiency, enhancing occupant comfort, and promoting environmental sustainability in buildings. As advancements in materials science and building technology continue, SHRCs will play an increasingly important

## Enhancing Building Performance with Solar Heating Reflective Coatings

role in the design and renovation of energy-efficient, climate-resilient buildings. The widespread adoption of SHRCs, supported by continued innovation and research, can significantly contribute to global efforts to mitigate the effects of climate change and foster sustainable development in the construction industry.

### **Conflict of Interest**

This project is supported by the DOE award: Alabama Building Training and Assessment Center



### References

- Abd-Elnaiem, A. M., Hussein, S. I., Ali, N. A., Hakamy, A., & Mebed, A. M. (2022). Ameliorating the mechanical parameters, thermal stability, and wettability of acrylic polymer by cement filling for high-efficiency waterproofing. *Polymers*, *14*(21), 4671.
- Ashhar, M., & Lim, C. (2023). *Thermal performance of reflective insulation system and comparison against ASHRAE Standard. 1278*(1), 012013.
- Athmani, W., Sriti, L., Dabaieh, M., & Younsi, Z. (2022). The potential of using passive cooling roof techniques to improve thermal performance and energy efficiency of residential buildings in hot arid regions. *Buildings*, *13*(1), 21.
- Cheekatamarla, P. K., Sharma, V., & Shrestha, S. (2022). Energy-efficient building technologies. In *Advanced Nanomaterials and Their Applications in Renewable Energy* (pp. 3–33).
- Chen, L., Zhang, K., Song, G., & Li, F. (2022). Study on the cooling performance of a radiative cooling-based ventilated roof for its application in buildings. *Building Services Engineering Research and Technology*, *43*(6), 685–702.
- Choi, H.-U., & Choi, K.-H. (2023). Electrical and thermal performances of a single-pass double-flow photovoltaic-thermal collector coupled with nonuniform cross-section rib. *International Journal of Energy Research*, *2023*(1), 4744558.
- Ekbatani, A., Mostajeran Goortani, B., & Karbalaei, M. (2024). Performance enhancement of photovoltaic module using a sun tracker with side reflectors (STSR system). *International Journal of Green Energy*, *21*(1), 64–73.
- Hamilton, I., Rapf, O., Kockat, D. J., Zuhair, D. S., Abergel, T., Oppermann, M., Otto, M., Loran, S., Fagotto, I., & Steurer, N. (2020). Global status report for buildings and construction. *United Nations Environmental Programme: Nairobi, Kenya*.
- Hu, J., Wang, X., Chen, W., Yin, Y., & Li, Y. (2023). OPV-PCM-ETFE foils in use for public buildings: Electrical performance and thermal characteristics. *Journal of Building Engineering*, *71*, 106427.

## Enhancing Building Performance with Solar Heating Reflective Coatings

- Jenree, R. M., Smith, R. L., Wu, S. J., & Weller, D. E. (2019). *U.S. Patent No. 10,253,493*. Washington, DC: U.S. Patent and Trademark Office.
- Khalvati, L., Sheykhshabani, Z. E., Balal, A., & Arbabzadeh, N. (2023, April). Boosting Solar Energy Production of a Building using New Architectural Design. In *2023 International Conference on Computational Intelligence and Sustainable Engineering Solutions (CISES)* (pp. 920-925).
- Liu, Q., Yan, B., Garrett, K., Ma, Y., Liang, X., Huang, J., Wang, W., & Cao, C. (2022). Deriving surface reflectance from visible/near infrared and ultraviolet satellite observations through the Community Radiative Transfer Model. *IEEE Journal of Selected Topics in Applied Earth Observations and Remote Sensing*, *15*, 2004–2011.
- Mahmoudi, M., Farzan, H., & Hasan Zaim, E. (2022). Performance of new absorber coating strategy in solar air heaters: An experimental case study. *Iranica Journal of Energy & Environment*, *13*(2), 124–133.
- Maiti, T., Parvate, S., Pragya, Singh, J., Dixit, P., E., B., Vennapusa, J., & Chattopadhyay, S. (2022). Plastics in coating applications. *Encyclopedia of Materials: Plastics and Polymers*. *4*, 126-135.
- McQuown, S. G., Slomski, J., Hellring, S. D., Holsing, L., & Gill, T. (2021). *U.S. Patent No. 11,118,068*. Washington, DC: U.S. Patent and Trademark Office.
- Middel, A., Turner, V. K., Schneider, F. A., Zhang, Y., & Stiller, M. (2020). Solar reflective pavements — A policy panacea to heat mitigation? *Environmental Research Letters*, *15*(6), 064016.
- Muradova, S., Negim, E.-S., Makhmetova, A., Ainakulova, D., & Mohamad, N. (2023). An overview of the current state and the advantages of using acrylic resins as anticorrosive coatings. *Kompleksnoe Ispolzovanie Mineralnogo Syra= Complex Use of Mineral Resources*, *327*(4), 90–98.

## Enhancing Building Performance with Solar Heating Reflective Coatings

- Murata, H., & Nakatani, K. (2023). *U.S. Patent No. 11,555,134*. Washington, DC: U.S. Patent and Trademark Office.
- Nguyen, T. V., Nguyen, T. A., & Nguyen, T. H. (2020). The synergistic effects of SiO<sub>2</sub> nanoparticles and organic photostabilizers for enhanced weathering resistance of acrylic polyurethane coating. *Journal of Composites Science*, 4(1), 23.
- Shapoval, S., Spodyniuk, N., Datsko, O., & Shapoval, P. (2022). Research of efficiency of solar coating in the heat supply system. *Pollack Periodica*, 17(1), 128–132.
- Shindy, H. (2016). Basics in colors, dyes and pigments chemistry: A review. *Chem. Int*, 2(29), 2016.
- Soumya, S., Mohamed, A. P., Paul, L., Mohan, K., & Ananthakumar, S. (2014). Near IR reflectance characteristics of PMMA/ZnO nanocomposites for solar thermal control interface films. *Solar Energy Materials and Solar Cells*, 125, 102–112.
- Speroni, A., Mainini, A. G., Zani, A., Paolini, R., Pagnacco, T., & Poli, T. (2022). Experimental Assessment of the Reflection of Solar Radiation from Façades of Tall Buildings to the Pedestrian Level. *Sustainability*, 14(10), 5781.
- Stuart-Fox, D., Newton, E., & Clusella-Trullas, S. (2017). Thermal consequences of colour and near-infrared reflectance. *Philosophical Transactions of the Royal Society B: Biological Sciences*, 372(1724), 20160345.
- Vicente, Gema San, Rocío Bayón, and Angel Morales. "Effect of additives on the durability and properties of antireflective films for solar glass covers." (2008): 011007. Health, Council, W. G. B. (2014). Health, wellbeing & productivity in offices. *World Green Building Council*.
- Wyon, D. P., & Wargocki, P. (2013). How indoor environment affects performance. *Thought*, 3(5), 6.

## Enhancing Building Performance with Solar Heating Reflective Coatings

- Zakaria, N. M., Omar, M. A., & Mukhtar, A. (2023). Numerical study on the thermal insulation of smart windows embedded with low thermal conductivity materials to improve the energy efficiency of buildings. *CFD Letters*, *15*(2), 41–52.
- Zhang, Y., Long, E., Li, Y., & Li, P. (2017). Solar radiation reflective coating material on building envelopes: Heat transfer analysis and cooling energy saving. *Energy Exploration & Exploitation*, *35*(6), 748–766.
- Zhou, A., Yu, Z., Chow, C. L., & Lau, D. (2017). Enhanced solar spectral reflectance of thermal coatings through inorganic additives. *Energy and Buildings*, *138*, 641–647.
- Zhu, X., Yu, Y., Chen, L., & Zhang, D. (2020). Solar heat reflective coating for sidewalks considering cooling effect, anti-skid performance, and human comfort. *Journal of Testing and Evaluation*, *48*(3), 2028–2039.

**Solar Energy Potential and Integration in Alabama Residential Buildings: A Photovoltaic System Feasibility Study**

Yizhou Yang<sup>1</sup>

Qihua Duan<sup>1\*</sup>

Babatunde Owolabi<sup>1</sup>

<sup>1</sup>Department of Civil, Construction, and Environmental Engineering, University of Alabama, Tuscaloosa, USA

[\\*gduan@ua.edu](mailto:*gduan@ua.edu)

## Abstract

This study examines the feasibility of integrating photovoltaic (PV) systems into residential buildings in Alabama to optimize solar energy use. Using Autodesk Revit 2024 for solar analysis on a prototype model from the U.S. Department of Energy, it assesses the efficiency, cost benefits, and payback periods of different PV panel types across five major Alabama cities. Results show substantial variations in energy output and savings, with payback periods between 11.6 to 14.1 years. Additionally, the study reviews Alabama's policy landscape, identifying gaps in net metering and suggesting improvements, including financial incentives and investment in solar technology. The findings offer valuable insights for advancing sustainable energy in Alabama's residential sector.

Keywords: solar photovoltaic, residential buildings, solar energy, Revit

## Introduction

Energy consumption in Alabama's residential buildings accounts for around 20% of the state's total energy use, contributing significantly to carbon dioxide emissions and climate change (2024 Electricity Rates by State, 2024). Solar energy offers a sustainable solution by meeting energy needs while reducing CO<sub>2</sub> emissions (Alabama, 2024.; Electric Rates & Providers in Tuscaloosa County, AL, 2024). Developing solar energy in Alabama's residential sector is a critical step toward aligning with global shifts to renewable energy sources.

Alabama's climate, with approximately 200 sunny days per year and four to five peak sunlight hours daily, makes it ideal for solar energy development, particularly rooftop photovoltaic (PV) systems (Aljundi et al., 2016). The state's conditions are favorable for solar production. Installing PV systems on residential rooftops holds significant potential for leveraging these advantages. However, Alabama's fragmented regulatory framework poses challenges. The absence of statewide net metering and reliance on individual utility companies complicate the adoption of solar energy. While financial incentive programs like AlabamaSAVES exist (Baghi et al., 2021), regulatory gaps and a lack of comprehensive data on residential solar installations, especially in cities like Birmingham and Montgomery, remain hurdles to broader implementation. Despite these challenges, advancements in solar technology and evolving policies present opportunities for future solar development in Alabama. As solar panel technology improves and legislation evolves, the potential for increased adoption of solar energy in the state's residential sector grows (Alabama Solar Incentives, 2023; Climate of Alabama, 2024; Jones et al., 2020).

This study used Autodesk Revit to assess the thermal performance of buildings and optimize PV panel placement. Revit's solar analysis tool helped evaluate the sun path and solar radiation impacts, enhancing solar energy efficiency (Kahle, 2024; Kneifel, 2012). Our analysis focuses on five major Alabama cities, assessing various PV panel types, energy production capacities, cost savings, and return on investment. Factors

such as temperature, humidity, and solar irradiance are considered. The findings highlight the significant potential for energy production and cost savings despite the regulatory challenges.

## Methodology

### *Residential building model*

In this study, we used the U.S. Department of Energy prototypical residential building model, which can accurately reflect the characteristics of typical residential structures across various U.S. regions. A single-family residential prototype building model with three bedrooms was chosen, which aligns with the 2021 International Energy Conservation Code. Illustrated in Figures 1 and 2, the building's orientation positions its longer axis east to west, with a length of 12 meters and a width of 9 meters from north to south, resulting in a total conditioned floor area (CFA) of 108 m<sup>2</sup>. The ceiling height on the first floor is set at 2.45 m. The roof, with a 4:12 slope, is equipped with one-foot overhangs on both the north and south facades, covering the CFA (Kumar et al., 2022).

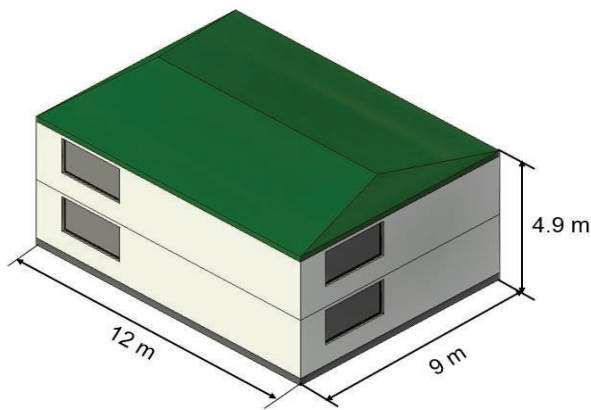


Fig. 1. Model 3D view of the building model

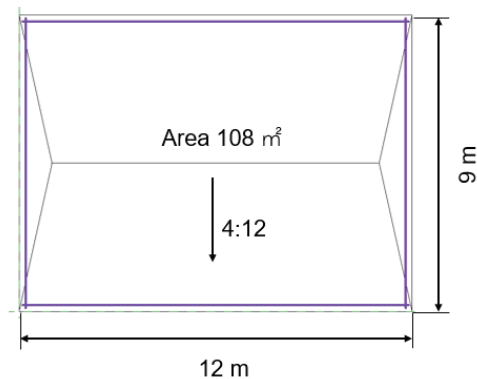


Fig. 2. Roof floor plan view of the building model

### *Selected cities and climate conditions*

To evaluate the potential and efficacy of solar PV systems across Alabama, this residential building model was examined in five major cities: Huntsville, Birmingham, Montgomery, Mobile, and Tuscaloosa. Huntsville, situated in the northern part of Alabama, experiences a humid subtropical climate, typically cooler than the western city of Tuscaloosa. Birmingham, located in the central-northern region, shares a similar climate to Huntsville but tends to have slightly cooler temperatures than the state's southern cities. Montgomery, positioned centrally, is characterized by hot summers and mild winters, indicative of its humid subtropical climate. Mobile, at the southern edge of Alabama, benefits from a Gulf-influenced subtropical climate, with notably hot, humid summers. Tuscaloosa, located in western Alabama, exhibits a humid subtropical climate

## Solar Energy Potential and Integration in Alabama Residential Buildings

with hot summers and mild winters, consistent with much of the state. Alabama is located in climate zone 3A, which is significant for solar PV system consideration (Larosa, 2024). The geographic and climatic characteristics of these cities are outlined in Table 1.

Table 1. The geographic information and climate conditions of the five major cities in Alabama

| Region           | City       | Geographic Location |           |          | Temperature |        |             |
|------------------|------------|---------------------|-----------|----------|-------------|--------|-------------|
|                  |            | Latitude            | Longitude | Altitude | Highest     | Lowest | Average     |
| Northern         | Huntsville | 34.73               | -86.59    | 581 ft   | 91°F        | 30°F   | 50°F - 70°F |
| Central-Northern | Birmingham | 33.52               | -86.81    | 597 ft   | 91°F        | 31°F   | 50°F - 70°F |
| Central          | Montgomery | 32.38               | -86.30    | 220 ft   | 92°F        | 35°F   | 50°F - 70°F |
| Southern         | Mobile     | 30.69               | -88.04    | 33 ft    | 91°F        | 40°F   | 50°F - 70°F |
| Western          | Tuscaloosa | 33.219              | -87.57    | 222 ft   | 94°F        | 32°F   | 60°F - 70°F |

### *Solar Analysis in Revit*

The Solar Analysis plugin for Autodesk Revit is a powerful tool to assess and visualize solar radiation on buildings. This plugin offers visual feedback through color-coded maps, indicating solar radiation distribution on building roofs (Kahle, 2024).

Using this Solar Analysis plugin, we evaluated solar radiation on the building model's roof through examining cumulative insolation, PV energy, and payback periods, comparing three types of PV panels integrated within Revit for each city. This analysis offers valuable insights into the solar energy potential. Here, cumulative insolation refers to the total amount of solar radiation energy received on the building's roof over a specific period, typically measured in kWh/m<sup>2</sup>. PV energy refers to the estimated energy production of PV panels, which is based on their placement, size, and efficiency. The payback period is the duration required for the initial investment in solar PV panels to be recovered through the savings from the electricity they produce. The analysis also considered seasonal variations in solar radiation such as daylight duration, cloud cover, and specific local climate conditions.

In Revit, three types of panels are categorized based on their efficiency and cost: Type 1 with 16.0% efficiency at \$2.86 per installed watt; Type 2 with 18.6% efficiency at \$3.47 per installed watt; and Type 3 with 20.4% efficiency, also at \$3.47 per installed watt. To calculate the PV energy cost for each city, we used the average electricity cost for residential buildings in each city expressed in dollars per kilowatt-hour (Padhee & Pal, 2018), as indicated in Table 2.



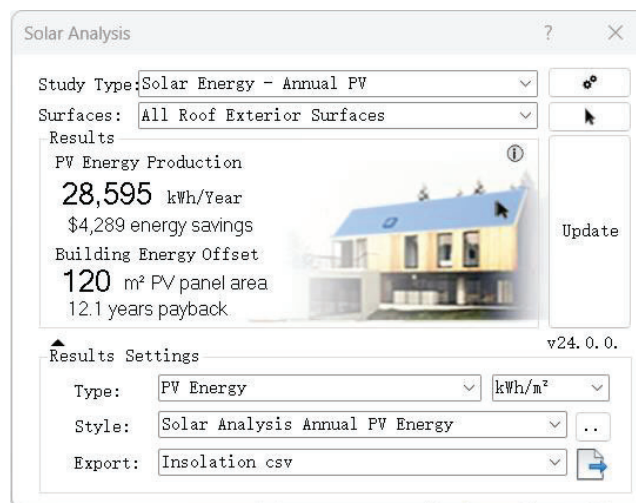
## Solar Energy Potential and Integration in Alabama Residential Buildings

Table 2. The average electricity price for residential buildings in the five major cities in Alabama (\$/kWh)

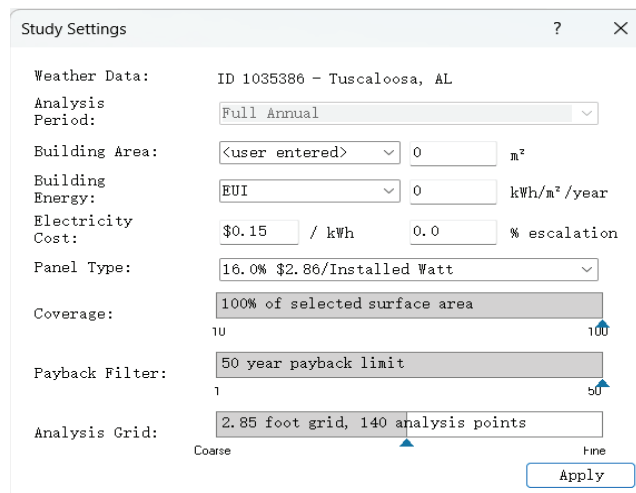
| City             | Huntsville | Birmingham | Montgomery | Mobile | Tuscaloosa |
|------------------|------------|------------|------------|--------|------------|
| Electricity Cost | 0.1146     | 0.1573     | 0.1174     | 0.1573 | 0.1525     |

### Results

As illustrated in Fig. 2(a), the “Study Type” was configured for “Solar Energy-Annual PV”, and the “Surfaces” was set to “All Roof Exterior Surfaces,” targeting a date range from 01/01/2023 to 12/31/2023. The “Style” in the results settings was set as “Solar Analysis Annual Insolation”, and the “Type” was set as “cumulative insolation”, “PV energy”, and “payback periods (years)” respectively.



(a) Solar Analysis Setting and Results interface



(b) Study settings

Fig. 3. Solar Analysis Setting and Results Interface

## Solar Energy Potential and Integration in Alabama Residential Buildings

Also, adjustments to the average residential electricity cost were made through the “Double gears” icon, identified as the study settings, shown in Fig 3(b). Fig. 3(a) shows the cumulative insolation results in Tuscaloosa. The analysis began upon selecting the “Update” option, and upon its completion, the results were summarized in the Solar Analysis dialog and visualized in a 3D view. Fig. 4 shows the 3D view of the solar analysis results. Yellow or orange color indicates that the area or surface receives a moderate amount of sunlight and is in a partially sunlit area. All results, including annual cumulative insolation, PV energy production, energy savings, and payback periods for the building model across five cities, will be summarized and elaborated on in the subsequent sections.

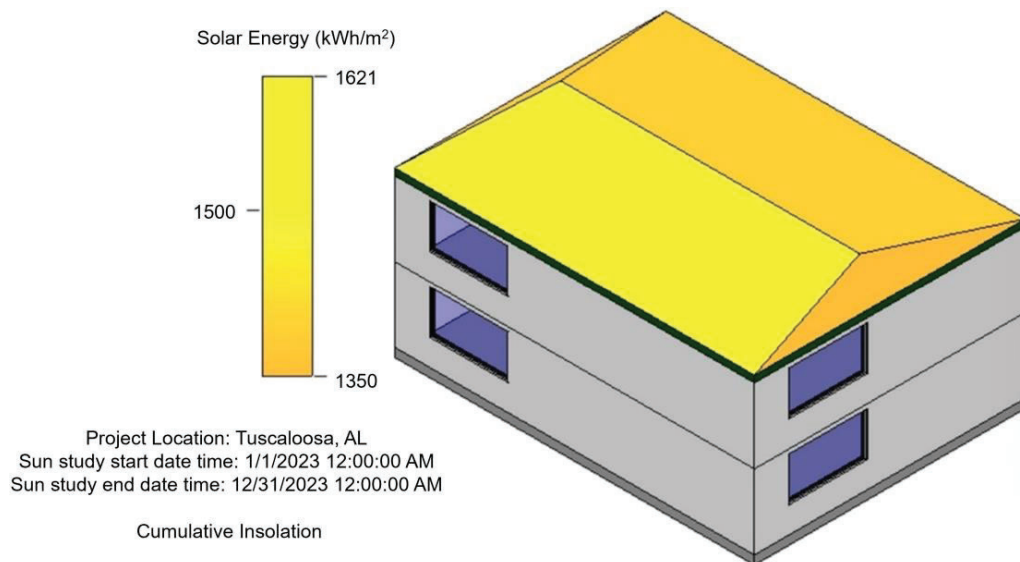


Fig. 4. 3D view of the solar analysis results

### *Solar Energy*

Table 3 presents the annual solar irradiance data for five cities in Alabama. Montgomery receives the highest amount of sunlight, with 180,638 kWh, which is 17% higher than Huntsville, the city receiving the lowest, at 153,898 kWh. Similar amounts of solar energy arrive at Birmingham, Mobile, and Tuscaloosa, with the differences among these three cities being less than 1.2%. These variations demonstrate the significance of geographical location and local climate in evaluating solar energy potential across different areas.

Table 3. Annual cumulative Insolation for the five cities (kWh)

| Huntsville | Birmingham | Montgomery | Mobile  | Tuscaloosa |
|------------|------------|------------|---------|------------|
| 153,898    | 177,691    | 180,638    | 179,891 | 179,197    |

## Solar Energy Potential and Integration in Alabama Residential Buildings

### *PV Energy Production*

Figure 5 reveals that the annual potential solar energy output from PV systems varies across Alabama. As the efficiency of PV panels increases from 16.0% to 20.4%, the annual PV energy production in Huntsville, Birmingham, Montgomery, Mobile, and Tuscaloosa increases by 6,754 kWh, 7,789 kWh, 7,926 kWh, 7,894 kWh, and 7,863 kWh, respectively. Higher efficiency PV modules, with improved conversion rates, can increase energy production. These results illustrate a clear efficiency-cost correlation. Regardless of the type applied to the residential building model, the annual PV energy production in Montgomery is always the highest, while that in Huntsville is the lowest. For instance, using Type 3 PV, Montgomery's output of 36,750 kWh surpasses Huntsville's output of 31,315 kWh by 5,435 kWh. This is because the flat terrain of Montgomery provides optimal conditions for PV installations, allowing for more exposure to sunlight and more efficient energy conversion, which is aligned with the maximum amount of sunlight received in Montgomery.

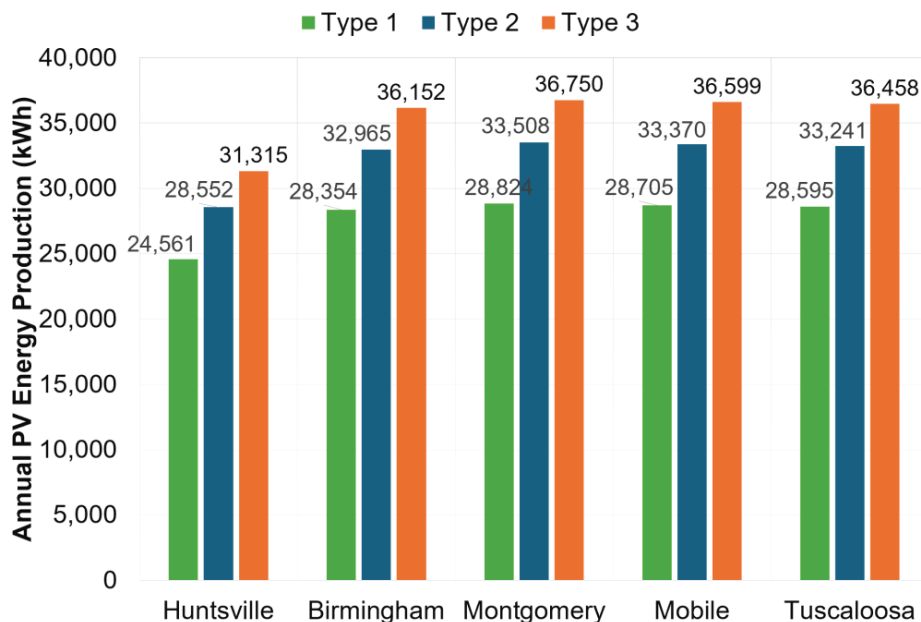


Fig. 5. Annual PV energy production for the five cities

### *Energy Savings*

Figure 6 demonstrates that higher-efficiency panels with higher installation costs will save more money in the field. Mobile has the highest energy savings, which range from \$4,593 to \$5,856 per year (increased by \$1,263) based on PV Type 16.0%- to 20.4%-efficiency panels. In comparison, Huntsville has the least energy savings, ranging from \$2,702 to \$3,445 (increased by \$743). This trend of higher-efficiency panels incurring greater initial costs reflects a widespread market phenomenon which is due to the sophisticated technology and materials required for superior performance, a factor that

## Solar Energy Potential and Integration in Alabama Residential Buildings

remains constant across different locations. We believe that higher-efficiency panels with higher installation costs can be used in each city. However, the extent to which this translates into cost-effectiveness for the homeowner can vary by city due to differences in solar insolation, local electricity rates, and other related factors which affect the overall savings and payback period.

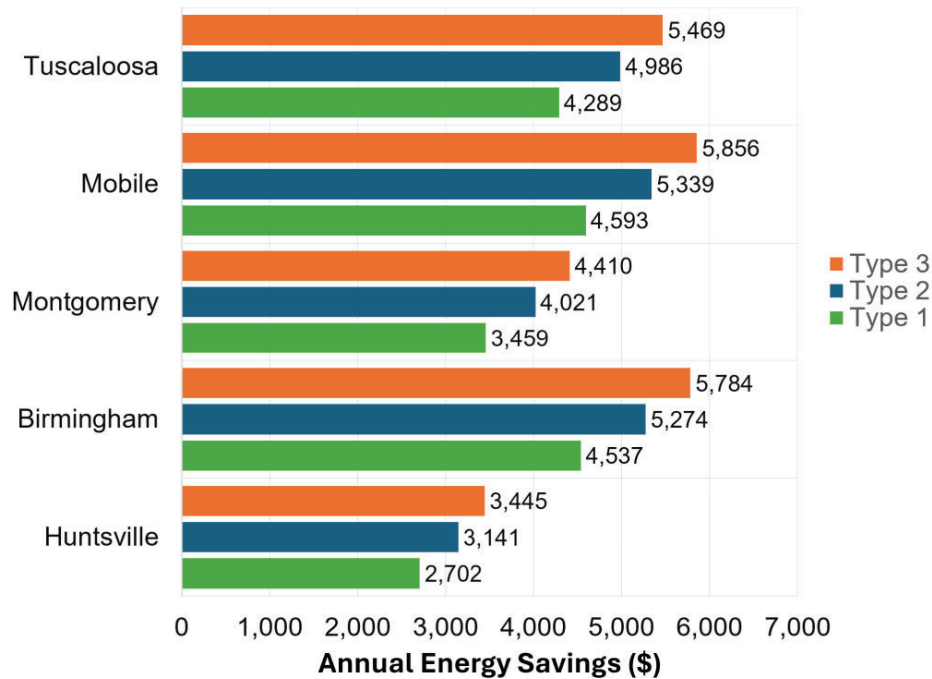


Fig. 6. Annual energy savings for the five cities

### *Payback Period*

From Figure 7, it is noticeable that the payback periods for solar panel installations in the five cities vary depending on the panel type, electricity costs, and locations. Higher solar energy production leads to greater electricity savings, reducing the payback period assuming electricity rates and other conditions are constant. Since Mobile has the highest energy savings, we should expect Mobile to have a shorter payback period (14.1 years) compared to the other cities we have analyzed. Huntsville has the lowest energy savings, so its payback period is also the longest (24.1 years). The difference in return on investment can be as much as 10 years just because of a few minor changes. This assumes that the factors like local electricity rates and solar insolation are favorable and that the increased savings from higher-efficiency panels outweigh the higher installation costs.

## Solar Energy Potential and Integration in Alabama Residential Buildings

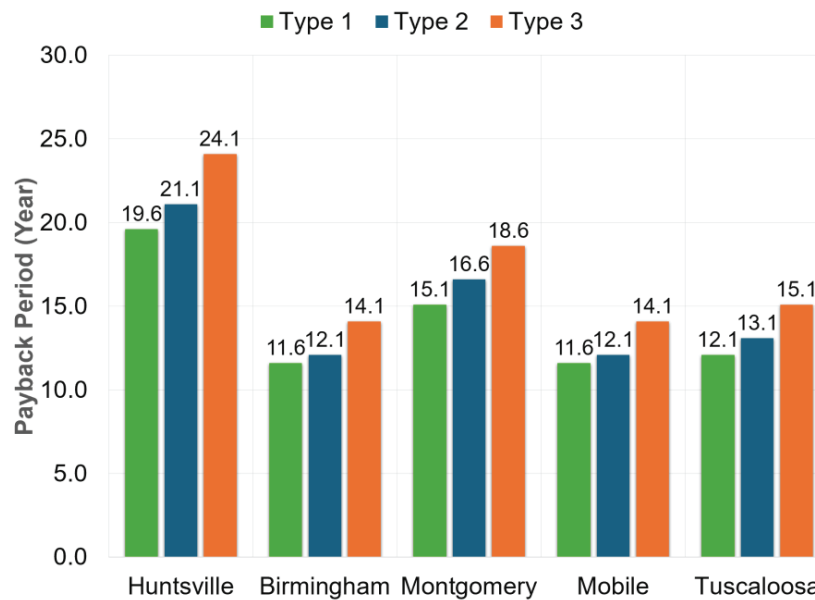


Fig. 7. Payback periods for the five cities

### Discussion

Based on the calculation and analysis of the solar potential in five different cities in Alabama, we can see:

1) Montgomery, located in central Alabama, receives the highest amount of sunlight and could generate the highest annual PV energy output: 36,750 kWh. Birmingham (3,6152 kWh), Mobile (3,6599 kWh), and Tuscaloosa (3,6458 kWh) have similar amounts of solar insolation and annual PV energy outputs. Huntsville, situated in northern Alabama, receives the lowest amount of sunlight and could generate the lowest annual energy output: 31,315 kWh. This indicates that more sunshine hours and higher solar radiation make PV energy systems more efficient due to climatic conditions and geographical location.

2) Mobile offers the highest energy savings, ranging from \$4,593 to \$5,856 per year, based on PV panel efficiency. In contrast, Huntsville has the least energy savings, ranging from \$2,702 to \$3,445. Energy production capacity is influenced by the efficiency of PV panels used. While high-efficiency PV panels come with a higher price tag, they offer superior solar radiation conversion, leading to greater annual energy output. This efficiency-to-cost tradeoff plays a vital role in optimizing returns on solar investments for residential buildings. Therefore, assessing the feasibility of solar PV installations in Alabama's homes must take into account both location and technological advancements to maximize benefits.

3) Mobile and Birmingham have shorter payback periods compared to the other cities, while Huntsville has the lowest energy savings and the longest payback period. The findings suggest that the PV systems integrated in residential buildings present a compelling avenue for advancing sustainable energy practices. While the energy output

## Solar Energy Potential and Integration in Alabama Residential Buildings

and financial savings vary across different regions, the overall trend indicates a promising potential for energy independence and economic benefits for homeowners.

Moreover, the analysis has shed light on the critical role of state policies and incentives in fostering the adoption of solar technologies. According to the Solar Energy Industries Association, Alabama has experienced significant growth in solar power generation, which comprised 3% of the state's renewable energy production in 2021 (Solar Energy Industries Association, 2024). The southeastern and Gulf Coast regions hold the best solar resources within the state (Alabama Solar Incentives, 2023).

Despite this growth, Alabama's solar landscape faces challenges, including the dominance of utility-scale solar generation and limited small-scale residential installations. Alabama's solar capacity growth, primarily through large-scale projects, contrasts with the nationwide trend of rapid solar expansion supported by federal policies and cost reductions. The state's approach to solar energy, particularly for homeowners, is hindered by minimal support from the state legislature and public utilities commission.

The primary incentives available in Alabama include the following:

- 1) The AlabamaSAVES loan program provides low-interest loans to Alabama businesses and nonprofits for energy efficiency and renewable energy projects, including solar installations.
- 2) Local utility rebate programs provided by some utility companies in Alabama offer rebate programs that provide financial incentives for installing solar panels.
- 3) The federal Solar Investment Tax Credit (ITC) offers a tax credit of 30% of the cost of installing a solar energy system.
- 4) Net metering programs are offered by some utilities which credit solar panel owners for excess electricity generated. This can lead to reduced utility bills over time.
- 5) Alabama provides a property tax exemption for renewable energy systems, ensuring that the value added by solar installations does not increase the property taxes (Guide to Alabama Incentives & Tax Credits, 2024; Why Choose Solar Panels?, 2024; Larosa, 2024).

However, Alabama Power, the largest utility, offers minimal compensation for excess solar energy generated by residential installations, contributing to longer payback times for solar panels, among the nation's worst (Whatstheweatherlike, 2024). Alabama does not mandate net metering statewide, although some local utilities may offer such programs. This restriction makes it difficult for solar owners to receive fair compensation for the electricity they generate and contribute back to the grid (Baghi et al., 2021).

These factors create a challenging environment for the adoption of solar PV in Alabama, indicating a need for a strategic reassessment of policy and incentive structures.

### **Conclusion**

This paper has examined the potential, challenges, and future direction of solar PV system integration in Alabama, with a focus on residential buildings. The feasibility study confirms that residential PV systems in Alabama offer a viable strategy for reducing CO<sub>2</sub> emissions and utility costs. With payback periods ranging between 11.6 to 14.1 years, the financial case for PV systems is clear, notwithstanding the initial investment. However, the study also indicates a unified policy approach is needed to maximize adoption and effectiveness. Recommendations include implementing statewide net metering policies, increasing investment in solar technology research, and providing financial incentives to lower entry barriers for homeowners. The use of Autodesk Revit 2024 for solar analysis demonstrates the importance of software tools in optimizing PV panel placement and efficiency. While improvements in building energy efficiency benefit overall energy savings, they do not directly affect the solar radiation received or the PV panels' efficiency as modeled in this study. These technological advancements facilitate precise calculations of energy production and savings, empowering stakeholders to make data-driven decisions.

### **Conflict of Interest**

This project is supported by the DOE award: Alabama Building Training and Assessment Center.



### References

- Aljundi, K., Pinto, A., & Rodrigues, F. (2016). Energy analysis using cooperation between bim tools (Revit and Green Building Studio) and Energy Plus. In *Proceedings of the 1º Congresso Português de Building Information Modelling, Guimaraes, Portugal*.
- Baghi, Y., Ma, Z., Robinson, D., & Boehme, T. (2021). Innovation in sustainable solar-powered net-zero energy Solar Decathlon houses: A review and showcase. *Buildings*, 11(4), 171.
- Jones, E. S., Alden, R. E., Gong, H., Frye, A. G., Colliver, D., & Ionel, D. M. (2020). The effect of high efficiency building technologies and pv generation on the energy profiles for typical us residences. In *2020 9th International Conference on Renewable Energy Research and Application (ICRERA)*. IEEE.
- Kahle, J. (2024). *The complete list of Alabama solar incentives*.  
<https://ecogenerica.com/alabama-solar-incentives/>
- Kneifel, J. (2012). *Prototype residential building designs for energy and sustainability assessment*. U.S. Department of Commerce and National Institute for Science and Technology.
- Kumar, M., Rawat, P., Maurya, A., Kumar, R., Bharadwaj, U., & Duggal, P. (2022). Analysing the institutional building for solar radiation and photovoltaic energy using autodesk-Revit. In *Journal of Physics: Conference Series* , 2178(1), p. 012024.



## Solar Energy Potential and Integration in Alabama Residential Buildings

Larosa, L. (2024). *Solar panel disposal laws — Section, AL guide*. Medium.

<https://medium.com/@leslie.larosa/solar-panel-disposal-laws-section-al-guide-e05322086878>

Padhee, M., & Pal, A. (2018). Effect of solar PV penetration on residential energy consumption pattern. In *2018 North American Power Symposium (NAPS)*.

Solar Energy Industries Association (2024). *Alabama state overview*.

<https://seia.org/state-solar-policy/alabama-solar/>

SolarReviews (2024). *Guide to Alabama incentives and tax credits*.

<https://www.solarreviews.com/solar-incentives/alabama>

Whatstheweatherlike.org. (2024). *What's the weather like in Alabama, U.S.A.*

<https://www.whatstheweatherlike.org/united-states-of-america/alabama/>

**Exploring the Impact of Spatial Factors on Circadian Daylight Distribution**

Neda Ghaeili<sup>1</sup>

Julian Wang<sup>1\*</sup>

Shevaa Beiglary<sup>1</sup>

Ying-Ling Jao<sup>2</sup>

1. Department of Architectural Engineering, Pennsylvania State University
2. Ross and Carol Nese College of Nursing, Pennsylvania State University

\* Corresponding author

### Abstract

Lighting strongly influences indoor well-being, yet existing metrics like "Daylight Autonomy" and "Annual Solar Exposure" overlook circadian light. Research highlights circadian light's significant impact on human performance, creating a need to explore spatial factors affecting its distribution. This study examines the influence of surface reflectance, proximity to windows, windows' optical properties, and gaze direction on circadian light. Using the Lark Plugin for Grasshopper, simulations were conducted in a box-model room with ten glazing systems varying in visible transmittance. The results show that windows with a visible transmittance below 0.3 fail to provide adequate circadian light unless the gaze is perpendicular. Among surface reflectance factors, wall reflectance proved more critical than ceiling reflectance in optimizing circadian light exposure.

Keywords: circadian light, spatial factors, window, wellbeing, daylight

### 1. Introduction

The impact of circadian light on the well-being of humans has been recently recognized. Several studies have investigated the effects of circadian light on human well-being, highlighting its significance and the consequences of insufficient exposure. For instance, some researchers have noted that circadian rhythm sleep-wake disorders are common in people suffering from mental disorders and that lighting therapy can help regulate this disorder (Blume, Garbazza, & Spitschan, 2019). Other research has proven that circadian cycles govern cellular functions and tissue processes by regulating gene expression and protein interactions (Grey & Koeffler, 2007). Disruption of these cycles may influence cancer susceptibility, highlighting the importance of circadian genes in tumor suppression. The impact of natural light on cognitive performance, physical activity, and alertness in students and workers has been discussed in the study (Shishegar & Boubekri, 2016). The study was done by Jao et al. (2022) also indicated that the ambient indoor lighting condition has positive influences on behavioral and psychological symptoms in people with dementia (Jao, et al., 2022). It is evident that indoor lighting is crucial for human well-being, given that Americans spend approximately 90% of their time indoors (Dodge, Daly, Huyton, & Sanders, 2012).

The intensity and duration of circadian daylight exposure received indoors depend on several factors, as outlined by Ghaeili, Ardabili et al. (2023). These factors encompass four key nodes:

- Node 1: Daylight source
- Node 2: Optical and morphological characteristics of windows
- Node 3: Optical properties of interior spaces

- Node 4: Occupant posture and gaze direction

Nodes 1 and 4 represent factors beyond the direct control of engineers and architects. However, for Node 2, in the context of glazing performance, optical characteristics encompass light transmittance, reflectance, and absorption, while morphological characteristics involve physical attributes such as window size, design, and glazing configuration. Node 3, on the other hand, emphasizes the importance of indoor surface light reflectance. Consequently, it is essential for professionals to thoroughly address all relevant aspects of Nodes 2 and 3 to effectively mitigate potential challenges posed by Nodes 1 and 4 in worst-case scenarios.

Regarding Node 2, various studies have examined this node from different perspectives. In most studies concerning the optical properties of windows, spectral transmittance has been the primary focus. For example, a study found no linear correlation between circadian stimulus and circadian light transmittance (Hraska, 2015). Similarly, others have suggested that windows could effectively meet indoor health standards for glazing systems with a visible transmittance ( $T_{vis}$ ) above 0.5 (Ghaeili, Beiglary, Wang, & Jao, 2023). For glazing with  $T_{vis}$  below 0.5, spectral transmittance weighted by circadian sensitivity provides a precise assessment of window performance.

On the other hand, architectural factors such as window-to-wall ratio (WWR), window orientation, and shading have been studied regarding the morphological properties of windows. For instance, some researchers have found that north windows require a higher WWR than south ones (Zeng, Sun, & Lin, 2021). Additionally, others noted that north-facing windows are less affected by changes in sky type compared to south-facing windows (Song, Jiang, & Cui, 2022). Concerning the impact of shading systems, research suggests that as long as the shading system does not obstruct the view of the sky from the window, it does not significantly impact the circadian performance of windows (Altenberg Vaz & Inanici, 2019). These studies focus on Node 2, and they all confirm that the impact of these variables is not independent; instead, there is an interconnected correlation among the variables that also affect the level of transmitted circadian light.

As noted elsewhere, a similar interconnected correlation exists among the parameters of Node 3 and Node 4, ultimately influencing the occupants' exposure to circadian light within a room (Ghaeili Ardabili, Wang, & Wang, 2023). Node 3, which examines interior architecture, surface reflectance, and spatial distance from the window, contributes to the fluctuation in the level and intensity of circadian daylight. Similarly, factors such as gaze direction and cornea height from Node 4 also impact the amount of exposure to circadian light. For instance, a study has demonstrated that when the gaze direction faces the window, there is a more significant reduction in circadian light as the distance from the window increases (Konis, 2018). Conversely, when the gaze is away from the window, there is less fluctuation in the reduction of circadian light exposure. Research indicates that wall reflectance is a key factor in determining exposure to circadian light

(Potočnik & Košir, 2021). This is not the case when the observer's gaze is perpendicular to the window.

This study aimed to explore the correlation between gaze direction, distance from the window, interior surface reflectance, and window  $T_{vis}$ . To achieve this, we utilized a box-modeled room simulated in Rhino, and the LARK plugin was employed to simulate various combinations of these variables. This approach allowed us to assess the impact of these variables and their correlation with circadian light exposure.

## 2. Methodology

This study involved the consideration of 10 windows selected from the International Glazing Data Base (IGDB), chosen based on their  $T_{vis}$  values. The objective was to select one glazing system from each 0.1 interval within the 0 to 1  $T_{vis}$  range. The selected windows' spectral transmittance curves are presented in Fig. 1.

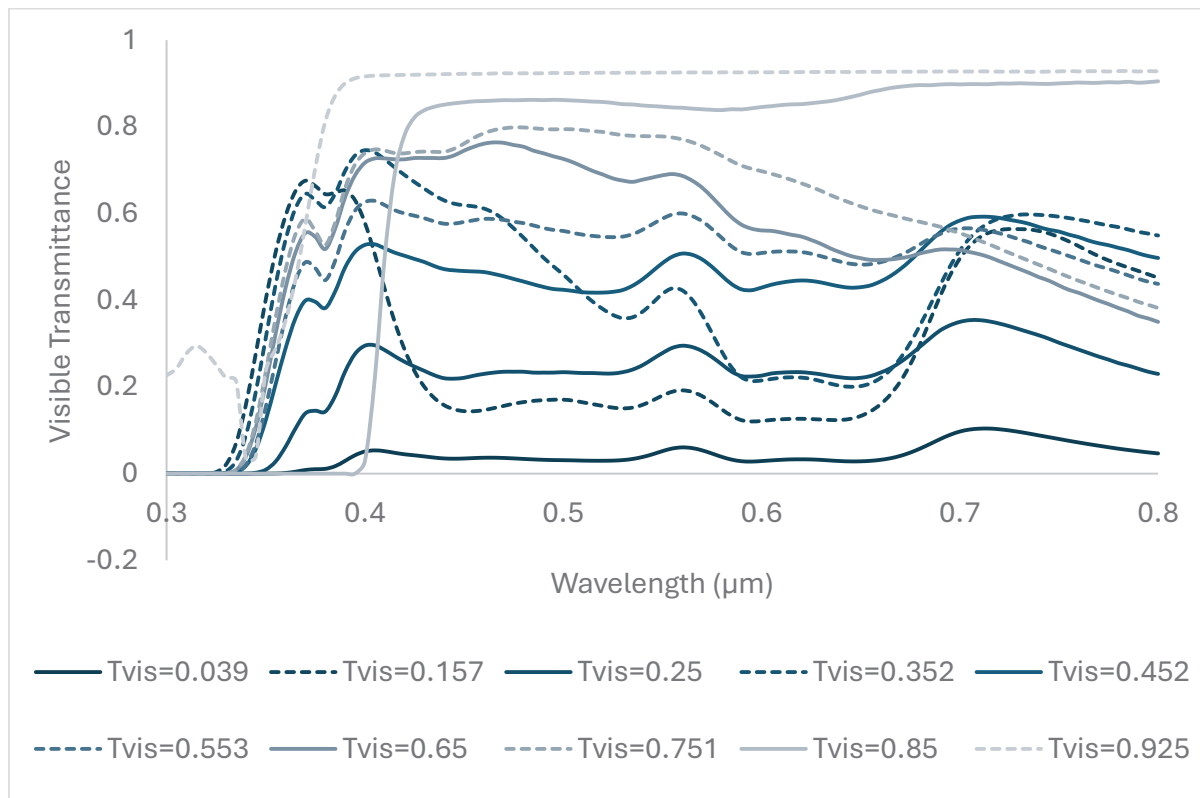


Fig. 1. Spectral transmittance of the selected glazings.

Regarding interior surface reflectance, ASHRAE recommendations were followed. The surface reflectance for ceilings ranged between 70% and 85%. For walls, it was between 50% and 70%. For floors, it was 20%. These ranges and values were also adopted for this research, with a 5% step interval for ceilings and a 10% step interval for walls to provide various scenario combinations.

This analysis was conducted using the LARK Plugin for Grasshopper. A box model measuring  $7 \times 7 \times 3 \text{m}^3$  was used, with a window featuring a 30% WWR on the model's south façade. The simulation was conducted in ASHRAE climate zone 4 in Denver, Colorado. As part of our simulation, we considered the noon fall equinox.

A grid measuring six by six, spaced 0.5 m away from the room walls, was employed for simulation. Four gaze directions were considered at each point on the grid: perpendicular to the window, parallel to the window (facing west and east walls), and away from the window. These gaze directions are denoted as S, W, E, and N, respectively.

The grid consists of 36 points, numbered from 1 to 36, for ease of reference in the paper. Fig. 2 illustrates the location and designation of these points and the four-gaze directions.

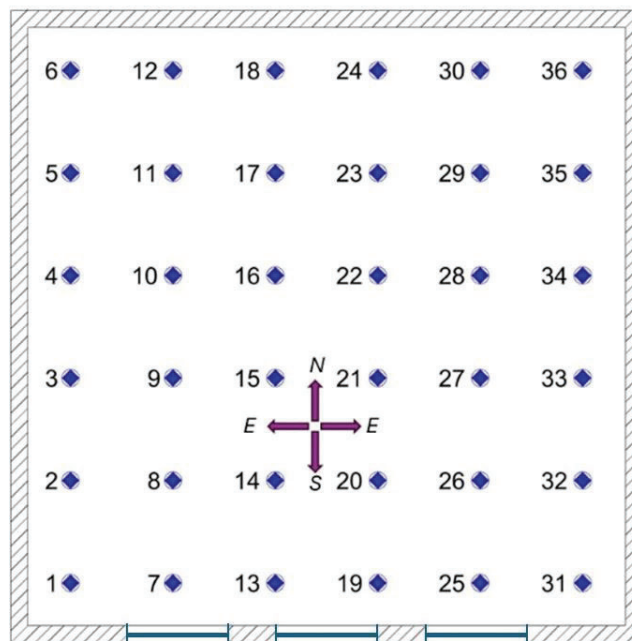


Fig. 2. Plan view: 36 sensors evenly spaced at 1m intervals in a  $7 \times 7 \text{m}^2$  room, 0.5m from walls.

### 3. Results

The level of circadian light, represented by  $m\_EDI$  (melanopic Equivalent Daylight Illuminance), was simulated for each point on the sensor grid and across four gaze

directions by adjusting wall and ceiling reflectance and window visible transmittance. The simulated values were analyzed using a decision tree regression to assess the impact of each variable on m\_EDI levels. The decision tree predicts m\_EDI by iteratively splitting the data into smaller subsets based on the most significant feature at each step. It chooses the feature (such as wall reflectance, ceiling reflectance, or window transmittance) and a threshold value that best separates the data, reducing the variance of m\_EDI within each new subset. By minimizing the variance, the tree ensures that the resulting subsets contain data points that are more similar in terms of their m\_EDI values, leading to more accurate predictions. At each "split," the tree focuses on improving how well the model can predict m\_EDI, ultimately breaking the data into groups that best explain the relationship between the variables and circadian light levels.

As depicted in Fig. 3, the gaze direction is the most influential parameter, followed by Tvis, in determining the condition of whether the space meets the required m\_EDI levels. In cases where the gaze direction is perpendicular to the window, regardless of Tvis value, exposure exceeds the 250 melanopic lux standard established by the WELL Building Standard (Circadian Lighting Design, 2022). However, if the gaze direction deviates from the perpendicular and Tvis falls below 0.301, circadian light exposure is below the threshold at 86.4 Lux.

Moreover, for points numbered above 30 that are positioned adjacent to the wall, a gaze direction parallel to the window facing the west wall yields higher circadian light compared to other directions. This may be due to the wall's obstruction of the south gaze direction, which makes the west direction a superior option. For finer adjustments, considering a southwest direction may offer even better results.

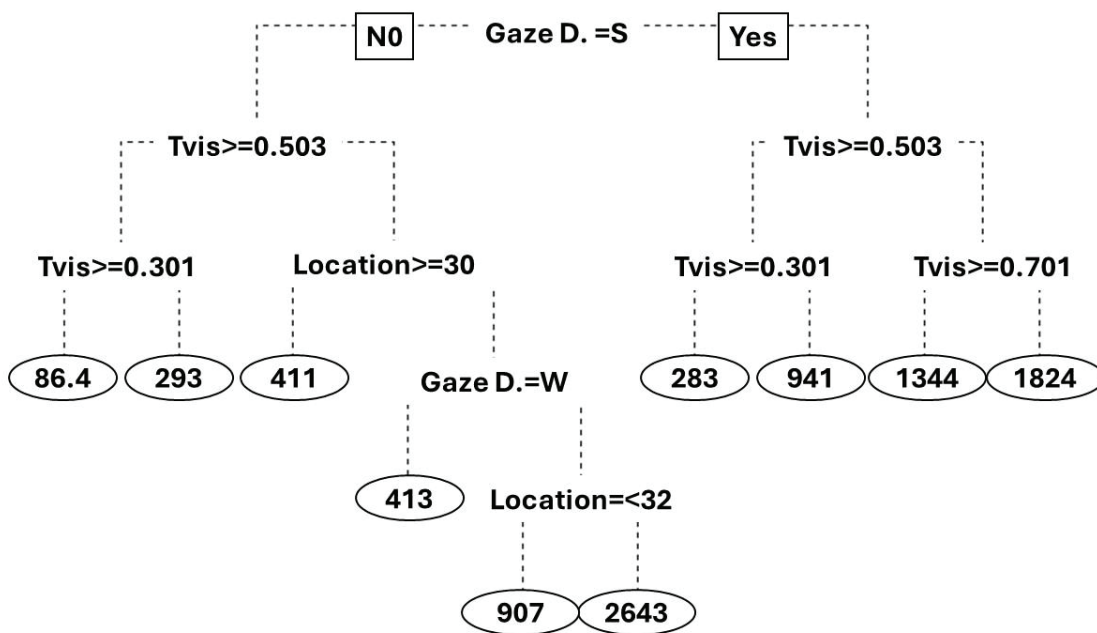
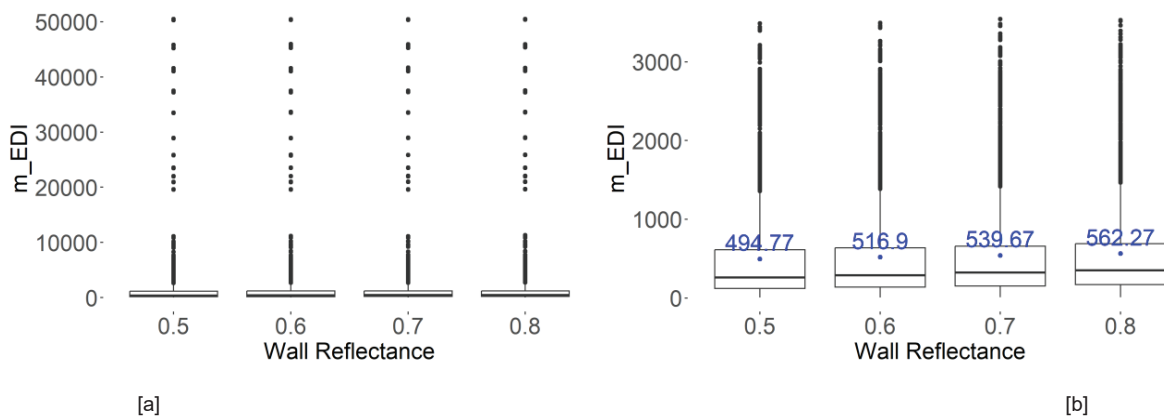


Fig. 3. Using Decision Tree Regression to assess the influence of variables on the level of m\_EDI.

Since surface reflectance did not appear in the decision tree plot, it indicates that surface reflectance has a minimal effect on the amount of m\_EDI. To provide a clearer understanding of m\_EDI variations across different wall and ceiling reflectance groups, side-by-side box plots were generated. Figures 4a and 4c show that the impact of surface reflectance on m\_EDI distribution is limited, and there are a series of outliers. Most outliers in the upper whisker of the plot are due to sensor points located in rows adjacent to the window. Consequently, data from the first three rows of the sensor grid were excluded to analyze further and check the impact of surface reflectance on circadian light in the deeper part of the room.

In Figures 4b and 4d, despite removing the first three rows, some outlier data points remain, especially when looking directly at the window. However, the reflectance of the walls becomes a significant factor in various scenarios, such as in areas far from the window and when the gaze direction is not perpendicular. A notable trend indicates that for every 10% increase in wall surface reflectance, there is approximately a 9% increase in m\_EDI levels. In contrast, ceiling reflectance exhibits less pronounced effects on m\_EDI levels.

Table 1 presents a more detailed examination of the impact of surface reflectance variation on the second half of the room.





### Circadian Daylight Distribution

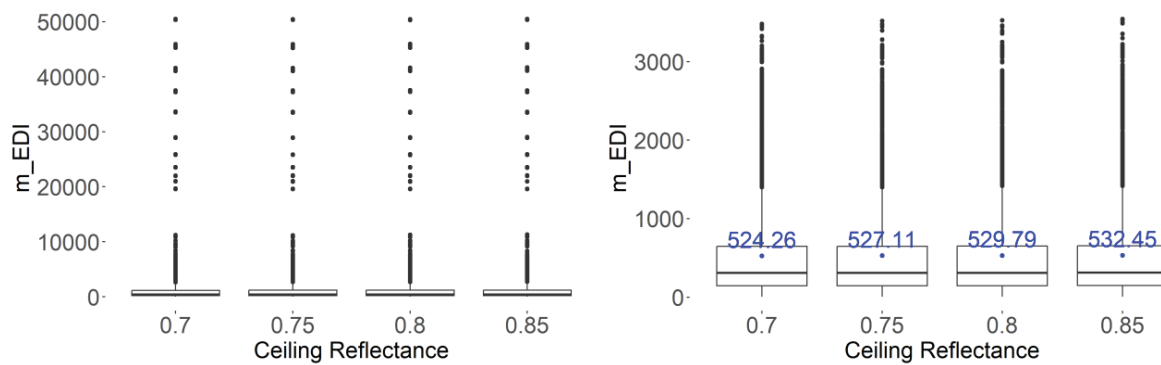


Fig. 4. The m\_EDI values distribution for different sensor points in simulation grids: a) all sensor points according to the wall reflectance, b) 18 sensor points in the second half of the room according to the wall reflectance, c) all sensor points according to the ceiling reflectance, d) 18 sensor points in the second half of the room according to the ceiling reflectance.

Table 1. Summary statistics of m\_EDI by surface reflectance

| Surface conditions |             | m-EDI values |          |          | Percentage variance<br>(relative to lowest reflectance) |
|--------------------|-------------|--------------|----------|----------|---|
| Type               | Reflectance | Mean         | Std Dev  | Variance |   |
| <b>Wall</b>        | 50%         | 494.7713     | 601.8083 | 362173.2 | -   |
|                    | 60%         | 516.8984     | 603.9540 | 364760.5 | 4.47  |
|                    | 70%         | 539.6673     | 607.9916 | 369653.8 | 9.07  |
|                    | 80%         | 562.2699     | 611.9694 | 374506.6 | 13.64   |
| <b>Ceiling</b>     | 70%         | 524.2582     | 602.5969 | 363123.0 | -   |
|                    | 75%         | 527.1096     | 605.3231 | 366416.0 | 0.54  |
|                    | 80%         | 529.7859     | 608.8238 | 370666.4 | 1.05  |
|                    | 85%         | 532.4531     | 611.0561 | 373389.5 | 1.56  |

The decision tree classification assessed the importance of various spatial variables, focusing on room depth and its influence on circadian light distribution. The analysis concentrated on the second half of the room, applying a 250 melanopic lux threshold to categorize data. Measurements below this threshold were labeled as 0 (insufficient light), and those equal to or above were labeled 1 (sufficient light). The decision tree plot visually distinguished these categories, with white nodes representing sufficient light and black nodes indicating insufficient light. Node percentages indicated how conditions met the threshold; for instance, 90.78% of cases with  $T_{vis}$  above 0.301 and a gaze direction of east, south, or west met the 250 lux threshold.

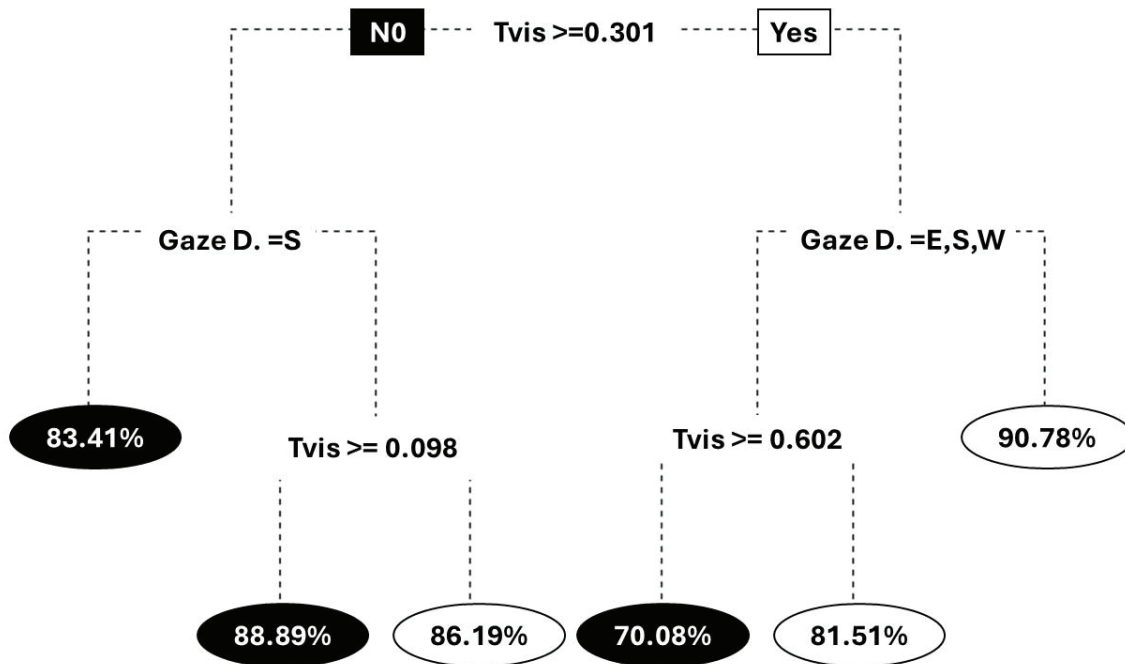


Fig. 5. Using Decision Tree Classification to assess the influence of variables on the level of m\_EDI in the second half of the room.

As illustrated in Fig. 5, Tvis emerges as the most influential variable. In 83.41% of instances where Tvis falls below 0.301, and the gaze direction is non-perpendicular to the window, the exposure to circadian light remains below 250 Lux. Furthermore, when the gaze direction is away from the window, and Tvis exceeds 0.602, the threshold is met in 81.51% of cases. Furthermore, for cases where Tvis is above 0.301, and the gaze direction is not opposite the window, the windows meet the threshold for 90.78% of cases.

#### 4. Conclusion

The exploration of circadian daylight encompasses a multitude of interconnected parameters, reflecting the complexity of indoor circadian lighting dynamics. There is an urgent need for a standardized metric to measure indoor circadian light distribution and ensure healthy indoor environments. This study simulated circadian light exposure levels within a room using a limited set of glazing samples and varying wall and ceiling reflectance.

Our research underscores the significance of gaze direction and window transmittance as essential variables in circadian light distribution. While a previous study has questioned the accuracy of Tvis in assessing circadian performance, our focus was to ascertain the predictive capability of existing properties in this research (Ghaeili, Beiglary, Wang, & Jao, 2023).

Wall reflectance emerged as a noteworthy factor, particularly in the deeper areas of the room, although Tvis and gaze direction overshadowed its impact. Acknowledging that these findings may evolve in more extensive and deeper spaces is important. This highlights the need for ongoing research to comprehensively understand and optimize circadian lighting in indoor environments.

### **Conflict of Interest**

This research was supported by the National Institutes of Health/National Institute of Aging (#1R21AG078544-01) for 'The Effect of Smart Ambient Bright Light for Nursing Home Residents with Alzheimer's Disease and Related Dementias,' and by the National Science Foundation (#2001207 CAREER) for 'Understanding the Thermal and Optical Behaviors of Near Infrared (NIR)-Selective Dynamic Glazing Structures.' All authors declare no conflicts of interest.

## References

- Altenberg Vaz, N., & Inanici, M. (2019). Syncing with the sky: daylight-driven circadian lighting design. *LEUKOS: The Journal of the Illuminating Engineering Society*, 291-309.
- Blume, C., Garbazza, C., & Spitschan, M. (2019). Effects of light on human circadian rhythms, sleep and mood. *Somnologie*, 147-156.
- Circadian Lighting Design*. (2022). <https://v2.wellcertified.com/en/wellv2/light/feature/3>
- Dodge, R., Daly, A., Huyton, J., & Sanders, L. (2012). The challenge of defining wellbeing. *Int. J. Wellbeing*.
- Ghaeili Ardabili, N., Wang, J., & Wang, N. (2023). A systematic literature review: Building window's influence on indoor circadian health. *Renewable and Sustainable Energy Reviews*.
- Ghaeili, N., Beiglary, S., Wang, J., & Jao, Y. (2023). Assessment of the window performance from the light provision and circadian light aspects. *Proceedings of the 52nd American Solar Energy Society National Solar Conference 2023* (pp. 43-51).
- Grey, S., & Koeffler, H. (2007). The role of circadian regulation in cancer. *Cold Spring Harbor Laboratory Press*, 72, 459-464.
- Hraska, J. (2015). Chronobiological aspects of green buildings daylighting. *Renewable Energy*, 109-114. doi:<http://dx.doi.org/10.1016/j.renene.2014.06.008>

Jao, Y.-L., Wang, J., Liao, Y.-J., Parajuli, J., Berish, D., Boltz, M., Calkins, M. (2022).

Effect of ambient bright light on behavioral and psychological symptoms in people with dementia: a systematic review. *Innov Aging*. doi: 10.1093/geroni/igac018.

Konis, K. (2018). Field evaluation of the circadian stimulus potential of daylight and non-

daylit spaces in dementia care facilities. *Building and Environment*, 112-123.

Potočnik, J., & Košir, M. (2021). Influence of geometrical and optical building

parameters on the circadian daylighting of an office. *Journal of Building Engineering*.

Shishegar, N., & Boubekri, M. (2016). Natural light and productivity: analyzing the

impacts of daylighting on students' and workers' health and alertness. *Int'l Journal of Advances in Chemical Engineering & Biological Sciences (IJACEBS)*.

Song, H., Jiang, W., & Cui, P. (2022). A study on nonvisual effects of natural light

environment in a maternity ward of a hospital in cold area. *BioMed Research International*.

Zeng, Y., Sun, H., & Lin, B. (2021). Optimized lighting energy consumption for non-

visual effects: A case study in office spaces based on field test and simulation. *Building and Environment*.

**Team SHUNYA: Harnessing Solar Power and Circularity in Urban Housing - A  
Student-Built Net Zero Home Case Study**

Ali Khan<sup>1</sup>

Prabhat Sharma<sup>1</sup>

Eshica Arya<sup>1</sup>

Venkata Santosh Kumar Delhi<sup>1</sup>

<sup>1</sup>Indian Institute of Technology Bombay, Mumbai, India

## Abstract

The subject of this case study is an operational two-story residential structure named Project Vivaan, situated within the campus of Indian Institute of Technology Bombay, in Mumbai, India. Designed and constructed by Team SHUNYA, Vivaan is an innovative prototype of a Net Positive Energy, Net Zero Carbon, and Net Zero Water residential building. Constructed with a focus on energy efficiency and sustainability, the house incorporates passive performance measures, second-life materials, advanced HVAC systems, and home automation. Preliminary data indicates that Vivaan performs as a Net Positive Energy house, with annual solar PV generation exceeding its energy demand. The project addresses increasing energy demand in residential buildings due to climate change and promotes circular economy principles by ensuring the structure's disassembly and material reuse at the end of its life cycle. The building has achieved significant recognition, including the 1<sup>st</sup> runner-up position at the 2023 US DOE Solar Decathlon Build Challenge.

Keywords: Solar Decathlon, net positive energy, net zero water, net zero carbon, material circularity

## Introduction

Vivaan is a Net Positive Energy, Net Zero Carbon, and Net Zero Water residential prototype designed and constructed by Team SHUNYA, a student team from Indian Institute of Technology (IIT) Bombay. Aimed to create a genuinely sustainable dwelling unit in an attempt at redefining residential construction in India, the building has been awarded multiple accolades for many of its innovative aspects. Vivaan also won the 1<sup>st</sup> runner-up position out of 32 international teams at the United States Department of Energy Solar Decathlon Build Challenge 2023, held at the National Renewable Energy Laboratory in Golden, Colorado in April 2023. The house incorporates features unique to the residential building stock in India, extensively uses second-life materials, and includes an in-house developed dehumidification system. A proprietary home automation system and accompanying app provide convenient controls for minimizing energy waste and maintaining adaptive thermal comfort levels in the house. The design also implements passive performance measures to maximize energy efficiency and extensively incorporates computational simulations to achieve a data-driven approach.

The major problem that this project addresses is the high demand for energy in residential buildings, which has been rapidly growing due to the effects of climate change. Moreover, Vivaan is designed with a circular economy approach, ensuring the disassembly of the structure and appropriate recycling or reuse after the end-of-life cycle. This system needs to be included in India, as traditional brick-and-mortar construction does not allow for such circularity.

## Approach

The residential building was constructed between December 2022 and April 2023, with a goal of testing and implementing various energy efficiency measures adopted





Fig 1. (a) Exterior view after completion. (b) Steel structure of Project Vivaan. (Credit: Prabhat Sharma)

after careful considerations and iterations with the help of multiple simulation software packages. Sensor-based monitoring and data analysis over the past year reveal that Vivaan is performing as a Net Positive Energy house. According to detailed comprehensive calculations, it is also Net Zero Water. Moreover, it is expected to achieve Net Zero Carbon within the next five years, owing to carbon-capturing measures implemented as part of the construction process.

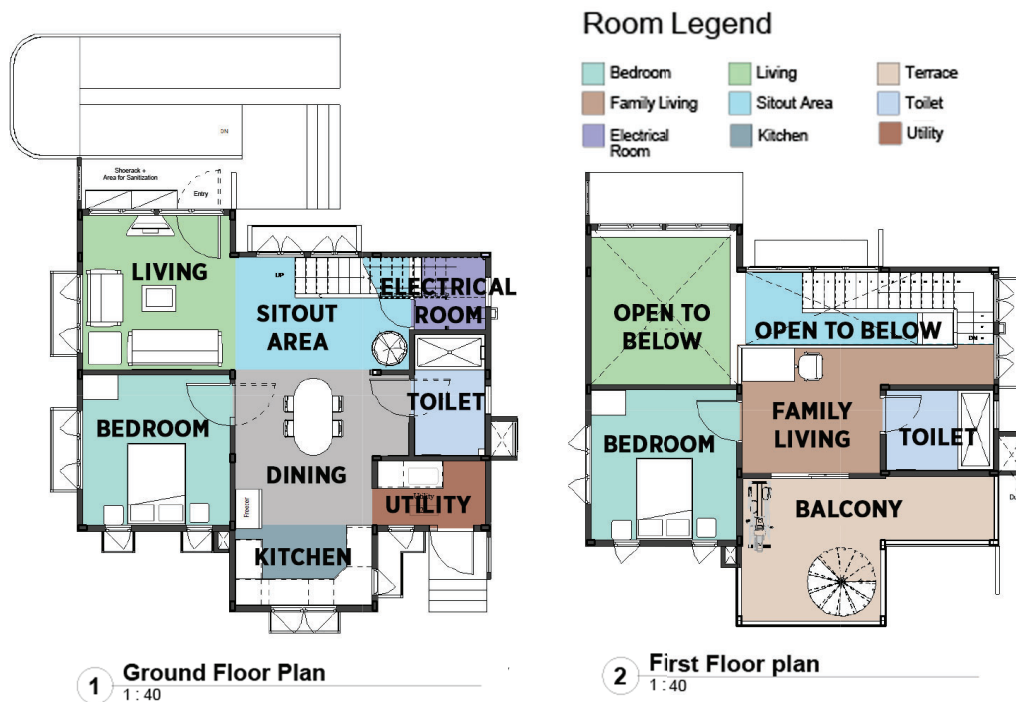


Fig 2. Floor plans of project Vivaan. (Credit: Ankan Karmakar)



With a total habitable area of 1,367 ft<sup>2</sup> (127 m<sup>2</sup>), the residence consists of two bedrooms, a dining hall, a kitchen, two washrooms, and a double-height living room. Among these, both the bedrooms and the living room are conditioned spaces, with a cumulative conditioned area of 34 m<sup>2</sup>. The spatial configuration is iteratively derived from floor plans of single-family detached dwelling units found in Mumbai and India to ensure a similarity between expected energy demand and physical parameters like room volume and occupancy schedule.

Mumbai is categorized in the Extreme Hot-Humid (0A zone) within the ASHRAE Climate Classification and warm-humid climate zone as per the National Building Code of India. The architectural typology resembles houses found in the coastal regions of Western India, with sloping roofs and inclined shades above windows. In terms of performance, the design and its elements are applicable to coastal areas of India that exhibit similar tropical warm and humid climates. The design incorporates data-informed passive performance measures, such as vertical fins and movable external shading to allow useful daylight intake and reduce heat gains from excessive solar radiation, double height spaces and open floor plans to allow for stack effect and cross ventilation, respectively, and window sizing (wall-window ratio) and their placement that are also iteratively optimized to aid in airflow and natural light. Before the design stage, rigorous micro and macro-climatic analysis of site conditions was performed and the weather files were calibrated using measured real-time outdoor ambient temperature data acquired onsite.



| <b>Material Selection</b>   |                            | <b>Thickness (mm)</b> | <b>U Value (W/m<sup>2</sup>K)</b> |
|---|----------------------------|-----------------------|-----------------------------------|
|  | AAC Blocks                 | 230                   | 0.8                               |
|   | Hollow Core Concrete Panel | 100                   | 0.37                              |
|   | Mineral Wool Insulation    | 100                   |                                   |
|   | Fiber Cement Board         | 12                    |                                   |
|  | Fiber Cement Board         | 12                    | 0.22                              |
|   | Polyurethane foam          | 100                   |                                   |
|   | Fiber Cement Board         | 12                    |                                   |
|   | Fiber Cement Board         | 6                     | 0.24                              |
|   | Eco-board Wall Panel       | 9                     |                                   |
|   | Glass Wool Insulation      | 100                   |                                   |
|   | Eco-board Wall Panel       | 9                     |                                   |

Fig 3. Wall assemblies considered for envelope and their U-value

Vivaan is carefully designed to ensure the building's resilience against natural and

manmade disasters. With a design life of 50 years, the prototype is constructed using precast steel sections for beams and columns, along with prefabricated metal decks for slabs. This decision was taken to ensure disassembly after the end of the design life. Additionally, a raft footing foundation of 1.8 m depth makes up the substructure of the building.

The primary criteria for envelope material selection were the climatic conditions of Mumbai and the Indian Energy Conservation Building Code (ECBC) compliance. A detailed comparative study of multiple envelope parameters derived from an analytical hierarchical process (AHP), considering thermal transmittance (U-value), embodied energy, local availability, durability, and life cycle cost was used to select appropriate combinations of materials for wall assemblies. An innovative and low carbon biodegradable board made of recycled agricultural waste material, named EcoBoard, has been used to reduce the embodied energy of the wall assemblies. The external wall, starting from the outermost layer (Layer 1), includes sections as follows:

| Layer | Material                 | Thickness (mm) | Key Feature           | Expected Life (years) |
|-------|--------------------------|----------------|-----------------------|-----------------------|
| 1     | Fiber Cement Board (FCB) | 6              | Durability            | 30                    |
| 2     | Moisture Barrier         | 2              | Impermeability        | 50                    |
| 3     | EcoBoard                 | 9              | Lower embodied energy | 20                    |
| 4     | Fiber wool Insulation    | 100            | Thermal resistance    | 50                    |
| 5     | EcoBoard                 | 9              | Lower embodied energy | 20                    |

The internal wall assembly does not incorporate the FCB and the moisture barrier and has a reduced insulation layer of 50 mm. The final U-value of the external assembly was calculated to be 0.24 W/K-m<sup>2</sup>, which is 70% less than that of AAC blocks, the material used most commonly in modern-day construction in India. The reduction in U-value is the first step to reducing the heat gain in the house. The envelope of Vivaan was designed to meet the Energy Conservation Building Code (ECBC) of India. To achieve ECBC compliance, a residential building in a warm and humid climate can have a maximum U-value of 0.4 W/m<sup>2</sup>-K for opaque external wall assemblies. The maximum U-values for an opaque external wall assembly in the same climatic zone for ECBC+ compliance is 0.34 W/m<sup>2</sup>-K. Vivaan is ECBC compliant with the existing assembly in 4 out of 5 climate typologies and ECBC+ in 3 out of 5.

A proprietary HVAC system designed by the student team has been deployed, which handles latent and sensible loads separately. A Fan Coil Unit at higher chilled water temperatures with a coefficient of performance (COP) of 4.2 handles the sensible load, while the liquid desiccant dehumidification system handles latent loads. This HVAC system has greater energy efficiency when compared to the split air-conditioning units primarily used in Indian households. Chilled water and strong liquid desiccant

are generated and stored to be used during non-solar hours. The waste heat produced from the condenser is then used to provide hot water. The system can also be controlled by an automation system created by the team. This system is suitable for application in regions with high humidity and temperatures throughout the year. A significant proportion of central and southern India exhibits these kinds of climatic conditions, along with the western and eastern coasts of the country. The system's efficiency is expected to increase with the simulated increase in demand, meaning that the system is to perform better in multi-family and low to mid-rise housing.

To meet the energy demand of the house, a solar power generation system with

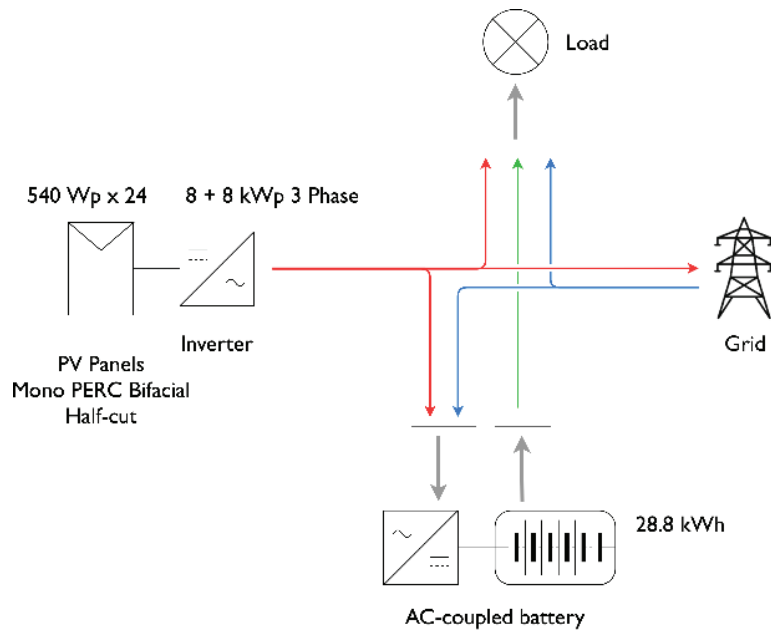


Fig 4. (a) Solar PV system design. (b) Installed bifacial solar panels. (Credit: Dany Hemanth)

12.96 kWp capacity is designed and installed on the roof. Monocrystalline bifacial

PV panels with a half-cut design were selected due to their higher power output per unit area and long-term durability. A 28.8-kWh lead acid battery is also part of the system to decrease the overall dependence on the grid. The total annual generation of the PV system is expected to be about 13,635 kWh, while the calculated annual energy demand is about 12,484 kWh. Due to the excess energy produced by the system, it was concluded that the house consumes less energy than it produces with onsite renewable energy generation making it Net Positive Energy. The solar PV panels are expected to last for 25 years, but the battery for energy storage will need replacement in about five years. Initially, the plan was for lithium-ion batteries, which can last up to 15 years, but the budget constraints led to the current battery system. A hybrid inverter with a life span of 10 years is used with a solar PV system for trading off excess annually generated electricity.

| (All values in kWh)   | Min  | Average | Max  | Annual |
|-----------------------|------|---------|------|--------|
| Loads                 | 24.5 | 34.2    | 44.5 | 12,484 |
| Generation            | 0.8  | 37.4    | 52.3 | 13,635 |
| Feed-in to Grid       | 0    | 10.2    | 26.6 | 3,724  |
| Consumption from grid | 0    | 9.5     | 33.0 | 3,464  |

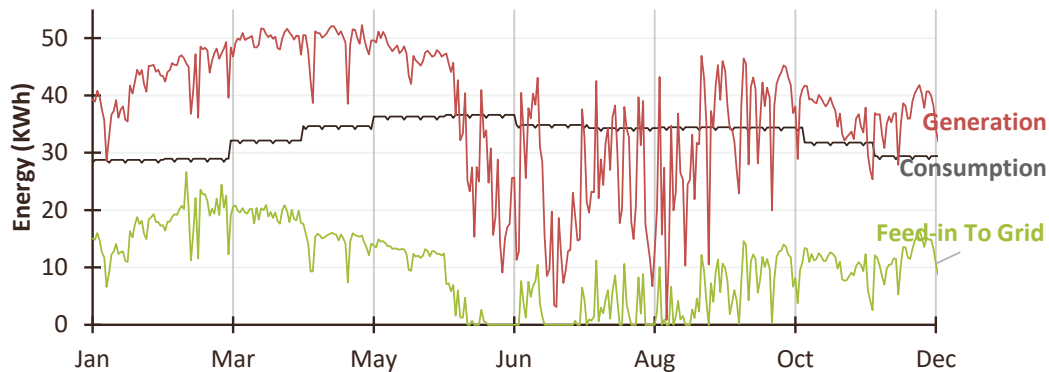


Fig 5. Annual electrical energy demand and production

### Data Collection and Analysis

Multiple sensors were installed in the house to measure the air temperature, humidity, and CO<sub>2</sub> concentration. Readings were taken at intervals of 10 seconds. Fig. shows the indoor air temperature, outdoor ambient temperature, and indoor relative humidity readings taken between April 3, 2023 and April 5, 2023. The HVAC system of the house was running during this experiment. The figure shows that the indoor air temperature can be easily maintained between 21°C to 26°C with the help of the chilled water system. Also, the relative humidity mostly lies in the range of 50% to 60%. This shows that the designed system has the potential to increase or decrease the temperature and relative humidity of the house based on desired occupant comfort. Owing to passive performance measures, the thermal cooling load of the house is reduced by 28%, and annual thermal comfort hours increased

by 16.4% with the use of the mentioned wall and roof assembly, as compared to a typical brick-concrete structure. A second measurement campaign was carried out, where surface temperature sensors were installed on the west and south walls of the ground-floor bedroom. The readings were taken as averages of 10-minute intervals under no active ventilation or cooling. No mechanical ceiling fans or air conditioning were active during this measurement period. The results, as illustrated in Fig , show that the internal surface temperatures of both walls remain consistently equal throughout the day, lying within the range of 27°C to 29°C when the external surface temperatures were between 25°C to 31°C.

### Results

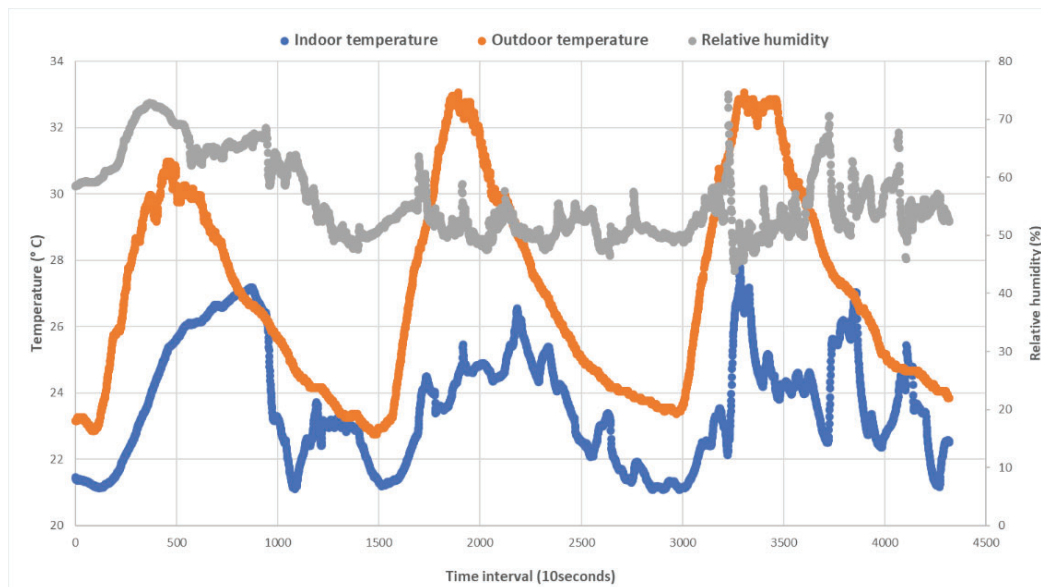


Fig. 6. Experimental readings from April 3, 2023 and April 5, 2023

The Ladybug and Honeybee libraries of Rhino3D, which run EnergyPlus on their back ends, were used for conducting incident solar radiation analysis, case-wise energy simulations, and daylight studies. OpenFOAM was deployed to simulate internal air flow using computational fluid dynamics and inform building geometry. All the analyses mentioned theoretically amount to a difference of 24% in energy consumption compared to the base case, i.e. the first design iteration.

Optimization of building geometry using Grasshopper's native genetic algorithm solver, Galapagos, suggested a reduction of 11% between the base case and the completed design. Similar optimization for building orientation minimized the average annual incident radiation and thus reduced the impact of heat gains from solar radiation. The proprietary automation system and its mobile application help reduce energy waste by about 18% by reducing energy waste and maintaining optimal adaptive thermal comfort and artificial lighting levels. The app monitors energy consumption in appliances using a home assistant platform. The open-source platform allows for customization, extensibility, and deplorability. It allows monitoring of temperature, humidity, CO<sub>2</sub>, and lux levels for each room and automates appliances based on occupancy. Remote monitoring and control of



systems are possible through a web interface and companion app. The total annual energy demand is predicted to be significantly less than the annual solar PV generation, making the house Net Positive Energy.

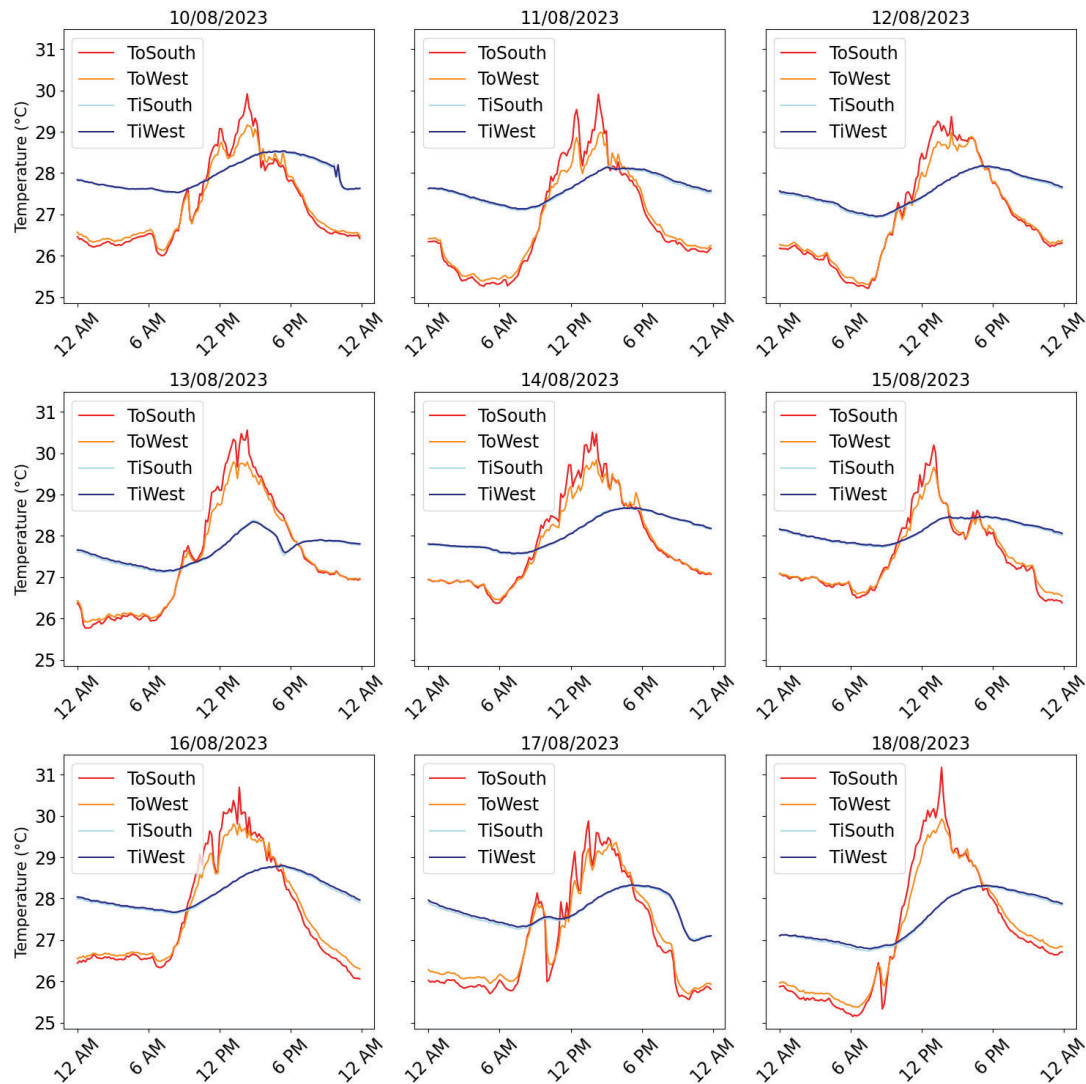


Fig 7. External ( $T_o$ ) and Internal ( $T_i$ ) wall surface temperatures between August 10, 2023 and August 18, 2023

As per the Uniform Indian Plumbing Code (UPC-I), 167 liters of water is consumed per capita per day (lpcd), but Project Vivaan uses only about 83 lpcd with the help of water-efficient fixtures and a greywater recycling system. An additional rainwater harvesting system with a storage capacity of 10,000 liters is installed, which can operate during all four months of the monsoon season and can provide non-potable water for up to 45 days in case of complete water shortage. The water-efficiency features result in an overall 82% water savings compared to a BAU home. Most of the freshwater purchased from the municipal corporation is used for drinking and cooking. As per Indian Green Building Council (IGBC) norms, if a house can use alternate water for more than 75% of the total consumption, it is characterized as a

near-net zero water house. Since Vivaan's water saving amounts to about 82%, i.e. 7% more than the baseline standard, it was concluded that the house is near Net Zero Water. Since Vivaan is still in the early operational period, there isn't enough measured data regarding water consumption or savings yet.

The building extensively incorporates second-life materials, such as biodegradable panels made of recycled agricultural waste. The EcoBoard panels are made using straw, husks, other organic materials, and a non-volatile binder. By using these boards, Vivaan reduces the environmental impact of the envelope when compared to traditional construction materials and promotes sustainable practices.

### **Conclusion**

The core philosophy behind Project Vivaan and Team SHUNYA is the drive and commitment to revolutionize the sustainable housing industry. Vivaan attempts to create a beacon of sustainability, embodying the principles of Net Zero Energy, Net Zero Water, and Net Zero Carbon. From selecting innovative second-life materials to implementing advanced fire-safety features, every aspect of Vivaan is designed to minimize environmental impact and prioritize the safety and wellbeing of its inhabitants. However, implementing these innovative features is challenging in India, as conventional construction laborers need more skills and experience to effectively execute the design onsite during construction.

The team needed to assist the construction labor with various issues and provide solutions to implement modern technologies efficiently. Several training and education sessions about new construction technology and materials were also conducted to educate the laborers about contemporary practices. Challenges arose when ensuring airtightness and aesthetic finishing, but were successfully tackled with correction methods and skilled labor.

Additionally, while using materials like EcoBoard, construction during monsoons becomes difficult as the material degrades from direct contact with water. Implementing in-house developed technology, such as liquid desiccant for dehumidification, requires a significant amount of time and an early start for timely implementation. Also, the financial budget becomes a prominent constraint when such experimental projects are implemented practically.

Project Vivaan is built to last, with structural durability of 50 years and precautions in place to handle electrical disruptions and emergencies caused by factors like climate change. By theoretically achieving Net Zero Carbon, we reduce our ecological footprint and establish a new standard for environmentally conscious construction. Furthermore, our focus on water conservation is evident through water-saving technologies that result in up to 82% savings, coupled with a robust 45-day water backup system.

Beyond sustainability and safety, Project Vivaan offers a sanctuary of comfort and serenity to its occupants. Innovative engineering elements are seamlessly integrated into the design, such as Jaalis (perforated window screens inspired by traditional Indian architecture) that aid in natural ventilation, cool roof tiles for maximizing energy generation of bifacial PV panels, and automation features for convenience and comfort. Through awareness and education, Vivaan strives to spread sustainable lifestyle principles to the masses, empowering individuals to

embrace sustainable living and meeting the growing demand for urban housing in an environmentally conscious manner. The objective is to create a future where sustainable housing is inclusively accessible, inspiring a collective movement towards a more resilient and harmonious world.

### **Conflict of Interest**

We are sincerely grateful to our sponsors, the dedicated members of IIT Bombay and Team SHUNYA, and the faculty advisors for their unwavering support and invaluable contribution to this project. Their generosity and belief in our vision have been instrumental in making this endeavor successful. We extend our heartfelt appreciation to our Associate sponsors, EcoBoard Industries Ltd and Prism Johnson Ltd; our Platinum sponsors, Design Builder Software Australia, Saint-Gobain Glass India Pvt Ltd, Pepperfry, Softtech Engineers Ltd, Seal for Life Group, Ecofirst Services Ltd, Prince Pipes and Fittings Ltd; Gold sponsors: Owens Corning India Pvt Ltd, Adani Solar, Polycab India Ltd, Signify Innovations India Ltd, Plan-M India Pvt Ltd, and Ameet Innovations LLP; our Silver sponsors, Saint-Gobain Gyproc India Ltd, SustLabs, CSD, SunInfra Energies Pvt Ltd, Origin Corporate Services Pvt Ltd, Upcycle Chakra LLP/ Anwasha Foundation, Wadbros Imports & Exports, Creatively Scientific Design, Rainy, Sugam Paryavaran Vikalp Pvt Ltd, Albatross Energetics, and Farmland Rainwater Harvesting System. Their deep commitment to sustainability has played a pivotal role in propelling this initiative forward. Their unwavering dedication to promoting sustainable housing and fostering a greener future for urban communities has been truly inspiring and has contributed significantly to the success of our project. We genuinely appreciate their trust, partnership, and shared commitment to creating a more sustainable world. Without their support, this transformative journey would not have been possible.



## References

2021 Uniform Plumbing Code. (n.d.). Retrieved September 17, 2024, from

<https://epubs.iapmo.org/2021/UPC/>

2023 Build Challenge Results. (n.d.). Retrieved September 17, 2024, from

<https://www.solardecathlon.gov/2023/build/2023-build-challenge-results.html>

2019 Energy Conservation Building Code. (BEE). Retrieved September 17, 2024,  
from

<https://beeindia.gov.in/sites/default/files/ECBC%20book%20final%20one%20%202017%20with%20Amendments.pdf>

**Designing High-Performance Buildings with a Focus on Equity: A U.S.  
Department of Energy Solar Decathlon Case Study**

Nea Maloo, FAIA  
Department of Architecture  
College of Engineering and Architecture, Howard University

**Author Notes**

Nea Maloo <https://orcid.org/0000-0002-1223-3149>

All graphics, design and research work produced in Equitable High-Performance class by Retro Booming student team presented at Solar Decathlon design competition. Retro Booming Team members: Darian Jacobs II, Ro Briscoe, Beleil Lamb, Jayla Wade, Sierra Gee, Eman Munoz, Elijah McKinnie, Malik Johnson, Ejovwokoghene Mushale, El Adon Bey

Acknowledgment: U.S. Department of Energy (DOE) Solar Decathlon® Design Challenge and all the faculty, partners who advised the students.

## Abstract

According to the Urban Economic Forum, around 80% of the buildings we have today will exist in 2050 which are responsible for 40% of global emissions. To effectively combat climate change, we must look for opportunities to design and retrofit existing buildings. This case study on the Mary Church Terrell House demonstrates an effective method to create high-performance buildings and enhance the focus on equity within a Historically Black College and University (HBCU) curriculum by leveraging the U.S. Department of Energy Solar Decathlon student competition framework — the design lessons integration with the guidelines and delivery of the competition entries. Through the design outcomes of an interdisciplinary cohort of students, the case study shows the application of energy outcomes to retrofit historic landmarks. It also discusses the impact of this exploration on the student's learning process to create equitable, net-zero buildings that promise to reduce carbon emissions by reducing their carbon footprint.

Keywords: Solar Decathlon; Howard University; historic landmark; house retrofit; net zero energy; case study; Washington, D.C.; historically Black college; HBCU

## 1. Introduction

Addressing climate change by getting cities to net zero and reducing the carbon in their buildings is an urgent cause, since buildings in cities account for almost 60% of carbon emissions (Grainger, 2022). For this reason, decarbonizing buildings is essential if we are going to slow global warming. The United Nations' Intergovernmental Panel on Climate Change's special report that addresses global warming of 1.5°C or greater makes clear that this urgency is an interdisciplinary matter among architects, builders, and manufacturers. What is also clear, according to the American Institute of Architects, is that more than 90% of 2025's building stock is already standing. Therefore, decarbonizing existing buildings offers our greatest chance of meeting this goal of keeping warming below 1.5°C. There is also evidence that retrofitting buildings strengthens the local economy. Compared to new construction, a greater proportion of a retrofit's budget typically goes to labor, creating more jobs for the dollars spent (Logan, 2019).

The design of retrofitted decarbonized buildings, with equity as the center of design, is essential to combat climate change and improve environmental justice. Breathing life into existing buildings with program and energy savings will also reduce the additional carbon emissions that new buildings create. Skills needed to create net zero buildings must be taught to the next generation of designers and builders. The design of high-performance buildings should consider the impact on the community and deliver

occupant comfort. This paper discusses a case study from the U.S. Department of Energy's annual Solar Decathlon Design Challenge, which offers students a way to propose new ways to decarbonize the built environment and test their theories on the project of their choosing showing impact and reach. The student projects provide ways to consider the impact of building design on the larger context of communities, too. Teaching decarbonization via this established competition is an effective way to address real opportunities for our communities to be stewards of our architectural heritage and empower students with concepts of sustainability, efficiency, and historic preservation.

The U.S. Department of Energy (DOE) Solar Decathlon® Design Challenge is an internationally recognized competition with different categories of residential, education, office, and multifamily high-performance buildings. Collegiate students compete on interdisciplinary teams to design these buildings. These designs' goals are to address real-world issues related to climate change, affordability, and environmental justice. Deepening their understanding of the global challenge, the competition asks them to consider architecture, energy performance, engineering, market analysis, durability and resilience, embodied environmental impact, integrated performance, occupation experience, and comfort and environmental quality.

This paper outlines the Terrell House, which was retrofitted by interdisciplinary student team from Howard University, both of which were the finalists in the Solar Decathlon competition and one of which received third place in their retrofit category.

### **1. Case Study: Mary Church Terrell House**

The interdisciplinary team of students from architecture, clinical studies, and environmental studies worked on the project during the course of spring semester in 2023.

#### *1.1 Site Context*

The house is located at 326 T Street NW, Washington D.C. in the LeDroit Park Historic District. The house occupies 1,618 square feet of the total lot size of 2,390 square feet and is surrounded on either side by residential rowhouses. The neighborhood is walkable and bikeable to surrounding areas with easy access to local small businesses and goods, as well as easy access to public transportation nearby with several metro and bus options available. LeDroit Park was originally a whites-only neighborhood in the 19th century and was even gated at one point in its history with guards to promote security for its residents. D.C. activists, as well as students from Howard University, helped integrate the area and, by the 1940s, LeDroit Park became a major focal point for the African American elite.

### *1.2 Historical Context*

LeDroit Park is notable for historical African-American figures who lived and worked there, including Walter Washington, the first mayor of Washington, D.C., elected under the D.C. Home Rule Act of 1973, and his wife, Benetta Washington, D.C, as well as General Benjamin O. Davis, the first African-American brigadier general in the U.S. Air Force, and Robert A. Terrell, the first African-American appointed as a District of Columbia Municipal Court judge, and his wife, Mary Church Terrell.

### *1.3 Mary Church Terrell*

Mary Eliza Church Terrell and her husband moved into 326 T Street in 1899 and stayed there until 1913. She was an African American educator, civil rights activist, and writer who was among the first Black women to receive a master's degree and the first Black woman to serve on an American school board. In 1909, Terrell was among the founders of the NAACP. During her residence, this house hosted a distinguished social network of prominent Black educators and public figures who lived in the affluent LeDroit Park neighborhood.

Her life's work focused on the notion of racial uplift, the belief that African Americans would help end racial discrimination by advancing themselves through education, community activism, and the motto "lifting as we climb."

Mary continued to advocate for civil rights until she died in 1954. The house remained and was occupied by multiple owners until as recently as 2002. During the 1970s, a fire destroyed half of the original duplex house while the other half was saved by a firewall (the existing western side of the house). This gives the house its distinct form today. In 1975, the house was registered as a National Historic Landmark.

### *1.4 Background*

Howard University purchased the residence in 2018 to keep the property and its history and provide renovations. A team of interdisciplinary students from Howard called Retro Booming used this project for the design challenge of the residential retrofit category of the Solar Decathlon to explore ways to redesign and repurpose the historic Terrell House.

### *1.5 Design Goals*

The project's primary goal is to renovate and achieve net zero energy. The students created three main design goals of "legacy," "equity," and "decarbonization" to embrace the community and history of the building. The legacy goal was achieved through retrofit design and appreciation of the historical ties of Mary Church Terrell and the LeDroit

Park Area. The design promoted social justice initiatives and practices through programming and design and achieved decarbonization of the building using renewable energy. The Retro Boomin' team's design proposal was developed to set a precedent for the LeDroit Historic Park District Community in showcasing a sustainable and resourceful home. Given the unique characteristics of the house compared to the other houses in the community, these design changes could be implemented throughout the community even more easily than they were with this development. The proposed design development would ultimately provide a pilot program for other homeowners in the neighborhood. The homeowners would each reap the benefits of a marketable, energy-efficient home that would significantly lower energy costs compared to the other traditional homes in the area, thus encouraging more sustainable approaches around.

### *1.6 Design Highlights*

The students iterated and created designs that addressed the categories of the competition including architecture, market analysis, integrated performance, embodied environmental impact, resilience, occupant experience, comfort, and environmental quality.

Retro Booming's proposal is to first, given the angle and shape of our roof, implement a backyard pergola system capable of hoisting the photovoltaic (PV) panel array as well as providing an outdoor space for the users of the home. The roof will, instead, offer an opportunity for a rainwater collection system, which will lower water usage bills and impact the users' cost of living. The building has also been designed to provide a more sealed envelope to protect residents while also further helping with energy efficiency and using sustainable materials. The various insulation layers like thermal, moisture, and air provide protection from the mixed climatic conditions that Washington D.C. so often experiences. Daylighting was a major consideration as well. To maximize light capabilities, the interior layout was redone.

Second, Retro Boomin's proposes to maximize energy savings on the interior through the passive design strategy of increasing the insulation of the building envelope with hemp wool. The proposed design had an open floor plan to maximize the use of cross-ventilation. It also reduced the sound pollution by adding green hedges near the road. The integrated systems and time-controlled lighting, energy-efficient appliances, and ease-of-use technologies lowered energy consumption and enhanced the environment for occupants. The design included the addition of new community space with added programming for the social justice center that will highlight the legacy of the Terrell House and LeDroit Park. The materials were locally sourced from the region to minimize the embodied carbon content. The operational carbon was reduced by efficient geothermal systems. In addition to the building's decarbonization goals, the students

achieved a low baseline energy use index (EUI) of 15 (down from 49) by incorporating more efficient systems.

Third, the Retro Boomin' team pursued geothermal HVAC systems to further improve energy efficiency and by designing zones for different floors. The selection of lighting fixtures and appliances can be replicated to reduce any house's lighting and plug loads. The design considerations were observed to obtain the goal of significantly reducing EUI. The building envelope has also been redesigned to provide a more sealed envelope to protect our users while also further helping with our energy efficiency and using sustainable materials. Daylighting was a major consideration as well, so to maximize tour capabilities for the historic home, the interior layout was redone. Students used a 4'x5' rainwater collection tank that can hold 470 gallons of graywater to redistribute for toilets and irrigation for the backyard. The system was also equipped with a backup tank and controls.

### *1.7 Financial Feasibility and Affordability*

The students had the goal of making this project affordable and financially responsible to the market. They did the arduous calculation of all the materials used for the design of retrofits in various categories including concrete rough carpentry, plumbing, and so forth, with unit rates of calculations of actual market information for construction projects within the DC metro region. The total cost was \$448,738 (compared to the cost of building from scratch at a cost of \$809,00) in this DC neighborhood. The financial feasibility and affordability of the Mary Church Terrell House retrofit is a testament to sustainable construction practices. The design achieved a 47% reduction in cost.

Students also proposed that a graduate student from Howard University will run the exhibitions and will receive reduced rent to live at the property as a resident caretaker. This community-led design provides a precedent for equitable decarbonized housing in the LeDroit Historic Park District, making homes safer, healthier, and more adaptable in our ever-changing environment. Furthermore, net-zero housing makes living more affordable and sustainable for present and future generations by reducing utility consumption costs and offering long-term savings via tax credits, renewable energy certificates, and stormwater retention credits. Most importantly, this project will amplify underserved community voices and create equity by providing a wide range of social justice resources.

## **2. Student Feedback Outcomes**

The students all completed self-evaluations and peer evaluations after the competition. In the evaluations, students highlighted the benefit of learning about net zero. One



student said they “learned about energy consumption and how the types of materials play a role in your building.” Another student said, “The information will allow me to continue the journey to make all architecture sustainable and healthy for people and the environment.” The students learned to manage time and learn from each other. They learned to communicate their ideas within the teams and in front of the public. They learned that retrofitting a building is not easy but important for decarbonized buildings and how to get to design net-zero high-performance buildings. The team made the finals and placed in the top three of the categories for the division.

### **3. Conclusion**

The case studies clearly demonstrate different ways of retrofitting historic buildings and the successful implementation of intentional goals. Teaching about real problems in society and the collaboration of an interdisciplinary team has helped with learning and applying design solutions. The students learned to take ownership of their designs, learned technical skills, and collaborated with peers and industry partners to complete the design. Their participation in the Solar Decathlon also gave them the opportunity to tackle the most complex problems facing the building industry and see other collegiate students design solutions. This has helped students develop market-ready design skills and connections through the network of global SD alumni. The design solutions clearly show the impact of having the focus on community and retrofit of buildings needs the intentional goals and technical skills of implementing high-performance buildings. The students achieved this residential retrofit design with a focus on the community and equity.

### **Conflict of Interest**

The paper is based on the Retro Booming team student work in the authors’ class at Howard University for Solar Decathlon Design Competition 24. There is no other conflict of interest.



Fig. 1. The unique form of the Terrell House is the result of a devastating fire in the 1970s that destroyed its western half. (Credit: Howard University Retro Booming Team)

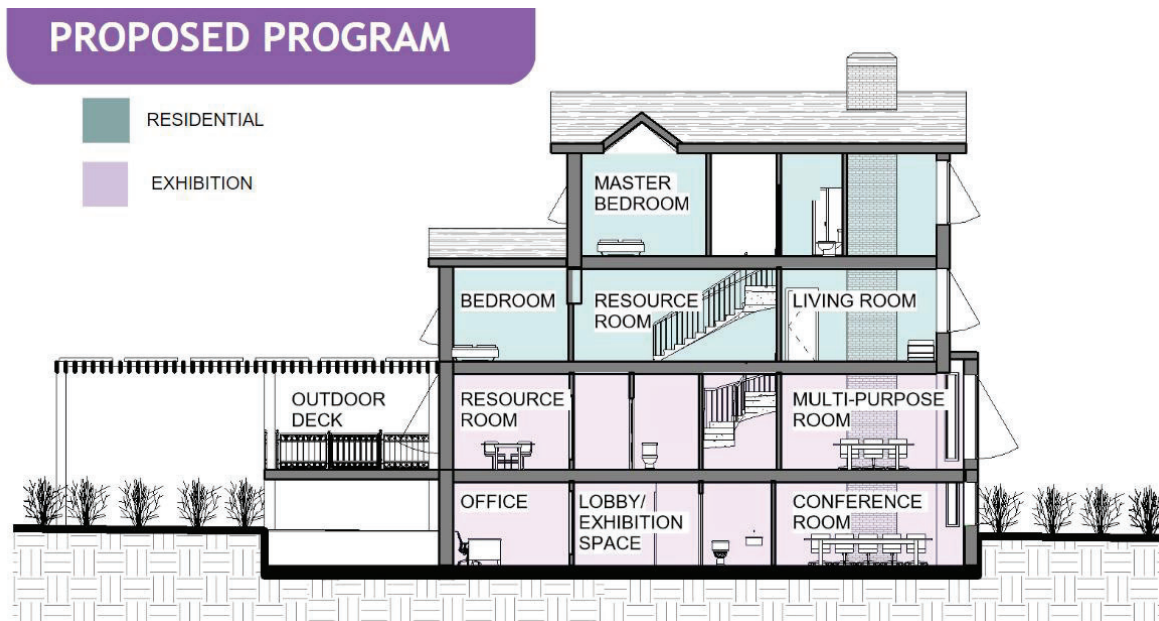


Fig. 2. Among the thematic goals of the project, “legacy” and “equity” are as important as decarbonization to tell the whole story of the Terrell House in a way that’s relevant to climate justice goals going forward. (Credit: Howard University Retro Booming Team, using Adobe and Revit software)



LEGACY & EQUITY

Fig. 3. The house, as a demonstration of its historical significance, will include exhibition space and meeting space for community events, as well as residential quarters for its caretaker. (Credit: Howard University Retro Booming Team, using Adobe, Revit and Photoshop software)

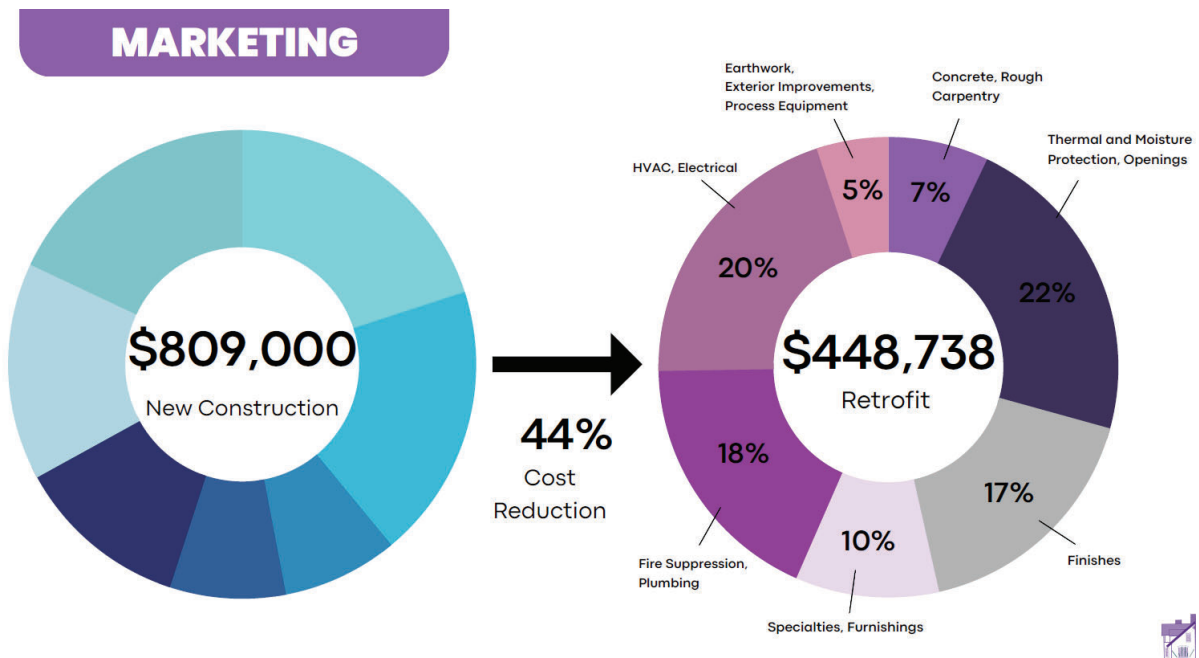


Fig. 4. Retrofitting our existing building stock has a real economic advantage in addition to an environmental one. The Terrell House’s retrofit costs are nearly half of the cost of new builds in this area of D.C. (Credit: Howard University Retro Booming Team, using adobe, Canva software)

## Solar Decathlon Case Study

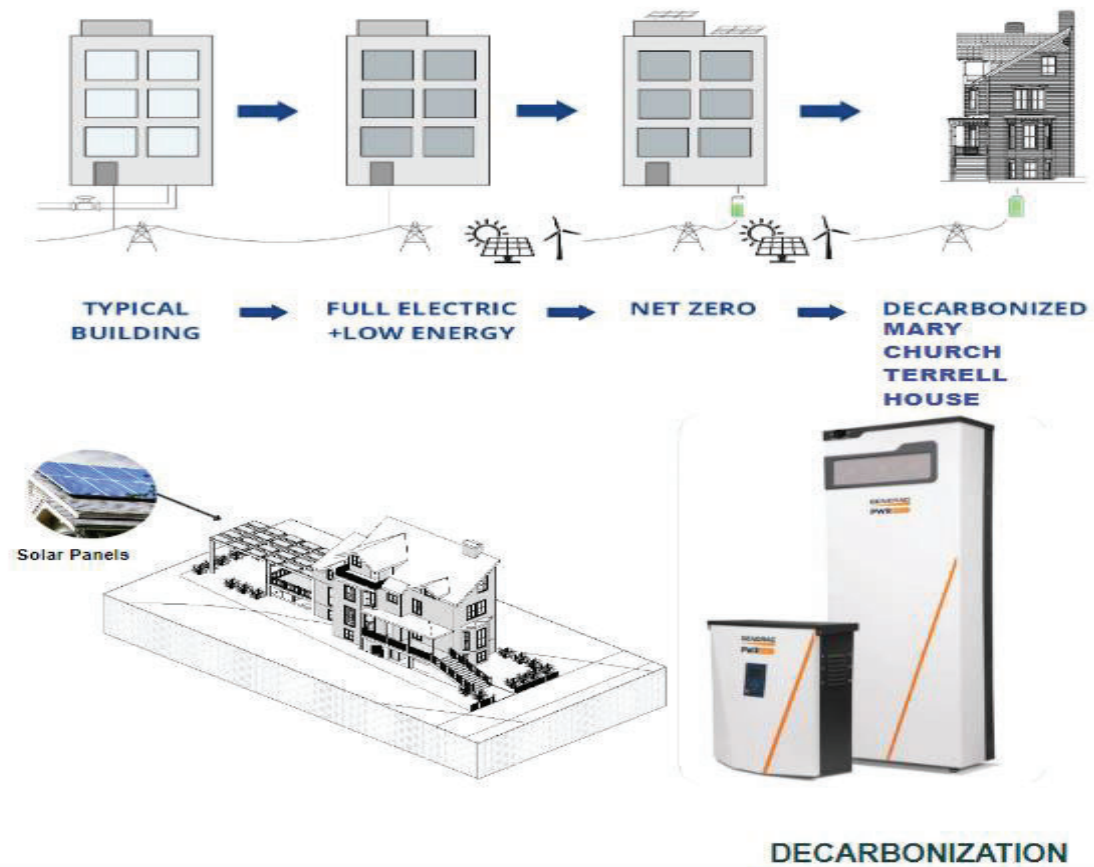


Fig 5. A PV array in the yard, which offers a canopy shade, helps the home get closer to net zero by producing as much energy (or more) than it consumes. (Credit: Howard University Retro Booming Team)



## References

U.S. Department of Energy. (2024.) *2024 design challenge rules*.

[www.solardecathlon.gov/2024/assets/pdfs/design-challenge-rules-2024.pdf](http://www.solardecathlon.gov/2024/assets/pdfs/design-challenge-rules-2024.pdf)

Grainger, G. (2022). “For Net-Zero Cities, We Need to Retrofit Our Older Buildings.

Here’s What’s Needed.” [www.weforum.org/agenda/2022/11/net-zero-cities-retrofit-older-buildings-cop27/](http://www.weforum.org/agenda/2022/11/net-zero-cities-retrofit-older-buildings-cop27/)

Logan, K. (2019). *Renovate, retrofit, reuse: uncovering the hidden value in America’s existing building stock*. Washington, D.C.: The American Institute of Architects.

**Early Experiences with a High-Elevation Off-Grid Solar Residence in Colorado**

David S. Renné  
Dave Renné Renewables, Boulder, CO  
Paulette B. Middleton  
Panorama Pathways, Boulder, CO  
[drenne@mac.com](mailto:drenne@mac.com)



## Abstract

A new off-grid high-elevation solar residence located in Colorado is described. Key design objectives were to size the solar/battery storage system to provide reliable power without the need for power backup. The residence features high R values for the walls and ceiling and low U values for the windows and uses highly efficient lighting and appliances. To date, the key lessons learned are: 1) The high building efficiency and its passive features, efficient appliances, and careful load management practices, have led to an off-grid system that in most cases does not require backup power; 2) Nevertheless, despite a favorable solar resource, adequate battery storage is mandatory at times of prolonged cold, cloudy, and snowy weather; 3) Selection of a design-build team with a deep understanding of sustainable building practices and making good use of incentives of the Inflation Reduction Act go a long way to ensuring a successful and cost-effective installation.

Keywords: Off-grid residence, rooftop PV, battery storage, net-zero plus, residential load management

## 1. Introduction and Design Considerations

During the spring of 2020, the authors purchased a 7.5-acre parcel of forested land just east of the Continental Divide near Nederland, Colorado. The parcel is part of an old gold-mining claim. Although the authors have yet to find the motherlode that early settlers had anticipated, they did set forth to build an off-grid solar-powered mountain home on the property. Construction began in the Spring of 2022 and was completed in late summer 2023. This paper provides early results of the performance of the residence as a case study for off-grid home design.

A local design-build team experienced in designing and building energy-efficient homes that perform extremely well in the harsh Colorado mountain winters was commissioned. The final design was a 1000-ft<sup>2</sup> main level with a kitchen, a utility room, a full bathroom, a bedroom, a living room, and an entryway plus a second-level 308-ft<sup>2</sup> open loft with a half-bath. The roof rises from the south to the north at a ~22° angle (somewhat less than ideal for this latitude). Most of the windows are located on the south and western side of the house, providing an effective passive heat source during winter. The site is flat, at an elevation of 8850 ft (~2700 m).

Water is supplied by a well. A septic system was required. Both systems require pumps, which add to the overall electricity load of the residence.

## 2. The Final Build

The final structure (see Figures 1 and 2) is a highly energy-efficient residence. High R values for the exterior walls (R = 27) and ceiling (R = 54) and low U values for the windows (U = 0.16), along with the use of highly efficient electrical appliances and the

installation of a wood stove, result in a Home Energy Rating System (HERS) Index of -53.

The solar system was sized based on estimated annual loads of approx. 10,000 – 12,000 kWh. The result is a 7.3-kW rooftop solar system (twenty 365 kW<sub>p</sub> rooftop-mounted panels totaling 36.6 m<sup>2</sup> in area) and a 24-kWh lithium ferrous phosphate battery storage system, using a 15 kW, 200-amp inverter.

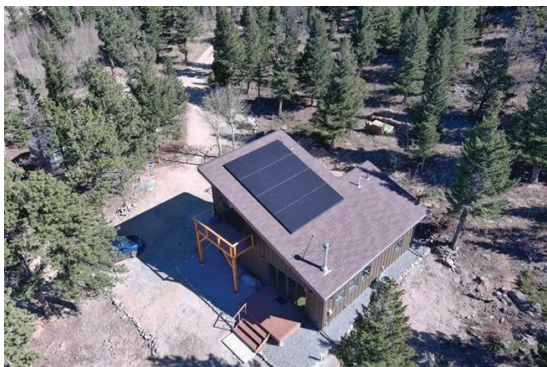


Photo courtesy Andrew Finanger, IPS Solar



Fig. 2. Authors in front of recently completed residence

Fig. 1. Aerial view of residence, looking NE

Although the original plan was to install the majority of the house on a concrete slab, the excavation work necessary to allow for burial of water pipes and a septic system resulted in the opportunity to place the entire dwelling over a fully conditioned crawl space. A ducted HVAC (Heating, Ventilating and Air conditioning) system using a centralized 3-ton (36K-BTU) variable-speed heat pump was installed. The heat pump provides both heating and cooling through an air handler located in the crawl space.

A 10-kW resistance heat backup system is included inside the air handler, but has not been commissioned, since adequate interior temperatures are generally maintained through the heat pump and the wood stove. Because the efficiency of the residence results in such an air-tight structure (ACH50<sup>1</sup> = 1.73), an auxiliary Energy Recovery Ventilator (ERV) is required to maintain fresh air. Although the ERV and the air handler add to the electricity load, the conditioned crawl space, which must be kept above freezing due to the fire sprinkler system, provides a “passive” geothermal heat source, causing temperatures in the space to remain well above freezing. Thus, the conditioned crawl space itself can be a source of heat to the house in winter, as well as cooling during summer, serving to moderate high temperature fluctuations inside the residence.

The well water head is approximately 80 feet (~26 m) from the house. A submersible 110-volt pump delivers water from the well to the house via a buried water conduit. A

---

<sup>1</sup> Air Changes per Hour at 50 pascals pressure differential

high-efficiency 40-gal. hybrid heat pump water heater is used to provide hot water to the residence.

The solar system was commissioned on August 21, 2023, and the HVAC system on September 7. The hybrid water tank was commissioned on September 11. The house was winterized in mid-November 2023 and the water turned back on in late April 2024.

### 3. Site Climatic and Solar Resource Characteristics

The site can be characterized as a cool montane continental climate. The site is near the top of the western side of a ridge that comprises part of the eastern Colorado Rockies foothills. To the west is a deep valley (Caribou Ranch), and further to the west is the Continental Divide. The site experiences frequent snowfall, sometimes heavy, from October to May. Summer rainfall comes primarily as afternoon thunderstorms. High winds are common, especially following winter storm events.

A Davis VantagePro2™ weather station was installed on a tripod in an open area near the residential site on August 16, 2020. The weather parameters (air temperature, barometric pressure, humidity, wind speed and direction at 2 m above ground, rainfall totals and rainfall rates) transmitted to a home computer on an hourly basis during the first year of operations, and since then have been transmitting at 15-minute intervals. The data are publicly available through a Davis WeatherLink™ subscription.<sup>2</sup>

The three full years of measurements (2021–2023) show a mean annual temperature ranging from 40.8°F to 42.6°F (4.9°C to 5.9°C). The warmest month is July, ranging from 62.6°F to 63.5°F (17.0°C to 17.3°C). But the coldest month in 2021 and 2022 was January (21.7°F and 22.0°F, or -5.7°C and -5.6°C), while in 2023 it was February (21.1°F, or -6.1°C). To date the highest recorded temperature was 89.6°F (32.0°C) in June 2021 and the lowest was -20.3°F (-29.1°C) in February 2021.

Heating Degree Days are tabulated for the site. These values are useful for assessing the heating requirements in a structure. Figure 3 provides the monthly average heating degree days along with the mean monthly temperatures over the 3 ¾ -year period that data are available. Annual average heating degree days (in °F) have ranged from 8410 to 8924, similar to regions in the upper Midwest and northern New England of the United States (Nadal and Fadali, [2024](#)).

---

<sup>2</sup> Accessible at [www.weatherlink.com](http://www.weatherlink.com); site name is “County Road 103, Nederland”.

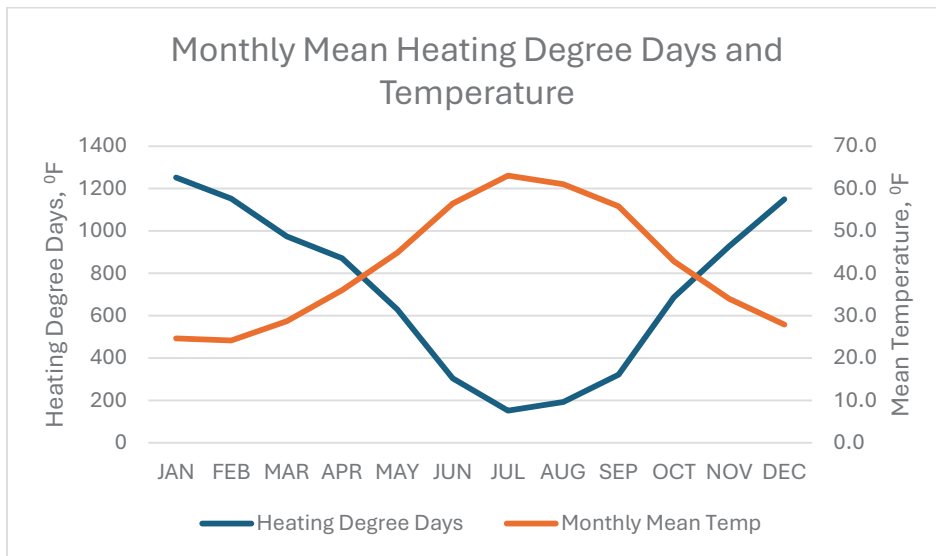


Fig. 3. Average total monthly heating degree days and monthly temperatures at the off-grid residence for the period August 2020 – May 2024, based on onsite measurements.

Average measured precipitation varied from 15.96 in (40.4 cm) in 2022 to 21.32 in (54.2 cm) in 2023. A significant source of annual precipitation is winter snowmelt.

There are no direct solar resource measurements at or near the site. Satellite-derived SolarAnywhere™,3 data have been provided by Clean Power Research (2021). All historic hourly data (2013 – 2023), in units of W/m<sup>2</sup> for the tile in which the site resides, were downloaded using the most recent Version 3.7 of SolarAnywhere. Figure 4 provides information on the monthly average daily total values of Global Horizontal Irradiance (GHI) for each of the 11 years in which data are available.

<sup>3</sup> <https://www.solaranywhere.com/>

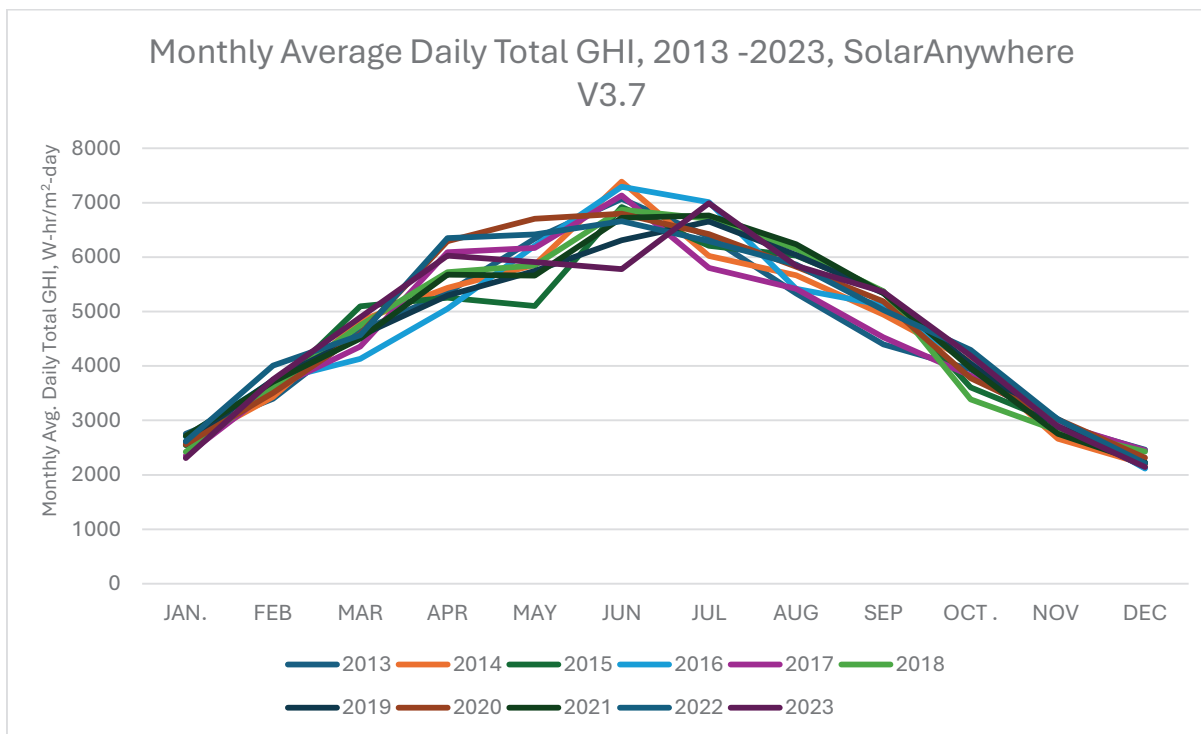


Fig. 4. Satellite-derived monthly average daily total GHI values at the location of the residence for the years 2013-2023. Data are from SolarAnywhere Ver. 3.7.

#### 4. Early Results on Residential Energy Performance

This section provides a preliminary analysis of system performance on the degree to which the domestic loads are met directly from the solar panels vis-à-vis the storage batteries. The intention is for this analysis to continue in the future, so that the residence can serve as a relevant case study for off-grid solar living.

Several apps are available to monitor the performance of the inverter, water heater, and HVAC systems in the residence. These include 1) PowerView™, an app<sup>4</sup> provided by the inverter manufacturer, which offers 5-minute data on the performance of the solar system (inverter, PV output, battery storage, backup generator output, residential loads, and numerous other parameters); 2) the ecobee™ app<sup>5</sup> that provides 5-minute digital data of the HVAC performance; and 3) EcoNet™, an app that monitors the performance of the hybrid hot water heater. More information regarding the solar and HVAC systems is provided in the Appendix. A NETGEAR Nighthawk™ wireless router was installed at the residence to provide subscription-based internet service through the regional 5G network, enabling the performance of the solar, water heating, and HVAC systems to be monitored remotely.

<sup>4</sup> <https://pv.inteless.com/plants>; recently renamed <https://www.solarkcloud.com/plants>

<sup>5</sup> <https://www.ecobee.com/consumerportal/index.html#/devices/thermostats/>

Fig. 5 shows an example of electrical flow information provided by the PowerView app.

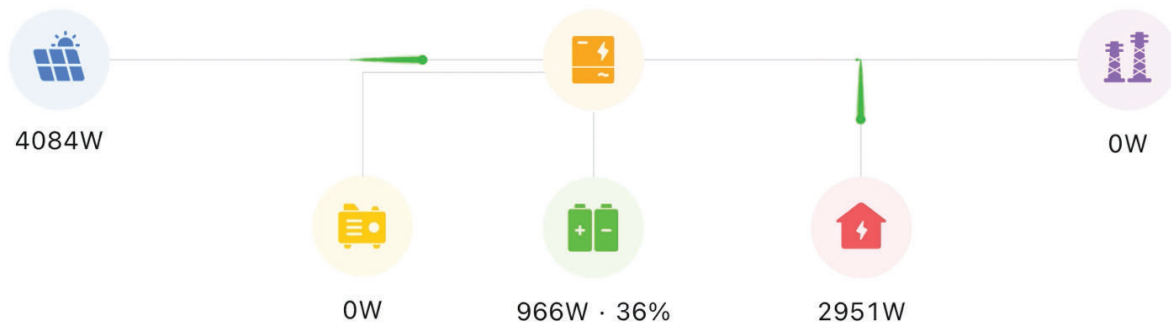


Fig. 5. Example PowerView power flow chart for the residence, taken on a sunny day in February when the HVAC system is operating. PV power flows from the panels (blue icon) to the inverter (orange icon), which then distributes the power to the batteries (green icon) and the electrical load (red icon). The backup generator (yellow icon) is not operating, and the grid (purple icon) is always zero since the residence is off the grid.

The app also provides daily summaries of these power flows. However, the app does not explicitly provide data on a “phantom load,” ranging from 60–90 W, that is required for the internal operation of the inverter and batteries. This phantom load must first be calculated from the daily data that are available, which includes the household load,  $L$ , total PV power output,  $PV_{OUT}$ , and the charge and discharge of the batteries. The total phantom load  $L_{PH}$ , can be expressed as the sum of the phantom load met by the PV system ( $PV_{L,PH}$ ) and the battery system ( $B_{L,PH}$ ):

$$L_{PH} = PV_{L,PH} + B_{L,PH} \quad (1)$$

The  $PV_{OUT}$  reported by PowerView represents only that output being used to meet the load ( $PV_L$ ), charge the battery ( $PV_{BAT}$ ) or meet the phantom load:  $PV_{OUT} = PV_{BAT} + PV_L + PV_{L,PH}$  or:

$$PV_{L,PH} = PV_{OUT} - PV_{BAT} - PV_L \quad (2)$$

Similarly, since battery charge comes exclusively from the PV when there is no external power source, the battery discharge ( $B_{OUT}$ ) is used to meet that portion of the load not met by the PV, plus the phantom load:  $B_{OUT} = B_L + B_{L,PH}$ , or:

$$B_{L,PH} = B_{OUT} - B_L \quad (3)$$



Combining (2) and (3) into (1), the total phantom load can be determined from:

$$L_{PH} = (PV_{OUT} - L) - \Delta B \quad (4)$$

Where  $\Delta B$  is the difference between the reported daily charge and discharge of the battery.

Once the phantom loads are calculated from (4) the relative daily contribution of PV vs. battery to meeting the total household load,  $L_T$ , which is the sum of the reported load and the phantom load, can be calculated as follows:

$$PV \text{ contribution to load} = L_T - B_{OUT} \quad (5)$$

$$Battery \text{ contribution to load} = B_{OUT} \quad (6)$$

Although the solar and HVAC systems were commissioned in late summer 2023, performance data available from the residence are limited due to a variety of reasons: 1) the residence has been primarily unoccupied, limiting the electrical loads to the HVAC and a few small appliances, such as the mini-fridge; 2) the residence was winterized in mid-November, further reducing the load requirements, except for the HVAC, which remained on with low indoor temperature settings; 3) the inverter failed on December 3, 2023 and was replaced on January 11, 2024, resulting in a loss of nearly seven weeks of performance data.

For this analysis, data on those occasions when the backup generator is running are excluded; data are evaluated only for those conditions when the batteries are being charged by the PV, and the battery discharge is being used to meet that portion of the load (including the phantom loads) not met by the  $PV_{OUT}$ . Figure 5 shows that  $PV_{OUT}$  is used both to charge the batteries (that is, until they are fully charged) and meet the residential and phantom loads.

Figure 6 provides an analysis of the monthly average contribution of PV and batteries in meeting residential loads for those days in which no backup generation is required, and power is fully available throughout the day. Due to the 7-week inverter failure, data for December 2023 and January 2024 are quite limited. Also, measurements did not begin until Aug. 21, limiting data availability for August 2023. Nevertheless, the figure shows a pattern of the household being much more reliant on battery storage during the cooler, cloudier winter months than the warmer spring, summer, and fall months, as would be expected.



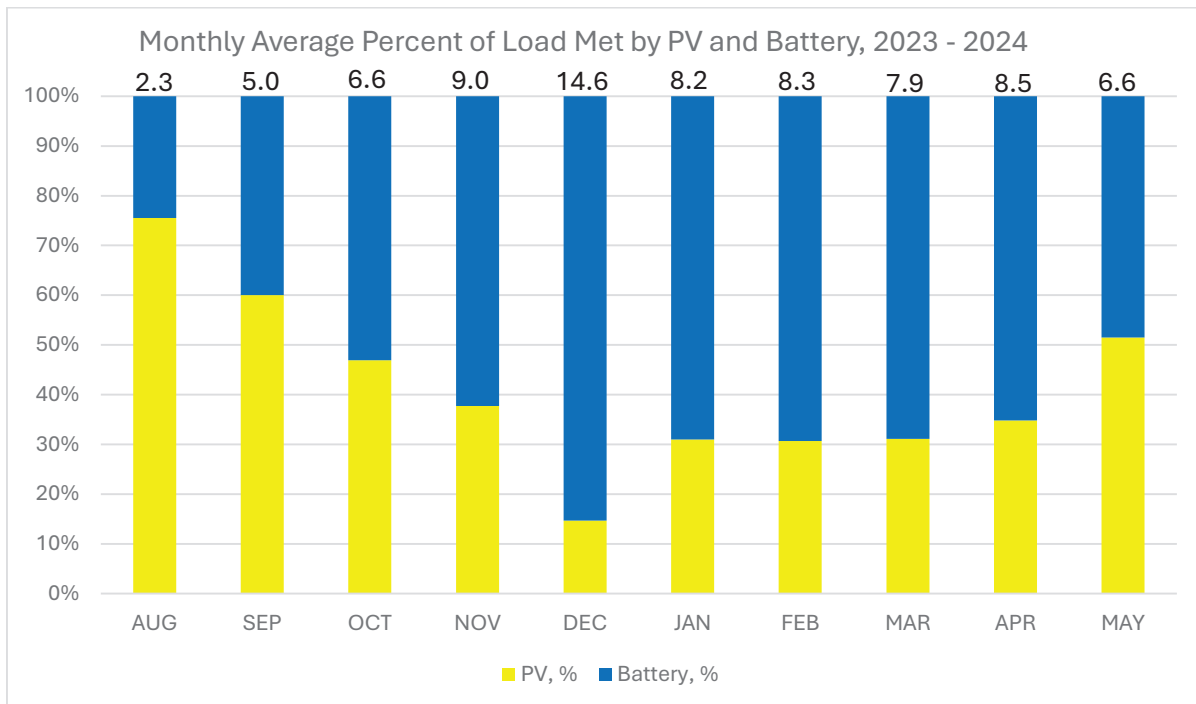


Fig. 6. Percentage of total monthly loads met by PV (yellow) and batteries (blue) when no external generator is used and inverter power to the house is fully on. Numbers above each bar represent the average daily load (kWh/day) for those days used in the analyses.

## 5. Summary and Future Plans

Some preliminary analysis of the performance of the off-grid solar system can be summarized here:

- Active load management is essential:** On a typical sunny day, the State of Charge (SOC) of the battery storage system can reach 100% well before noon. This means that any further production of solar from the panels is “curtailed”, other than what is used to meet the current loads. Accordingly, activities requiring high electricity use (e.g. clothes washing, EV charging, etc.) should be done during this period of full charge. In late afternoon and evening hours, electricity demand should be minimized to avoid too much reduction in SOC. Alternatively, during times of extensive cloudiness or snow-covered panels, electricity usage must be minimized at all times to avoid SOC dropping below 20%, at which point the inverter is designed to shut power off to the house to protect the batteries.
- Steps need to be taken to minimize the impacts of long-term curtailment of electricity production:** A significant problem in this environment is caused by multi-day periods when the solar panels are covered with snow, or during periods of prolonged cloudiness. Under these conditions the batteries are unable to build

up a sufficient charge to meet all electricity demands, especially those associated with HVAC operations. This situation can be mitigated only through extreme load management practices or adding additional backup storage capacity to the solar system.<sup>6</sup> Of course, a backup generator can bridge these extreme events, although the overall goal of the residence is to be able to rely completely on a 100%-renewable energy system, independent of the regional grid.

- ***The solar system and electrical loads need to be designed and planned appropriately for the intended use of the dwelling:*** Although the house is not yet fully occupied, and the load patterns have not yet been clearly established, early indications are that the solar system may have been oversized while the battery storage system is significantly undersized.
- ***Make full use of local expertise and state and federal incentives:*** The authors commissioned an architectural firm knowledgeable in net-zero and passive home design and local building requirements and a contractor familiar with modern-day construction methods required for highly efficient homes. Although these efficiency measures can result in a higher initial cost for the build, the Inflation Reduction Act, along with State of Colorado incentives, have helped significantly in keeping initial costs at a manageable level and encouraging the use of only the most energy-efficient building materials and appliances.

In summary, despite the challenges, a properly functioning and well-designed off-grid system is cost-effective in the long run and provides a highly desirable place to call home.

## 6. Conflicts of Interest

This research is self-funded. There are no conflicts of interest.

---

<sup>6</sup> Plans are underway to install an additional 8 kW of battery storage.

## References

Clean Power Research (2021). *Solar anywhere system check*.

[https://go.cleanpower.com/rs/369-HBZ-605/images/Solar-Data-Lifecycle-  
Overview\\_FINAL-LINKS\\_060421.pdf](https://go.cleanpower.com/rs/369-HBZ-605/images/Solar-Data-Lifecycle-Overview_FINAL-LINKS_060421.pdf)

## Appendix: Building and Equipment Specifications

| <b>Construction</b>      | <b>Company/Manufacturer</b>  | <b>Comments</b>  |
|--------------------------|--|--|
| Design;<br>Contractor    | Rob Ross, AIA, TRAD Design/Build; Jacob Neathawk, Neathawk Building Company LLC  | Business located in Boulder, CO  |
| External wall insulation | Johns Mansville™   | ClimatePro Blow-in fiberglass + foam   |
| Ceiling insulation       | Johns Mansville™   | ClimatePro Blow-in fiberglass + HFO closed cell foam   |
| Roofing material         | GAF™   | Timberline Armor Shield ASII   |
| Siding material          | James Hardie™  | Fibre-cement, board and batten style   |
| Bldg. eff. ratings       | Scott Home Services LLC, Boulder, CO   | HERS Index Score = -53 (Note: A zero-energy grid-tied home would be HERS = 0)  |
| <b>Solar System</b>      | <b>Manufacturer</b>  | <b>Comments</b>  |
| Solar Panels             | REC™ 365 N-Peak 2 monocrystalline n-type, black<br><a href="https://www.recgroup.com/de/products/rec-n-peak-2">https://www.recgroup.com/de/products/rec-n-peak-2</a>   | Each panel rated at 365 W <sub>p</sub> ; 20% efficiency; 7.3 kW <sub>p</sub> total; 36.6 m <sup>2</sup> total area; roof-mounted, south-facing at 22° tilt |
| Inverter                 | Sol-Ark™ 15-2p-N<br><a href="https://www.sol-ark.com/sol-ark-15k-all-in-one/">https://www.sol-ark.com/sol-ark-15k-all-in-one/</a>  | 15 kW Max Power delivered to batteries; 200 amp service; suitable for both off-grid and on-grid  |
| Battery storage          | Blue Planet Energy™ Blue Ion HI<br><a href="https://www.blueplanetenergy.com/">https://www.blueplanetenergy.com/</a>   | 24 kWh in two cabinets; expandable to 32 kWh (expansion will take place in 2024)   |
| <b>HVAC</b>              | <b>Manufacturer</b>  | <b>Comments</b>  |
| Heat Pump                | Bosch™ BOVA-36HDN1-M20G<br><a href="https://www.budgetheating.com/Bosch-3-Ton-20-SEER-Inverter-BOVA-36-BVA-36-p/52077.htm">https://www.budgetheating.com/Bosch-3-Ton-20-SEER-Inverter-BOVA-36-BVA-36-p/52077.htm</a> | 3-ton (36K BTU) variable speed inverter system   |
| Air handler              | Bosch™ BVA2.0<br><a href="https://www.bosch-homecomfort.com/us/en/ocs/residential/bva20-air-handler-unit-1115667-p/">https://www.bosch-homecomfort.com/us/en/ocs/residential/bva20-air-handler-unit-1115667-p/</a>   | Includes 10 kW resistance auxiliary heat (not used)  |
| Thermostat               | Ecobee™ Smart Thermostat Premium<br><a href="https://www.ecobee.com/en-us/smart-thermostats/smart-thermostat-premium/">https://www.ecobee.com/en-us/smart-thermostats/smart-thermostat-premium/</a>                  | Extra room sensor installed in crawl space   |

## Solar Residence in Colorado

|                  |   |  |
|------------------|---|--|
| Hot water supply | Rheem™ Performance Platinum Hybrid<br><a href="https://www.rheem.com/products/residential/water-heating/">https://www.rheem.com/products/residential/water-heating/</a> | 40-gallon; heat pump with resistance heating coil backup |
| Wood Stove       | Lopi™ Evergreen NexGen-Fyre<br><a href="https://www.lopistoves.com/product/evergreen-nexgen-fyre/">https://www.lopistoves.com/product/evergreen-nexgen-fyre/</a>        | 12,772 – 70,720 BTU (EPA Tested); up to 77.1% efficiency |

**Evaluation of Retrofit Passive Solar Heating for Emergencies**

Martin Smallen  
Metallurgical Engineer, Retired

## Abstract

During war or natural disasters, the heating infrastructure of a nation can be damaged, and temporary heating is necessary. Emergency generators are often employed until infrastructure restoration. This project proposes to add a simple and inexpensive passive solar Trombe water wall consisting of individual containers as an emergency energy option. An experiment determined that the conversion efficiency of solar radiation into stored heat was 60% for the water wall. The average yearly heating performance was then calculated at two locations: Morgan Hill, CA (37.1°N latitude) and Bozeman, MT (45.6°N latitude). The performances were predicted using two methods that agreed with each other. The predictions show that the water wall can supply 98% of the yearly heating requirement for Morgan Hill and 85% for Bozeman. The heating performance can be improved if the containers are tilted so that the sun's rays are perpendicular to the absorbing surface on the winter solstice.

Keywords: passive solar; Trombe wall; retrofit; emergency heating

## 1. Introduction

In times of war and natural disasters, the heating infrastructure of a nation can be damaged. In these situations, there is a need for emergency heating of buildings. While some energy can be restored with backup solar or fossil fuel generators, this may only supply a few hours a day on a rotating basis. A temporary retrofit passive solar system could add to that emergency energy mix by providing a warm room(s) in unheated buildings. In addition, passive solar could reduce the load on power plants.

The first use of passive solar designs for heating date back to the Greeks, Chinese, Romans, and Anasazi (U.S. Department of Energy, 2004; Wikipedia, 2023). Passive solar heating is usually incorporated into the building structure (Wikipedia, 2023; U.S. Department of Energy, n.d.; Duffie & Beckman, 1974). However, this report evaluates a temporary retrofit system that can be added to existing buildings. The concept is to build a Trombe water wall out of inexpensive and easily available materials, such as wood, plastic, or metal containers; flat black paint; water; and polystyrene insulation (Wikipedia, 2024). Alternate materials can also be used. The materials need not be new either. They can be salvaged from landfills or damaged buildings.

The Trombe water wall would be built in front of an equator-facing ( $\pm 30^\circ$ ) window. The water wall would consist of flat black-painted containers on a shelf. During the day, the sun's rays would warm the water in the containers. At night, insulation between the water wall and the window would direct the heat into the room. The advantages of the design are that it is: 1) decentralized, 2) inexpensive, 3) constructed of common materials, 4) electricity-free, 5) easy to assemble and disassemble, and 6) low in carbon emissions. It would take a semiskilled person 1 to 2 days to do the assembly.

## 2. Theory



The Trombe water wall was analyzed as a flat-plate collector. According to Duffie and Beckman (1974), the solar energy balance equation for a flat-plate collector is given in eq. 1.

$$A(\tau\alpha)S = Q_U + Q_L + Q_S \quad (1)$$

$A$  is the solar collector area,  $(\tau\alpha)$  is the transmittance-absorptance product for the clear cover,  $S$  is the rate of total solar radiation per unit area,  $Q_U$  is the rate of useful heat transfer to a working fluid,  $Q_L$  is the rate of energy loss, and  $Q_S$  is the rate of energy storage. But  $Q_U$  is the same as  $Q_S$  in the case of the Trombe water wall since the heat stored in the water wall is the useful heat, so  $Q_S = 0$ . The modified balance equation then becomes eq. 2.

$$A(\tau\alpha)S = Q_U + Q_L \quad (2)$$

This modified energy balance equation was used to evaluate the Trombe water wall. Also, the rate of energy terms were converted to energy in kWh, a common unit used by utilities.

$Q_U$  was determined by using the water's specific heat capacity as shown in eq. 3.

$$Q_U = 2.78 \times 10^{-7} (mC\Delta T) \quad (3)$$

where  $m$  is the mass of the containers' water,  $C$  is the specific heat capacity of water,  $\Delta T$  is the water temperature increase, and  $2.78 \times 10^{-7} \text{ kWh/J}$  converts  $J$  to  $kWh$ .

The containers were isolated by setting them on four 7-mm diameter felt pads so the heat loss would be mainly by radiation. It was then assumed that conduction and convection heat losses were negligible. The radiation heat losses,  $Q_L$ , were calculated using eq. 4, which assumes that the six containers in this experiment are a small convex object surrounded by a large enclosure, the room (Duffie & Beckman, 1974).

$$Q_L = \frac{t_1 \varepsilon_1 A_1 \sigma (T_2^4 - T_1^4)}{1000} \quad (4)$$

where  $t_1$  is the time of energy collection in hours,  $\varepsilon_1$  is the emissivity of the flat black-painted containers,  $A_1$  is the total surface area of the containers,  $\sigma$  is the Stefan-Boltzmann constant,  $T_1$  is the average room temperature,  $T_2$  is the average container temperature and  $1000$  converts  $W$  to  $kW$ .

The heat stored in the containers at the end of the day  $H_b$  is given in eq. 5. The heat loss from the containers was added to the heat gain since that heat loss is heat gain to the room.

$$H_b = \frac{Q_U + Q_L}{A} \quad (5)$$

The predicted heating performance  $P$  is given in eq. 6.

$$P = \frac{100SEA_w}{Q_r} \quad (6)$$

$P$  is the percentage of heating supplied by solar,  $E$  is the conversion efficiency of solar radiation into heat in the containers,  $A_w$  is the total window area, and  $Q_r$  is the space heating requirement.

In addition to the above method, the Trombe water wall was analyzed by a second method (Mazria, 1979). The method is not reproduced here but the source is listed in the references.

Finally, the predicted daily average indoor temperature  $t_i$  is given in eq. 7 (Mazria, 1979).

$$t_i = \frac{HG_{sp}}{U_{sp}} + t_0 \quad (7)$$

$HG_{sp}$  is solar heat gain,  $U_{sp}$  is the overall coefficient of heat transfer, and  $t_0$  is the average daily outdoor temperature.

### 3. Methodology

#### *Equipment*

The experimental setup is shown in Figure 1 and is a scaled-down version of a Trombe water wall. The containers on the lower shelf are tilted at 60° and those on the upper shelf are tilted at 90°. The equipment was set up in an unheated room of a house where the equator side of the house faced 160° south. The house is located near Morgan Hill, CA at 37.1°N latitude. Even though the room was unheated, two adjacent rooms were heated. Prior to setup, the containers were painted with a flat black paint. The containers were placed on the wood shelf 28 cm from a double-pane window that is made of standard window glass. A single container's fluid capacity is 3.875 L (1 gallon). Calibrated thermocouple temperature meters measured the water, room air, and outside air temperatures. Calibrated solar power meters measured cumulative solar radiation at 60° and 90° tilts.



Fig. 1. Experimental setup showing six flat black painted and water-filled containers on a shelf. The containers on the lower shelf are tilted at 60° and those on the upper shelf are tilted at 90°. (Photo credit: Martin Smullen)

The equipment list is shown in Table 1.

Table 1. Equipment List

| Item                            | Manufacturer Model Number |
|---------------------------------|---------------------------|
| Solar Power Meter (2 ea)        | TES-132                   |
| Thermocouple Thermometer (3 ea) | Perfect Prime TC41        |

*Procedure*

In the morning of each day, the polystyrene insulation was removed from the space between the water containers and the window. The initial temperature and solar radiation measurements were recorded in the morning and the final measurements were recorded in the afternoon. There were no measurements in between. At the end of the day, the polystyrene insulation was placed back between the containers and the window. A typical data sheet is shown in Table 2.

## Passive Solar Heating for Emergencies

Table 2. Typical data sheet.

| Site Info.                  | Tilt (°) | Date   | Start and Stop Time | Bottle Temp. 1 (°K) | Bottle Temp. 2 (°K) | Bottle Temp. 3 (°K) | Bottle Temp. 4 (°K) | Avg. Bottle Temp. (°K) | Room Temp. (°K) | Outside Temp. (°K) | Cum. Solar Rad. (kWh/m <sup>2</sup> -Day) | Heat Gain in Bottles (kWh) | Heat Loss From Bottles (kWh) | Net Heat Gain to Bottles (kWh) | Norm. Heat Gain in Bottles (kWh/m <sup>2</sup> -Day) |
|-----------------------------|----------|--------|---------------------|---------------------|---------------------|---------------------|---------------------|------------------------|-----------------|--------------------|---|----------------------------|------------------------------|--------------------------------|--|
| Morgan Hill, CA             | 90       | 4/9/23 | 9:30                | 291.6               | 291.8               | 291.5               | 291.1               | 291.5                  | 291.3           | 283.0              | 0   | 0                          | 0                            | 0                              | 0  |
| Collector Facing 160° South |          |        | 15:30               | 300.8               | 300.6               | 301.8               | 300.8               | 301.0                  | 298.3           | 298.0              | 3.069                                     | 0.250                      | 0.029                        | 0.279                          | 1.552  |

Constants used in the calculations are given in Table 3.

Table 3. Constants used in calculations.

| Constant  | Symbol       | Value                                      |
|---|--------------|--|
| 1. Solar collector area (6 containers)            | $A$          | 0.180 m <sup>2</sup>                       |
| 2. Heat capacity of water                         | $C$          | 4182 J/Kg-°K at 20°C                       |
| 3. Mass of water (6 containers)                   | $m$          | 22.86 Kg                                   |
| 4. Emissivity of flat black paint                 | $\epsilon_1$ | 0.95                                       |
| 5. Area of containers subject to radiation losses | $A_1$        | 0.510 m <sup>2</sup>                       |
| 6. Stefan-Boltzmann constant                      | $\sigma$     | 5.67x10 <sup>-8</sup> W/m <sup>2</sup> -°K |
| 7. Window area of test room                       | $A_w$        | 2.90 m <sup>2</sup>                        |

The predicted heating performance of the Trombe water wall was determined for two locations, one in Morgan Hill, CA (37.1°N latitude) and one in Bozeman, MT (45.6°N latitude). To do this,  $E$  was obtained from Figure 2 and was used along with National Renewable Energy Laboratory historical solar data (Marian & Wilcox, 1990) plus historical heating data from Morgan Hill (23 years) and Bozeman (3 years). In addition to this, the performance in Morgan Hill was predicted using as a check on the Duffie & Beckman method, except that actual coefficient of heat transfer ( $U_{sp}$ ) was used for the Mazria method instead of the calculated  $U_{sp}$  (Mazria, 1979). The predicted room temperatures were calculated per the Mazria method. Finally, the cost was determined to build a water wall.

### 4. Results

Figure 2 shows that the heat stored in the containers at the end of a day is a linear function of the solar radiation. Approximately 60% of sunlight is stored as heat in the containers for both tilt angles ( $E = 60\%$ ). This curve is used to predict the performance of the Trombe water wall.

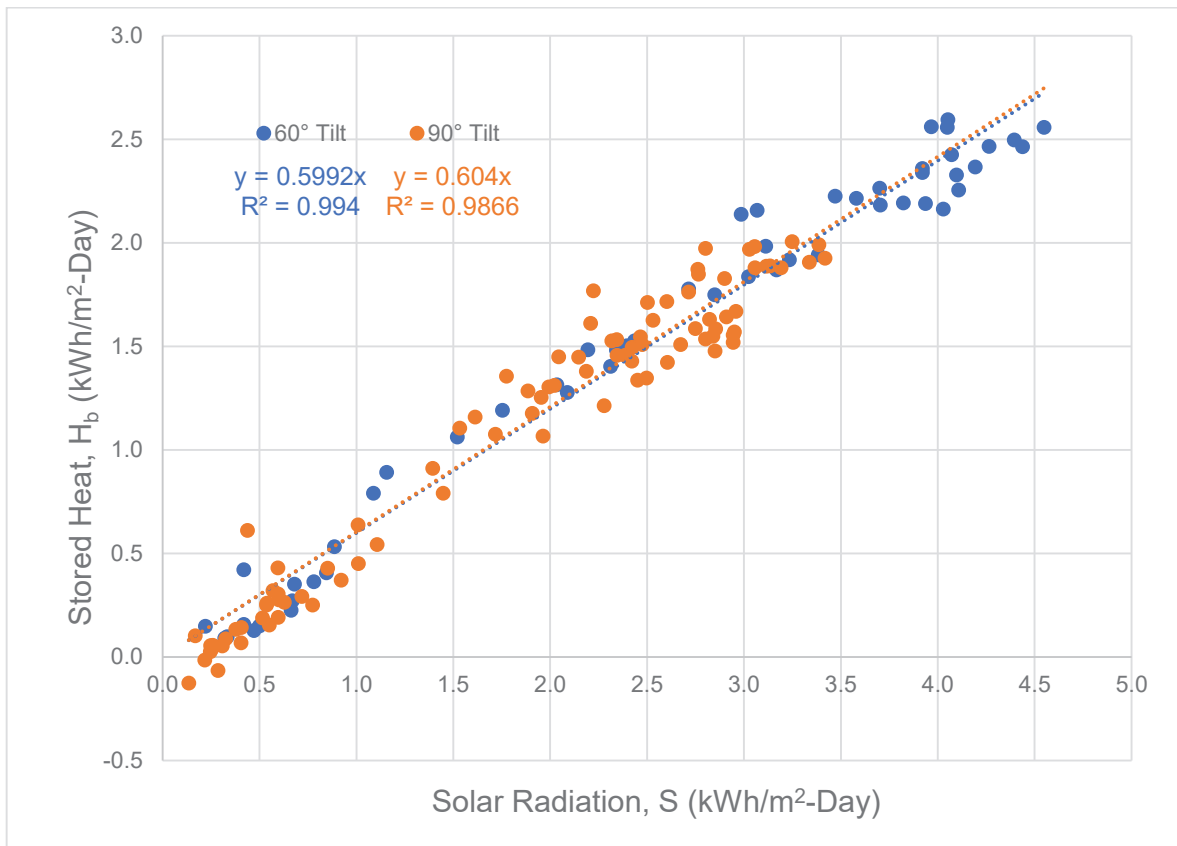


Fig. 2. Heat stored in containers at the end of each day as a function of solar radiation.  $S$  is shown in Eq. 1 and comes from solar energy meter measurements.  $H_b$  is shown in Eq. 5 and comes from temperature measurements. The slope gives  $E$  in Eq. 6.

Figure 3 shows the predicted heating performances in Morgan Hill, CA and Bozeman, MT. In Morgan Hill, the Trombe water wall supplied 66%, 71%, and 98% of the heating requirement for December, January, and the total heating season, respectively when the container tilt angle was 90°. Those numbers increased to 97% for both months and 162% for the total heating season when the container tilt angle was 60°. A 60° tilt makes the sun's rays perpendicular to the absorbing surface of the containers on December 21<sup>st</sup>, the winter solstice. Figure 3 also shows the predicted heating performance in Bozeman, MT. Here the Trombe water wall supplied 56%, 50%, and 85% of the heating requirement for December, January, and the total heating season, respectively when the container tilt angle was 90°. Those numbers increased to 66%, 61%, and 108% when the container tilt angle was 69°. A 69° tilt makes the sun's rays perpendicular to the absorbing surface of the containers on December 21<sup>st</sup>. The asymmetric shape of the curves is due to dividing a large number (stored heat) by a small number (heating requirement) in November and March compared to the rest of the heating season. The reason the water wall exceeds 100% for the total heating season is that some months exceed 100%.

## Passive Solar Heating for Emergencies

In Mazria's method, the solar contribution is truncated for those months when it exceeds the heating requirement. If that is done with the Duffie and Beckman method, then the percentage of the yearly heating requirement supplied by solar for Morgan Hill is 87% for the Duffie and Beckman method and 79% for the Mazria method.

The predicted average daily indoor temperature for the rooms at each location is given in Table 4. In Morgan Hill, monthly temperatures range from 18.1°C to 27.0°C for a 90° tilt and 19.0°C to 30.3°C for a 60° tilt. In Bozeman, monthly temperatures range from 8.7°C to 27.0°C for a 90° tilt and 9.4°C to 31.2°C for a 60° tilt. The December and January indoor temperatures are cool in Bozeman but still substantially warmer than outside, which is -4.4°C to -5.6°C.

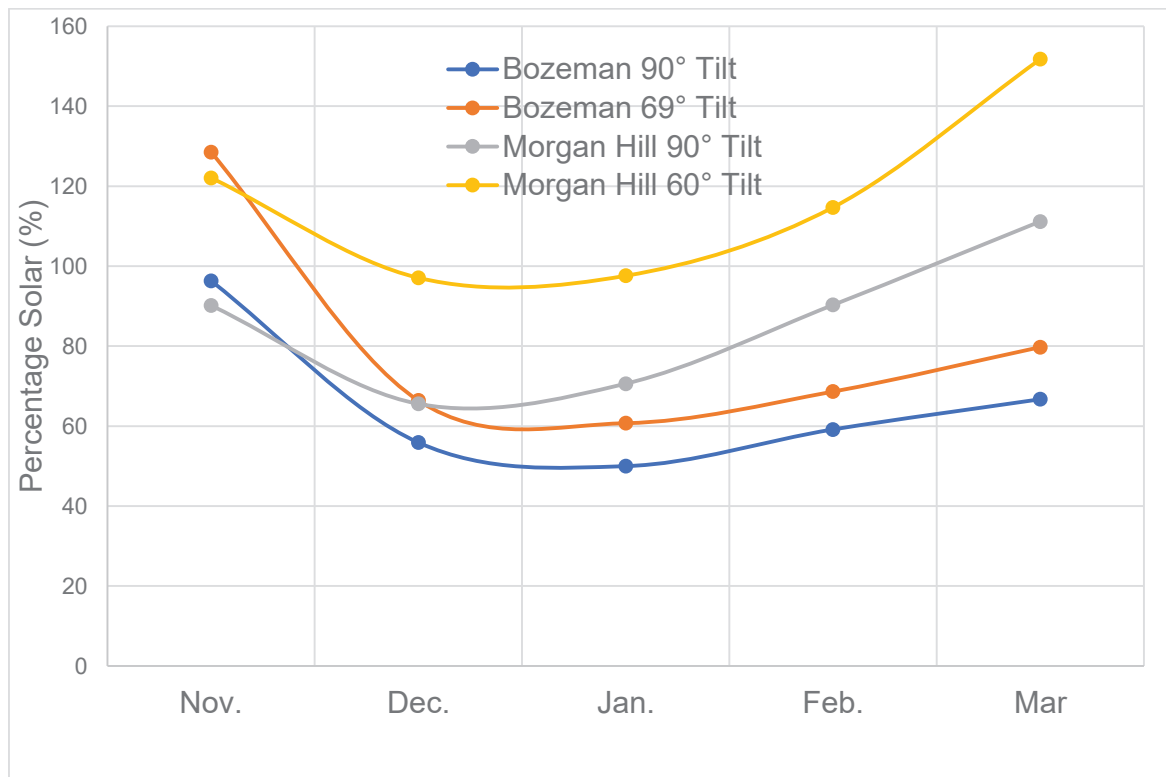


Fig. 3. Predicted heating performance for Morgan Hill, CA, USA (37.1°N latitude and window area = 2.90 m<sup>2</sup>) and Bozeman, MT, USA (45.6°N latitude and window area = 1.78 m<sup>2</sup>).

Table 4. Predicted daily average indoor temperature for each month

| Month | Room Temperature (°C) |          |             |          |
|-------|-----------------------|----------|-------------|----------|
|       | Morgan Hill, CA       |          | Bozeman, MT |          |
|       | 60° Tilt              | 90° Tilt | 69° Tilt    | 90° Tilt |
| Sept. | 30.3                  | 27.0     | 31.2        | 27.0     |
| Oct.  | 27.7                  | 25.6     | 25.1        | 22.8     |
| Nov.  | 22.3                  | 21.1     | 16.1        | 15.0     |
| Dec.  | 19.0                  | 18.1     | 9.4         | 8.7      |
| Jan.  | 19.7                  | 18.5     | 12.3        | 11.2     |
| Feb.  | 21.7                  | 19.5     | 16.2        | 13.8     |
| Mar.  | 22.9                  | 19.4     | 20.6        | 16.3     |
| Apr.  | 23.8                  | 19.4     | 22.3        | 16.4     |

The cost to construct a passive solar Trombe water wall was determined from 2023 USA prices and comes to \$221/m<sup>2</sup>, excluding labor. The price can be lowered by using second-hand or salvaged materials.

## 5. Discussion

This project evaluated a Trombe water wall that would provide a warm room(s) in nations where the heating infrastructure has been damaged by war or nature. The water wall was designed so that it would be 1) decentralized, 2) inexpensive, 3) constructed of common materials, 4) electricity-free, 5) easily assembled and disassembled, and 6) a low-carbon emitter.

To evaluate the water wall, a curve was generated to determine the conversion efficiency of sunlight into stored heat. With that curve plus the sites' solar radiation, heating requirement and window area, the percentage of heat supplied by the water wall was calculated for each month of an average heating season in Morgan Hill, CA, USA and Bozeman, MT, USA. The same was done for the predicted room temperatures.

As expected, the predicted heating performance and room temperatures were better for Morgan Hill because it was at a lower latitude and had a larger window area. In addition, the performance improved when the container tilt angle was decreased from 90° to 60°. The water wall provided more than 100% of the heating requirement for some months of the heating season. Shading, insulation, or fewer containers would be needed for those months.

The predicted heating performance and room temperatures for the higher latitude site, Bozeman, was not as good because of the lower solar radiation and smaller window area. There was not as much performance improvement in Bozeman for December and January by decreasing the container tilt angle. That is because the solar elevations are ~9° lower in Bozeman and the sun's rays are closer to perpendicular to a 90° tilt.



The Mazria method was used as a check on the Duffie and Beckman method for both locations. It was found that both methods gave fairly similar results for the yearly solar contribution to the heating requirement. The differences are due to the literature sources for solar radiation.

There are several ways to improve the performance at higher latitudes. They are by adding another window, using a reflector, or applying a selective surface to the containers. Of course, these techniques increase the complexity and cost of the water wall.

There are several disadvantages of the Trombe water wall. The first is that the containers will block a substantial amount of sunlight from entering the rooms. But some containers can be removed to allow sunlight to enter the room(s). The second disadvantage is appearance. But maybe this is a small price to pay for warmth in an emergency.

One also must be aware of the loading of the water wall on the floor. The wall could weigh 227 to 454 kg (500 to 1000 lbs.) so the weight distribution on the floor needs to be considered. Lastly, the water wall should be anchored to the wall that borders the window.

### **6. Conclusion**

Approximately 60% of sunlight can be stored as heat in a retrofit, passive solar Trombe water wall that is both simple and inexpensive. With that high conversion efficiency, two methods predict that a water wall could supply a substantial portion of the heating requirement in rooms with equator facing windows. The predictions show better results at lower latitudes. Nevertheless, enhancements can be made to improve the performance at higher latitudes such as by adding windows, reflectors, or selective surfaces.

It is proposed that this retrofit be used in countries where their heating infrastructure has been damaged by war or nature to supplement other emergency energy sources. Government policies could aid in the implementation of such a system. Those policies could include tax incentives and storage facilities with water wall kits available for emergencies.

Some limitations of this concept are loading considerations on wood floors, room sunlight blockage and aesthetics. Future work could entail comparing room temperatures with and without the water wall. Also, detaching the collector from the storage unit to alleviate overloading wood floors could be another future research topic.

### **Acknowledgement**

I would like to thank William D. Smallen for supplying his historical heating data for Bozeman, MT, USA.

**Conflict of Interest**

The author does not report any conflicts of interest.

## References

- Duffie, E. and Beckman, W. (1974). *Solar energy thermal processes*. New York: Wiley-Interscience.
- Marian, W. and Wilcox, S. (1990). *Solar radiation data manual for flat-plate and concentrating collectors*, National Renewable Energy Laboratory.
- Mazria, E. (1979). *The passive solar energy book*. Emmaus, PA: Rodale Press.
- U.S. Department of Energy. (2004). *The history of solar*.  
[https://www1.eere.energy.gov/solar/pdfs/solar\\_timeline.pdf?utm\\_id=64753&sfmc\\_id=4732353](https://www1.eere.energy.gov/solar/pdfs/solar_timeline.pdf?utm_id=64753&sfmc_id=4732353)
- U.S. Department of Energy (n.d.) *Passive solar homes*.  
<https://www.energy.gov/energysaver/passive-solar-home-design>
- Wikipedia (2023). *History of passive solar building design*.  
[https://en.wikipedia.org/wiki/History\\_of\\_passive\\_solar\\_building\\_design#:~:text=Ancient%20Greeks%2C%20Romans%2C%20and%20Chinese,after%20the%20Fall%20of%20Rome.](https://en.wikipedia.org/wiki/History_of_passive_solar_building_design#:~:text=Ancient%20Greeks%2C%20Romans%2C%20and%20Chinese,after%20the%20Fall%20of%20Rome.)
- Wikipedia (2024). *Trombe wall*.  
[https://en.wikipedia.org/wiki/Trombe\\_wall](https://en.wikipedia.org/wiki/Trombe_wall)

**Thermal Comfort in Hot, Humid Weather  
in a Dome-Shaped Building**

Roya Taheri, PhD, AIA, LEED AP  
Taheri Architecture, Inc.  
Email: [rtaheri@taheriarch.com](mailto:rtaheri@taheriarch.com)

## Abstract

This study considers natural ventilation in various climates where a hot, humid season exists. Effort was made to reduce the reliance on commonly used mechanical systems and incorporate natural ventilation to achieve higher levels of comfort and IEQ. Simulations were performed using Computational Fluid Dynamics (CFD) modeling software, with natural ventilation and a solar chimney, as well as combined natural and mechanical ventilation, in a building with a domed roof. The total amount of solar radiation on a hemispherical dome surface was calculated using equations. The average solar radiation per unit of roof surface area was then calculated. Next, the temperature on the dome surface and heat transfer were simulated. The impact of the air velocity on human comfort was examined using different combinations of windows and skylights. The results indicated that because of a high elevation of the skylight, the velocity in the room increased, exceeding the comfort zone.

Keywords: natural ventilation, thermal comfort, hot weather, dome

## Introduction

More than 10% of the building energy consumption is reported to be for ventilation (U.S. EIA, 2022). With the trend of global warming, the energy usage of ventilation as well as cooling can be expected to increase. Studies have shown the impact of poor prevalent mechanical ventilation systems on human health and/or comfort could be adverse, considering sick building syndrome or stress resulting from indoor pollutants, VOCs, office work-related stressors, humidification, and odors associated with moisture and bioaerosol exposure (Ibrahim et al. 2022; Nag, 2018). Moreover, the issues related to overcooling have drawn attention (Chong, 2014; Sekhar, 2015). It is important to enhance energy savings while maintaining indoor air quality, especially in hot, humid weather, when it is more critical.

Proper design of overall building configuration, temperature distribution, and airflow are important to achieve thermal comfort and save energy and resources. To meet thermal comfort without spending excessive energy, this research explored the potential of natural ventilation in a hot, humid environment in a building with a dome roof. It examined thermal comfort under various combinations of air inlets and outlets, while changing temperature, relative humidity and air velocity. The study uses a CFD software program to simulate these indoor conditions.

## Thermal Comfort

There are predictions that the frequency and duration of intensified, humid heat events are expected to increase in the coming years. We often experience excessive temperatures both in the summer and the winter in urban buildings. According to Sekhar (2015), “The findings suggest that overcooled buildings are not a consequence of occupant preference but more like an outcome of the HVAC system design and operation”.

Ming-Tse et al suggest that thermal comfort may be achieved at higher temperatures by adding airflow around the body. Proper design of the overall building configuration, considering temperature distribution, humidity, and airflow, would help achieve thermal comfort and save energy and resources.

### **Temperature Range**

A study in China indicates that “the neutral temperatures in naturally ventilated and air-conditioned buildings were 28.3°C and 27.7°C, respectively” (Yang and Zhang, 2008). It suggests a temperature of not lower than 26°C for a conditioned space with natural ventilation, and an increase in the air velocity to achieve greater comfort.

According to Caetano et al., “Based on the Predictive-Mean-Vote (PMV)-Model, the thermal comfort zone is defined to be between 22.5°C to 25.5°C operative temperature when relative humidity is above 65% and 23.0°C to 26.0°C operative temperature when relative humidity is above 35%”.

The acceptable thermal comfort range in Malaysia was reported to fall within 23.4°C – 31.5°C for a natural, ventilated space in a field study by Abdul Rahman & Kannan, as quoted in research by Ahmad and Abdul Rahman (2017).

### **Humidity**

A study about humidity in hot, humid climates indicated “the impact of humidity on human responses was not significant when the relative humidity was below 70% and was significant and increased with an increase in air temperature when the relative humidity was above 70%.” (Jin et al., 2017). “The upper limit for people in hot, humid climates who engaged in sedentary activity and dressed in summer clothing (0.57 clo) was determined to be 30.3 °C in ET\* for the 90% acceptable range and 32.3 °C in ET\* for the 80% acceptable range.” ET\* is the new effective temperature.

For simulation in this study, temperature was set at 30°C and relative humidity was set at 70%. A simulation for 35°C and 80% humidity was explored as well.

### **Air Velocity**

According to Zhou et al. (2023), “For a long time, the air speed in a typical indoor office environment was restricted to a level below 0.2 m/s, with the highest acceptable air temperature controlled at 26°C.” Per ASHRAE 55-2010, the same research quotes, “Under the upper air speed limits of 0.8 m/s and 1.2 m/s, the maximum operative temperatures would be extended to around 30.5°C and 31.0°C, respectively”.

Evaporative heat loss decreases when humidity rises due to a reduced water vapor pressure gradient between the ambient air and the skin’s surface. According to Sobolewski et al. (1990), “Despite access to drinking water, a hot and humid environment causes more serious problems to living organisms than a dry

environment.” They continue that, “In these circumstances, any chance of physical activity is only possible in conditions of intense air flow.”

### Solar Radiation on Dome

In earlier research, the total amount of solar radiation on a hemispherical dome surface was assumed to be equal to the sum of the radiation shone on two surfaces  $S_1$  and  $S_2$  (Figure 1) (Taheri, 1990):

$$I_{tD} = S_1 I_{DN} \sin h + S_2 I_{DN} = \pi r^2 I_{DN} (\sin h + 1)$$

The average solar radiation per unit of roof surface area was expressed as

$$I_{uD} = I_{tD}/S = \pi r^2 I_{DN} (\sin h + 1)/2(2\pi r^2) = I_{DN} (\sin h + 1)/(4 I_{tD})$$

is the total normal radiation on the roof surface,  $I_{DN}$  is the normal solar radiation, and  $I_{uD}$  is the normal solar radiation per unit area of the roof.

The temperature on the dome surface and the heat transfer were then calculated. A hybrid simulation based on this calculation was performed and airflow within a model showed turbulence within the model.

In this study, a CFD model was used to explore the airflow and velocity in a similar building, producing similar results for patterns of airflow.

### Natural Ventilation

The airflow in natural ventilation may be obtained from the equations below (Taheri et al., 1987).

$$\gamma (T) = 1.293 * 273.16 / T = 353.20 / T$$

$$p (z) = (10332.3 - \gamma * z) g$$

$$\Delta p = \gamma * 273.16 * z (1/T_i - 1/T_o)$$

$$v : \sqrt{[2g * \Delta p / (\xi \gamma)]}$$

$\gamma$  is the density of air at 30°C (303.16°K), 1.164 kg/m<sup>3</sup>. The density at 0°C is 1.293 (kg/m<sup>3</sup>).

$z$  is the height from the top opening to the center of the low opening.

$\xi$  is pressure loss coefficient, which is 1.

$v$  is the air velocity at the opening [m/s].

$g$  is the gravity acceleration constant, 9.8 m/s<sup>2</sup>.

$\Delta p$  is the pressure loss Kg/m<sup>2</sup>.



$T_o$  is the outdoor temperature in Kelvin.

$T_i$  is the indoor temperature in Kelvin.

Air velocity at the openings was calculated for natural ventilation in two cases of cross-ventilation and stack ventilation and generally agreed with the results of the CFD simulations.

## Simulation

For this study, as the location of a building with a hot, humid summer, Washington, DC, is selected. A psychrometric chart for Washington DC is indicated in Graph 1.

### *Simulation Settings*

The simulations are under ambient temperature of 30°C and 70% relative humidity.

Our goal is to obtain a velocity of between 0.2 and 0.8 m/s at the seating-area level. The initial velocity at the perimeter inlets was assumed to be 0.1 m/s. The second set of simulations use 2.5 m/s, as the wind or mechanical ventilation-induced scenario. The building is circular with a dome roof. The overall height is 50 meters and the wall height is 25 meters. The simulations are performed for three cases of:

- (A) Four openings at a low level with the bottom of the opening 2 m above floor finish.
- (B) Four openings at a low level and a 2-m diameter skylight,
- (C) Four openings at a low level and four openings at a high level.

### *Simulation Results*

The net radiative heat flux is shown on the first model for cross ventilation (case A) at 8 a.m. (Figure 2).

The velocity in the room with four air inlets at a low height and a skylight opening indicates a combination of cross ventilation with a stack effect. The opening at the top is circular with a 2-meter diameter. In this simulation, with an initial velocity of 2.5 m/s, a high air velocity was observed at the seating area in the middle of the room, at the height of about 1.5 meters (about 1 m/s at 10 a.m. and 1.8 m/s at 2 p.m.). This is beyond the comfort level we would like to achieve, which is between 0.2 to 0.8 for indoors. The humidity level, on the other hand, was not alleviated (Figure 4), conceivably because the outside humid air was brought inside at a higher speed compared to the scenarios with an initial velocity of 0.1 m/s. The velocity in the middle of the room seating area fluctuates between 0.05 and 0.6 m/s (Figure 3). Considering that according to the psychrometric chart (Graph 1), a relative humidity of 70% and a

temperature of 30°C is close to the comfort zone, it may be assumed that a mild breeze could help provide comfort.

In case C, with four high and four low openings, with an induced initial velocity of 2.5 m/s, the air velocity in the middle of the room at the seating area ranges between 0~2.7 m/s. With initial velocity of 0.1 m/s, the seating area velocity remains under 0.4 m/s and reaches as low as 0.1 m/s.

In the case of 2.5 m/s initial velocity, a wider range of humidity is observed. The increase of humidity at the lower outlet opening may be attributed to the concentration of air accumulating to exit the space. In the case of eight openings, the lower row of outlets has a higher humidity caused by the higher weight of air due to gravity.

#### *Increase in Temperature and Humidity*

A scenario of 35°C and 80% relative humidity was simulated. With an increased velocity of 2.5 m/s, this scenario may fall in the comfort zone for the outdoor environment; however, for indoor sedentary activities, the combination is not assumed to be acceptable. The 0.1 m/s does not provide comfort under this thermal condition.

Case C, with two rows of openings, did not provide an optimal environment for either the 0.1 or 2.5 initial velocities.

We may conclude that with lower temperature and humidity levels, it is possible to obtain comfort in this building with natural ventilation only. However, with humidity of 80 and temperature of 35°C, dehumidification and/or cooling may be needed.

## Conclusion

Thermal comfort seems to be achievable in a hot, humid summer in a climate similar to Washington, DC, by natural ventilation in a circular building with a 33-meter radius with a dome roof and an overall height of 50 meters according to the simulations performed using a CFD software.

Generally, a higher level of air velocity may be achieved in the seating area by inducing a wind or mechanical air flow of 2.5 m/s. However, as the velocity in this zone surpasses the 0.2 to 0.8 m/s optimum velocity for seated individuals, a lower initial velocity is desirable. Simulations with a skylight indicate a higher level of turbulence and air velocity. For this study which represents a large hall, it can be concluded that an opening in the roof to achieve stack ventilation is not necessary. The cross ventilation between the four low openings, as well as the case of four low openings and four high openings, produce a more uniform indoor thermal environment and are easier to predict and control. At a higher temperature of 35°C and 80% relative humidity, natural ventilation alone was not adequate and dehumidification and/or cooling may be needed to obtain thermal comfort.

## References

- Ahmad, N. H., Abdul Rahman, A. M. (2017). The potential of evaporative cooling window system using labu sayong in tropical Malaysia: A review. *Advanced Journal of Technical and Vocational Education*, 1(1): 262-272.
- Caetano, D. S., Kalz, D. E., Lomardo, L. L. B., Rosa, L. P. (2017). Evaluation of thermal comfort and occupant satisfaction in office buildings in hot and humid climate regions by means of field surveys. *International Conference – Alternative and Renewable Energy Quest, Energy Procedia 115*, 183-194.
- Chong, K. I. K. (2014). *Natural ventilation in buildings: modeling, control and optimization*. Massachusetts Institute of Technology.
- Ibrahim, F., Samsudin, E. Z., Ishak, A. R., and Sathasivam, J. (2022). *Hospital indoor air quality and its relationships with building design, building operation, and occupant-related factors: a mini-review*. Frontiers.org.
- Jin, L., Zhang, Y., Zhang, Z. (2017). Human responses to high humidity in elevated temperatures for people in hot-humid climates. *Building and Environment*, 114, 257-266.
- Lin, M.T., Wei, H.Y., Lin, Y.J., Wu, H. F., Liu, P.H. (2010). *Natural ventilation applications in hot-humid climate: A preliminary design for the College of Design at NTUST*. Proceedings of the 17th Symposium for Improving Building Systems in Hot and Humid Climates: Austin, Texas.
- Marsh, A. J. (2018). *PD: Psychrometric Chart online*.  
<https://drajmarsh.bitbucket.io/psychro-chart2d.html>

Nag, P. K. (2018). *Sick building syndrome and other building-related illnesses*. Springer

Nature, DOI: 10.1007/978-981-13-2577-9\_3, PMID: PMC7153445

Sekhar, S.C. (2015). Thermal comfort in air-conditioned buildings in hot and humid

climates – why are we not getting it right? *Indoor Air*. 26(1), p. 138-152.

<https://onlinelibrary.wiley.com/doi/full/10.1111/ina.12184>

Sobolewski, A., Młynarczyk, M., Konarska, M., & Bugajska, J., (2021). The influence of

air humidity on human heat stress in a hot environment. *International Journal of*

*Occupational Safety and Ergonomics*.

<https://doi.org/10.1080/10803548.2019.1699728>

Taheri, R. (1990). Comparison between design criteria for various warm climates.

*Proceedings of the Indoor Air Quality and Ventilation Conference: Lisbon, Portugal*.

p. 55.

Taheri, R. (1987). Hybrid simulation of a ventilation system based on natural

convection. *Transactions, SHASE*, 345, pp. 51-69.

U.S. Energy Information Administration (2022). *Use of energy explained, Energy use in*

*commercial buildings, 2018 Commercial Buildings Energy Consumption Survey*.

<https://www.eia.gov/energyexplained/use-of-energy/commercial-buildings.php>

Yang, W., Zhang, G. (2008). Thermal comfort in naturally ventilated and air-conditioned

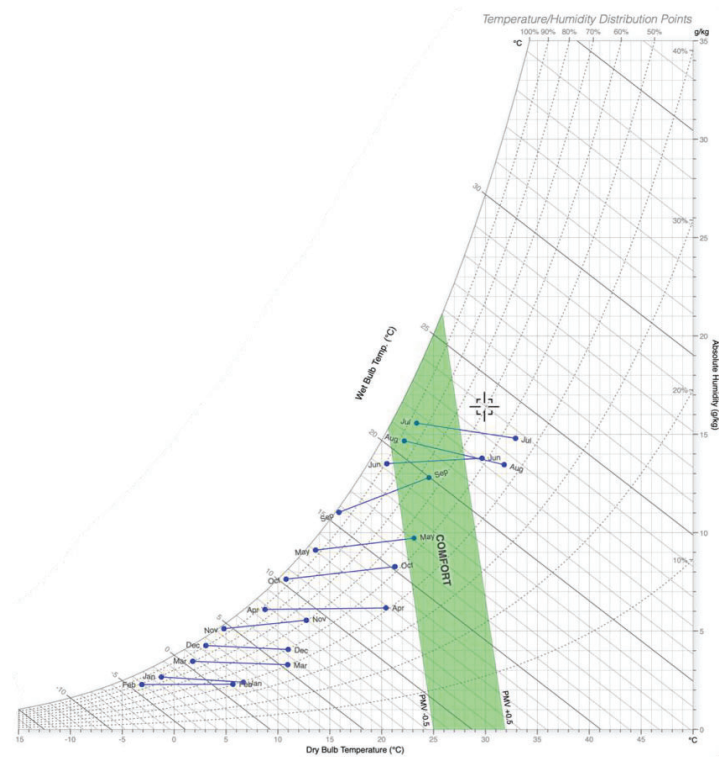
buildings in humid subtropical climate zone in China. *International Journal of*

*Biometeorology*. 52(5), 38598.

Zhou, J., Zhang, X., Xie, J., Liu, J. (2023). Effects of elevated air speed on thermal

comfort in hot- humid climate and the extended summer comfort zone. *Energy and*

*Buildings*, 287, 112953.



Graph 1. Thermal comfort in hot and humid summers in Washington D.C..(Marsh, A.D. 2018)

In the summer seasons, the temperature and relative humidity ranges between;

23°C to 35°C and 45% RH to 90% RH

Mean radiant temperature: 20°C

Air velocity: 0.70 m/s

Metabolic activity: 1.2 met (seated and light activity)

The comfort temperature and relative humidity according to the psychrometric graph:

June between 28°C-30°C and 55% RH

July between 30°C-34°C and 50%-60% RH

August between 29°C-33°C and 50% RH

### Psychrometric Chart

ASHRAE 55-2017

Dry Bulb: 29.90 °C

Rel Humidity: 60.68%

Sensation: Slightly Warm

SET: 28.48 °C

PMV: +0.89

PPD: 7.1%

Figures

Fig. 1. Solar Radiation on Dome

*“Total amount of solar radiation on a hemispherical dome surface was assumed equal to the sum of radiation shone on two surfaces  $S_1$  and  $S_2$ ” (Taheri, 1990).*

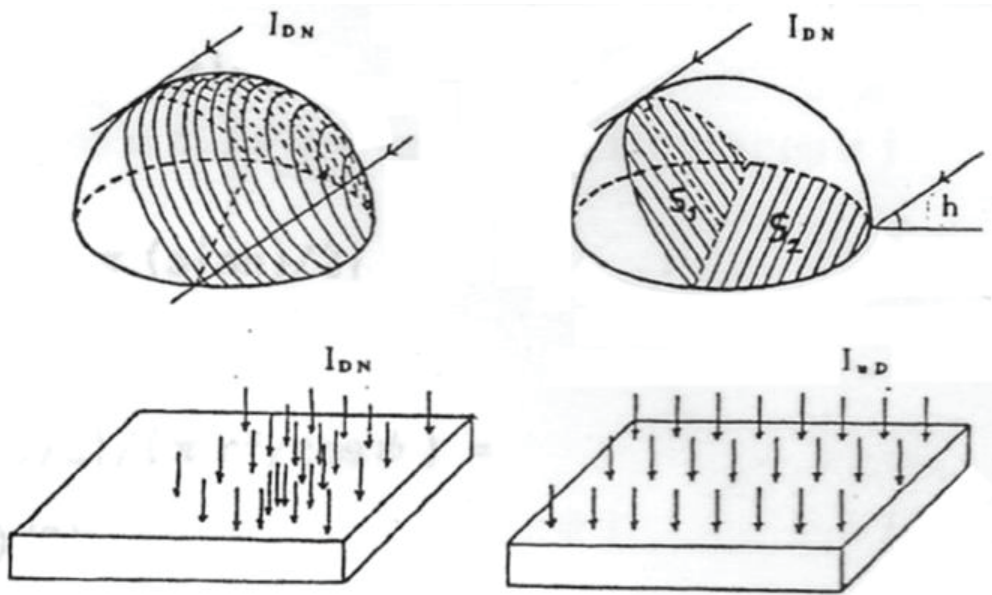


Fig. 2. Net radiative heat flux (A)  
Net radiative heat flux in Case A, cross ventilation, 8 a.m.

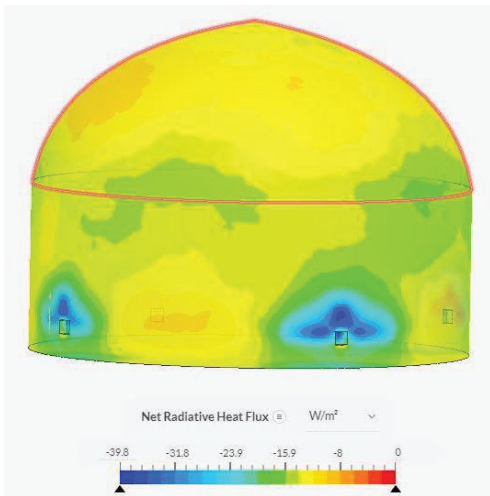
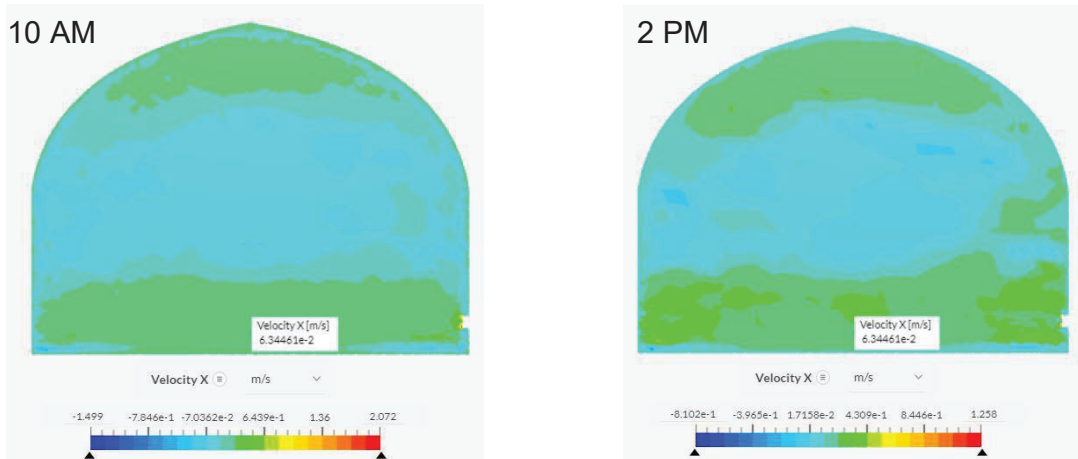


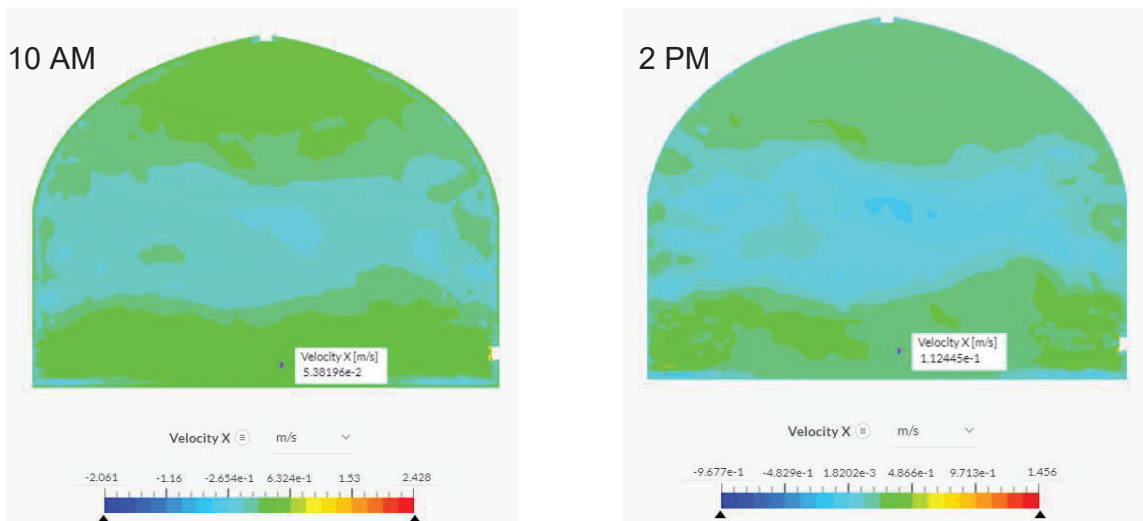


Fig. 3. Air velocity

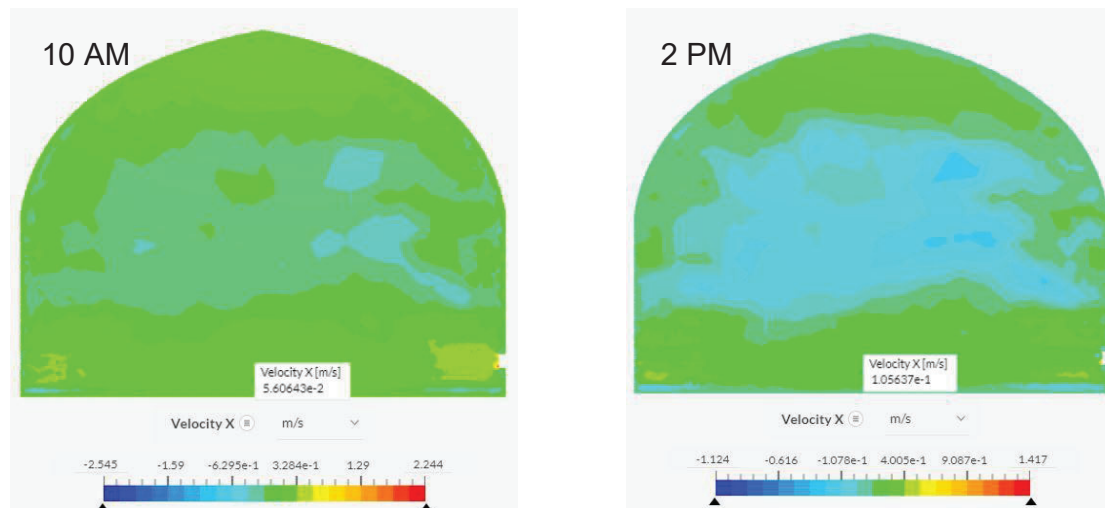
Velocity distribution, Scenario A, (4 openings at low level), Initial velocity 0.1 m/s



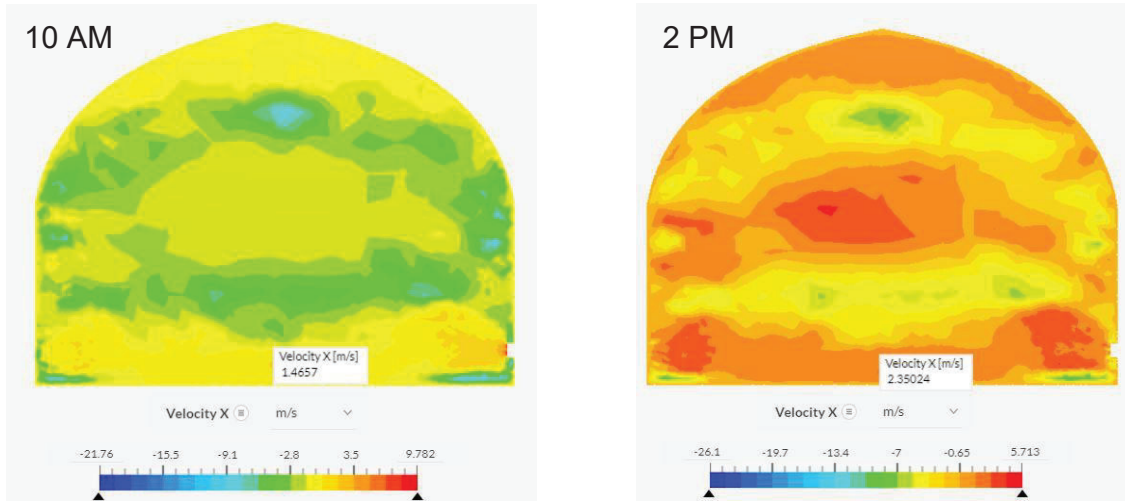
Velocity distribution, Scenario B (4 openings at low level with skylight), Initial velocity 0.1 m/s



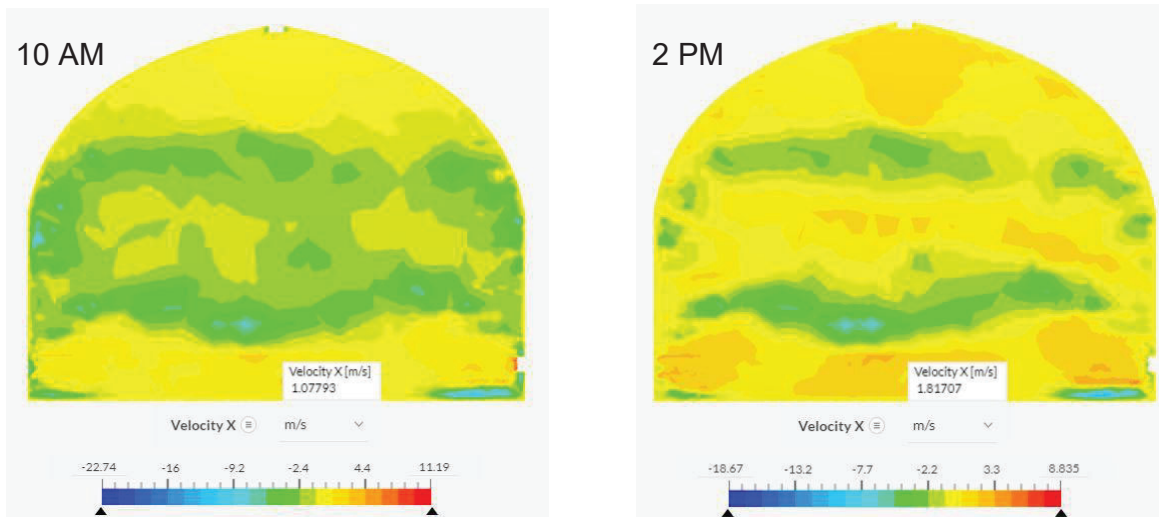
Velocity distribution, Scenario C (4 openings at low and 4 at high level), Initial velocity 0.1 m/s



Velocity distribution, Scenario A, (4 openings at low level), Initial velocity 2.5 m/s



Velocity distribution, Scenario B, (4 openings at low level with a skylight), Initial velocity 2.5 m/s



Velocity distribution, Scenario C (4 openings at low and 4 at high level), Initial velocity 2.5 m/s

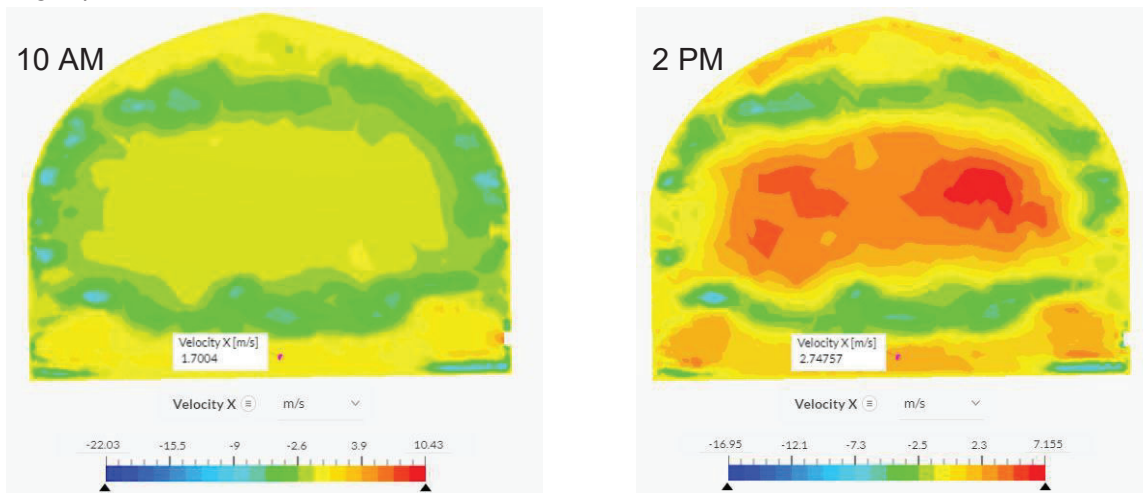
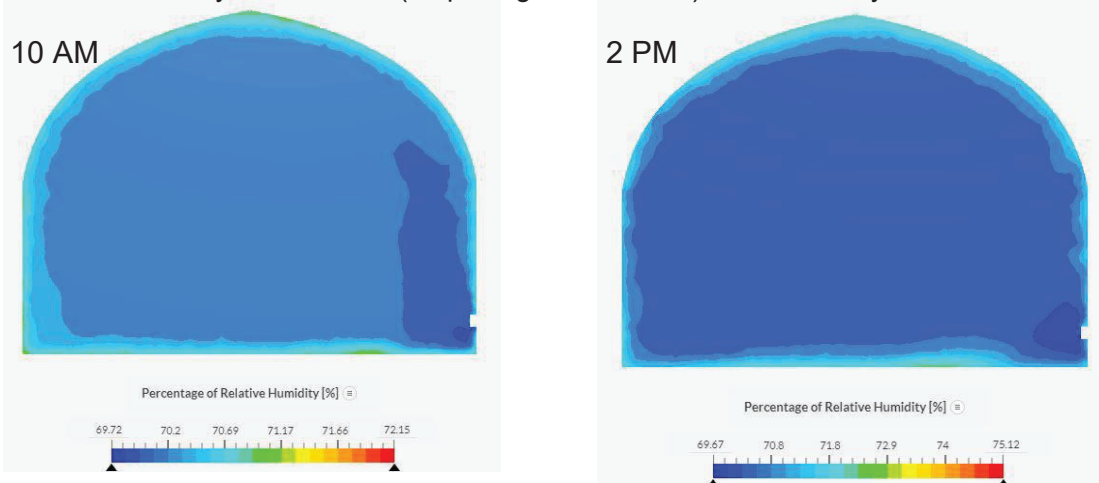
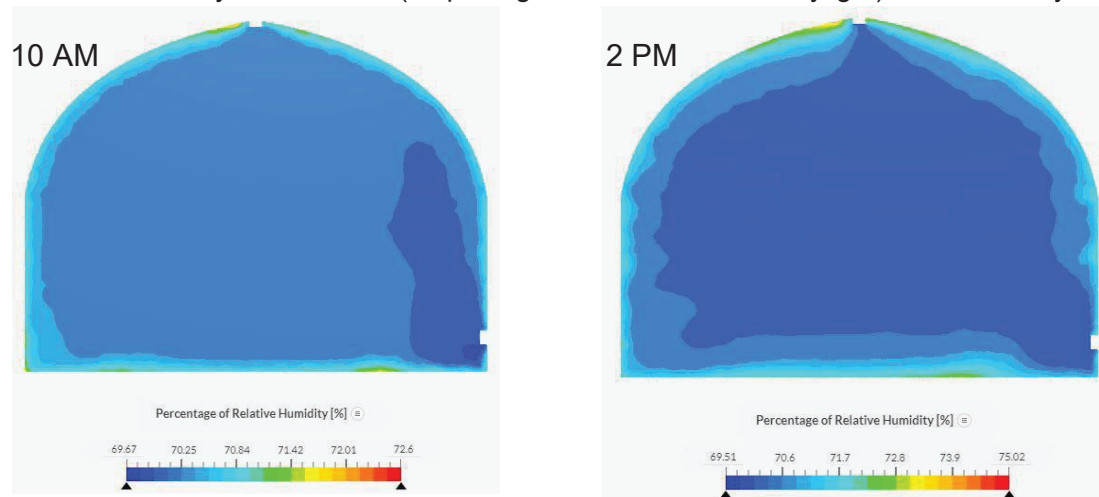


Fig. 4. Relative humidity

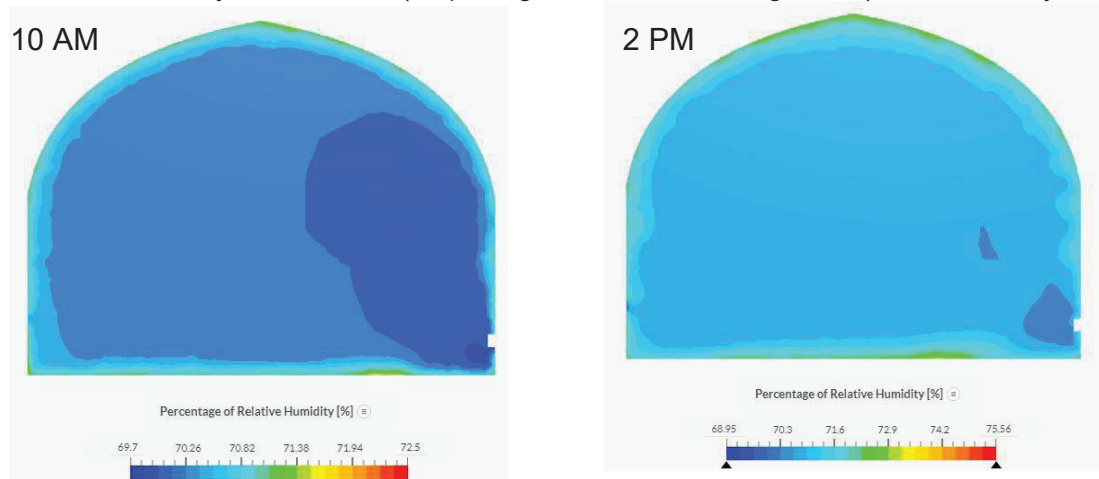
Relative Humidity, Scenario A, (4 openings at low level), Initial velocity 0.1 m/s



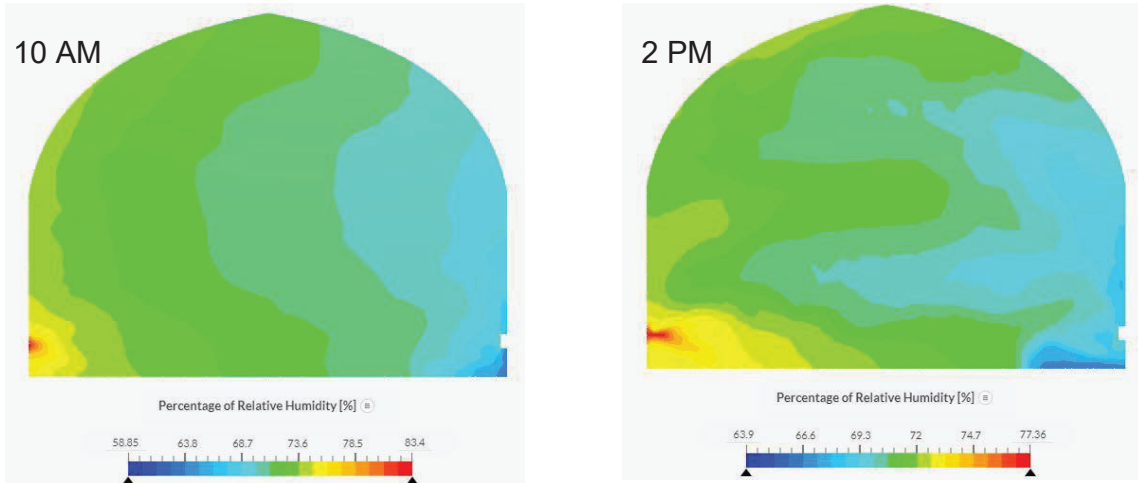
Relative Humidity, Scenario B, (4 openings at low level with a skylight), Initial velocity 0.1 m/s



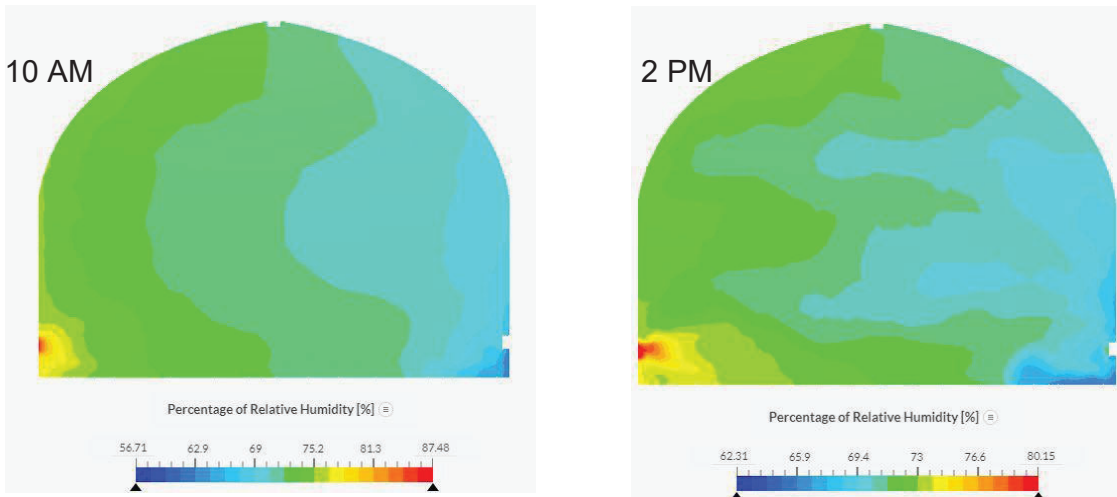
Relative Humidity, Scenario C, (4 openings at low and 4 at high level), Initial velocity 0.1 m/s



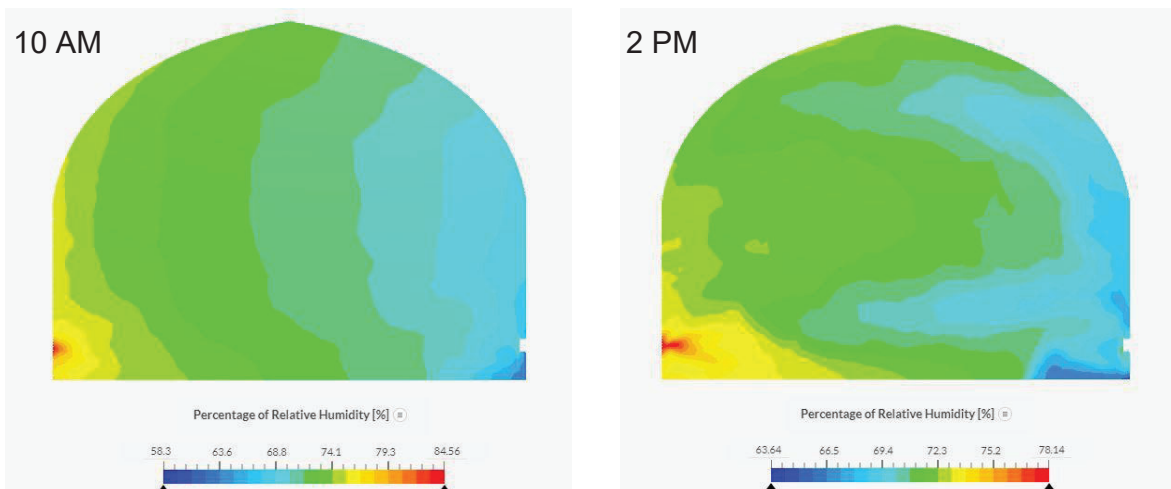
Relative Humidity, Scenario A, (4 openings at low level), Initial velocity 2.5 m/s



Relative Humidity, Scenario B, (4 openings at low level with a skylight), Initial velocity 2.5 m/s



Relative Humidity, Scenario C, (4 openings at low and 4 at high level), Initial velocity 2.5 m/s



**Energy and Economic Analysis of Combined Use of Phase Change Material  
with Insulation in Residential Buildings**

Prabhat Sharma <sup>a\*</sup>

Anish Modi <sup>a</sup>

<sup>a</sup> Department of Energy Science and Engineering, Indian Institute of Technology  
Bombay, Powai, Mumbai 400076, India

\* Corresponding author. ORCID: <https://orcid.org/0009-0008-5740-4918>,  
Email: [19i170005@iitb.ac.in](mailto:19i170005@iitb.ac.in)



## Abstract

The increase in energy demand in residential structures has obtained substantial attention in recent decades. One of the solutions to reduce the energy demand could be using phase change materials (PCMs) and insulation. Researchers have primarily focused on using PCMs and insulation in building envelopes to enhance energy efficiency, despite the associated costs. In this research, various cases were generated by varying the thickness and location of PCM and insulation among different building components. Technoeconomic analyses were conducted to identify the optimal thickness and placement of PCM and insulation in various building components. The results of the building simulations indicated that PCM thickness of up to 10 mm can be incorporated into the roof of a residential building in Mumbai. The best-performing case resulted in a 17.3 % reduction of the cooling load compared to the base case, with a payback period of 5 years.

Keywords: EnergyPlus, phase change material, simple payback period, thermal insulation

## 1. Introduction

The demand for primary energy consumption in the building sector is consistently increasing due to a rise in occupants' thermal comfort expectations (Kalbasi & Afrand, 2022). India is the third largest energy-consuming country after the United States and China. It is expected to decrease its energy demand to meet the net zero targets in 2070 (Jaganmohan, 2024). As per India's Cooling Action Plan, the national and space cooling demand are projected to rise 8 times and 11 times by factors of 700% and 1000%, respectively, by 2037-38, compared to the 2017-2018 levels (Cell, 2019). This underlines the need for passive cooling strategies in buildings to conserve energy.

As a passive measure, using thermal insulation is an easy-to-install and cost-effective method to reduce the cooling or heating demand. The researchers have tried to optimize the thickness, location, and type of material to increase the insulation's usefulness. Kaynakli (2023) focused on finding the optimum insulation thickness, while Ozel and Pihtili (2007) determined the optimum insulation location in the wall to maximize the time lag and minimize the decrement factor. Time lag refers to the difference in the time between peak outdoor temperature and peak indoor temperature whereas decrement factor is a parameter to quantify the reduction of temperature variation between external and internal surface.

Similar to thermal insulation, phase change material (PCM) has also gained attention to reduce the energy demand in the buildings due to its advantages such as high energy storage density and the ability to store and release thermal energy with minimal temperature variation. A PCM can be incorporated into the bricks, walls, roofs and windows of the building envelope (Beemkumar et al., 2019; Lamrani et al., 2021; Li et al., 2022; Saxena et al., 2020).

To effectively use the PCM in the buildings, researchers have tried to optimize the location, thickness, and melting temperature of the PCM. Jin et al. (2016) found that the optimal location of the PCM shifts to the outer side of the wall with an increase in the PCM thickness. In another numerical study, after simulating five different PCMs,

Kalbasi (2022) found the optimal melting temperature of PCM for different climatic conditions.

In previous research, PCM and insulation was separately used in different building components, and their thermal performance was evaluated. Insulation increases the thermal resistance of the building and reduces heat transfer, whereas PCM increases the thermal mass and thermal resistance of the building as it uses both sensible and latent heat. Therefore, the combination of insulation and PCM could increase energy savings and reduce the thermal load of the building.

Only a limited number of studies have investigated the thermal performance of insulation and PCM combinations. The results of the study by Kalbasi and Afrand (2022) show that combining PCM and insulation reduces the annual energy demand by 12.6%. Another study by Arumugam et al. (2022) focused on identifying the optimal position of the PCM and insulation. The results suggested using them on the outer surface, irrespective of the building's location.

To the best of the author's knowledge, no study has examined the combined use of PCM and insulation from an economic perspective. Also, the two known studies combining PCM and insulation have not evaluated the optimum building component, i.e. walls or roof, for integrating PCM and insulation. Therefore, the objective of this study is to find an optimum component to integrate the combination of PCM and insulation to maximize energy savings and minimize the payback period. This was done for residential buildings in Mumbai, which have warm and humid climate conditions.

## 2. Methodology

### 2.1 Building model description

Figure 1 shows the building's floor plan, used for current study, with a total carpet area of 1367 ft<sup>2</sup>. The building drawings were provided by Team SHUNYA, which was developed for the U.S. Solar Decathlon Build Challenge 2023 (Team SHUNYA, 2023). The building had two bedrooms, a double-height living room, a dining room, a kitchen, two toilets, a utility area, and a battery area.

To restrict the scope of the analysis to building envelope-related thermal load and performance, the building was considered unoccupied, with no lighting, computers, or office equipment. The infiltration through the building envelope was assumed to be 0.35 ac/hr.

## Analysis of Combined Use of Phase Change Material with Insulation



Fig. 1. Floor plan of the building's ground floor and first floor.

For analyzing the thermal performance, a building model was developed with typical wall, roof, and floor structures commonly used in India. The “typical wall” is composed of gypsum plaster (12 mm), brick (210 mm), and gypsum plaster (12 mm). The typical roof and floor for the study are made of cast concrete (200 mm). Clear glass (3 mm) with single glazing is used for windows.

After we analyzed the typical configuration, the combination of PCM and insulation was incorporated on the exterior side of the external wall of the building. The PCM and insulation used for the study were BioPCM®M182/Q25 and mineral wool, respectively.

Table 1. Thermophysical properties of materials (DesignBuilder, 2022).

| Material   | $k$ ( $W\ m^{-1}\ K^{-1}$ ) | $\rho$ ( $kg\ m^{-3}$ ) | $c_p$ ( $J\ kg^{-1}\ K^{-1}$ ) |
|------------|-----------------------------|-------------------------|--------------------------------|
| Plaster    | 0.16                        | 600                     | 1000                           |
| Brick      | 0.62                        | 1700                    | 800                            |
| Concrete   | 1.4                         | 2100                    | 840                            |
| Glass      | 0.9                         | -                       | -                              |
| PCM        | 0.2                         | 235                     | 1970                           |
| Insulation | 0.04                        | 48                      | 1381                           |

### 2.2 Mathematical Modeling

DesignBuilder (2022) and EnergyPlus (2022) were used for drawing and energy simulation of the building, respectively. In DesignBuilder, a new building was drawn and envelope materials were input. Then, the performance of the building was evaluated annually or for a specific period, depending on the requirement. The conduction finite-difference (CondFD) method was used to simulate PCM. In CondFD, the layer of PCM was divided into several nodes. The thermal behavior of



the PCM was assumed to be an unsteady state without internal heat generation. Eq. (1) was used to numerically solve each node of PCM under the Crank Nicholson scheme.

$$C_p \rho \Delta x \frac{T_i^{j+1} - T_i^j}{\Delta t} = \frac{1}{2} \left( k_w \frac{T_{i+1}^{j+1} - T_i^{j+1}}{\Delta x} + k_E \frac{T_{i-1}^{j+1} - T_i^{j+1}}{\Delta x} + k_w \frac{T_{i+1}^j - T_i^j}{\Delta x} + k_E \frac{T_{i-1}^j - T_i^j}{\Delta x} \right) \quad (1)$$

Here,  $C_p$  is the specific heat of PCM,  $\rho$  is density,  $\Delta x$  is the PCM thickness,  $\Delta t$  is the time step,  $k_w$  is the thermal conductivity of PCM between node  $i$  and node  $i + 1$ ,  $k_E$  is the thermal conductivity of PCM between node  $i$  and node  $i - 1$ ,  $T$  is the node temperature,  $i$  is the node being modeled,  $i + 1$  is the adjacent node towards indoor space,  $i - 1$  is the adjacent node towards ambient space,  $j$  is the current time step, and  $j + 1$  is the next time step.

The enthalpy-temperature curve was given as input to calculate the enthalpy change during the phase change process. The specific heat of the PCM was updated using the enthalpy-temperature function at each time step.

### 2.3 Simple payback period (SPP)

In this study, the SPP was determined to find the time required after which a reduction in the required cooling electricity will recover the initial cost of the PCM and the insulation in the walls and the roof. The initial cost of the PCM and the insulation (50 mm) was taken as 165 Indian Rupees per kg and 400 Indian Rupees per m<sup>2</sup> of the insulated area, respectively (Mishra et al., 2012; Saxena et al, 2019). The electricity price was assumed to be 8 Indian Rupees per kWh for calculating the annual savings (Global Petrol Price, 2023).

$$SPP = \frac{C_{PCM} + C_{insulation}}{Annual\ savings} \quad (2)$$

### 2.4 Procedure

Initially, parametric simulations were conducted by varying the thickness of the PCM and the insulation in the roof to determine the optimal thickness of the PCM and the insulation. A similar approach was applied to find the optimal insulation thickness in the external walls. Subsequently, a set of 50 cases was formulated, using various combinations of PCM in the roof, roof insulation, and wall insulation. The initial model incorporated construction materials representative of a typical wall and typical roof, denoted as the "base case." These cases were simulated to find the optimal configuration concerning cooling load and SPP.

## 3. Results and Discussion

Fig. 2 shows the annual cooling load and required annual cooling electricity at different thicknesses of PCM in the roof for residential buildings in Mumbai. The graph shows that the incorporation of the 10 mm PCM in the roof reduces the cooling load by 8%. The further increase in the thickness of PCM in the roof did not reduce the cooling load or cooling electricity. Therefore, a typical roof and a roof with 10 mm PCM were considered for further study while creating different combinations with the insulation.

## Analysis of Combined Use of Phase Change Material with Insulation

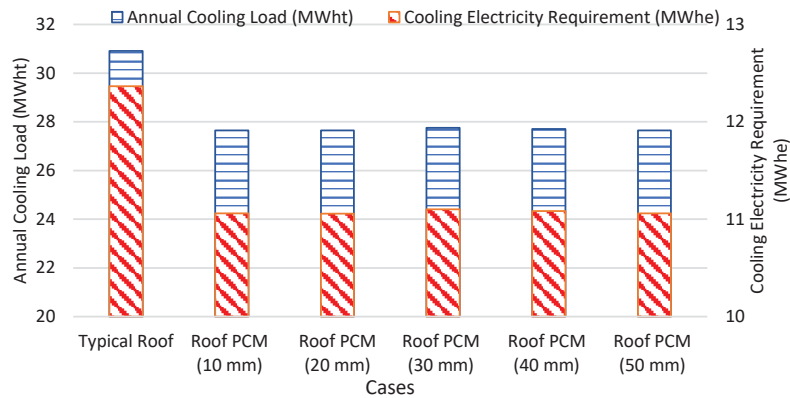
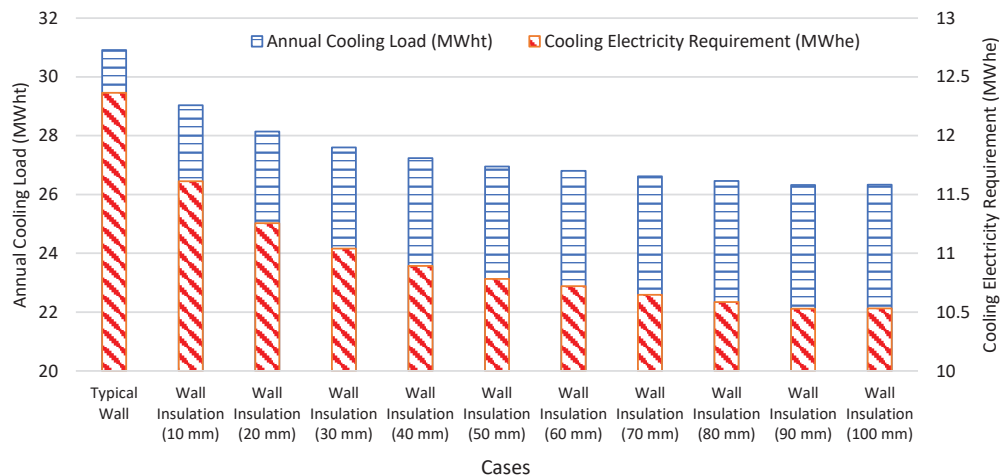


Fig. 2. Comparison of annual cooling load and annual cooling electricity requirement at different PCM thicknesses incorporated in the roof.

Similarly, a parametric study was performed with different thicknesses of insulation in the roof of the building. The cooling load of the building dropped from 2.6% to 4.7%, with an increase in insulation thickness from 10 mm to 100 mm. The reduction in the cooling load did not increase linearly with the increase in the insulation thickness and became almost constant after 50 mm of insulation. Therefore, 10 mm, 20 mm, 50 mm, and 100 mm of insulation thickness were taken into consideration when making a combination with roof PCM and wall insulation.

A parametric study involving the variation of PCM thickness within walls had not been conducted in current study. The PCM in the wall was omitted as it would lead to high capital costs. Then, the thermal performance of the building with insulation in the wall was evaluated. Fig. 3 shows the annual cooling load and annual cooling electricity with a variation of insulation in the walls. The cooling load reduced by 6 %, 9.6 %, 11.8 %, 13.3 %, 14.5 %, 15.3 %, 16 %, 16.7 %, 17.3 %, and 17.4 % with 10 mm, 20 mm, 30 mm, 40 mm, 50 mm, 60 mm, 70 mm, 80 mm, 90 mm, and 100 mm wall insulation, respectively. The increase in the reduction of the cooling load of the building is less than the uncertainty of the software used. Thus, 10 mm, 20 mm, 50 mm, and 100 mm of wall insulation were considered for making a combination with PCM and insulation in the roof.



## Analysis of Combined Use of Phase Change Material with Insulation

Fig. 3. Comparison of annual cooling load and annual cooling electricity required at different insulation thicknesses incorporated in the wall.

Based on the selected thickness from the parametric studies of the insulation in walls and roof and PCM in the roof, 50 different cases were created to perform the technoeconomic analysis. Table 2 presents all the cases developed and evaluated using different thicknesses of the insulation and PCM in the walls and the roof. The SPP and cooling load for all the cases were calculated and plotted in Fig. 4.

Table 2. The various cases with a combination of different thicknesses of PCM and insulation in the roof and the walls.

|                                   |      | Roof without PCM |         |         |         |         | Roof with PCM (10 mm) |         |         |         |         |
|-----------------------------------|------|------------------|---------|---------|---------|---------|-----------------------|---------|---------|---------|---------|
| Roof insulation \ Wall insulation |      | 0 mm             | 10 mm   | 20 mm   | 50 mm   | 100 mm  | 0 mm                  | 10 mm   | 20 mm   | 50 mm   | 100 mm  |
| 0 mm                              | 0 mm | Base case        | Case 1  | Case 2  | Case 3  | Case 4  | Case 5                | Case 6  | Case 7  | Case 8  | Case 9  |
| 10 mm                             | 0 mm | Case 10          | Case 11 | Case 12 | Case 13 | Case 14 | Case 15               | Case 16 | Case 17 | Case 18 | Case 19 |
| 20 mm                             | 0 mm | Case 20          | Case 21 | Case 22 | Case 23 | Case 24 | Case 25               | Case 26 | Case 27 | Case 28 | Case 29 |
| 50 mm                             | 0 mm | Case 30          | Case 31 | Case 32 | Case 33 | Case 34 | Case 35               | Case 36 | Case 37 | Case 38 | Case 39 |
| 100 mm                            | 0 mm | Case 40          | Case 41 | Case 42 | Case 43 | Case 44 | Case 45               | Case 46 | Case 47 | Case 48 | Case 49 |

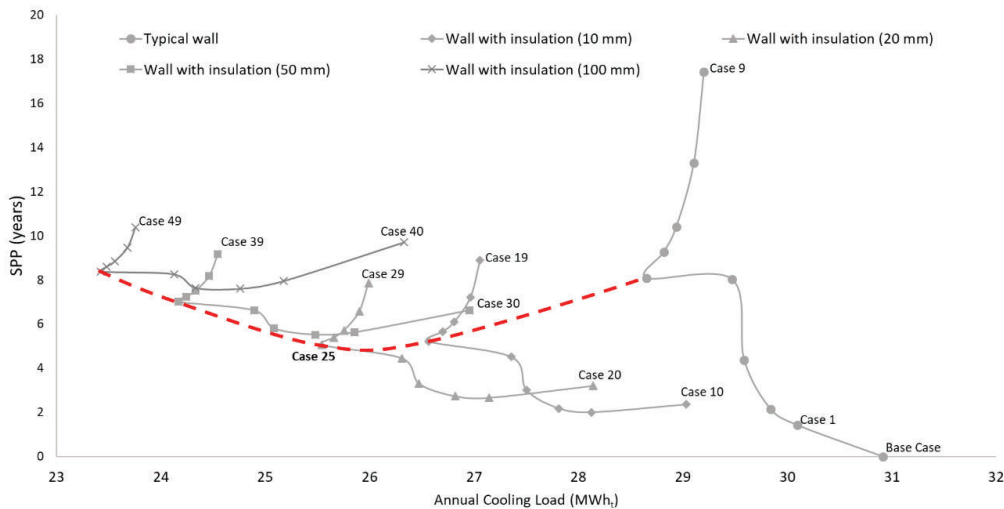


Fig. 4. Optimum case based on the cooling load and payback period (Dashed line connects least cooling load cases of wall with different insulation thickness)

Figure 4 shows that the base case had the highest cooling load, i.e., 31 MWh. The red dashed line connects the cases with minimum cooling load for different thicknesses of wall insulation. Our optimized case would be a case with minimum SPP on the dashed line. Case 25, a roof with 10-mm PCM and walls with 20 mm insulation, was the optimal case, as going to any other point from Case 25 will result in an increase in the cooling load or the SPP. The cooling load for Case 25 was

25.5 MWh, which is 17.3 % less than the base case with a payback period of 5 years.

### 4. Conclusion

In this study, the cooling load of the residential building was reduced by adding a combination of PCM and insulation. Different cases were developed based on the suitable thickness of PCM and insulation in the roof and walls. The main findings are summarized as follows:

- 1) For the roof, the optimum PCM thickness is 10 mm, as a further increase in PCM thickness does not reduce the cooling load. The increase in thickness above 10 mm makes it difficult to undergo a complete cycle of melting and freezing.
- 2) At the same thickness, it was discovered that the thermal performance of insulation in walls performs better than insulation in roofs with an increase in SPP. This is because the wall insulation reduces the overall heat gain of the building as its total surface area is more than the roof.
- 3) A combination of 20 mm wall insulation with 10 mm of PCM in the roof performs best regarding cooling load and SPP. The cooling energy performance index drops by 17.6 % compared to the base case.

The above conclusion was achieved for Mumbai's warm and humid climate conditions but needs to be examined for other climate conditions. In this study, the optimum case was found by calculating the SPP of the initial investment. However, SPP does not account for cash flows after the payback is achieved and treats all cash flows as equivalent. Because of these limitations of SPP, the lifetime energy savings are not considered and may lead to a different optimum case. Therefore, a detailed economic analysis needs to be performed in future work, including the discount rate, inflation rate, and life of the material.

### Conflict of Interest

The authors declare that they have no known competing financial interests or personal relationships that could have appeared to influence the work reported in this paper.

### References

- Arumugam, P., Ramalingam, V., & Vellaichamy, P. (2022). Optimal positioning of phase change material and insulation through numerical investigations to reduce cooling loads in office buildings. *Journal of Energy Storage*, 52, 104946.
- Beemkumar, N., Yuvarajan, D., Arulprakasajothi, M., Ganesan, S., Elangovan, K., & Senthilkumar, G. (2019). Experimental investigation and numerical modeling of room temperature control in buildings by the implementation of phase change material in the roof. *Journal of Solar Energy Engineering*, 142(1), 011011.
- Cell, O. (2019). India cooling action plan. *New Delhi: Ministry of Environment, Forest and Climate Change, Government of India*. Retrieved on January 18, 2024, from <https://aeee.in/wp-content/uploads/2020/10/INDIA-COOLING-ACTION-PLAN-e-circulation-version080319.pdf>
- DesignBuilder. (2022, December 2). *Release software*. Retrieved February 15, 2024, from <https://designbuilder.co.uk/download/release-software>
- EnergyPlus. (2022). *Latest release*. Retrieved February 22, 2024, from <https://energyplus.net/downloads>.
- Global Petrol Price. (2023). Retrieved February 26, 2024, from [https://www.globalpetrolprices.com/India/electricity\\_prices/](https://www.globalpetrolprices.com/India/electricity_prices/)
- Jaganmohan, M. (2024). *Primary energy consumption worldwide in 2022, by country*. Statista. Retrieved February 10, 2024, from <https://www.statista.com/statistics/263455/primary-energy-consumption-of-selected-countries/>

## Analysis of Combined Use of Phase Change Material with Insulation

- Jin, X., Medina, M. A., & Zhang, X. (2016). Numerical analysis for the optimal location of a thin PCM layer in frame walls. *Applied Thermal Engineering*, *103*, 1057–1063.
- Kalbasi, R. (2022). Usefulness of PCM in building applications focusing on envelope heat exchange – Energy saving considering two scenarios. *Sustainable Energy Technologies and Assessments*, *50*, 101848.
- Kalbasi, R., & Afrand, M. (2022). Which one is more effective to add to building envelope: Phase change material, thermal insulation, or their combination to meet zero-carbon-ready buildings? *Journal of Cleaner Production*, *367*, 133032.
- Kaynakli, F. (2023). Thermal insulation thickness optimization based on energy cost for internally insulated walls. *ZeroBuild Journal*, *1*, 30–34.
- Lamrani, B., Johannes, K., & Kuznik, F. (2021). Phase change materials integrated into building walls: An updated review. *Renewable and Sustainable Energy Reviews*, *140*, 110751.
- Li, D., Yang, R., Arıcı, M., Wang, B., Tunçbilek, E., Wu, Y., Liu, C., Ma, Z., & Ma, Y. (2022). Incorporating phase change materials into glazing units for building applications: Current progress and challenges. *Applied Thermal Engineering*, *210*, 118374.
- Mishra, S., Usmani, J., & Varshney S. (2012). Energy saving analysis in building walls through thermal insulation system. *International Journal of Engineering Research and Applications* *2*, 2(5), 128–135.

## Analysis of Combined Use of Phase Change Material with Insulation

Ozel, M., & Pihtili, K. (2007). Optimum location and distribution of insulation layers on building walls with various orientations. *Building and Environment*, 42(8), 3051–3059.

Saxena, R., Rakshit, D., & Kaushik, S. C. (2019). Phase change material (PCM) incorporated bricks for energy conservation in composite climate: A sustainable building solution. *Solar Energy*, 183, 276–284.

Saxena, R., Rakshit, D., & Kaushik, S. C. (2020). Experimental assessment of Phase Change Material (PCM) embedded bricks for passive conditioning in buildings. *Renewable Energy*, 149, 587–599.

Team SHUNYA, IITB. (2023). *U.S. Department of Energy Solar Decathlon*.

Retrieved February 24, 2024, from

<https://www.solardecathlon.gov/event/competition-team-indian-institute-of-technology-bombay.html>



**Integrating Energy Technology and Policy: A New Graduate-Level Course**

Kristin L. Field\*  
Mark Alan Hughes  
Russell J. Composto

## Integrating Energy Technology and Policy Course

As part of a five-year National Science Foundation Research Traineeship (NRT) program, called *Interdisciplinary Training in Data Driven Soft Materials Research and Science Policy*, at the University of Pennsylvania (Penn), we started a new, semester-long (14-week) course. This course, EAS 5110/ENMG 5100, *Societal Grand Challenges at the Interface of Technology and Policy*, is a partnership between Penn's School of Engineering and Applied Science (SEAS) and the Penn Kleinman Center for Energy Policy (KCEP) and is cross-listed as Engineering & Applied Science (EAS) and Energy Management and Policy (ENMG), respectively.

Graduate students are recruited to build a class enrollment where half of the students are pursuing degrees in SEAS or one of the science, technology, engineering, or math (STEM) degrees and the other half are involved with KCEP-related programs (e.g., students pursuing business, law, city planning, design, or social science degrees and/or energy policy certificates in addition to their primary degrees).

This new course is structured around the basics of energy policy and energy technologies and incorporates case studies, pre-class assignments based on readings, small group activities, and student team projects. The class offers an opportunity for STEM students to work with policy students and vice versa. One goal of this course is to have students appreciate that both science and policy are needed to successfully advance climate initiatives.

This course was offered for the first time in Spring 2023 (with 16 students) and for a second time in Spring 2024 (with 15 students). Although having not been co-instructors previously, the teaching team from SEAS and KCEP designed the course with an intentional integration of technology and policy from perspectives across Penn's 12 schools as well as centers and institutes. At the time of the ASES SOLAR 2024 conference, this team was currently teaching the 2024 course and building on instructor and student experiences from 2023. Even after only one year, the instructors have observed the need to continually update the course content because of the rapidly evolving technology and policy landscapes of the energy transition.

### Key Findings

These findings are ongoing. For the course design, it became apparent how different courses from different schools tend to be taught in different ways (e.g., amount and types of course reading materials, types of questions asked of the students, expectations of synthesis of large amounts of material more superficially versus focused, specific understanding of incrementally built knowledge, and student engagement). Learning how to integrate and balance these norms was important for the instructors and for the students.

For the course content, the enormity of topics relevant to the energy transition, even when focusing on those that were rich sources for illustrating the overlap of technology and policy issues, provided opportunities (and challenges). Offering this course once a year around this pool of dynamic topics (e.g., renewable energy, energy storage,

## Integrating Energy Technology and Policy Course

hydrogen economy) also requires a substantial amount of reviewing and updating of the content.

The last general observation is that *process* is a critical component of this type of course that brings together professional graduate students with research-based PhD students from a variety of disciplines. To help promote a collaborative, engaged cultural norm, as well as productive, final group projects that are rewarding for the students, the teaching team continues the intentional mixing of students for in-class small group activities, emphasizes the focus on group-level (rather than individual-level) outcomes as a grading metric, and has refined guidelines and guardrails for final projects. In summary, initial feedback from both STEM and policy students is that this type of interdisciplinary course has impacted how they think about current interests and future career paths.

Keywords: interdisciplinary graduate education, energy transition, energy technology, energy policy, STEM education, climate change

### **Conflict of Interest**

The development and execution of this course are supported by the National Science Foundation under Grant #2152205. Any opinions, findings, and conclusions or recommendations expressed in this material are those of the authors and do not necessarily reflect the views of the National Science Foundation.

**Mobilizing to Support Large-Scale Solar and Storage Goals**

Jill K. Cliburn

Cliburn and Associates, Santa Fe, NM

[jkcliburn@cliburnenergy.com](mailto:jkcliburn@cliburnenergy.com)

## Abstract

Nearly one year since the Inflation Reduction Act supercharged the transformation to clean energy for the U.S., progress in one sector has noticeably lagged: large-scale renewable energy generation and storage. Interest rates and transmission access are partly to blame, but so is the intensity of public opposition to many of these projects. This paper summarizes existing and original research on the roots of this opposition, on their interconnected campaigns and on the role that disinformation plays. It offers an assessment of responses from local or state agencies and from nascent groups of citizens that are beginning to challenge their arguments. It explores an original proposal, drawing on resources of the American Solar Energy Society to create a framework for plain-talk, fact-based outreach, negotiation of community benefits and advocacy to meet solar deployment goals. Considerations for adoption of this proposal and of alternative solutions are included.

Keywords: siting, permitting, disinformation, delays, large-scale solar, utility-scale solar, battery storage, ASES, advocacy, mobilizing

## Introduction: A Need for Outreach and Advocacy

The U.S. Department of Energy (U.S. DOE) goal to achieve 100% decarbonized electricity is unprecedented in its scale and speed. Driven by climate imperatives and supported by the Inflation Reduction Act (IRA), the electricity sector has been challenged to deliver about two terawatts of solar and wind generation by 2035, deploying at a rate that varies by scenario up to eight times faster than at the beginning of this decade, according to the National Renewable Energy Laboratory (NREL) Energy Futures Study (Denholm et al., 2022). According to NREL, an accompanying need for two- to 12-hour energy storage will require even faster growth in deployments than for solar and wind generation.

An assessment of first-year progress towards IRA decarbonization goals showed that progress lags in the deployment of large-scale renewables and storage (Clean Investment in 2023, 2024). Interest rates and transmission access are largely to blame, but so is the intensity of public opposition to many large wind or solar generation and battery projects. A recent survey of developers, led by Berkeley Lab, confirmed that opposition to large-scale solar is “more frequent and more expensive to address than it was five years ago” (Robi et al., 2024). The same study found that permitting challenges and community opposition closely followed grid-interconnection constraints as the top three reasons for large-scale solar- project cancellations.

The early response to rising public opposition to large-scale renewables has included increasing legal and regulatory authority at the federal and state level. Legislation in 13 states takes varying degrees of authority for siting away from local agencies and places it at the state level (Cappelletti & Hanna, 2024). This helps where state governments currently support a clean energy transition, but it poses risks if state or federal policy support shifts against that transition.

Our research on consequences and remedies to local project opposition began with frontline work to understand and address opposition to conditional-use zoning for a 100-MW solar project with a 48-MW (4-hour) battery system, proposed by AES Corp. for a private site near Santa Fe, NM.

In 2023, Cliburn and Associates assessed public comments on that proposal, using artificial intelligence (AI) to spot themes, strategies or likely sources of factual as well as false statements (Cliburn & Adams, 2023). We have continued to document the Santa Fe case study, increasingly motivated to quell disinformation and public opposition that has spilled from the country zoning board into the broader local and state policy landscape. We also have broadened our scope to include a literature review and interviews with local and state agency staff, social science researchers, and citizen-advocates who are working to resolve siting challenges. Some of that research is summarized in the Spring 2024 issue of *Solar Today* in the article “It’s Time to Stand up for Solar” (Cliburn, 2024).

As detailed below, we find that while an academic understanding of this opposition contributes to remedial strategies, their successful execution relies on support from citizens on the ground. Prevailing distrust in experts, misrepresentation of risks, and social media’s immediacy are hard to overcome. Conventional expertise cannot win public support for the clean energy buildout unless it is supported by local envoys. Our proposed solution, building on existing ASES member networks and programs, offers one strong option to deliver on these needs.

## **Research Basis for the Proposed Solution**

### *From General Permitting Guidance to Opposition Research*

The study of opposition to large-scale renewable energy projects is a relatively recent field of research. In 2022, when we began citizen advocacy in relation to a proposed solar and storage project near Santa Fe, NM, one source of information that was often recommended was *Solar@Scale: A Local Government Guidebook for Improving Large-Scale Solar Development Outcomes* (Solar@Scale, 2022). This still-popular guidebook includes many references, but little discussion of local opposition as a source of project delays and cancellations. This is evidenced by only a handful of returns on searches in text and references in the guidebook for terms such as *opposition*, *protest*, or *deny*. Further, it did not anticipate the prevalence of battery storage and associated controversies.

Research teams at institutions such as the University of Michigan, Columbia University, Massachusetts Institute of Technology, University of Minnesota, and Yale University have begun to investigate where assumptions of public support have gone wrong. For example, the paper “Sources of opposition to renewable energy projects in the United States” assessed 53 large-scale renewable energy projects dating back to 2008 and derived seven major sources of opposition (Susskind et al., 2022).

More recent survey-based research (summarized in Figure 1) identifies 14 sources of opposition to large-scale solar and wind, though it can be noted that the veracity of specific complaints was not explored (Nilson et al., 2024).

*Good fences make good neighbors: Stakeholder perspectives on the local benefits and burdens of large-scale solar energy development in the United States* draws on more than 50 interviews of those living near solar energy developments to examine trends in their concerns, satisfaction with outcomes and advice for improving processes (Bessett et al 2024).

Another effort looked at how information about proposed projects emerged and moved via media and informal channels through stakeholder communities (Michaud & Hao, 2023).

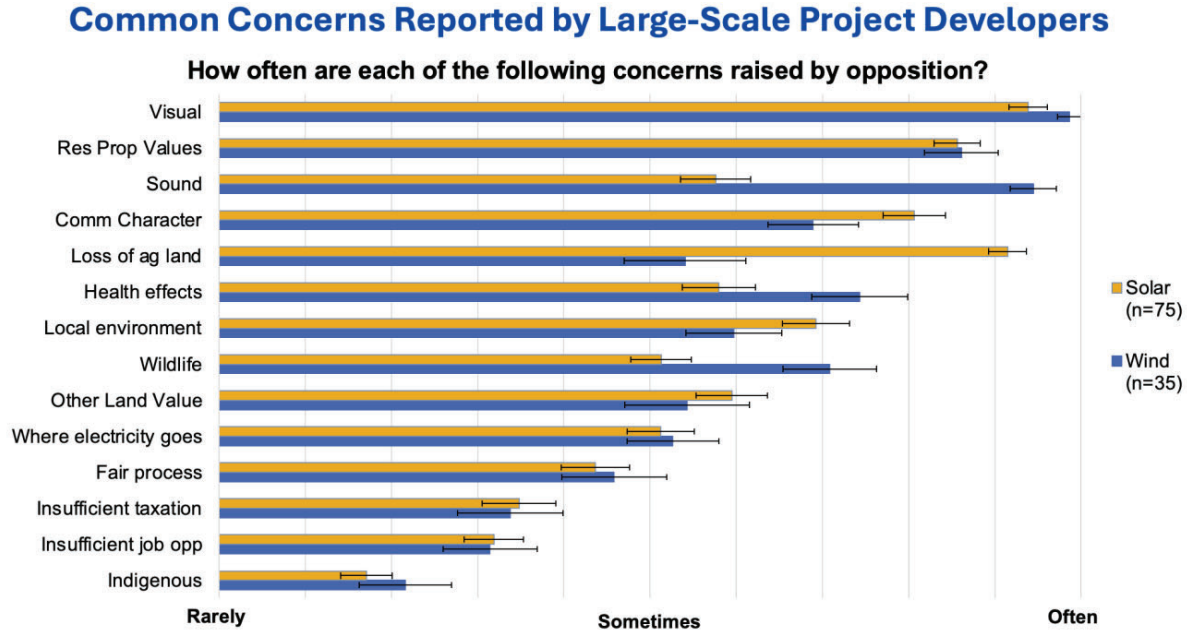
Our own research used online tools, including ChatGPT, to track opposition concerns and map them in relation to project sites, neighborhood characteristics, and specific language used by opposition leaders. Among other findings, we found a strong correlation between disinformation in public comments and specific language offered on opposition websites and in fliers circulated in specific neighborhoods (Cliburn & Adams, 2023).

Across recent research, there is confirmation of the power of disinformation from unconventional sources, ranging from online chats to unsourced video clips posted on social media. The survey of project developers and related professionals cited above indicates that the average cost to a developer of a delay in large-scale solar deployment, often driven by public concerns, is about \$200,000 per megawatt (MW) (Robi et al. 2024).

Industry associations have begun to respond, forming and sponsoring conferences to discuss research and possible solutions. These are led by American Clean Power (ACP) association and institutions such as the Electric Power Research Institute and the U.S. DOE, including Sandia National Laboratories and Berkeley Lab among others. Enterprises, such as the storage division of DNV GL and Wood Mackenzie, as well as some nonprofit organizations, recently began to promote research-based solutions that incorporate public engagement .



Fig. 1. Common concerns reported by 123 survey respondents from about 60 companies engaged in large-scale U.S. solar or wind development. The frequency of a reported concern does not indicate its veracity, but the repetition of concerns can affect public acceptance. (Berkeley, 2024)



*Applied Research for Better Policies, Outreach, and Public Processes*

Some efforts to address permitting and siting outcomes focus on applying research to improve policy, processes, and outreach. One nexus for this work is the U.S. Department of Energy Renewable Energy Siting Through Technical Engagement Program, or R-STEP (Office of Energy Efficiency and Renewable Energy, 2024). This program funds research, technical assistance, and state-based collaboratives. Collaboratives involve state, industry, and local partners, following models first introduced in leading states such as New York and Minnesota. For example, the Clean Energy Resource Teams (CERTs) program in Minnesota involves the state energy office and the historically trusted University of Minnesota Extension among other partners. The CERTs mission is to provide education and tools to local communities to support a swift and equitable energy transition. Much of its work is focused on building stakeholder trust (M. Birch, personal communication, January 25, 2024).

The first round of R-STEP awards, announced in April 2024, have funded programs in Indiana, Iowa, Michigan, Mississippi, North Carolina, South Carolina, and Wisconsin. Each state will emphasize a different set of partners, resources, and information channels, but the focus on fact-based outreach and trust-building is a throughline.

### **Disinformation Messaging and Messengers**

Those who have been on the frontline of local solar and storage development controversies recognize the impact of disinformation. The author has tracked a currently delayed conditional-use zoning process for a project near Santa Fe, New Mexico. Through this effort, we documented misinformation and disinformation about the Santa Fe County project, including in formal and informal comments and — as our research expanded — in reviewing opposition information networks nationwide. We focused on content and processes, avoiding most judgments of credentials. These are fraught, since our society values “out of the box” thinkers and must credit activists from typically excluded classes for many far-reaching societal contributions.

Nevertheless, solar opposition websites typically misapply information from their sources and favor charged language about “industrial solar” from “corporate energy developers” who plan to sell their generation to utilities that will send it (disregarding laws of physics) to cities far away. They often feature dramatic, unsourced photos (e.g., abandoned PV panels and battery fires). Their websites bear confusing names, such as Citizens for Responsible Solar and the Clean Energy Coalition for Santa Fe County.

There are relatively few grassroots organizations or voluntary efforts that focus on building informed grassroots advocacy to counter the opposition. The New York-based United Solar Energy Supporters (USES) provides one example. USES board members and advisors come from solar technical fields, local planning and permitting, project development and communications backgrounds to assist frontline, non-expert volunteers (Cliburn, 2024). By encouraging neighbor-to-neighbor outreach, USES has built public trust and contributed to project approvals. (Scanlon, personal communication, January 5, 2024).

Recognizing the extent of the need for informed advocacy, a nonprofit called Greenlight America recently emerged as “an independent, philanthropically funded nonprofit to support local groups and volunteers who want to get utility-scale clean energy projects built in their communities.” Founders of Greenlight America have political campaign experience. Their expertise and access to industry, labor, and political networks are strong, but at this time they are offset by minimal evidence of an authentic local presence (Greenlight America, n.d.).

The playbook for quelling disinformation and encouraging public engagement has been evolving over decades. The study of research-based behavioral strategies for clean energy adoption that could be used alongside or instead of economic incentives was institutionalized in 2007 with the advent of a biannual Behavior, Energy and Climate Change Conference. This conference is co-sponsored by the American Council for an

Energy-Efficient Economy and programs at Stanford University and the University of California at Berkeley. Archived proceedings sometimes refer to the importance of choosing the right messengers and information channels, as potentially greater than the importance of crafting the right message. Rebuttals to energy disinformation, such as one recent resource from the Sabin Center may not be effective unless strategically delivered (Eisenson et al., 2024). Broad explorations of disinformation techniques, such as the winner of the 2024 Harvard Goldsmith Book Prize, *Foolproof: Why Misinformation Infects Our Minds and How to Build Immunity*, may be helpful in developing any strategic solar advocacy plan (Van der Linden, 2023).

### Research Takeaways That Inform This Proposal

The success of opposition campaigns depends on vulnerable information gaps, misperception of risks, and genuine uneasiness about the pace of change in our technologies and our landscapes. Opposition thrives in an atmosphere of ignorance regarding both the electric grid and the scale of investment needed to transform the energy system. Distrust of utilities, big tech, science, and government or corporate power is a common theme that drives solar and storage disinformation. Calls for delay until “the facts are better known” or for alternative solutions are common.

Expertise is increasing in many fields that can support large-scale solar and storage siting, such as process management, training for planning and zoning officials, and policy development at every level. Yet we are focused on one key gap: the need to identify authentic, local messengers and resources they can use. Efforts to fill this gap are complemented by best practices, such as:

- *Offering proactive outreach about utility-scale battery technology.* The public needs early dialog about the need for battery storage and its performance. This includes understanding the role of field testing and continuous improvement, instead of assuming that lab-perfected solutions can be deployed at some future date.
- *Sharing success stories through social media, testimonials, and public tours.* Those who oppose large-scale projects often circulate outdated or out-of-context information. Timely, relevant examples are needed.
- *Facilitating community dialog.* This may require finding reasonably neutral cosponsors, outside the official permitting processes. Public distrust may extend to local agency staff, officials, or anyone who could profit economically in any way.
- *Promoting negotiation of community benefits agreements, relatively early in the siting process* can be a game-changer. Many solar advocates and local officials do not know about these tools, which may improve outcomes and build local wealth (Eisenson & Webb, 2023).

- *Familiarizing solar advocates with local and state agencies and processes.* This includes encouraging process leaders to involve fire safety and infrastructure officials early and to provide resources to them.

### **ASES: A Model for Mobilizing Effective Citizen Advocacy**

A review of needs and best practices for speeding successful deployment of large-scale solar and storage, as described in this paper, suggests that ASES could play a powerful role. Twenty thousand ASES members nationwide can provide location-specific presence and a core group of potential advocates. ASES membership includes longtime leaders in renewable energy-technology development and deployment, as well as in design, social science research, and policy. About 40 local and student chapters across the U.S. already exist. Membership includes thousands who have used ASES's relationship with the Clean Energy Credit Union to invest in clean energy for their homes and vehicles. All members regularly receive information from ASES, and many participate in at least some of the organization's educational online dialogs, technical divisions, webinars, tours, conferences, and media.

Taken together, ASES members could be described as neighbors; they share the pain of accepting the changes in their communities to achieve a clean energy transition. They often reside in or near communities where large-scale renewable energy developments could change landscapes and economies. Through their involvement in ASES programs, many are primed to support strong community-benefit strategies, while rejecting outright disinformation and injustice. The ASES vision for "a world equitably and sustainably transformed to 100% renewable energy" is generally known across the membership, and the climate's non-negotiable timeline is understood.

Table 1 summarizes three key aspects of a proposal to mobilize ASES membership to help achieve large-scale solar and storage deployment goals. The effort involves establishing partnerships among ASES Solar Envoys and some of the most trusted sources of relevant, research-based technical and policy solutions. Many of these partnerships already exist, for example, through the involvement of scientists in ASES technical divisions, conferences, and publications. These kinds of partnerships are exemplified in the discussion above regarding how USES functions (USES members include members of ASES). Other targeted partnerships include developing ties with the U.S. DOE R-STEP state collaboratives, as well as with like-minded nonprofits.

Most of the ASES resources summarized in Table 1 already exist. For example, the ASES National Solar Tour is a long-time success story. It was expanded and improved in recent years with the option to host tours of community-scale solar projects and to include site videos. The tour is an opportunity to bring the public into contact with large-scale solar success stories and to answer their questions in specific terms.

The addition of a siting resource archive would be one new aspect of the proposed resource package. ASES has ready access to many resources for this archive through its divisions and conferences and through partnerships, as discussed above.

| <b>Hypothetical Mobilization of ASES Membership<br/>to Help Achieve Solar Deployment Goals</b>  |   |
|---|---|
| <p>This proposal for mobilizing membership of the American Solar Energy Society (ASES) is currently hypothetical; yet it exemplifies how strategies to quell misinformation and opposition to large-scale solar and storage could be applied.</p> |   |
| <p><b>Partnerships</b></p>  | <ul style="list-style-type: none"> <li>• ASES Solar Envoys who are volunteers from among the ASES state and student chapters and the 20K+ at-large members. Semi-autonomous in-state groups bring more partners.</li> <li>• DOE Renewable Energy Siting Through Technical Engagement in Planning (R-STEP) program and state grant recipients, including state agencies and nonprofits.</li> <li>• Formal or informal relationships with NREL, Sandia, PPNL, Berkeley Lab, universities and broad-based research centers.</li> <li>• Professional planning associations, associations of counties, etc.</li> <li>• Solar and storage companies, associations and foundations.</li> </ul> |
| <p><b>Resources</b></p>   | <ul style="list-style-type: none"> <li>• ASES Technical Divisions that assist with factual research, strategy and a Solar Envoy training program.</li> <li>• ASES communications, including Solar Today magazine, Solar@work social media, and the National Solar Conference.</li> <li>• The ASES National Solar Tour, which may showcase community and large-scale solar and storage projects, as well as homes.</li> <li>• A new ASES web page that could support curated resources and links to active campaigns and partner resources.</li> </ul>   |
| <p><b>Training, Networking &amp; Evaluation</b></p>   | <ul style="list-style-type: none"> <li>• A Solar Envoy training that would cover topics from grid basics to media literacy, including understanding risk perception, busting solar and storage myths, and community benefit agreements. Technical Divisions and various partners would assist.</li> <li>• ASES communications resources could support peer networking and further their replication.</li> <li>• A “wiki” do-it-yourself database could track successes and setbacks. If funding is secured, the program would set goals for replicating process and policy improvements and would pursue annual evaluation and planning.</li> </ul>                                     |

Table 1. Summary of a proposal for development of a Solar Envoy program option.

Relevant training and informal certification might be valuable for the many ASES members who — like most Americans — have knowledge gaps and misperceptions about the topics that swirl at the center of siting controversies. It is fair to assume that many ASES members would initially oppose large-scale solar development. Large-scale solar does not exemplify the self-sufficiency that many ASES members value; it is, however, a practical necessity for meeting critical climate goals.

ASES training topics might include grid basics, media literacy, understanding risk perception, busting common solar and storage myths, options for community benefit agreements, and local agency process improvements. ASES technical divisions offer expertise that could assist in implementing this training. Training could be offered for a fee to non-members. Network development could motivate “graduating” Solar Envoys to initiate action. A few environmental non-profits, such as Climate Reality Project and Environmental Defense Fund offer examples of how the preparation and support of local envoys could work.

It is beyond the scope of this paper to suggest a budget and funding pathway for this proposed solution. Because the proposal builds on many of ASES’s existing strengths and resources, the budget could be relatively modest. We can think of no other organization that is so prepared for this effort. It has focused on solar energy and related technologies as key to the climate solution, and it has a unique diversity of expert and citizen-science members. There may be opportunities for federal funding or to join various collaborative programs. Private foundations and donors are likely to support the plan. There is also an opportunity for partial, no-cost implementation. For example, expanding the vision for the National Solar Tour could be an option presented to ASES chapters. Interest groups and organizations, such as the Solar and Storage Industries Institute, may be willing to work with ASES chapters to help showcase large projects. It is not advisable for industry to dominate this effort, but it may offer support.

The review of research on improving outreach and siting processes for large-scale solar and storage has led us to suggest this effort, centered at ASES, as a strong response to an urgent need. The timeline for deploying clean energy is inescapable. So is the importance of public engagement to ensure broad-based equity and support energy democracy in this far-reaching energy transition.

### **Conflict of Interest**

The author’s research and preparations for this paper, including related presentations and an op-ed explainer published in *Solar Today* magazine (Spring 2024), were provided by Cliburn and Associates with no direct, external funding. Research contributions to this work by Colter Adams in 2023 was supported in part through an undergraduate research grant from Bodoin College.



## References

- Bessette, D. L., Hoen, B., Rand, J., Hoesch, K., White, J., Mills, S. B., & Nilson, R. (2024). Good fences make good neighbors: Stakeholder perspectives on the local benefits and burdens of large-scale solar energy development in the United States. *Energy Research & Social Science*, 108. <https://doi.org/10.1016/j.erss.2023.103375>
- Cappelletti, J., & Hanna, J. (2024, January 13). States with big climate goals strip local power to block green projects. *Associated Press*. <https://apnews.com/article/wind-solar-energy-projects-local-opposition-eb300574867f53f8abba85127574adc3>
- Clean investment in 2023: Assessing progress in electricity and transport* (2024). Rhodium Group LLC and MIT Center for Energy and Environmental Policy Research. Retrieved from <https://rhg.com/research/clean-investment-in-2023-assessing-progress-in-electricity-and-transport/>
- Cliburn, J. K., & Adams, C., (2023, August 10). The specter of big solar “NIMBY”: Personal encounters and a research-based response. American Solar Energy Society Solar 2023 Conference: Boulder, Colorado.
- Denholm, P., Brown, P., Cole, W., Mai, T., Sergi, B, Brown, M., Jadun, P., Ho, J., Mayernik, J., McMillan, C., & Sreenath, R. (2022). *Examining supply-side options to achieve 100% clean electricity by 2035*. NREL/TP-6A40-81644. National Renewable Energy Laboratory. <https://www.nrel.gov/docs/fy22osti/81644.pdf>

Eisenson, M. (2023). *Opposition to renewable energy facilities in the United States: May 2023*

*Edition*. Sabin Center for Climate Change Law.

[https://scholarship.law.columbia.edu/sabin\\_climate\\_change/200/](https://scholarship.law.columbia.edu/sabin_climate_change/200/)

Eisenson, M., & Webb, R. M. (2023). *Expert insights on best practices for community benefits agreements*. Sabin Center for Climate Change Law.

[https://scholarship.law.columbia.edu/sabin\\_climate\\_change/206/](https://scholarship.law.columbia.edu/sabin_climate_change/206/)

Eisenson, M., Elkin, J., Fitch, A., Ard, M., Sittinger, K., & Lavine, S. (2024). *Rebutting 33 false claims about solar, wind, and electric vehicles*. Sabin Center for Climate Change Law.

[https://scholarship.law.columbia.edu/sabin\\_climate\\_change/217/](https://scholarship.law.columbia.edu/sabin_climate_change/217/)

Greenlight America. (n.d.). <https://www.greenlightamerica.org/>

Michaud, G., & Hao, S. (2023, November 9-11). *Utility-scale solar projects in the rural Midwest:*

*An assessment of knowledge flows and processes*. APPAM 2023 Fall Research

Conference: Atlanta, GA, United States.

Office of Energy Efficiency & Renewable Energy. (2024). *Renewable Energy Siting Through Technical Engagement and Planning (R-STEP)*. U.S. Department of Energy.

<https://www.energy.gov/eere/renewable-energy-siting-through-technical-engagement-and-planning>



Robi, N., Hoen, B., & Rand, J. (2024). *Survey of utility-scale wind and solar developers report*.

Berkeley Lab. <https://emp.lbl.gov/publications/survey-utility-scale-wind-and-solar>

*Solar@Scale: A local government guidebook for improving large-scale solar development outcomes* (2nd ed.). (2022). ICMA and American Planning Association.

<https://icma.org/page/solarscale-guidebook>

Susskind, L., Chun, J., Gant, A., Hodgkins, C., Cohen, J., & Lohmar, S. (2022). Sources of opposition to renewable energy projects in the United States. *Energy Policy*, 165.

<https://doi.org/10.1016/j.enpol.2022.112922>

Van der Linden, S. (2023). *Foolproof: Why misinformation infects our minds and how to build immunity*. W. W. Norton & Company.

**To What Extent Are the United States and Nigeria Able to Balance Economic Growth Against Emission Reduction Goals?**

Bolu Ayankojo  
Old Dominion University  
[bayan001@odu.edu](mailto:bayan001@odu.edu)

## ABSTRACT

The paper examines the link between economic growth and greenhouse gas emissions reduction, focusing on the United States and Nigeria. The study addresses the Nationally Determined Contribution (NDC) targets that ensure average surface temperatures do not exceed 1.5°C above preindustrial levels and are intended to achieve net-zero GHG emissions by 2050. It examines emission reduction strategies in five common sectors: electricity, transportation, industry, cooking, and building. The United States is ahead of Nigeria in achieving its emissions-reduction goals, but challenges persist in some sectors. The study suggests that economic prosperity can be achieved without relying solely on fossil fuels, but Nigeria has yet to establish a clear pathway to overcome these hurdles.

Keywords: greenhouse gas, net zero, United States, Nigeria

### 1. Introduction

Industrialized and developing countries have to balance economic growth against emissions-reduction goals to limit global warming to less than 1.5°C above the preindustrial level (Coopers, 2016, pp. 1-2). Developing countries face different trade-offs between economic growth and emissions reduction due to varying degrees of regional dependence on fossil fuels, differing economic structures, and distinct vulnerabilities to climate change (Ritchie, 2021). Industrialized countries have made significant progress in transitioning away from coal consumption and reducing carbon intensity (Alagidede et al., 2016). Developing countries are vulnerable when it comes to creating policies for growth and emission reductions that are affordable and achieve the set emissions-reduction targets.

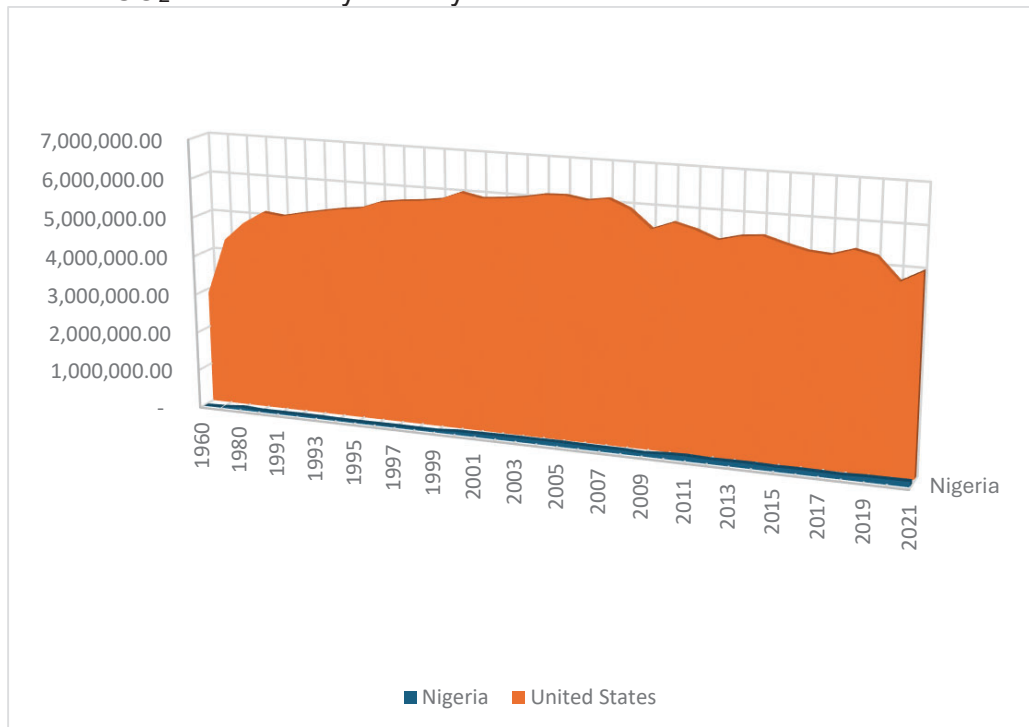
This study aims to evaluate and examine the efforts of the United States (US) and Nigeria to reduce emissions by 2050 and 2060-2070, respectively, by conducting a comprehensive review of secondary data. It reveals that the US has devised a more effective strategy for reducing emissions than Nigeria. This research aims to shed light on the disparities and cooperation between industrialized and developing countries and reveal the crucial role of climate finance in supporting developing countries like Nigeria in achieving net zero objectives. This research aims to assess how well industrialized and developing countries can balance economic growth against emissions reduction goals, focusing on the US and Nigeria.

The US and Nigeria are economic partners with a focus on oil, mining, and investment in sectors like electricity, transport, manufacturing, technology, retail, and tourism (Tai 2022, p. 9). They have substantial trade ties, with the US exporting billions and Nigeria importing millions. However, the two countries have significantly different economic performance (USTR, 2024). CO<sub>2</sub> emissions data from 1960 to 2021 show a significant disparity between the two countries, with the US emissions four times those of Nigeria. Both countries have experienced a reduction in emissions, particularly following their commitments to the Paris Agreement.

## United States and Nigeria Economy and Emissions

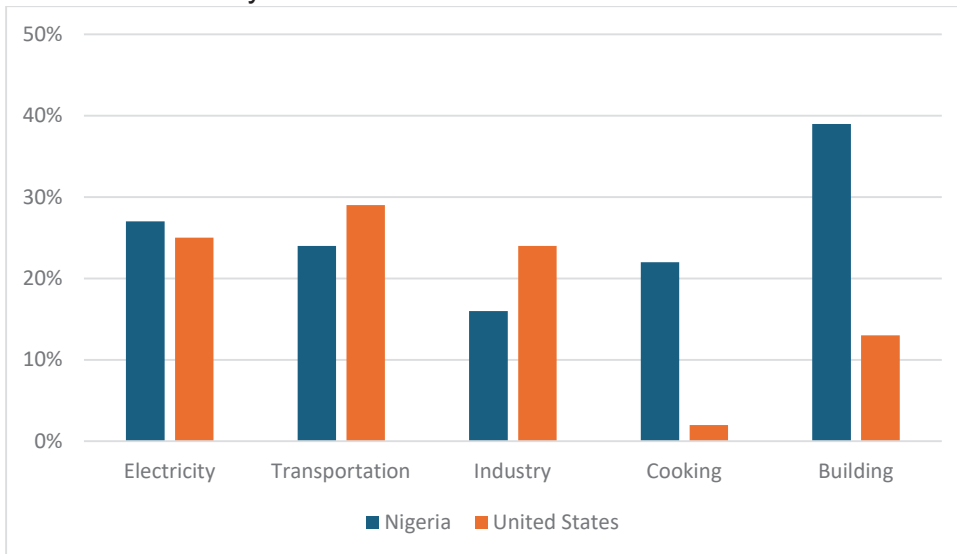
Data for this research was collected from various search engines using words such as “emission reduction”, “greenhouse gas sources”, “country targets”, and “GDP per capita”. The historical trajectory of emissions shows that emissions were relatively low before the Industrial Revolution, with gradual growth until the mid-20th Century. As seen in Fig.1, the US emitted 5.01 billion tons, peaking in the early 2000s, contributing to the global emissions burden. Nigeria emitted less due to unreliable and inadequate national grid electricity supply. Rapid sea level rise in Nigeria could cause erosion, flooding, and migration, among other consequences.

Fig. 1. Annual CO<sub>2</sub> emissions by country



Source: Our World in Data based on the Global Carbon Project (2023).  
[OurWorldInData.org/co2-and-greenhouse-gas-emissions](https://OurWorldInData.org/co2-and-greenhouse-gas-emissions).

Fig. 2. Total Emissions by Sector



Sources: Nigeria energy transition plan. [Energytransition.gov.ng/transport-2-2/](https://energytransition.gov.ng/transport-2-2/); Center for Climate and Energy Solutions. [www.c2es.org](http://www.c2es.org)

## 2. Emission Pledge of the United States and Nigeria

The US aims to reduce emissions by 26% to 28% by 2025, while Nigeria aims to reduce emissions by 45% under specific conditions and achieve a 20% reduction below current levels by 2030. However, ambitious measures are proposed in the National Development Goals and revised National Policy on Climate Change (Dioha & Emodi, 2018, pp. 29-30).

### 2.1. Net zero sectors' strategies

The United Nations Framework Convention on Climate (UNFCCC) Conference of Parties introduced Low-Carbon Development Strategies to reduce GHG emissions. The US has committed to reducing GHG emissions to zero by 2050, including through actions in electricity, transportation, building, industry, and cooking for both short and long-term objectives (Horowitz et al., 2022; Whitehouse, 2021).

#### 2.1.1. US net zero strategies

The US aims to achieve carbon-free electricity by 2035 by incorporating renewables and reducing coal-fired power generation. A 90% clean grid will be achieved by 2035 without new coal plants. From 2005 until 2019, the US marked a 32% decrease in CO<sub>2</sub>

## United States and Nigeria Economy and Emissions

generated (McGrath, 2021). New policies, incentives, and market reforms are essential to meet growing electricity demand (Phadke et al., 2020). Cost reductions in renewable energy generation, batteries, and storage technologies are expected to reduce emissions by 70-90% by 2030. Existing nuclear energy will remain in service, while solar and wind generation will continue to expand until 2050.

The US transportation sector is working to reduce emissions to have half new light-duty cars by 2030, produce 3 billion gallons of sustainable aviation fuel, and reduce costs across all modes of transportation by increasing fuel economy and emissions standards, providing incentives for zero-emission vehicles, expanding biorefineries, and investing in infrastructure to support all clean transportation modes.

The US building sector accounts for US electricity consumption, causing emissions from gas, oil, and other fuels. The goal is to achieve 100% clean power generation by 2035, eliminating emissions and facilitating efficient electrification of building appliances. Partnerships like the EPA's Energy Star program and building energy requirements will enhance efficiency.

The US has seen a significant reduction in space heating GHG emissions due to the widespread use of electric stoves, natural gas, and propane in household cooking appliances (Berrill et al. 2021, p. 6). Cooking accounts for a portion of the overall amount of electricity used by households in the US. 61% of household stoves use electricity, 31% using natural gas, and 5% using propane (Wright et al., 2020, p. 123).

Industries emit GHGs through energy consumption, onsite fossil fuel combustion, and non-CO<sub>2</sub> emissions. Achieving carbon-free electricity by 2035 will eliminate emissions and electrify low- and medium-temperature heat processes. Decarbonization strategies include energy efficiency, electrification, low-carbon fuels, feedstock management, and energy optimization (USDS, 2021, p.17).

### *2.1.2. Nigeria net zero strategies*

Nigeria's Climate Change Act aims for net zero emissions by 2050, with the Renewable Energy Master Plan (REMP) aiming to increase renewable electricity's share from 13.5% in 2015 to 36% by 2030. By 2025, renewable energy will make up 10% of Nigeria's total energy consumption (IEA, 2013). Nigeria's emissions are primarily from electricity, transportation, oil and gas, cooking, and industry, accounting for 65% of the country's total emissions shown in Figure 2 (ETP, 2022, p.2).

Nigeria's energy strategy is the Nigeria electricity vision 30-30-30, which aims to generate 30 GW of electricity by 2030, with 30% coming from renewable sources. This will be done by replacing diesel and petrol generators with sustainable energy sources like solar and wind (Ibrahim et al., 2021, pp. 3-4).

The Nigeria Energy Transition Plan (ETP) places a strong emphasis on reducing transportation emissions, particularly from passenger vehicles, and promotes the use of

## United States and Nigeria Economy and Emissions

low-emission technologies and mode-shifting with a focus on transitioning from gasoline/diesel and hybrid vehicles to electric buses and two- to three-wheelers.

The decarbonization strategy for cooking prioritizes the transition from traditional firewood, charcoal, and kerosene to Liquefied Petroleum Gas by 2030 and the promotion of efficient electricity usage and biogas, particularly in rural areas. Strategies for reducing emissions in the industrial sector include substituting clinker with calcined clay in cement production and reducing its demand by 20% by 2050, adopting bioenergy with carbon capture and storage and replacing grey hydrogen with green and blue hydrogen (Yetano Roche, 2023, p. 3).



## United States and Nigeria Economy and Emissions

Table 1. Net Zero Action Plan

| <b>Sectors</b> | <b>United States</b>   | <b>Nigeria</b>   |
|----------------|--|--|
| Electricity    | Switch to clean fuels through efficient appliances, increase renewable energy use, and decrease coal-fired power through new policies, incentives, and market reforms by 2050. | Expand gas generation capacity by integrating renewable energy. By 2030, solar will be deployed through decentralized deployment in 2040, 2050, and 2060.  |
| Transportation | Achieve dominance of zero-emission vehicle sales by 2030, and alternative modes.   | Use low-emissions technology and mode-shifting, focusing on passenger vehicles by 2030.  |
| Industry       | Adopt low-carbon fuels and feedstocks to reduce emissions by 69-95% by 2050.   | Replace clinker with calcined clay, using bioenergy.   |
| Cooking        | Enhance energy efficiency through increasing sales of clean and efficient electric appliances.   | Transition to liquefied petroleum gas (LPG) from wood, charcoal, and kerosene by 2030.   |
| Building       | Achieve 100% clean power generation in public buildings, government facilities, schools, and universities by 2035 through investment.  | Developers have three ways to ensure building compliance, along with the green star rating system (rated from 1 to 4). Renewable sources are expected to account for 50% of hot water usage in both residential and non-residential buildings. |

The National Building Energy Efficiency Code (BEEC) requires all new buildings to adhere to the 1977 national building regulation for compliance (Lombe, 2017, p. 60). Since 2011, developers have been mandated to choose one of the three compliance route-prescriptive, performance, and reference route which are used for both residential and non-residential buildings. The prescriptive methods targets roof insulation, 50% of the hot water generated from non-electrical resistance heating, fenestration shading, and walls, while performance routes allow buildings to mimic performance and pass regulation using energy simulation to achieve projected energy savings. Nigeria has

adopted the green star rating tool to minimize environmental impact and promote green building standards (Edeoja, & Edeoja, 2015, p. 120). This tool assesses a building adherence to BEEC initiative on a scale of 1-4 stars where higher ratings indicate efficiency in building operations (Lombe, 2017, p. 2).

### 3. Conclusion

The US and Nigeria share a common goal of reducing GHG emissions with strategies that complement each other. They both focus on different strategies. The US uses incentives to encourage cleaner energy adoption and Nigeria focuses on diversifying its energy sources through foreign support. The US and Nigeria's electricity sectors are closely interrelated, as seen in Table 1. The US building sector is actively pursuing a novel approach through extensive research to reduce emissions in the construction industry.

The US leverages its existing regulatory policies and offers various incentives to encourage cleaner energy adoption including financial incentives, tax credits, rebates, and policies related to net metering. This initiative encompasses and targets residential, commercial, government, institutional, and nonprofit entities. Furthermore, 30 states have actively mandated renewable energy requirements, while others have set voluntary goals for renewable energy (NSCL, 2021). And the Rural Energy for America Program (REAP) and low-income communities bonus credit programs provide renewable energy certificates, net metering, and feed-in tariffs to low-income households and rural areas (EIA, 2022). These programs are projected to increase employment opportunities by 2035, contributing to job creation, government revenue, and investment attraction (O'Boyle et al., 2021). These initiatives do not only aim to promote energy efficiency, but also to set up clean electricity guidelines, and attract investments in wind power, solar, and energy storage technologies. Conversely, there is room for improvement in the emissions reduction policy, particularly in the transportation sector, as this may pose a long-term concern while addressing the short-term goals.

Thus, the US transportation sector can examine battery decomposition that usually occurs with EV cars that potentially lead to increased battery combustion which is often associated with GHG emissions over the lifespan of a battery. Further investigation and research are crucial to determine the long-term effects on the economy and the environment. Additional obstacles faced in the transportation sector encompass upfront expenses associated with vehicle acquisition and inadequate charging infrastructure (Phadke et al, 2021). On the other hand, Nigeria's lack of a clear strategy for transitioning to cleaner energy sources is contributing to inequality, poor health, inadequate education, and poverty. Implementation remains uncertain across various ministries with various proposed plans.

Nigeria's emissions strategy aims to diversify energy sources, including hydropower (2111 MW), solar energy (19 MW), biofuels (10 MW), and wind (3 MW). The country's potential to generate more biogas from 227,500 tons of animal waste could improve

electricity supply (Olanipekun & Adedokun, 2020; Posibi, 2023; Kazimierczuk, 2019). The transportation sector is shifting toward electric vehicles and biofuel-based cars. It is expected that by 2030, 20% of private cars will be biofuel-based cars, and this percentage is expected to increase to 25% by 2050 for the market share for vehicles fueled by biofuel. This transition is expected to yield substantial benefits with a projected adoption rate of 10% for private cars and 35% for taxis by 2030 and 2050 respectively (IRENA, 2023, p. 13). The government encourages renewable energy investments through fiscal and market incentives under the REMP, aiming to create up to 840,000 net jobs by 2060.

Nigeria's electricity sector faces significant challenges, with its population of 213 million currently receiving about 7,200 megawatts of electricity, resulting in a significant gap between demand and supply (Monyei et al., 2018, p. 1583). Nigeria's transition to clean energy relies on foreign investors, donors, and climate funding, and the transportation sector is targeting the adoption of electric vehicles by 2050, which is expected to reduce CO<sub>2</sub> and boost GDP. However, attracting investors has been slow, and incentives and energy tax reductions have not attracted private and local investors. The reduction in emissions is expected to generate new job opportunities, while the oil and gas sector may experience job losses. A comprehensive database to track renewable energy investments and prioritize clean fuels from solar, wind, carbon-free hydrogen, and sustainable biofuels could enhance efficiency, which would be a significant step toward a sustainable future and Nigeria's goal to achieve net zero emissions by 2060.

### **Conflict of Interest**

The author did not receive funding, grant, or other support from any organization for the submitted work.

## References

- Alagidede, P., Adu, G., & Frimpong, P. B., (2016). The effect of climate change on economic growth: evidence from Sub-Saharan Africa. *Environment Economic Policy Studies*. 18, 417–436. URL: <https://doi.org/10.1007/s10018-015-0116-3>
- Berrill, P., Gillingham, K. T., & Hertwich, E. G. (2021). Drivers of change in US residential energy consumption and greenhouse gas emissions, 1990–2015. *Environmental Research Letters*, 16(3), 034045. URL: [10.1088/1748-9326/abe325](https://doi.org/10.1088/1748-9326/abe325)
- Center for Climate and Energy Solutions (2024). *Energy/emission data: US emissions*. URL: <http://c2es.org/>
- Coopers, P. (2016). *The Paris Agreement: A turning point? The low carbon economy index 2016*. Pricewaterhousecoopers. URL: <https://www.pwc.com/ee/et/publications/pub/low-carbon-economy-index-2016.pdf>
- Dioha, M. O., & Emodi, N. V. (2018). Energy-climate dilemma in Nigeria: Options for the future. In *IAEE Energy Forum*, 2, 29-32. URL: [https://www.researchgate.net/profile/Nnaemeka-Emodi-2/publication/323830158\\_Energy-Climate\\_Dilemma\\_in\\_Nigeria\\_Options\\_for\\_the\\_Future/links/5aad28b0a6fdcc1bc0bad5af/Energy-Climate-Dilemma-in-Nigeria-Options-for-the-Future.pdf](https://www.researchgate.net/profile/Nnaemeka-Emodi-2/publication/323830158_Energy-Climate_Dilemma_in_Nigeria_Options_for_the_Future/links/5aad28b0a6fdcc1bc0bad5af/Energy-Climate-Dilemma-in-Nigeria-Options-for-the-Future.pdf)
- Edeoja, J. A., & Edeoja, A. O. (2015). Carbon emission management in the construction industry – Case studies of the Nigerian construction industry. *American Journal of Engineering Research*, 4(7), 112-122. URL: <https://api.semanticscholar.org/CorpusID:112014491>

- Energy Information Administration (EIA) (2022). *Renewable energy explained Incentive: Renewable energy requirements and incentives*. U.S. Energy Information Administration. URL: [https://www.eia.gov/energyexplained/renewable-sources/incentives.php#:~:text=Government%20financial%20incentives&text=The%20federal%20tax%20incentives%2C%20or,%2DRecovery%20System%20\(MACRS\)](https://www.eia.gov/energyexplained/renewable-sources/incentives.php#:~:text=Government%20financial%20incentives&text=The%20federal%20tax%20incentives%2C%20or,%2DRecovery%20System%20(MACRS).).
- Energy Transition Plan (ETP) (2022). *Investing in Nigeria's energy transition opportunity*. URL: <https://www.energytransition.gov.ng/wp-content/uploads/2022/05/Investing-in-Nigeria-Energy-Transition.pdf>
- Horowitz, R., Binsted, M., Browning, M., Fawcett, A., Henly, C., Hultman, N., McFarland, J., & McJeon, H. (2022). The energy system transformation needed to achieve the US long-term strategy. *Joule*, 6(7), 1357-1362 <https://www.cell.com/action/showPdf?pii=S2542-4351%2822%2900251-3>
- International Energy Agency (IEA) (2013). *Nigeria renewable energy master plan*. IEA/IRENA Policy and Measures Database. <https://www.iea.org/policies/4974-nigeria-renewable-energy-master-plan>
- Ibrahim, I. D., Hamam, Y., Alayli, Y., Jamiru, T., Sadiku, E. R., Kupolati, W. K., Ndambuki, J. M., & Eze, A. A. (2021). A review on Africa energy supply through renewable energy production: Nigeria, Cameroon, Ghana, and South Africa as a case study. *Energy Strategy Reviews*, 38, 100740. <https://doi.org/10.1016/j.esr.2021.100740>
- IRENA (2023). *Renewable energy roadmap: Nigeria*. International Renewable Energy Agency, Abu Dhabi. [https://www.irena.org/-/media/Files/IRENA/Agency/Publication/2023/Jan/IRENA\\_REMap\\_Nigeria\\_2023.pdf](https://www.irena.org/-/media/Files/IRENA/Agency/Publication/2023/Jan/IRENA_REMap_Nigeria_2023.pdf)

- Kazimierczuk, A. H. (2019). Wind energy in Kenya: A status and policy framework review. *Renewable and Sustainable Energy Reviews*, 107, 434-445. URL: <https://doi.org/10.1016/j.rser.2018.12.061>
- Lombe, C., (2017). Development of the National Building Energy Efficiency Code. *Federal Ministry of Power, Works, and Housing (Housing Sector)*. URL: [https://worksandhousing.gov.ng/themes/front\\_end\\_themes\\_01/images/download/1510059611415.pdf](https://worksandhousing.gov.ng/themes/front_end_themes_01/images/download/1510059611415.pdf)
- McGrath, G. (2021). *Electric power sector CO<sub>2</sub> emissions drop as generation mix shifts from coal to natural gas*. US Energy Information Administration. URL: <https://www.eia.gov/todayinenergy/detail.php?id=48296>
- Monyei, C. G., Adewumi, A. O., Obolo, M. O., & Sajou, B. (2018). Nigeria's energy poverty: Insights and implications for smart policies and framework towards a smart Nigeria electricity network. *Renewable and Sustainable Energy Reviews*, 81, 1582-1601. URL: <https://doi.org/10.1016/j.rser.2017.05.237>
- NSCL (2021). *State renewable portfolio standards and goals*. National Conference of State Legislatures. <https://www.ncsl.org/energy/state-renewable-portfolio-standards-and-goals>
- O'Boyle, M., Baldwin, S., Spengeman, S., Mcnair, T., Phadke, G. A., Abhyankar, N., & Paliwal, U. (2021). *A national clean electricity standard to benefit all Americans*. Energy and Innovation Policy and Technology. <https://energyinnovation.org/wp-content/uploads/2021/04/A-National-Clean-Electricity-Standard-to-Benefit-All-Americans.pdf>

Olanipekun, B. A., & Adelokun, N. O. (2020). Assessment of renewable energy in Nigeria: challenges and benefits. *International Journal of Engineering Trends and Technology (IJETT)*. 68. <http://dx.doi.org/10.2139/ssrn.3568592>

Our World in Data (2023). *Annual CO<sub>2</sub> emissions*. <http://OurWorldInData.org/co2-and-greenhouse-gas-emissions>

Phadke, A., Paliwal, U., Abhyankar, N., McNair, T., Paulos, B., & O'Connell, R. (2020). *Plummeting solar, wind, and battery costs can accelerate our clean electricity future*. Goldman School of Public Policy. <http://www.2035report.com/wp-content/uploads/2020/06/2035-Report.pdf?hsCtaTracking=8a85e9ea-4ed3-4ec0-b4c6-906934306ddb%7Cc68c2ac2-1db0-4d1c-82a1-65ef4daaf6c1>

Phadke, A., Abhyankar, N., Kersey, J., McNair, T., Paliwal, U., Wooley, D., Ashmoore, O., Orvis, O., O'Boyle, M., O'Connell, R., Agwan, U., Mohanty, R., Sreedharan, P., and Rajagopal, D. (2021). *2035 transport*. University of California, Berkeley. <https://www.2035report.com/transportation/>

Ritchie, H., (2021). *Many countries have decoupled economic growth from CO<sub>2</sub> emissions, even if we take offshored production into account*. <https://ourworldindata.org/co2-gdp-decoupling>

Tai, K. (2022). *Biennial report on the implementation of the African growth and opportunity act*. United States Trade Representative. URL: <https://ustr.gov/sites/default/files/files/reports/2022/2022AGOImplementationReport.pdf>

## United States and Nigeria Economy and Emissions

US Department of State (USDS) (2021). *U.S. relations with Nigeria: Bilateral relations fact sheet Bureau of African Affairs*. <https://www.state.gov/u-s-relations-with-nigeria/>

US Trade Representative (USTR) (2024). *Nigeria trade & investment summary*.  
<https://ustr.gov/countries-regions/africa/nigeria>

U.S. Energy Information Administration (EIA) (2022). *What is U.S. electricity generation by energy source?*  
<https://www.eia.gov/tools/faqs/faq.php?id=427&t=3#:~:text=About%2060%25%20of%20this%20electricity,was%20from%20renewable%20energy%20sources>

Wright, C., Sathre, R., & Buluswar, S. (2020). The global challenge of clean cooking systems. *Food Security*, 12(6), 1219-1240. <https://doi.org/10.1007/s12571-020-01061-8>

Yetano Roche, M. (2023). Built for net-zero: Analysis of long-term greenhouse gas emission pathways for the Nigerian cement sector. *Journal of Cleaner Production*, 383, 135446.  
<https://doi.org/10.1016/j.jclepro.2022.135446>



**What Is the Future of Photovoltaics in the Electrification of Africa?**

Moses S Bass<sup>1</sup>

Zita Ngagoum Ndalloka<sup>2</sup>

1 Department of Physics, Rúa Xosé María Suárez Núñez, s/n. (Campus Vida)  
Universidade de Santiago de Compostela ,15782, Santiago de Compostela, Spain

2 Department of Electrical and Computer Engineering, University of Massachusetts  
Lowell, USA

Corresponding author: [mosessbass@gmail.com](mailto:mosessbass@gmail.com)

## ABSTRACT

This paper examines the current state of electrification and photovoltaics in Africa, shedding light on existing challenges and opportunities for solar energy. With a focus on PV technology, we aim to contribute to the discourse on energy access in Africa and stimulate the interest of policymakers and the global solar industry. We underscore the imperative of prioritizing renewable energy investments to breach the electrification gap in Africa, where 567 million people are still living without energy access. Considering the huge potential for the application of PV technology in Africa due to solar resource availability and PV technology maturity, we therefore call on African governments to boost investments in solar PV, to subsidize PV systems and their installations, and to particularly put in place clear policies and regulations to allow both utility companies and private solar energy service providers a level playing ground.

Keywords: electricity, solar energy, photovoltaic, Africa, renewables

## Introduction

The potential of solar energy, particularly through photovoltaic (PV) technology, to power the African continent is immense. In this paper, we aim to explore this potential by examining the current landscape of electrification and photovoltaics in Africa. Our goal is to contribute to the discourse on PV adoption in Africa, urging policymakers to prioritize its advancement and encouraging global solar industry intervention to enhance universal electricity access in Africa in the near future.

Despite significant progress in global electrification rates over the past decade, millions of people, particularly in the global South, still lack access to electricity. Between 2010 and 2021, the global electrification rate improved from 84% to 91%. However, a staggering 675 million people worldwide remain without electricity, with 567 million residing in sub-Saharan Africa alone (IEA, IRENA, UNSD, World Bank, & WHO, 2023). Without substantial changes, Africa is poised to continue grappling with limited electricity access, especially considering its rapidly growing population of 1.3 billion people. By 2050, Africa's population is expected to reach 2.5 billion people (IRENA & AfDB, 2022).

The International Energy Agency (IEA) emphasizes the necessity of increased investments and policy support mechanisms to bridge the electricity access gap in Africa. Without such actions, millions will still lack electricity access by 2030, the target year for achieving the Sustainable Development Goals (SDGs). SDG 7 is centered on

ensuring universal access to modern energy that is affordable, reliable and sustainable, but Africa still has a long way to go in achieving this goal.

As the world's second most populous continent, Africa is projected by the IEA to require a total installed capacity of energy of 510 GW by 2030 to meet its rising power needs (IEA, 2022). Renewable energy sources are expected to dominate this capacity, with solar photovoltaics alone accounting for 125 GW (IEA, 2022). Previous research has already shown renewable energy is suitable for Africa's energy transformation, as it is both low-cost and climate-compatible (Oyewo et al., 2022). Despite solar energy and photovoltaic technology being proclaimed as pivotal for breaking the energy poverty cycle in Africa, PV's total installed capacity on the continent in 2021 represented only 1% of the global total (IEA, 2022). Over the past decade, Africa installed 10.4 GW of solar capacity, with the majority being PV and this total is only about 8% of the projected required capacity by 2030 (IRENA & ADB, 2022). What then needs to be done from now on to accelerate the contributions of solar energy in the electrification of Africa?

Illustrated in Figure 1 is the present electrification rate achieved in each of the 54 African countries. It ranges from 8% (lowest) to 100% (highest). While almost all North African countries have achieved universal electrification, the majority of sub-Saharan Africa still grapples with low electricity access rates. Libya is the exception, with 70% electricity access. In Sub-Saharan Africa, on the other hand, the island nations of Mauritius and Seychelles are the only two to have attained 100% electrification. Very low electricity access rates can be observed in countries like South Sudan, Burundi, and Chad, which have only managed to attain 8%, 10%, and 11% respectively. In total, 21 countries in Sub-Saharan Africa have less than 50% electricity access. This is concerning and risks failing to meet the universal access target set for 2030 by the United Nations.

Disparities in electricity access levels in Sub-Saharan Africa can be attributed to various factors, including energy resource availability, economic strength, and energy planning efficacy. The present electricity system in most parts of the African continent is untenable for any meaningful development. For this reason, electrification needs to be prioritized and be made sufficient to cater for present and future needs.

## Photovoltaics in the Electrification of Africa

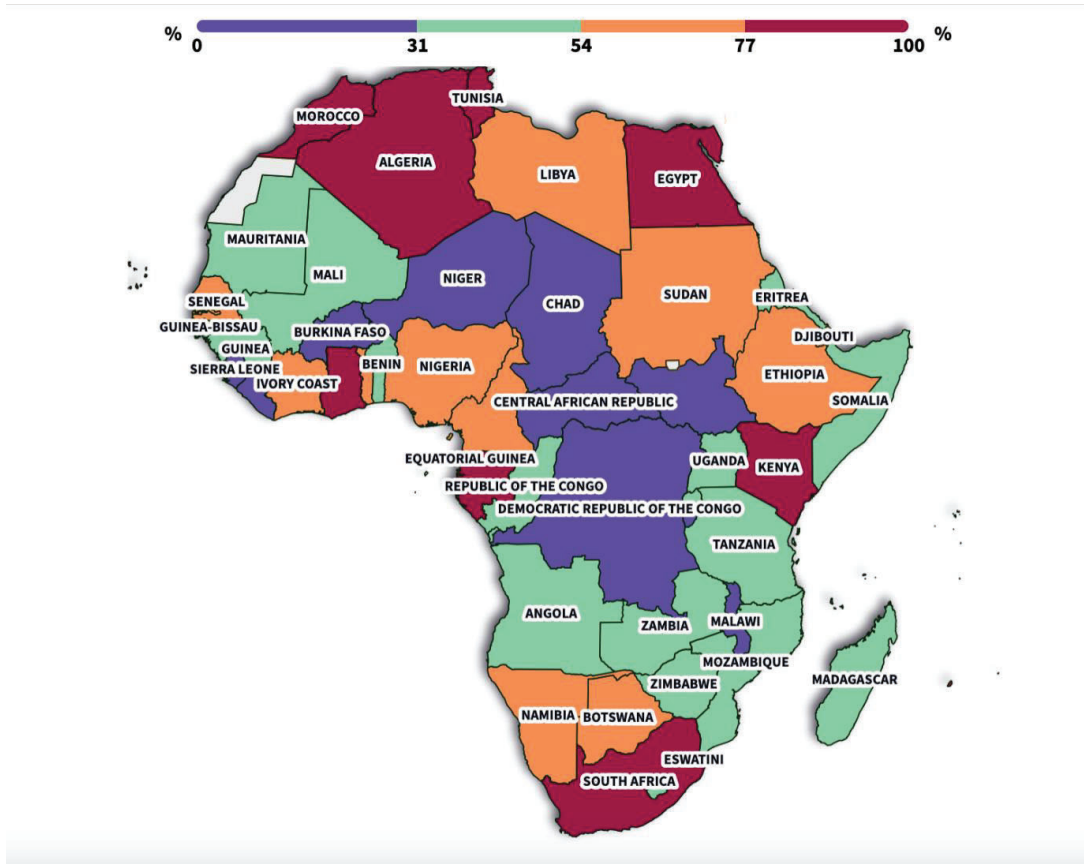


Fig. 1. Access to electricity in Africa by country in 2021.

For Africa to achieve SDG7 by 2030 and boost growth for its over one billion people through the emergence of numerous economic opportunities, more investments in renewable energy capacity will be required to break the current fossil fuel dominance in its electricity mix. Gas and coal are presently large components of the African electricity generation mix, respectively comprising 40.27% and 27.14% of electricity generation capacity in 2021 according to data from Ember. Expanding the utilization of Africa's renewable energy resources will be a game changer, especially for solar energy. The next sections provide details on the solar energy potential in the African continent and the performance of solar energy in electrification within Africa and across regions between 2017 and 2021.

### Solar Energy Potential in Africa

Africa has 60% of the world's best solar resources, with an estimated average annual solar irradiation of 2,119 kilowatt-hours per square meter (kWh/m<sup>2</sup>) (IEA, 2022; IRENA and AfDB, 2022). However, due to the continent's diverse geographical attributes,

## Photovoltaics in the Electrification of Africa

solar irradiation levels vary across regions as shown in Figure 2. Countries in the west, north, and south typically receive an annual average irradiation of around 2,100 kWh/m<sup>2</sup>, whereas those in the east and central regions receive less, averaging below 1,800 kWh/m<sup>2</sup> annually. Despite this variability, Africa's technical solar potential is estimated at a staggering 7,900 GW. What is yet utilized is approximately 1%.

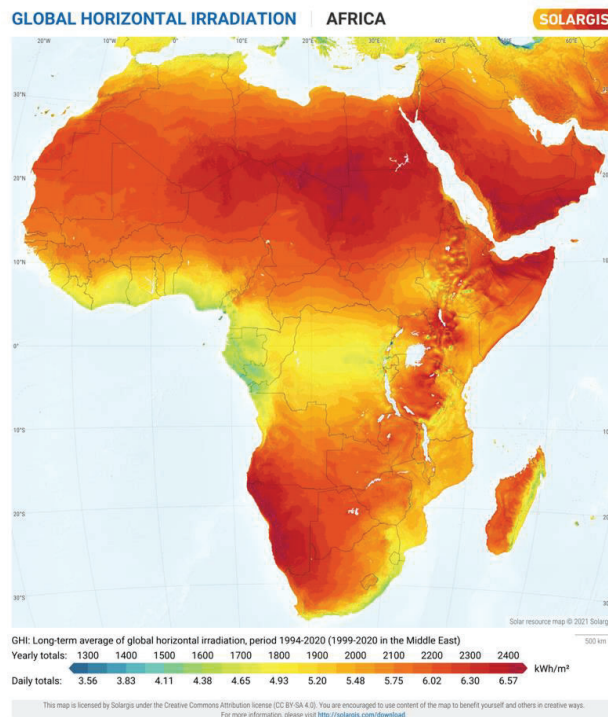


Fig. 2. Global Horizontal Solar Irradiation in Africa. (Solargis, 2021)

Despite this immense potential, the contribution of solar energy to electrification remains low in Africa when compared to other parts of the world. Figure 3 provides a comparative analysis of solar energy contributions to electricity generation globally across regions from 2017 to 2021. Only 2% of the electricity generated in Africa came from solar energy in 2021 while it was 4% in China, the United States and India respectively. The European Union (EU) had the largest share of 6% in the same year. More effort is required from Africa, since it faces the greatest electrification challenge. Africa taking advantage of its rich solar resource is a necessary step forward. Over the period from 2000 to 2021, the share of solar energy in the world's electricity mix has experienced significant growth, rising from 1.1 TWh to 1,284 TWh. Africa should

therefore take advantage of the growing trend toward solar energy, particularly through the deployment of photovoltaics.

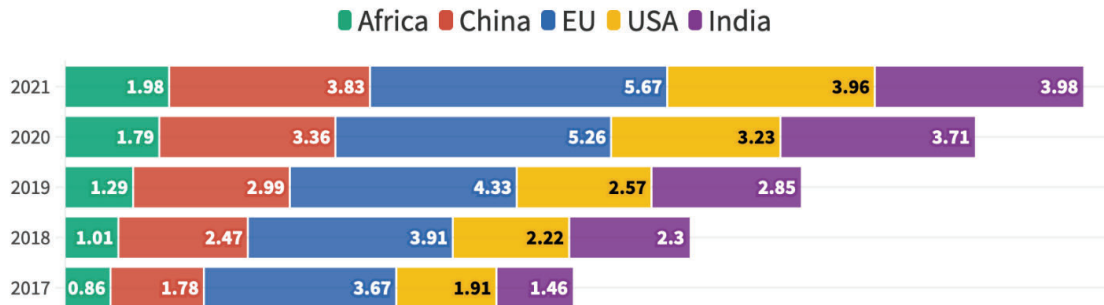


Fig. 3. Percentage share of solar energy in electricity generation across five regions (2017-2021)

### Photovoltaics (PV) Technology

Among the various technologies for converting solar energy into electricity, photovoltaics (PV) stand out as one of the most economically and technically viable options. Years of research and development have led to significant improvements in PV efficiency and cost reduction, contributing to the rapid increase in PV installations worldwide. Over 90% of the global PV market consists of crystalline silicon (c-Si) (Heath et al., 2020, p. 1). The capacity of PV has experienced remarkable growth, rising from 1.4 gigawatts (GW) in the year 2000 to 512 GW by 2018 (Heath et al., 2020, p. 1). As of 2022, the global installed capacity of solar energy has further surged to 1,185 GW, underscoring the increasing importance and adoption of PV technology in meeting global energy needs (REN21, 2023).

Despite the global rise in PV adoption rates, Africa lags behind in installed capacity, accounting for just 1% of the global total. Recent data indicates that the continent currently has 261 operational solar farms, with capacities ranging from 1 megawatt, 95 under construction, and a further 195 announced (Global Energy Monitor., 2024). PV technology has helped bridge the electrification gap in Africa and has the potential to do more if action from policymakers and industry practitioners intensifies. Several African countries have expanded electricity access through mini-grids and solar home systems. According to the International Energy Agency, more than half of the electricity expansion in sub-Saharan Africa in 2022 was due to solar home systems. Moving forward in the race to achieve universal electricity access by 2030 and beyond, there is still more to be done. Figure 4 compares the renewable electricity (RE) targets by 2030 to the electricity generated from solar in 2021 in nine countries in sub-Saharan Africa.

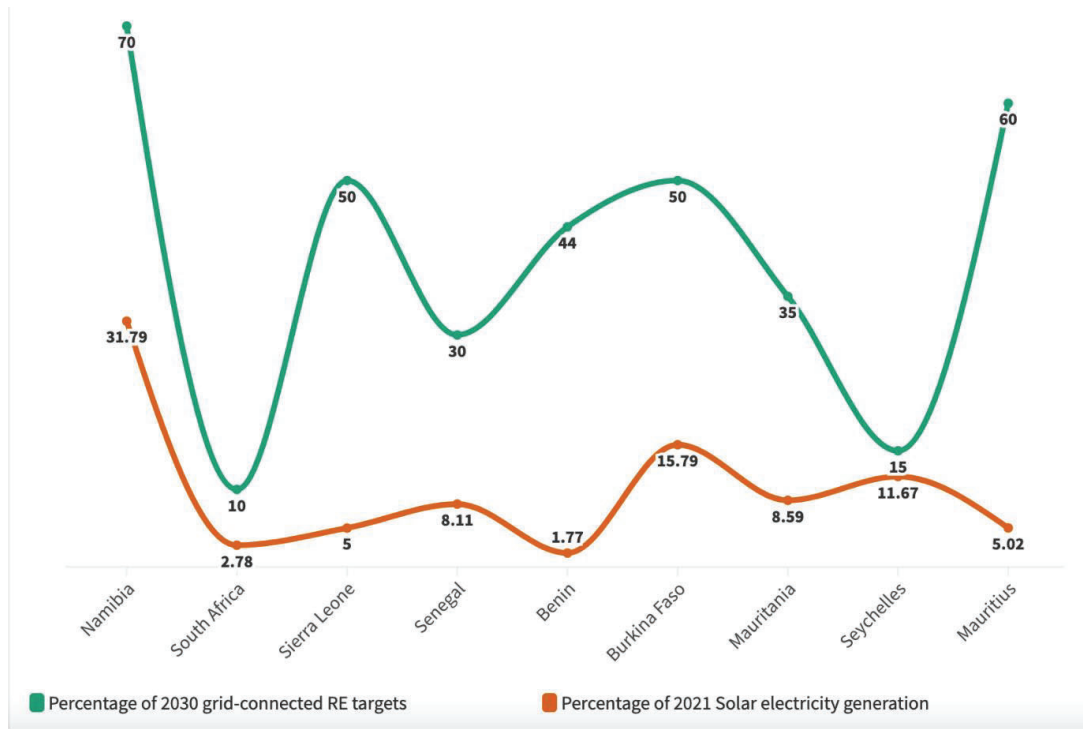


Fig. 4. Renewable electricity targets and solar electricity generation in Africa.

A great disparity exists between the RE targets and the electricity generated from solar in the nine countries compared. An exception is Seychelles, which is close to achieving its target. Solar electricity is quite minimal in Africa, and this is evident even in South Africa, which has the largest solar capacity installed in Africa, yet produces just about 3% of its electricity from solar. Namibia is commendable for generating the largest share of solar electricity in Africa in 2021. For clarity, almost all the African countries not included in Figure 4 produce about 1% or less of electricity from solar. Given this unfortunate situation, urgent action is therefore needed in tackling the electrification challenge in Africa with photovoltaics. We provide the following recommendations toward that goal.

### Policy Recommendations

1. African governments should boost investments in solar PV to upscale its role in electricity generation. This can be done by providing prevailing policy instruments that have worked in countries or regions with thriving solar markets, especially China and the European Union.



2. The total cost of installing a solar system need to be subsidized within African countries to encourage widespread adoption of PV technology. While there is evidence of the falling prices of PV panels, the cost remains a challenge and therefore requires curtailment to reduce the burden on the customers.
3. Establish clear policies and regulations to provide a level playing field for both utility companies and private solar investors to avoid conflicts and uncertainties in electricity service provisions. This can prevent conflicts over customers and create room for coordinated electricity service provision.
4. Local manufacturing of solar photovoltaics should be focused on the first- and second-generation PV technologies (Si-based and thin film, respectively), given their maturity. Third-generation technologies are yet to be commercialized and may not be appropriate for the African context.
5. African countries should initiate discussions around PV recycling, adopting favorable policies that will enhance the development of PV recycling companies to avert a PV waste challenge soon.

### **Conclusion**

Africa has a huge solar potential for various PV applications including floating, off-grid, and utility-scale installations. To achieve the various African RE targets by 2030 and accomplish 100% electrification, African countries must enhance their commitment to the development and installation of RE projects over the continent in the next few years. Furthermore, efforts need to be intensified by all stakeholders within and outside Africa. Just as put forward by (Oyewo et al., 2022), a renewable future for Africa will require strong institutional support, regional cooperation as well as the strengthening of systematic innovation.

### **Conflict of Interest**

This research did not receive any specific funding, and the authors declare no conflict of interest.

### **Acknowledgments**



This work utilized data from Ember and employed Flourish for visualizing electrification in Africa and the percentage share of solar energy, specifically in Figures 1, 3, and 4.

## REFERENCES

- Heath, G. A., Silverman, T. J., Kempe, M., Deceglie, M., Ravikumar, D., Remo, T., Cui, H., Sinha, P., Libby, C., Shaw, S., Komoto, K., Wambach, K., Butler, E., Barnes, T., & Wade, A. (2020). Research and development priorities for silicon photovoltaic module recycling to support a circular economy. *Nature Energy*, 5(7)10.1038/s41560-020-0645-2
- IEA. (2022). *AfricaEnergyOutlook2022*. <https://www.iea.org/reports/africa-energy-outlook-2022>
- IEA, IRENA, UNSD, World Bank, & WHO. (2023). *Tracking SDG7: The energy progress report*. Washington DC: World Bank. <https://trackingsdg7.esmap.org/data/files/download-documents/sdg7-report2023-full-report.pdf>
- IRENA and ADB. (2022). *Renewable energy market analysis: Africa and its regions*. International Renewable Energy Agency and African Development Bank.
- Oyewo, A. S., Bogdanov, D., Aghahosseini, A., Mensah, T. N. O., & Breyer, C. (2022). *Contextualizing the scope, scale, and speed of energy pathways toward sustainable development in Africa*.
- REN21. (2023). *Renewables 2023 global status report collection, global overview*. REN21 Secretariat.
- Global Energy Monitor. (2024). *Solar Farm Phase Count by Region*. <https://globalenergymonitor.org/projects/global-solar-power-tracker/>
- Solargis. (2021). *Global Horizontal Solar Irradiation in Africa*. [Map]. Solargis. <https://solargis.com>

**Firm-Dispatchable Power and Its Requirement in a Power System Based on  
Variable Generation**

Stephen R. Clark\*  
Craig McGregor

Department of Mechanical and Mechatronic Engineering, Stellenbosch University,  
Stellenbosch, South Africa\*

[Sclark@sun.ac.za](mailto:Sclark@sun.ac.za)

### Abstract

Many countries have commenced a transition from fossil fuel-based electricity generation systems to sustainable systems based on wind and solar generation. It is often noted that the least-cost approach would involve a massive scale-up in variable renewables supported by battery storage and gas-peaking plants. However, the requirement is for firm-dispatchable generation rather than peaking power. Firm-dispatchable power is not defined, and the specific requirements are poorly understood. This study seeks to define firm-dispatchable power in this context and its requirement in the sustainable generation system. The study compares 100% renewable generation scenarios from South Africa, Texas, and the United Kingdom (UK) to demonstrate the requirement for this firm-dispatchable generation. The results indicate that firm-dispatchable generation must be available for all three systems to completely back up the variable generation. The installed capacity for this firm-dispatchable generation does not vary with the distinct demand profiles of the different locations or their comparative renewable generation profiles. It also does not change significantly with the amount of storage. The annual energy required from this firm-dispatchable generation varies due to its use's comparative economics, but the required installed capacity does not change.

**Keywords:** variable generation, peaking power, firm-dispatchable power

### Introduction

The transition from fossil fuel-based electricity generation systems to sustainable systems based on wind and solar generation is a significant step toward meeting international greenhouse gas emission reduction targets. Most countries have also recognized that these systems have a lower cost than maintaining conventional fossil fuel-based systems.

It has been noted in South Africa and elsewhere that the least-cost approach would involve a massive scale-up in variable renewables supported by battery storage and gas-peaking plants (Creamer, 2023; Roy et al., 2020). Rather than peaking power, firm-dispatchable power must be available to fill shortfalls when these renewable sources do not meet the demand. However, "firm-dispatchable power" is not defined, and its specific requirements are poorly understood. This study aims to define firm-dispatchable power in this context and its requirement in the sustainable generation system.

### Background

A traditional fossil fuel-based electricity generation system consists of a combination of baseload, load following, and peaking power plants, with each source serving as a firm supply source. Thermal power plants, including fossil-fuelled, nuclear-fuelled, geothermal, and biofuel plants, generally have high capital and low fuel costs. Compared to peaking plants, thermal plants are slower to ramp up and down, making

them less suitable for backup power for low-cost systems based on wind and solar generation (Kumar et al., 2012).

The variability of wind and solar generation is a significant concern for generation systems, leading to the need for a rapid ramp-up of peaking power (Jain, 2023; Roy et al., 2020). This can be achieved through energy storage mechanisms such as battery electric storage, pumped hydro, compressed air storage, and other options (Spector, 2019; Teske et al., 2016). However, these systems have limitations, as their costs are generally energy-based rather than power-based, such as batteries, where the capital cost is related to the number of MWh of energy stored rather than the MW of power that can be generated. For longer-term use (days or weeks), additional units for each added usage period quickly increase costs (Cole & Frazier, 2019).

The terms peaking, dispatchable power, and firm power are often discussed in the energy literature (Enel, 2023; University of Calgary, 2023; US EIA, 2023b). While there does not appear to be any discussion of the concept of firm-dispatchable power in the literature, combining the accepted definitions for firm and dispatchable generation would give the following definition for the term in the context of a system based on wind and solar generation.

**Firm-dispatchable power is generating capacity (to replace the wind and solar sources completely) that is always available, that can be turned on or off or can adjust its power output according to market need.**

Generation sources such as combustion engines, turbines, and fuel cell generators can meet these needs with ample flexibility on fuel types, including fossil fuels, biofuels and green hydrogen (Siemens, 2020; Wartsila, 2023). Fuel cell plants are currently more expensive but are expected to approach the cost of engines or turbines in the future (Papageorgopoulos, 2019).

In a generation system based primarily on variable sources, the firm-dispatchable generation must always guarantee the ability to meet demand. In South Africa, dispatchable generation requirements can last for several days at certain times of the year in a typical year (Clark et al., 2022). As shown in Figure 1, this firm-dispatchable power must provide nearly all the needed generation for four to five days. Without this generation, the grid would collapse. The long demand period for this firm-dispatchable generation makes it impossible to address using only peaking generation, storage, or demand management.

Reports from Germany, the UK, the U.S., and Australia indicate similar periods where firm-dispatchable power is required to provide most of the generation for some period in typical years (Baraniuk, 2018; Brower, 2016; Runyon, 2018; Wert et al., 2023). In some worst-case scenarios, firm-dispatchable generation could be needed for several weeks to handle "droughts" in wind and solar generation (The Royal Society, 2023). The required characteristics for this generation source include quick ramp-up and ramp-down, availability to be economically used for as long or short as needed, and large installed capacities.

## Firm-Dispatchable Power and Variable Generation

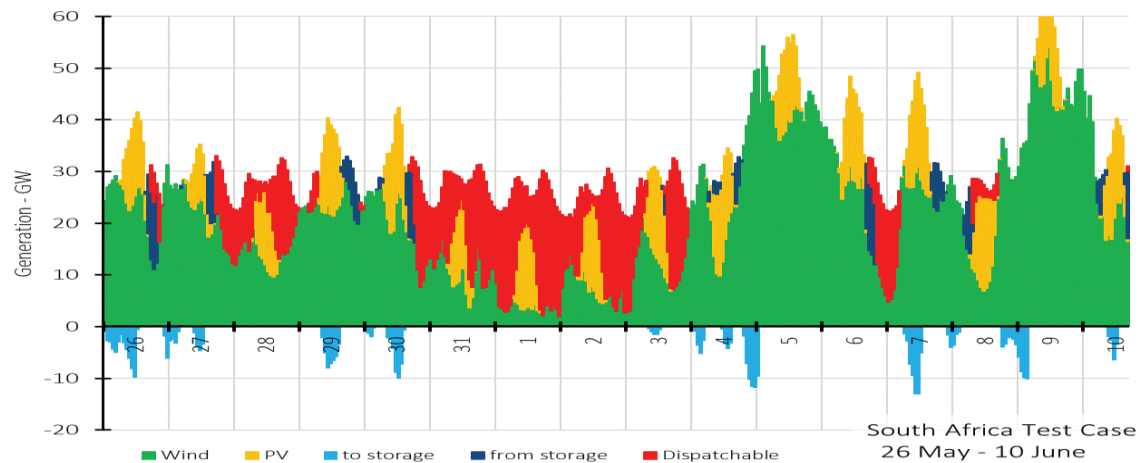


Fig. 1. This is a snapshot of the model output showing the South Africa test case defining the shortfall based on 2019 data.

### Firm-Dispatchable Energy Requirement

The analysis presented here focuses on firm-dispatchable generation requirements for balancing power systems based on variable wind and solar sources. The analysis uses hypothetical scenarios based on wind and solar with no baseload generation to demonstrate the need for firm-dispatchable power. Energy storage is considered a part of the lowest-cost mix of generation sources.

This analysis compares the cost of firm-dispatchable generation, solar generation, wind resources, and battery storage in these three systems based on publicly available data from 2022 for Texas, the UK, and 2019 for South Africa (Elexon, 2023; ERCOT, 2023).

As indicated in Table 1, the South Africa test case shows that with these assumptions, the model indicates that the system is balanced at the lowest cost with installed wind at 188% of peak demand and solar PV at 70%. The analysis indicates that firm-dispatchable generation must be installed to meet at least 109% of the average demand and 84% of the peak demand to balance the system when the variable sources do not meet the demand.

The overall demand for firm-dispatchable energy generation in the South African system is 8% of the overall energy generation in the lowest-cost scenario. It is possible to build more wind and solar generation and add more storage from batteries or other technologies to reduce the amount of firm-dispatchable energy required. However, this comes at an increased cost to the overall system with no impact on the required installed firm-dispatchable generation capacity.

Comparing the situation in South Africa with international experience is vital to understanding how the situation compares with other systems. Two examples fit the criteria for comparison in size and isolation: Texas and the UK. At 431 TWh per year demand, the Texas ERCOT grid is 187% the size of the South African Eskom network. The UK National Grid is the same size as the Eskom grid, with a net demand of approximately 230 TWh of electricity per year. In all three scenarios, wind resources

## Firm-Dispatchable Power and Variable Generation

must be built significantly more than peak demand, with solar PV making a lesser contribution. Battery energy storage also makes similar contributions in South Africa and Texas but adds almost no value to the UK system.

### **Analysis Parameters**

To assess the firm-dispatchable generation requirements in renewable-heavy electricity systems, this study modelled hourly electricity supply and demand scenarios for three regions: South Africa (Eskom), Texas (ERCOT), and the United Kingdom (National Grid). The analysis utilized historical hourly demand profiles from 2019 (South Africa) and 2022 (Texas and UK), combined with historical hourly wind and solar generation data from the same years (Elexon, 2023; ERCOT, 2023; Eskom, 2019).

Several renewable energy deployment scenarios were developed for each region by scaling historical wind and solar generation to various assumed installed capacities based on historical capacity factors. The model then calculated the required firm-dispatchable generation installed capacities and hourly dispatch to ensure supply meets demand for every hour in each scenario, assuming no other generation sources. The model aimed to minimize overall system costs, considering installation and generation costs for renewables, energy storage, and firm-dispatchable plants.

Costing for least-cost cases was based on National Renewable Energy Laboratory (NREL) 2040 forecasts: wind – 1200 USD/kW, PV – 1000 USD/kW, and dispatchable generation – 800 USD/kW. The NREL forecast of 200 USD/kWh for energy storage was used for base cases, with tests for lower-cost energy storage, as discussed in the following section (NREL, 2023).

Several sensitivity analyses were conducted to assess the impact on firm-dispatchable generation requirements, including scenarios with very low-cost energy storage. The results, presented in the following tables and figures, provide insights into the capacity and utilization of firm-dispatchable plants needed to complement renewable-dominant electricity systems in each region.

## Firm-Dispatchable Power and Variable Generation

Table 1. Test Cases Summary Information

|  | <b>South<br/>Africa-<br/>Eskom</b> | <b>Texas -<br/>ERCOT</b> | <b>UK – NG</b> | Units                         |
|--|------------------------------------|--------------------------|----------------|-------------------------------|
| <b>Current Parameters based on 2022</b>                        |                                    |                          |                |                               |
| Annual Demand  | 231                                | 431                      | 230            | TWh                           |
| Peak Rate  | 34                                 | 80                       | 43             | GW                            |
| Average Rate   | 26                                 | 49                       | 26             | GW                            |
| <b>Lowest-Cost Case Parameters with no Baseload Generation</b> |                                    |                          |                |                               |
| Installed Wind   | 64                                 | 130                      | 95             | GW                            |
| Wind Energy  | 204                                | 392                      | 256            | TWh                           |
| Wind CF (1)  | 36                                 | 34                       | 31             | %                             |
| Wind Percent of Peak Capacity                                  | <b>188</b>                         | <b>163</b>               | <b>220</b>     | Percent of Peak Gen. Capacity |
| Installed PV   | 24                                 | 63                       | 5              | GW                            |
| PV Energy  | 54                                 | 129                      | 4              | TWh                           |
| PV CF (1)  | 26                                 | 23                       | 9              | %                             |
| PV Percent of Peak Capacity                                    | <b>70</b>                          | <b>79</b>                | <b>11</b>      | Percent of Peak Gen. Capacity |
| Battery Capacity   | <b>13</b>                          | <b>14</b>                | <b>0</b>       | GW                            |
| Battery Hours  | 4                                  | 4                        | 0              | Hours                         |
|  |                                    |                          |                |                               |
| Installed Dispatch   | 29                                 | 58                       | 30             | GW                            |
| Dispatch Energy  | 21                                 | 45                       | 51             | TWh                           |
| <b>Dispatchable Generation Parameters for Lowest-Cost Case</b> |                                    |                          |                |                               |
| Dispatch CF (1)  | 8.6                                | 8.9                      | 19.3           | %                             |
| % Peak demand  | 84                                 | 73                       | 68             | %                             |
| % Average demand   | <b>109</b>                         | <b>118</b>               | <b>110</b>     | % <sup>1</sup>                |

<sup>1</sup> CF refers to the capacity factor, that is the actual energy output divided by the energy output that would be produced if operated at its rated output for the entire year.

## Firm-Dispatchable Power and Variable Generation

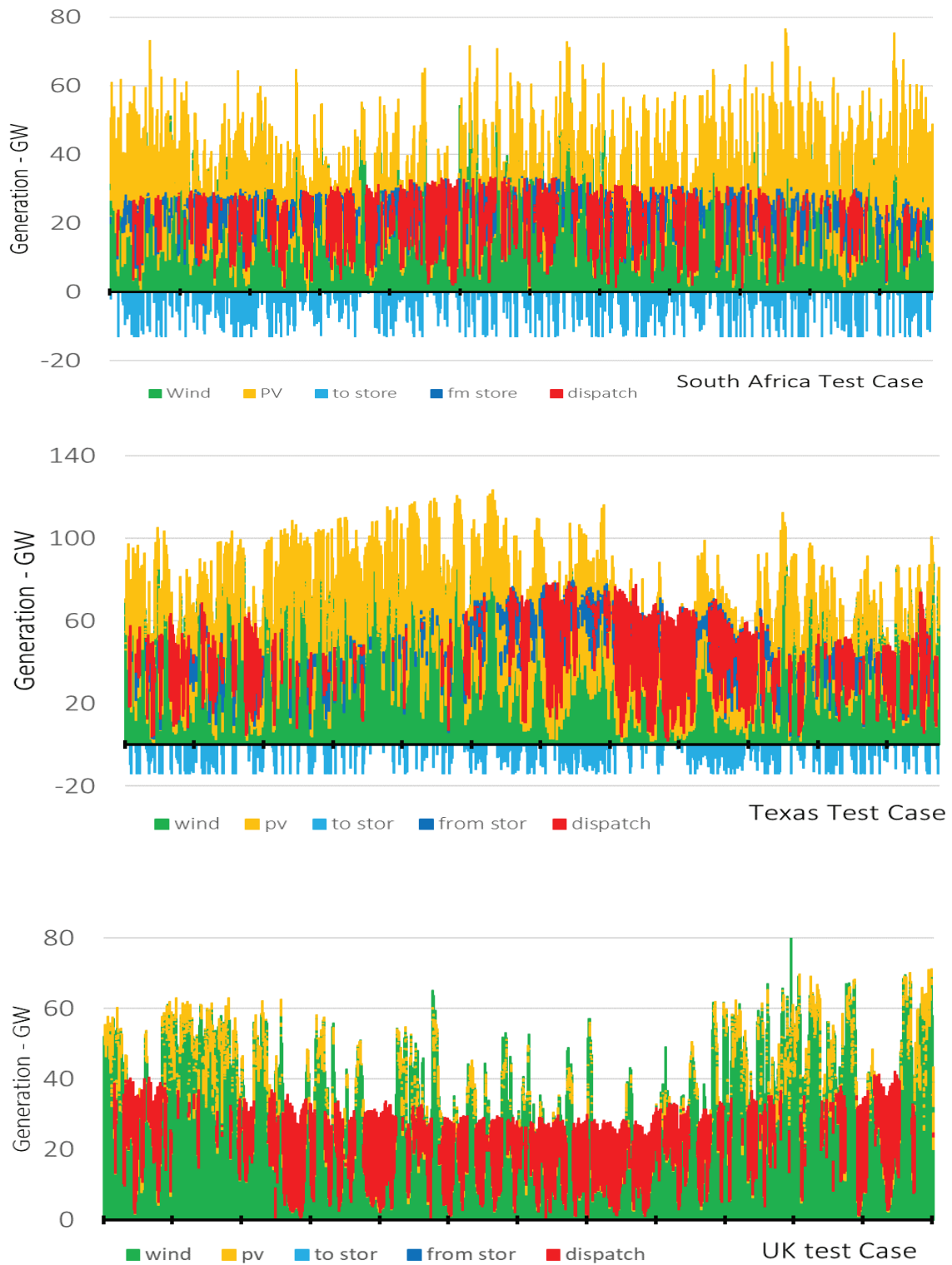


Fig. 2. These are annual summaries of the model output showing the base case test results.



## Firm-Dispatchable Power and Variable Generation

While each regions has distinct demand and renewable generation profiles, the three systems have similar requirements for firm-dispatchable generation. Based on annual average demand, the required installed capacity ranges from 109% for South Africa to 110% in the UK and 118% for Texas. The usage factor for the dispatchable generation for South Africa and Texas was slightly below 9%, and the UK factor was 19% for the lowest-cost scenario. The three comparison cases all show similar requirements for firm-dispatchable power in proportion to the amount of wind and solar generation.

The cost of storage is one of the significant unknown factors, and it is expected to decrease significantly in the coming years (Goldie-Scot, 2019; Rao, 2021). There is the possibility that the requirement for firm-dispatchable generation might be affected or eliminated with low-cost storage. Test cases were run for storage costs as low as 10 USD/kWh. With this extremely low storage cost, the amount of dispatchable energy generated has been significantly reduced, as shown in Table 2 and Figure 3. However, even though the amount of energy provided by the firm-dispatchable generation is minimized, there was no reduction in the required installed capacity.

Table 2. Low-cost test cases summary information

|   | South Africa-<br>Eskom | Texas -<br>ERCOT | UK – NG | units |
|---|------------------------|------------------|---------|-------|
| <b>Lowest Cost Case Parameters with no Baseload Generation and Very Low Storage Cost</b>  |                        |                  |         |       |
| Installed Wind  | 66                     | 122              | 102     | GW    |
| Installed PV  | 26                     | 73               | 4       | GW    |
| Battery Capacity  | 27                     | 55               | 67      | GW    |
| Battery Hours   | 24                     | 35               | 21      | Hours |
| <b>Dispatchable Generation Parameters for Lowest Cost Case with Very Low Storage Cost</b> |                        |                  |         |       |
| Installed Dispatch  | 29                     | 51               | 30      | GW    |
| Dispatch Energy   | 7                      | 16               | 27      | TWh   |
| Dispatch CF   | 2.6                    | 3.7              | 10.4    | %     |
| % Peak demand   | 84                     | 63               | 68      | %     |
| % Average demand  | 109                    | 104              | 110     | %     |

### Firm-Dispatchable Power and Variable Generation

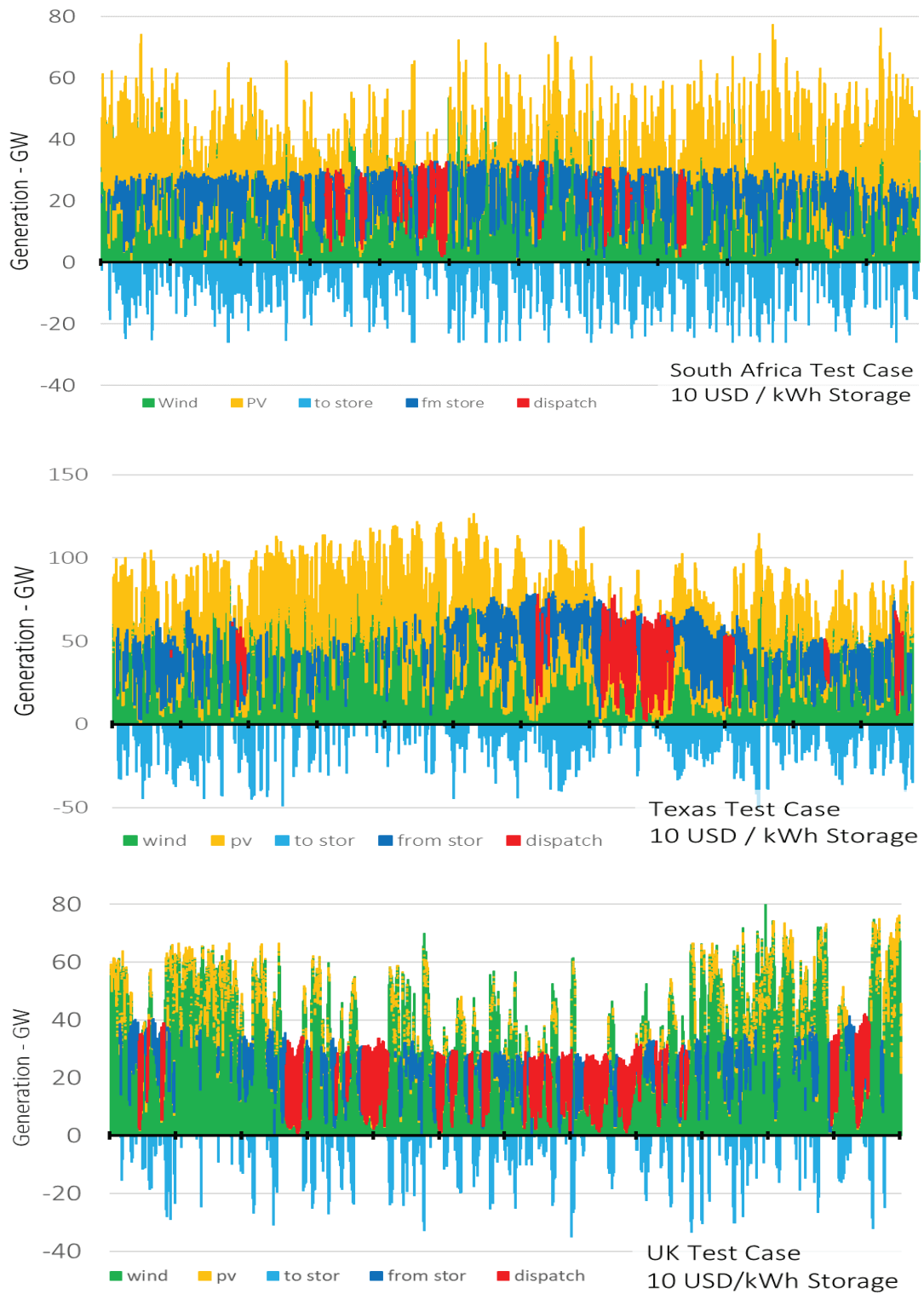


Fig. 3. These are the annual summaries of the model results for the low-cost storage test cases.

### **Cost Impact of Firm-Dispatchable Generation**

The US Energy Information Agency estimates that onshore wind and solar PV are the lowest-cost generation sources, with levelized costs of energy (LCOE) of 40 USD/MWh and 36 USD/MWh, respectively (EIA, 2023a). Firm-dispatchable generation is often argued to be expensive, but it does not significantly add to the cost of a wind and solar-based system if correctly implemented. The cost of installing the required generation capacity and providing electricity from the installed capacity must be considered. According to the modelling results for each of the three scenarios, installing the required firm-dispatchable generation would add approximately 14 USD/MWh to the overall system tariff, with a use cost of approximately 100 to 200 USD/MWh for the firm-dispatchable generation, depending on fuel price. The high energy production cost would limit the use of this generation source.

When decision-makers consider implementing a dispatchable generation program, the topic of fuel choice is often discussed. However, with minimal usage of the firm-dispatchable generation, fuel choice has a lower cost impact than the installation cost. Fuel costs are the cost of fuel delivered to the generator, including transport and seasonal storage at the plant in volumes sufficient to be able to meet the demand for several days (Clark et al., 2022). Generators based on combustion engines or turbines can use many types of fuels, both hydrocarbons such as natural gas, LPG or diesel and those from renewable sources such as biofuels and hydrogen in all its forms and derivatives (Siemens, 2020; Wartsila, 2023). The fuel choice can also change over time as costs and other considerations change.

### **Results**

Scenarios have been tested for the three markets with an assumed nominal 100% supply from wind and solar resources. Installed backup generation is required to meet approximately 110% of the average annual demand in all cases. The firm-dispatchable generation must be available to meet most of the peak demand. The usage of this installed firm-dispatchable generation capacity varies significantly depending on wind, solar, and storage costs.

In conclusion, a generation system based on wind and solar is the cheapest way to achieve a sustainable and low-carbon generation system. However, provision must be made for the firm-dispatchable generation to completely replace the variable supply from wind and solar for days to weeks as needed.

### **Conflict of Interest**

This work was supported by the Strategic Fund of Stellenbosch University through the Hydrogen Engineering Research Platform. The authors appreciate and thank Stellenbosch University for its commitment to advancing sustainable hydrogen technologies.

## References

- Baraniuk, C. (2018). Weird 'wind drought' means Britain's turbines are at a standstill. *New Scientist*. <https://www.newscientist.com/article/2174262-weird-wind-drought-means-britains-turbines-are-at-a-standstill>
- Brower, M. (2016). The North American 'Wind Drought': Is it the new normal? *Renewables*. <https://aws-dewi.ul.com/the-north-american-wind-drought/>
- Clark, S., van Niekerk, J., Petrie, J., & McGregor, C. (2022). The role of natural gas in facilitating the transition to renewable electricity generation in South Africa. *Journal of Energy in Southern Africa*, 33(3), 22–35. <https://doi.org/10.17159/2413-3051/2022/v33i3a8362>
- Cole, W., & Frazier, A. W. (2019). *Cost Projections for Utility Scale Battery Storage Cost*. <https://www.nrel.gov/docs/fy19osti/73222.pdf>
- Creamer, T. (2023). Least-cost foundation. *Engineering News*. <https://www.engineeringnews.co.za/>
- Elexon. (2023). *BMRS*. <https://www.bmreports.com/bmrs/?q=eds/main>
- Enel. (2023). *What Is a Peaking Power Plant?* <https://www.enelnorthamerica.com/insights/blogs/what-is-a-peaking-power-plant>
- ERCOT. (2023). *2022 Wind and Solar Generation*. <https://eur03.safelinks.protection.outlook.com/?url=https%3A%2F%2Fwww.ercot.com%2Fmisdownload%2Fservlets%2FmirDownload%3FdoclookupId%3D890277261&data=05%7C01%7C%7C7cdb41bb68d540b0092c08dbcc9b8b2e%7Ca6fa3b030a>

[3c42588433a120dffcd348%7C0%7C0%7C63832874121846](https://doi.org/10.52202/077496-0026)

- Eskom. (2019). *Renewables January 2015 - December 2019 (incl Sere) (Public Release)*. <https://www.eskom.co.za/dataportal/data-request-form/>
- Goldie-Scot, L. (2019). *A Behind the Scenes Take on Lithium-ion Battery Prices*. BNEF. <https://about.bnef.com/blog/behind-scenes-take-lithium-ion-battery-prices/>
- Jain, P. (2023). India needs to ramp up power system flexibility to meet 450GW renewable energy target. In *IEEFA*. <https://ieefa.org/resources/india-needs-ramp-power-system-flexibility-meet-450gw-renewable-energy-target>
- Kumar, N., Besuner, P., Lefton, S., Agan, D., & Hilleman, D. (2012). *Power plant cycling costs*. <https://doi.org/10.2172/1046269>
- Papageorgopoulos, D. (2019). *Fuel cell R & D overview*. [https://www.hydrogen.energy.gov/pdfs/review19/plenary\\_fuel\\_cell\\_papageorgopoulos\\_2019.pdf](https://www.hydrogen.energy.gov/pdfs/review19/plenary_fuel_cell_papageorgopoulos_2019.pdf)
- Rao, R. (2021). *Chart: behind the three-decade collapse of lithium-ion battery costs cheap lithium-ion batteries now dominate consumer electronics; look out, auto industry*. IEEE Spectrum. <https://spectrum.ieee.org/chart-behind-the-three-decade-collapse-of-lithium-ion-battery-costs>
- Roy, S., Sinha, P., & Shah, S. I. (2020). Assessing the techno-economics and environmental attributes of utility-scale PV with battery energy storage systems (PVS) compared to conventional gas peakers for providing firm capacity in California. *Energies*. <https://www.mdpi.com/1996->

[1073/13/2/488?type=check\\_update&version=2](https://doi.org/10.52202/077496-0026)

Runyon, J. (2018). European wind operators face wind drought while solar power production. *Renewable Energy World*, 1–18.

<https://www.renewableenergyworld.com/2018/08/14/european-wind-operators-face-wind-drought-while-solar-power-production-rises/#gref>

Siemens. (2020). *Siemens gas turbine portfolio*.

<https://assets.new.siemens.com/siemens/assets/api/uuid:10f4860b140b2456f05d32629d8d758dc00bcc30/gas-turbines-siemens-interactive.pdf>

Spector, J. (2019). *The biggest batteries coming soon to a grid near you*.

<https://www.greentechmedia.com/articles/read/the-biggest-batteries-coming-soon-to-a-grid-near-you>

Teske, S., Leung, J., Crespo, L., Bial, M., Dufour, E., Richter, C., & Rochon, E. (2016). Solar thermal electricity - Global Outlook 2016. In *European Solar Thermal Electricity Association, Greenpeace International and SolarPACES*.

The Royal Society. (2023). *Large-scale electricity storage*. <https://royalsociety.org/-/media/policy/projects/large-scale-electricity-storage/Large-scale-electricity-storage-report.pdf>

University of Calgary. (2023). Dispatchable source of electricity. In *Energy Education*. [https://energyeducation.ca/encyclopedia/Dispatchable\\_source\\_of\\_electricity](https://energyeducation.ca/encyclopedia/Dispatchable_source_of_electricity)

US EIA. (2023a). *Cost and performance characteristics of new generating technologies, annual energy outlook 2023*.

[https://www.eia.gov/outlooks/aeo/assumptions/pdf/elec\\_cost\\_perf.pdf](https://www.eia.gov/outlooks/aeo/assumptions/pdf/elec_cost_perf.pdf)

US EIA. (2023b). *US EIA glossary*. <https://www.eia.gov/tools/glossary/>

US NREL. (2023). *Annual technology baseline 2023*.

<https://atb.nrel.gov/electricity/2022/data>

Wartsila. (2023). *Peaking power plants*.

<https://www.wartsila.com/encyclopedia/term/peaking-power-plants>

Wert, J. L., Safdarian, F., Gonce, A., Chen, T., Cyr, D., & Overbye, T. J. (2023). Wind resource drought identification methodology for improving electric grid resiliency.

*IEEE Xplore*. <https://ieeexplore.ieee.org/document/10078708>

**Policy and Data Needs for Increased Grid Reliability and Energy Equity**

Clifford K. Ho<sup>1</sup>

Tess Carter<sup>2</sup>

Anaïs Borja<sup>3</sup>

<sup>1</sup>Legislative Fellow, Office of U.S. Senator Martin Heinrich

[Clifford\\_Ho@heinrich.senate.gov](mailto:Clifford_Ho@heinrich.senate.gov)

<sup>2</sup>Senior Policy Analyst, Joint Economic Committee Democratic Staff

[Tess\\_Carter@jec.senate.gov](mailto:Tess_Carter@jec.senate.gov)

<sup>3</sup>Senior Policy Advisor, Office of U.S. Senator Martin Heinrich

[Anais\\_Borja@heinrich.senate.gov](mailto:Anais_Borja@heinrich.senate.gov)



### Abstract

Identifying, sharing, and analyzing the right types of data are key to ensuring reliability and resilience of the electric grid and improving long-term reliability assessments. This is especially important in light of increasing occurrences of extreme weather, the changing mix of power generation and demands on the grid, and the need to ensure reliability and resilience in rural and disadvantaged communities. Currently, data are not consistently reported at a sufficiently granular level to provide necessary information for models of weather-dependent resources and loads, or to identify where disparities in reliability or resilience may exist on a city or community level. This paper describes policies that can enable the collection and sharing of these data to help ensure equitable reliability for all.

### 1. Introduction

Our nation's electrical grid is experiencing significant changes and uncertainties: (1) increasing loads from projected growth in manufacturing, data centers, and electrification of homes, businesses, and vehicles; (2) a changing mix of centralized and distributed generation resources; (3) an increasing number of severe weather events; and (4) aging infrastructure. As a result, we need to identify ways to collect and share more data that will enable utilities, grid operators, and customers to model, monitor, and maintain reliability and resilience in the face of these growing changes and uncertainties. Outages currently cost the U.S. economy approximately \$150 billion each year (Joint Economic Committee, 2024). Data to quantify where, when, and why these outages occur will enable more efficient and equitable solutions. Two forms of data are addressed in this paper: (1) energy-related weather data and (2) distribution-level reliability data.

Energy-related weather data includes solar irradiance, wind speed, temperatures, precipitation, and other weather data that can impact weather-dependent resources, such as solar photovoltaics, concentrated solar power, and wind turbines. Solar and wind power have become the fastest-growing generation resources on the U.S. grid. The U.S. Energy Information Administration (EIA) forecasts that solar and wind generation will grow 75% and 11%, respectively, from 2023 to 2025 (U.S. EIA, 2024). In 2023, renewable sources from solar, wind, hydro, biomass, and geothermal accounted for 22% of total generation in the U.S., surpassing nuclear generation for the first time in 2021 and coal generation for the first time in 2022. Increasing contributions from these weather-dependent, variable resources require more granular data to improve both real-time grid operations and longer-term reliability planning.

Distribution-level reliability data includes information regarding the duration and frequency of customer outages typically caused by severe weather or animals that cause faults or downed power lines. Eto et al. (2019) and Lawson (2022) found that more than 90% of outages on the grid were caused by the distribution system, as opposed to the bulk power system, which comprises power generation and transmission systems. In addition, increasing amounts of distributed (and sometimes bi-directional) energy resources and loads, such as solar panels, battery storage systems, and electric

vehicles, are being added to the grid. While distribution-level reliability data is currently collected by the EIA, the frequency, duration, and recovery times of outages are currently averaged and reported at an entire utility level (U.S. EIA, 2023). Identifying ways to collect and share more granular distribution-level reliability data could help increase reliability, resilience, and energy equity on a city or community level.

## 2. Data Needs

### 2.1. Energy-Related Weather Data

#### 2.1.1. Existing Weather Data and Use

Models of solar energy, wind energy, and other weather-dependent electric generation resources and loads require meteorological data such as solar irradiance, wind speed, and temperature. Utilities, public utility commissions, regional transmission organizations (RTOs), and independent system operators (ISOs) use these data in resource-adequacy models. These models aim to ensure that electric loads throughout the year can be met by a portfolio of generation resources (e.g., gas-fired turbines, wind turbines, solar farms) with consideration of expected electrical loads in future years.

However, many models and available data sets are based on historical weather data. Climate change and greater frequency of extreme weather events increases the uncertainty in these data and models. Improved modeling methods, such as probabilistic modeling, that can accommodate these uncertainties have been recommended by the North American Electric Reliability Commission (NERC, 2016), industry (EPRI, 2022), academia (Gao and Gorinevsky, 2020), and national labs (Ho et al., 2023).

Although various energy-related weather datasets exist that can be used in these models, they are disparate and decentralized. Also, the type of data, spatial and temporal frequency of the data, and amount of data available varies by source. Below is a sampling of existing energy-related weather databases:

- National Solar Radiation Database (NSRDB): The NSRDB is managed by the National Renewable Energy Laboratory. The NSRDB contains hourly and sub-hourly values of meteorological data for the United States and a subset of international locations, including solar radiation (global horizontal, direct normal, and diffuse horizontal irradiance).
- Wind Data Hub: The Wind Data Hub is managed by the Pacific Northwest National Laboratory and provides modeled and observational wind data from remote sensing systems and in-situ measurements of meteorological variables.
- Open Energy Data Initiative (OEDI): The OEDI is managed by the U.S. Department of Energy (DOE) and provides datasets uploaded from researchers working for DOE programs, offices, and national laboratories. It provides

access to data resulting from specific projects across the broad spectrum of energy programs and projects funded by DOE.

- **U.S. Energy Atlas:** The U.S. Energy Atlas is managed by the DOE Energy Information Administration and provides data and interactive maps of energy infrastructure and resources in the United States.
- **NCAR Data for Climate and Weather Research:** The National Science Foundation (NSF) National Center for Atmospheric Research (NCAR) manages the Research Data Archive, which contains a collection of meteorological and oceanographic data, as well as model outputs from NCAR's Computational and Information Systems Lab.
- **NASA's LANCE and FIRMS Databases:** The National Aeronautics and Space Administration (NASA) manages the LANCE and FIRMS databases. The Land, Atmosphere Near real-time Capability for Earth observations (LANCE) website provides near real-time data and satellite imagery for monitoring natural and human-made phenomena. The Fire Information for Resource Management System (FIRMS) provides near real-time fire data from satellites that can be used to analyze potential impacts on solar irradiance and solar-energy resources.

### 2.1.2. *Weather Data Needs*

To improve models of weather-dependent resources and loads, the energy-related weather data should span long periods (~30 years), be sampled frequently (at least every hour) and contiguously, include a wide range of available meteorological data, span numerous regions (preferably in a gridded fashion) across the United States, and enable modeling of future impacts of climate change and extreme weather on weather-dependent energy resources and loads (ESIG, 2023). Very few current datasets meet these criteria. In addition, DOE should serve as a centralized clearinghouse for these data. A central portal that provides access to vetted and secure data specifically for resource-adequacy modeling and long-term electric-reliability planning would greatly benefit the modeling community.

## 2.2. *Distribution-Level Reliability Data*

### 2.2.1. *Existing Reliability Data and Use*

The IEEE 1366 Standards provide distribution-system reliability metrics that are widely used and reported by utilities (IEEE, 2022). Some examples of these reliability metrics include the following:

- **Customer Average Interruption Duration Index (CAIDI):** A metric that indicates the average time required to restore service to a customer after a sustained interruption lasting more than five minutes

- **System Average Interruption Frequency Index (SAIFI):** A metric that indicates how often the average customer experiences a sustained interruption lasting more than five minutes over a predefined period of time

Although these distribution reliability metrics are required to be reported by larger utilities via EIA form 861, the data are averaged over the entire utility, which can span large regions. This makes it difficult to identify trends in reliability or resilience at the city or community level.

### 2.2.2. Reliability Data Needs

The California Public Utilities Commission Energy Division presented an overview of electric system reliability and several recommendations (Enis, 2021). They stated that more granular reliability data “can show where recurring issues are happening and areas where the greatest improvement is needed” and also “how widely the metrics vary over entire service territories.”<sup>1</sup> The CPUC recommends future improvements that include increased data granularity and “determining possible equity impacts of unreliable service.” They also recommend improvements to the “usability of data presented in annual reports.”

Fig. 1 shows a plot of two reliability metrics, CAIDI and SAIFI, reported by the Public Service Company of New Mexico, from 2013 to 2022. CAIDI and SAIFI represent the average duration and number of customer outages per year. The average number of outages has been fairly consistent at approximately one sustained interruption (lasting more than five minutes) per year. However, the duration of the average customer outage appears to be trending upward since 2017. Fig. 2 shows the spatial variability in CAIDI and SAIFI reported in 2022 from four service providers in New Mexico. These service providers include three investor-owned utilities (Public Service Company of New Mexico, Southwestern Public Service Company, and El Paso Electric Company) and the Western Area Power Administration (WAPA), which provides federal hydropower to various state and federal agencies, municipalities, Native American tribes, and rural electrical cooperatives. The “heat maps” of CAIDI and SAIFI shown in Fig. 2 illustrate the potential spatial variability of reliability metrics across New Mexico. However, because these reliability data are reported as average values over an entire utility, it is difficult to identify if disparities exist and where improvements are needed at a city or community level.

---

<sup>1</sup> Oak Ridge National Laboratory manages the Outage Data Initiative Nationwide (ODIN) website, which provided real-time outage information provided on a voluntary basis by utilities across the United States. However, temporal and spatial trends in reliability are not tracked to inform where improvements are needed.

## Increased Grid Reliability and Energy Equity

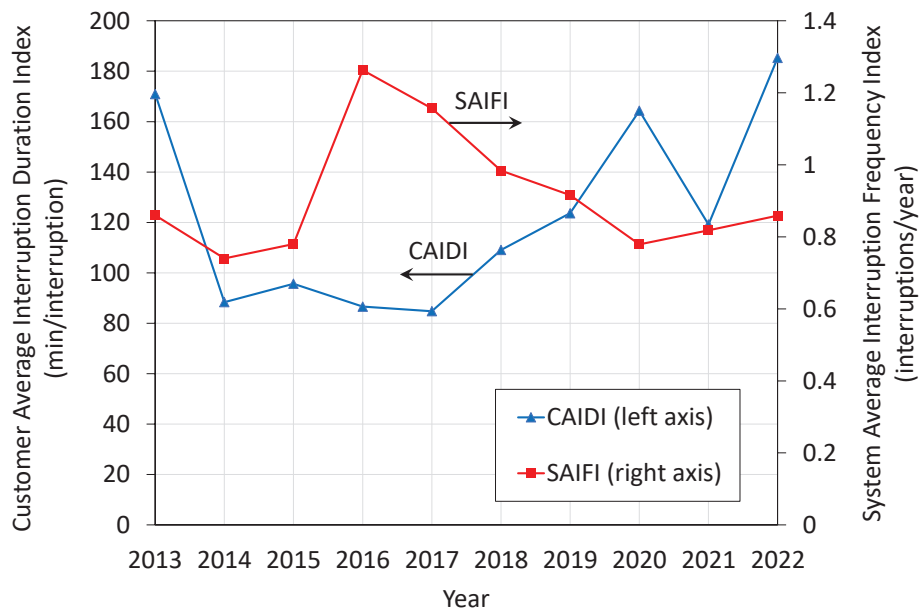


Fig. 1. Plot of CAIDI and SAIFI reliability metrics reported by the Public Service Company of New Mexico from 2013 to 2022 (from data reported to U.S. EIA, 2023)

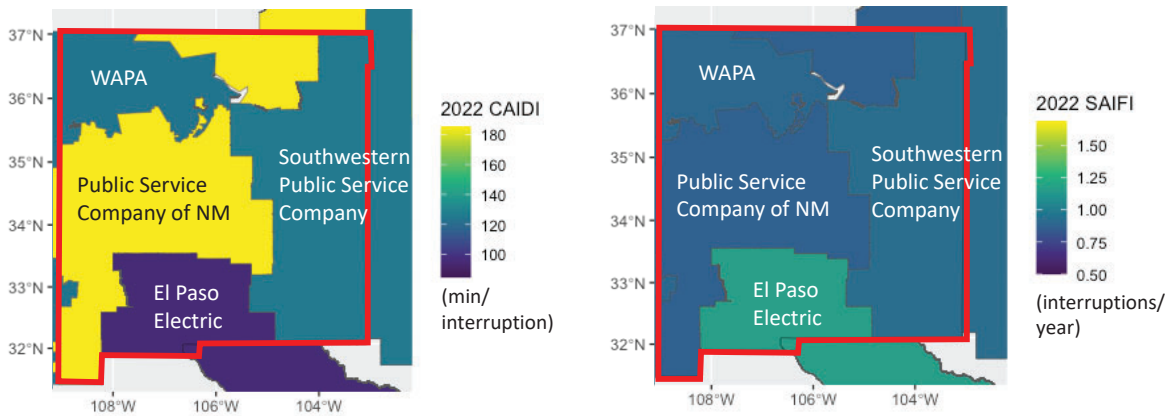


Fig. 2. Approximate regions depicting 2022 CAIDI and SAIFI reliability metrics reported in New Mexico (Note: WAPA provides electricity to several electric cooperatives in NM). (from data reported to U.S. EIA, 2023)

### 3. Other Policy Needs

In addition to the need for more granular weather and distribution-level reliability data, improvements are also needed to expand and improve our transmission infrastructure and to increase accountability for grid reliability.

## Increased Grid Reliability and Energy Equity

Regarding transmission expansion and improvements to alleviate the growing congestion and interconnection queues on the U.S. grid, three barriers are often cited: (1) planning, (2) paying, and (3) permitting (Gramlich, 2019).

Planning for new transmission lines and upgrades needs to focus on longer-term requirements (>10 – 15 years) with consideration of increasing weather impacts on generation resources and loads on the grid. Interregional transmission planning also needs to be coordinated among multiple states, as required by Federal Energy Regulatory Commission (FERC) Order No. 1000 (FERC, 2011), to help alleviate local power shortages. Two Congressional Research Service (CRS) reports provide a summary of issues, federal policies and legislation aimed at addressing shortcomings in transmission planning and siting (Lawson, 2023; Lawson, 2024).

Paying for large transmission infrastructure and improvements, or cost allocation, can be contentious if customers need to pay for projects that do not directly benefit them. FERC Order No. 1000 establishes cost allocation that follows the “cost causation” principle of electricity ratemaking, which requires that beneficiaries of a grid asset pay for the costs (FERC, 2011). This requires a determination of who benefits from a transmission line or upgrades and what the share of costs should be to each beneficiary. A FERC Notice of Proposed Rulemaking also addressed cost allocation for transmission infrastructure (FERC, 2022). Federal policies and legislation that address transmission cost allocation have been summarized by CRS (Lawson, 2024).

Permitting for large, interstate transmission requires approvals from multiple states and local governments along the path of the transmission line. This process can be long and arduous, and recommendations to streamline the process and provide federal authorities for projects serving the national interest have been proposed by Congress (Lawson, 2024).

In addition to planning, paying, and permitting for transmission improvements, there is a need to ensure that innovations that can improve capacity and efficiencies on the grid are incentivized for adoption. These grid-enhancing technologies include dynamic line ratings, advanced transmission conductors, power flow controls, and topology optimization (U.S. DOE, 2022). Other innovations at various stages of deployment that can increase the reliability and resilience of the grid include distributed energy resources and storage systems (including electric vehicles), artificial intelligence for grid operations and planning, and virtual power plants. Policies that appropriately monetize and incentivize these technologies and their integration on the grid will also help to increase electric reliability and resilience for both bulk-power and distribution systems.

Finally, policies to enhance accountability for grid reliability are needed, especially in deregulated markets. Angwin (2020) notes that there is a general lack of accountability for grid reliability in deregulated markets run by RTOs and ISOs due to the diversified nature of electricity generation, transmission, and distribution in those markets. “Pay for performance” or performance-based regulation have been implemented in a number of states to improve utility performance by changing the way they make money. However,



## Increased Grid Reliability and Energy Equity

national standards for ensuring accountability and payments based on grid reliability are lacking. Some challenges include the following:

- Different electricity requirements and resources that will necessitate location-specific features of performance-based regulations

Diversity of owners and operators of electricity generation, transmission, and distribution systems, especially in RTO areas, and the different authorities of regulated and deregulated markets

Providing accountability in this multifaceted and diverse ecosystem, both at the federal and state levels, can pose significant challenges. However, general approaches for performance-based regulation and ratemaking based on best practices are needed to provide accountability for grid reliability and resilience.

### 4. Conclusions

The U.S. electric grid is facing challenges with increased frequency of extreme weather, uncertainty associated with weather-dependent resources and loads, and aging infrastructure. These factors can impact the reliability and resilience of the grid. This paper has identified and recommended the following needs to address these challenges:

- A centralized repository or portal for weather data required for models of weather-dependent electric generation resources and loads
- More granular distribution-level electric reliability data that can be used to identify where improvements are needed at the city or community level
- Policies that enable or incentivize necessary transmission expansions, upgrades, and other innovative technologies that improve reliability, resilience, and efficiency of the grid
- Policies that ensure accountability of grid reliability and resilience through performance-based regulation and ratemaking

### Conflict of Interest

No financial conflicts of interest.

The views and opinions expressed in this paper are those of the authors and do not necessarily reflect the Senate or Committee offices to which the authors belong.

## References

Angwin, M. (2020). *Shorting the grid - the hidden fragility of our electric grid*. Wilder, VT: Carnot Communications.

Electric Power Research Institute (EPRI). (2022). *A guide to resource adequacy concepts and approaches*. Palo Alto, CA: EPRI.

Energy Systems Integration Group (ESIG). (2023). *Weather dataset needs for planning and analyzing modern power systems*. Reston, VA.

<https://www.esig.energy/weather-data-for-power-system-planning>

Enis, J. (2021). *Electric System Reliability*. Retrieved 2023, from

<https://www.cpuc.ca.gov/-/media/cpuc-website/transparency/commissioner-committees/emerging-trends/2021/2021-02-17-electric-system-reliability-presentation---final.pdf>

Eto, J. H., LaCommare, K. H., Caswell, H. C., & Till, D. (2019). Distribution system versus bulk power system: identifying the source of electric service interruptions in the US. *IET Generation, Transmission & Distribution Journal*, 8.

Federal Energy Regulatory Commission (FERC). (2011). *FERC order 1000; transmission planning and cost allocation by transmission owning and operating public utilities*. Retrieved 2024, from <https://www.ferc.gov/sites/default/files/2020-04/OrderNo.1000.pdf>

Federal Energy Regulatory Commission (FERC). (2022). *FERC issues transmission NOPR addressing planning, cost allocation*. Retrieved 2024, from



<https://www.ferc.gov/news-events/news/ferc-issues-transmission-nopr-addressing-planning-cost-allocation>

Gao, W., & Gorinevsky, D. (2020). Probabilistic modeling for optimization of resource mix with variable generation and storage. *IEEE Transactions on Power Systems*, 9.

Gramlich, R. (2019). *A grid new deal - testimony to roundtable on electricity transmission infrastructure, U.S. House of Representatives Select Committee on the Climate Crisis*. Retrieved 2023, from <https://gridprogress.files.wordpress.com/2019/06/testimony-to-roundtable-on-electricity-transmission-infrastructure-.pdf>

Ho, C. K., Roesler, E. L., Nguyen, T., & Ellison, J. (2023). Potential impacts of climate change on renewable energy and storage requirements for grid reliability and resource adequacy. *J. Energy Resources Technology, JERT-23-1127*, 12.

Institute of Electrical and Electronics Engineers (IEEE). (2022). *IEEE guide for electric power distribution reliability metrics*. New York, NY: Transmission and Distribution Committee of the IEEE Power and Energy Society.

Joint Economic Committee. (2024). *How renewable energy can make the power grid more reliable and address risks to electricity infrastructure*. Washington, DC: U.S. Senate <https://www.jec.senate.gov/public/index.cfm/democrats/2024/1/how-renewable-energy-can-make-the-power-grid-more-reliable-and-address-risks-to-electricity-infrastructure>

## Increased Grid Reliability and Energy Equity

Lawson, A. J. (2022). *Maintaining electric reliability with wind and solar sources: background and issues for Congress*. Washington DC: Congressional Research Service.

Lawson, A. J. (2023, April 25). *Electricity: overview and issues for Congress*, Congressional Research Service. Retrieved 2024, from <https://crsreports.congress.gov/product/pdf/R/R47521>

Lawson, A. J. (2024, February 9). *Electricity transmission permitting reform proposals*, Congressional Research Service. Retrieved 2024, from <https://crsreports.congress.gov/product/pdf/R/R47627/11>

North American Electric Reliability Corporation (NERC). (2016). *Probabilistic assessment technical guideline document*. Atlanta, GA: NERC.

U.S. Department of Energy (DOE). (2022). *Grid-enhancing technologies: a case study on ratepayer impact*. Washington DC.

U.S. Energy Information Administration (EIA). (2023). *Annual electric power industry report, Form EIA-861 detailed data files*. Retrieved December 2023, from <https://www.eia.gov/electricity/data/eia861/>

U.S. Energy Information Administration (EIA). (2024, January 16). *Today in energy*. Retrieved February 2024, from In-Brief Analysis: <https://www.eia.gov/todayinenergy/detail.php?id=61242>

**Maximizing DPV Hosting Capacity with Regional Firm VRE Power**

Marc Perez<sup>\*</sup>  
Richard Perez<sup>\*,+</sup>  
Upama Nakarmi  
Thomas E. Hoff<sup>\*</sup>  
Jeffrey Freedman<sup>+</sup>  
Elizabeth McCabe<sup>+</sup>  
Marco Pierro<sup>&</sup>  
Jan Remund<sup>#</sup>

<sup>\*</sup>Clean Power Research, Napa, CA

<sup>+</sup>Atmospheric Sciences Research Center, SUNY, Albany, NY

<sup>&</sup>EURAC, Bolzano, Italy

<sup>#</sup>Meteotest, Bern, Switzerland

### Abstract

A growing body of work demonstrates that Variable Renewable Energy resources (VREs) such as weather-driven wind and solar could firmly and economically meet current and future regional electric demand 24/365 nearly anywhere on the planet if effective regulations and market rules enabling their transformation from intermittent to firm are implemented. The question we pose in this paper is whether Distributed PV (DPV) hosting capacities could be enhanced if DPV systems actively participated in the larger [transmission] grid's firm VRE power generation objective. We show that this is indeed the case with the possibility of multifold DPV hosting capacity increases.

Keywords: grid integration, high renewable penetration, distribution system utilities (DSO), distributed PV, saturation, load growth

### Introduction

The International Energy Agency (IEA) defines firm power generation as the capability for a generating resource or an ensemble of resources to meet electrical demand 24x365 (Perez et al., 2023). PV and wind are weather/season-driven Variable Renewable Energy (VRE) resources that inherently do not meet the firm power criterion. Their intermittency does not pose issues at low grid penetration, operating at the margin of conventional baseload and dispatchable generation.

However, as penetration increases, load-management issues gradually arise (steeper ramps, deeper duck curves, etc.) until deployment reaches the limits of what power grids can absorb, leading to a host of issues such as reactive curtailments, negative market prices, and a growing opposition to further renewable deployments, particularly at the distribution level. The left side of Figure 1 illustrates the intensifying VRE supply/demand imbalance as penetration increases for a hypothetical 50%/50% wind/PV blend on the New York City power grid that has been traditionally supplied with baseload and dispatchable resources.

The IEA work (Perez et al., 2023) shows that it is possible to economically transform VREs from intermittent to firm so their output can match a given load shape, removing imbalances and enabling a seamless gradual displacement of underlying conventional resources. The right side of Figure 1 illustrates the penetration of VREs, transformed from weather-driven to firmly matching the load shape of dispatchable generation.

The transformation requires an optimum blend of technologies and strategies that include energy storage, coupling solar and wind, supply or demand-side flexibility, and most importantly, overbuilding VREs and proactively curtailing (i.e., apparently wasting) a portion of their generation. The overbuilding/curtailment (implicit storage) strategy reduces real energy storage requirements and allows for realistic firm power generation costs.

A number of studies undertaken as part of IEA Task 16 suggest that, by 2040 or before, these enabled VREs could firmly supply nearly 100% of electric demand in most regions of the world at generation costs equal or below that of current conventional generation (Perez, 2020; Remund et al., 2022; Rey-Costa et al., 2023). However, the overbuilding/implicit storage strategy that is essential to achieving this objective cannot be implemented today. This is because remuneration pathways for VREs are guided by energy-market rules that inherently penalize curtailment. As a result, VREs continue to deploy unconstrained at the margin (left side of Figure 1). Such unconstrained deployments are self-limiting beyond a small margin because of the grid imbalances they engender. A recent article by the IEA team of experts argues that firm VRE deployments could be fostered with capacity-based market rules applied to VREs in parallel to and independently of conventional energy markets (Remund et al., 2023). This article also makes the case that flexibility

## Maximizing DPV Hosting Capacity

provided on the supply side with a small amount (<5%) of 100% renewable e-fuel-powered dispatchable generation is very effective at minimizing firm power electricity costs, despite the cost of e-fuels (Viscardi et al., 2021) that can be 4-5 times higher than conventional [fossil] fuels. This small amount of clean dispatchable generation also constitutes a fail-safe insurance in case of extreme VRE droughts (more extreme than what could be captured in the 20 years analyzed).

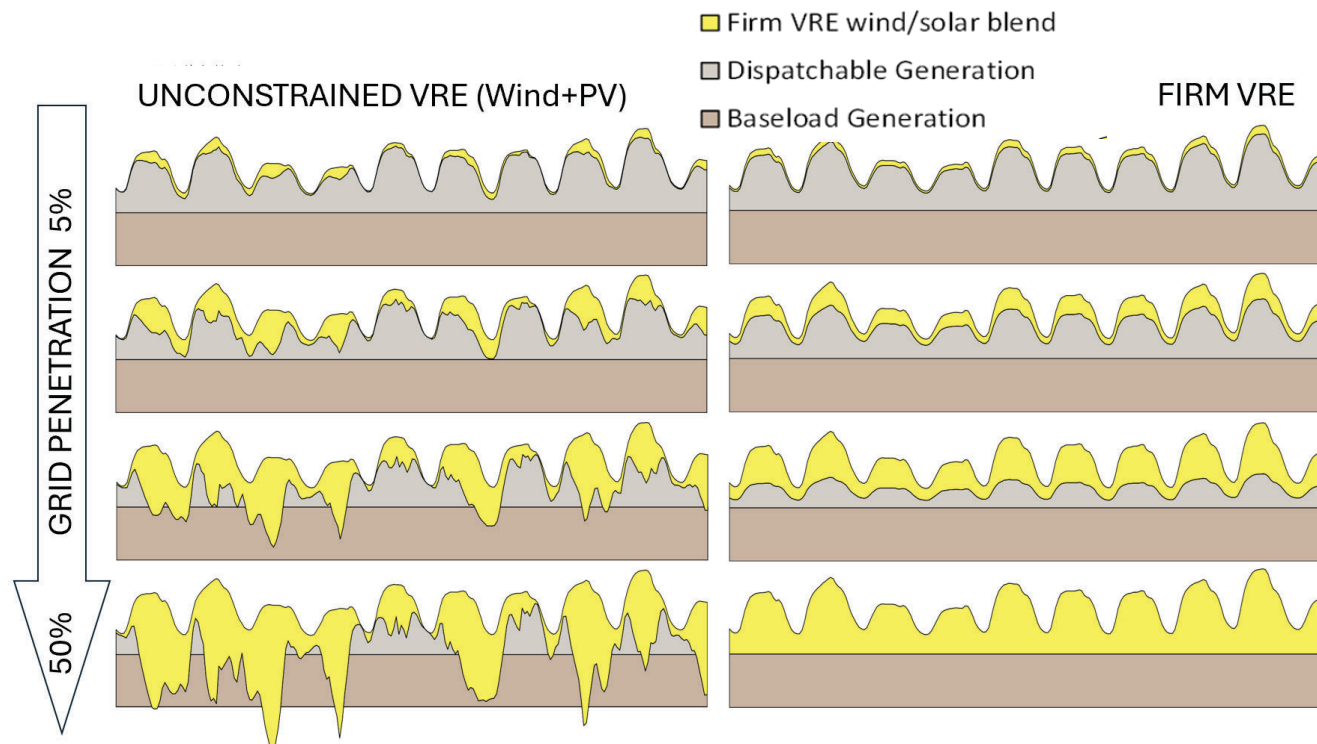


Fig. 1: Contrasting the grid penetration impact of unconstrained VRE (left) and firm VRE (right). This qualitative illustration assumes a 50/50% wind PV energy contribution on a grid traditionally served with dispatchable and baseload generation.

## DPV Hosting Capacity

DPV includes user-sited residential and commercial systems, community solar systems etc., that are located on utility distribution circuits. As their number increases, congestion issues arise, increasingly leading to deployment restrictions. The well-documented California industry slowdown in residential deployments attributable to NEM3 (Balaraman, 2024) and the deployment moratoriums imposed on a growing number of distribution circuits in New Jersey [e.g., PSEG, 2024] are two symptomatic examples of this emerging issue.

The question we pose is the following: Given effective market rules enabling the deployment of regional (transmission-level) firm VRE solutions — with an optimized blend of PV, wind, real and implicit storage, as well as a small contribution from clean dispatchable generation (supply-side flexibility) — how would distribution-level hosting capacities be affected, assuming that distribution-side resources would fully participate in the regional firm power strategy (Perez, 2020; Remund et al., 2022; and Rey-Costa et al., 2023)? Distribution-side resources would consist of DPV and storage systems only, assuming that wind and thermal dispatchable units could only operate at the transmission level.

## Maximizing DPV Hosting Capacity

DPV hosting capacity is typically defined in static terms as a function of the maximum DPV output and the minimum load on a distribution circuit, (e.g., Wang et al., 2022) an upper limit over which voltage and thermal overloading problems would occur. There is a growing push to consider 'dynamic' hosting capacities involving storage and a degree of DPV curtailment that would limit DPV production peaks and thereby increase a circuit's effective hosting capacity (Wang et al., 2022). Assuming a linear relationship between peak DPV and hosting capacity, the distribution hosting capacity increase, DHCI, resulting from a dynamic operation of DPV can be calculated from:

$$DHCI = \frac{DPV_{max_u}}{DPV_{max_m}} - 1$$

$DPV_{max_u}$  represents the unconstrained DPV production peak and  $DPV_{max_m}$  represents the managed DPV production peak, embedding distributed storage and DPV curtailment. The firm power approach discussed in this paper is fully consistent with this dynamic view while it is also much broader, since in this case DPV curtailment and storage would not be circuit-specific but operated in the context of least-cost regional firm VRE power generation.

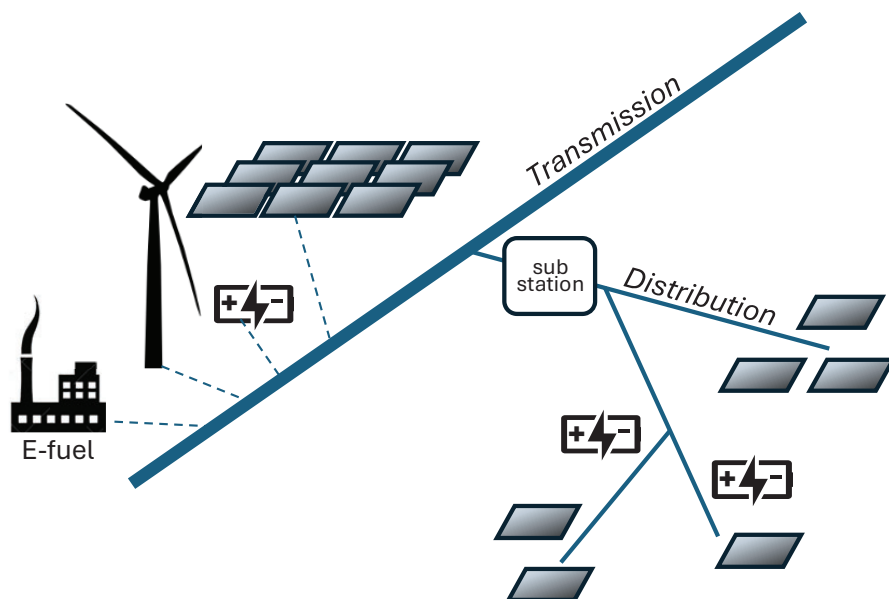


Figure 2. Distribution of firm VRE assets on a power grid. While wind and e-fuel thermal would likely be interconnected on the transmission grid, PV and storage assets can be interconnected, either upstream or downstream of distribution substations.

### Illustrative Case Case Studies

We illustrate distribution hosting capacity impacts with two regional firm power case studies that were undertaken as part of IEA PVPS Task 16 for electrical regions 9 and 3 of the Midcontinent Independent System Operator (MISO), respectively corresponding to the states of Louisiana and Iowa (Perez et al., 2023). For the present case studies and for the sake of generalization, we

consider that the regional firm power requirement consists of serving a constant load 24/365 (i.e., equivalent to what would be supplied by baseload generation).

Least-cost firm VRE configurations were determined by simulating 20 years' worth of hourly latitude-tilt PV generation and 90-m hub height wind power generation. Simulations apply SolarAnywhere/PVLib for PV and ERA5 reanalysis wind data extrapolated to turbine hub height using measurement using tower-validated models and nominal wind power curves (Hersbach et al., 2020; NOAA, 2003; Saint-Drenan, 2020; SolarAnywhere, 2024).

Optimum firm VRE configurations and generation LCOEs are a function of the capital and operating costs (CapEx and OpEx) of the technologies involved: PV, wind, storage, and dispatchable e-fueled powered generation (assuming a supply-side flexibility contribution of 5% for the latter). For the present case studies, we consider future (2040) costs summarized in Table 1 (NREL Annual Technology Baseline, 2023).

Table 1.

|       |                    |                     |
|-------|--------------------|---------------------|
| CapEx | PV                 | \$466/kW            |
|       | Wind               | \$525/kW            |
|       | Battery *          | \$65/kWh<br>\$49/kW |
| OpEx  | PV                 | 2.3% of CapEx/yr    |
|       | Wind               | 4.5% of CapEx/yr    |
|       | Battery            | 2.5% of CapEx/yr    |
|       | e-fuel Thermal Gen | 18 c/kWh            |

*Note that Battery CapEx, unlike how it is often reported, includes two components per kW and kWh capacities.*

The least-cost optimum VRE configurations and resulting firm power levelized costs of energy (LCOEs) determined for Iowa and Louisiana are presented in Table 2. The table also reports the wind and PV capacity factors in each region.

While the least-cost firm power regional VRE blend is equal part wind and solar in Iowa, it is 100% solar in Louisiana — i.e., adding any proportion of would result in higher LCOEs. While capacity factors are comparable, the small economic advantage of PV and the more pronounced wind droughts lead to a solar-only optimum.



Table 2.

|                                     | Iowa              | Louisiana       |
|-------------------------------------|-------------------|-----------------|
| PV capacity factor                  | 14.6%             | 15.4%           |
| Wind capacity factor                | 41.3%             | 15.3%           |
| Optimum PV energy contribution      | 47.5%             | 95%             |
| Optimum wind energy contribution    | 47.5%             | 0%              |
| Assumed e-fuel thermal contribution | 5%                | 5%              |
| Optimum VRE curtailment             | 24%               | 55%             |
| Optimum battery storage             | 11.8 load hours   | 39 load hours   |
| Optimum LCOE                        | 3.9 cents per kWh | 6 cents per kWh |

### Case Studies Results

We assume that DPV systems and associated distributed storage systems directly contribute to larger [regional transmission] grid's firm power generation objective. In effect, these distributed assets operate as part of the optimum regional VRE configuration discussed above. Dynamic curtailment, when needed, is applied to the total VRE output, and apportioned to the PV and wind output available at the time. We further assume that all PV plants on the regional grid (utility-scale and DPV) are operated in an analogous manner in terms of dynamic curtailment.

Looking at Louisiana first with its 95% PV 5% e-fuel optimum, we assume that battery storage is distributed proportionally to the installed PV capacity installed at the transmission or distribution level below a substation. In effect, all PV plants on the grid operate identically in terms of storage management, with storage possibly co-located on their DC sides, but not necessarily so. Figure 3 (top) illustrates several days' worth of DPV generation on an arbitrary feeder in MISO Region 9 (Louisiana). It shows the apportionment of DPV output between the direct feed to the circuit, the storage charge, and the curtailment. The solid black line is the sum of the direct feed of PV to the grid and storage output. It is nearly constant — matching the baseload firm power generation assumption — except for brief PV droughts when (transmission-side) e-fuel flexible power generation ensures load requirements.

However, the most important observation in this figure is the difference between unconstrained DPV and firmed DPV peaks (respectively  $DPV_{max_u}$  and  $DPV_{max_m}$  in the above equation). This translates into a DPV hosting capacity increase of 650% in this case study. Therefore, in effect, a regional firm VRE power strategy would increase the amount of DPV a distribution circuit can sustain by more than sevenfold.



## Maximizing DPV Hosting Capacity

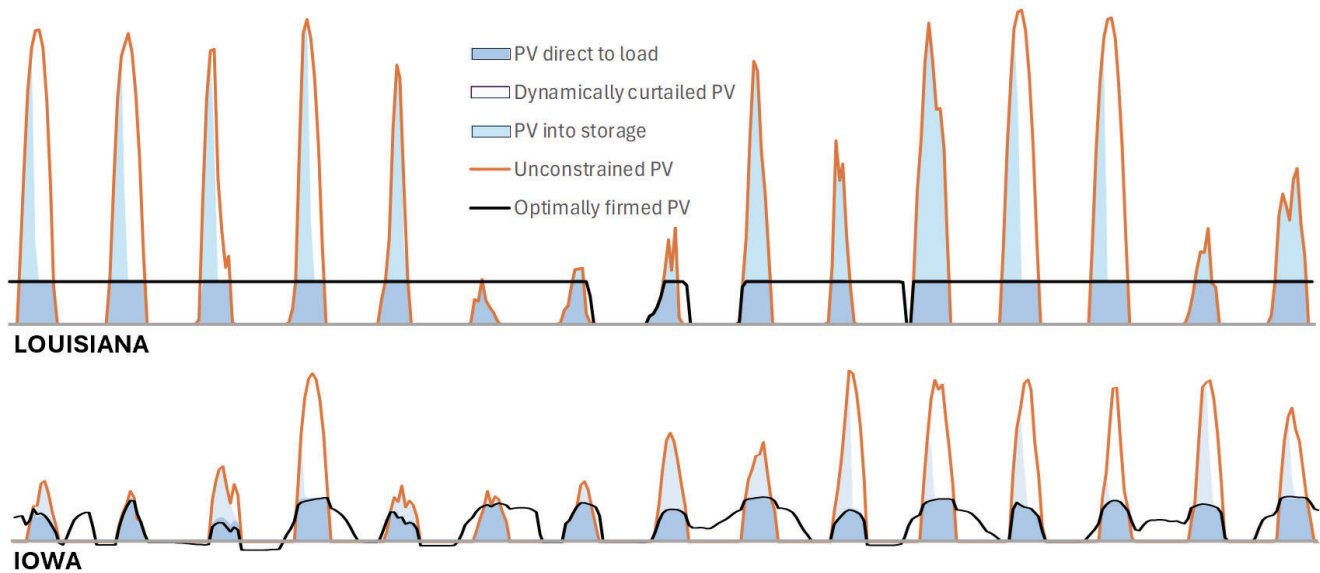


Fig. 3. Contrasting distribution-level unconstrained DPV and firm DPV contribution in two power grids, where PV is the unique VRE (top) and where VRE consists of a blend of wind and PV (bottom)

The situation in MISO Region 3 (Iowa) is illustrated in the bottom of Figure 3. This situation is more complex because the management of firm DPV must be responsive to wind output on the larger grid to maintain overall load-shape requirements. This impacts storage management on both distribution and transmission parts of the grid. Because wind and solar seasonal patterns can be different, the independent operation of storage associated with PV on the distribution side and with wind on the transmission side would result in considerably more storage (~3 times more) than if PV, wind, and storage were colocated, penalizing the optimum firm power bottom line LCOE shown in Table 2. The issue can be resolved by transferring electricity between storage units on each side of substations at the cost of small additional substation traffic (thus slightly reducing the possible hosting capacity gains). This storage-to-storage exchange is apparent in Figure 3 with the negative firm power solid black line, indicating a transfer from grid-level storage to feeder-level storage needed to maintain overall minimum storage requirements.

Nevertheless, in this more complex DPV operation case in a region with optimized PV/wind firm power operations, the distribution hosting capacity gain remains substantial at 260%.

### Conclusion

The case studies analyzed, representing a limited but diverse sample of firm VRE power generation configurations, indicate that operating DPV systems to directly contribute to the regional firm power objectives, results in a multifold increase of distribution-level hosting capacities. This increase is largest when the optimum VRE blend is dominated by PV generation

## Maximizing DPV Hosting Capacity

but remains remarkable when wind plays a significant role as well. An important task ahead is thus to create the regulatory and market rules environments where two major power generation benefits — (1) lowest-cost 100% renewable power generation for a region, and (2) a significant increase in DPV market size even where currently constrained — can be realized.

### **Conflict of Interest**

The authors of this document declare no conflicts of interest related to the content presented. There are no financial, personal, or professional affiliations that could bias the information provided.

## References

- Balaraman, K. (2024.) California rooftop solar had a tough year following NEM 3.0.  
<https://www.utilitydive.com/news/california-rooftop-solar-nem-30-outlook/702498/>
- Hersbach H., Bell, B., Berrisford, P., et al. (2020.) The ERA5 global reanalysis. *Q J R Meteorol Soc.* 146: 1999–2049. <https://doi.org/10.1002/qj.3803>
- NOAA (2003.) *Earth system research laboratories. Chemical sciences laboratory. LLLJP wind shear formula.* <https://csl.noaa.gov/projects/lamar/windshearformula.html>
- NREL Annual Technology Baseline (2023). <https://atb.nrel.gov/electricity/2023/data>
- Perez, M. (2020). *Pathways to 100% renewables across the MISO region.*  
<https://www.osti.gov/biblio/1668266>
- Perez, R., Perez, M., Remund J., et al. (2023). *Firm power generation.* <https://iea-pvps.org/wp-content/uploads/2023/01/Report-IEA-PVPS-T16-04-2023-Firm-Power-generation.pdf>
- Remund, J., Perez, R., Perez, M., Pierro, M., & Yang, D. (2023). *Firm photovoltaic power generation: Overview and economic outlook.*  
<https://onlinelibrary.wiley.com/doi/abs/10.1002/solr.202300497>
- Remund J., Perez, M., & Perez, R. (2022). Firm PV Power Generation in Switzerland. *IEEE*.  
<https://ieeexplore.ieee.org/abstract/document/9938518>
- Rey-Costa, E., et al. (2023). Firming 100% renewable power: Costs and opportunities in Australia's National Electricity Market. *Renewable Energy*, 219(1), 119416.
- Saint-Drenan, Y., Besseau, R., Jansen, M., Staffell, I., Troccoli, A., Dubus, L., Schmidt, J., Gruber, K., Simões, S. & Heier, S. (2020). A parametric model for wind turbine power curved incorporating environmental conditions. *Renewable Energy*, 167.

SolarAnywhere (2024).

[https://www.solaranywhere.com/?gclid=CjwKCAiAzJOtBhALEiwAtwj8tm5ak504TwWMyHJEXFdX6SO4gkJfADOQBdJ\\_hK3oHWUC9I5Bz6vV-RoCkIkQAvD\\_BwE](https://www.solaranywhere.com/?gclid=CjwKCAiAzJOtBhALEiwAtwj8tm5ak504TwWMyHJEXFdX6SO4gkJfADOQBdJ_hK3oHWUC9I5Bz6vV-RoCkIkQAvD_BwE)

Viscardi, R., Bassano, C., Nigliaccio, G., & Deiana, P. (2021). The potential of e-fuels as future fuels. ENEA Magazine, Energia, ambiente e innovazione | 1/2021. pp. 112-116. DOI: 10.12910/EAI2021-022.

Wang, W. et al. (2022). PV hosting capacity estimation: experiences with scalable framework; National Renewable Energy Laboratory. <https://www.nrel.gov/docs/fy22osti/81851.pdf>

**The Practical Implementation of Distributed Solar CHP With Thermal and EV  
Battery Storage for Schools**

Steven B. Smiley  
Energy Economist  
Seattle, WA

**Author Note**

Correspondence concerning this article should be addressed to Steven B. Smiley,  
[smiley27@earthlink.net](mailto:smiley27@earthlink.net)

## Abstract

As much as five percent of energy consumption in a typical U.S. city comes from K-12 and higher education schools. Retrofitting these schools to be 100% renewable-heated and powered, with thermal and electric battery storage, can accelerate community clean energy. This is a concept plan for the implementation of 100% solar energy for a middle school with an approximate four megawatt electric and thermal load, with 4 million kW-hours/year energy, including school bus electric vehicle (EV) charging. An evaluation is provided for solar photovoltaics (PV), vehicle to grid (V2G), thermal and electric storage systems, including hot water, hot bricks, and stationary batteries. Distribution interconnection and infrastructure applications are considered. This paper is an extension of the author's paper "Accelerating 100% Renewable Energy Plans" (Smiley 2023).

Keywords: renewable energy for schools, accelerating renewable energy

## 1 Introduction

This is a "electrification" plan, increasing the present consumption of electricity 2.74 times for a school utilizing solar PV, thermal and electric storage, bus EV V2G (and other school vehicles) batteries with bi-directional infrastructure upgrades, policies, and smart grid controls. The goals of this plan include:

- Elimination of fossil greenhouse gases (GHG).
- Use of 100% renewable energy of > 4 million kW-hours/year.
- Expansion of solar PV site availability — installing 3,400 kWac of solar PV.
- Purchase and operation of electric V2G buses lowering operating costs while providing electric peak shaving capabilities.
- Installation of solar PV, electrical and thermal storage to cover both electric (37%) and thermal energy (63%) needs. See Figure 1 below.
- Distribution of municipal electricity increased by 2.74 times
- Decrease in overall energy costs to the school and public utility
- Connection into the distribution system substation with limited electric grid upgrades
- Elimination of interconnection delays, avoiding "Independent System Operator" (ISO) requirements and transmission upgrades
- Use of "high load-factor" electric rates, providing lower cost, off-peak electricity 80% of the time
- Use of electricity (mostly off-peak) at a price competitive with natural gas and much lower than petroleum for space, water heating, and vehicle fuels

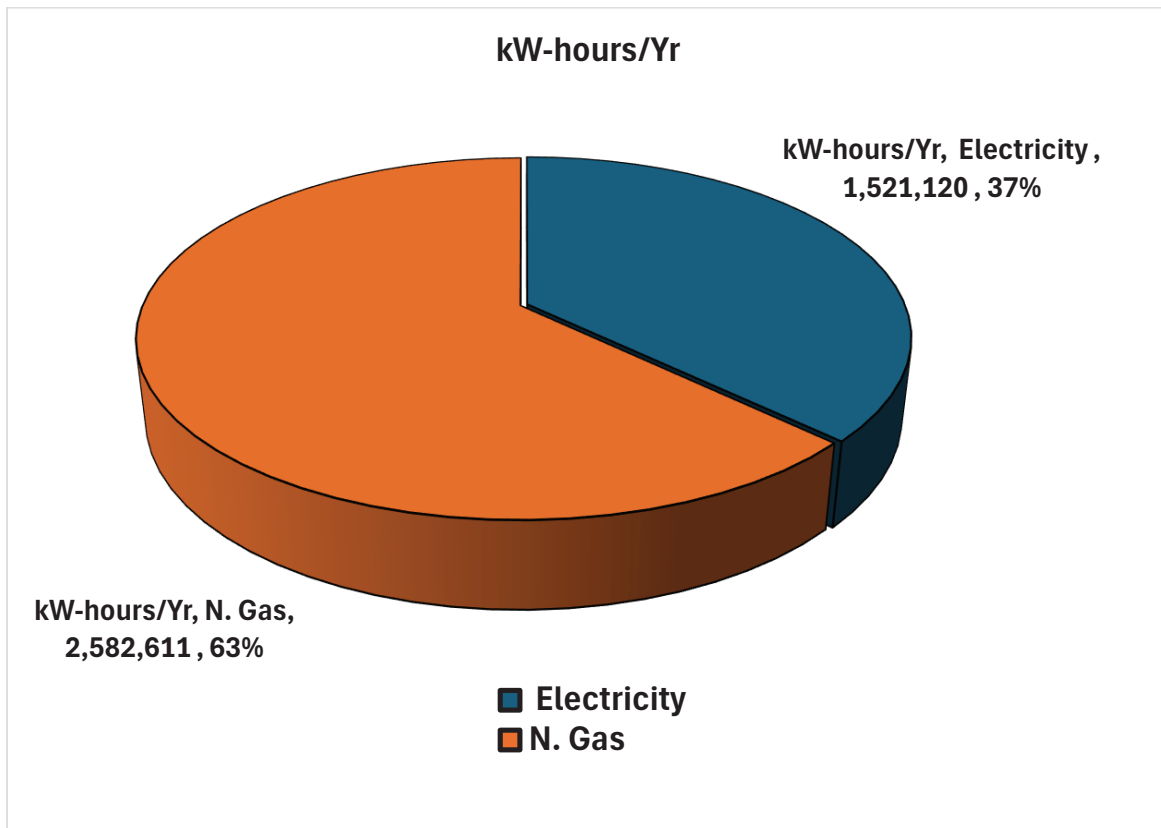


Fig. 1. Total energy breakdown

## 2. Discussion

This plan combines policy applications and project installations consisting of school, community, and utility mid-scale solar with storage. The applicable policies include:

- Community, public utility, and/or cooperative mid-scale solar installations for improved economies of scale — inside the distribution system, avoiding transmission issues
- Federal “direct pay incentives” via the U.S. Inflation Reduction Act (IRA)
- Local utility rebates
- School bonds, green bonds, and/or utility on-bill financing
- High load-factor time of use (TOU) electric rates
- Unlimited fair value net metering
- External benefits accounting for democratic, environmental, social, and economic categories (including economic multiplier benefits)
- Avoidance of market failures that negatively impact project developments

With mid-scale solar PV, whether owned by the school district, the public (municipal) utility, community, or cooperatively, the economies of scale for a 3- to 5-MW solar array

provide a levelized price of 4 cents/kWh or lower — especially with the federal direct pay incentive (30%) or production incentive of 2.6 cents/kWh.

However, local ownership and control within the distribution system is critical, in contrast to outside power purchase agreement (PPA) projects. Solar projects under a PPA can eliminate the advantages of local solar distribution projects.

With locally owned projects, financial incentives can include rebates, tax credits, and non-taxable direct payments, on-bill financing, lower-interest school bonds, and green bond financing. This improves the economics for solar, wind, energy storage, fuel-switching, efficiency, and infrastructure upgrades. And these financial incentives internalize some of the heretofore unpaid environmental external costs.

As outlined in the Database of State Incentives for Renewables and Efficiency (2024), “Under the federal Inflation Reduction Act (IRA), there are 30% investment direct pay credits now available for infrastructure, assuming the renewable energy system is sized less than 5 MW per installation. This applies to interconnection property associated with the installation of renewable energy property with a maximum net output of not greater than 5 MW-AC to provide for the transmission and distribution of the electricity produced or stored by such property, and which are properly chargeable to the capital account of the taxpayer.

“The direct-pay option allows non-taxable entities to directly monetize certain tax credits. The provisions apply to nonprofits, a state or political subdivision and such applicable entities can elect to be treated as having made a tax payment equal to the value of the tax credit they would otherwise be eligible to claim. The entity can then claim a refund for the excess in taxes they are deemed to have paid. The option effectively makes this tax credit refundable for these nonprofit entities.”

Should the solar PV installation be community or cooperatively owned, in contrast to the public municipal utility, a fair value unlimited net metering policy should be implemented offsetting peak power grid purchases, roughly 9 cents per kWh or more.

Local ownership maximizes the democratic, environmental, and economic benefits by reducing additional costs associated with market imperfections. These include transaction costs, transmission interconnection costs, transmission fees, transmission efficiency losses (2% minimum, up to 10%), price markups, higher interest rates, permitting delays, long supply chain environmental impacts, potential low regional transmission market revenue prices (even negative on occasion), and loss of local grid optimization and harmonization.

Low-cost net energy is available by applying high load-factor rates offered to large primary customers, such as the “Primary Service-High Load Factor Rate I1”. See Figure 2.



**PRIMARY SERVICE-HIGH LOAD FACTOR**

(Rate "I1")

**Availability:**

Open to any customer desiring primary voltage service for general use where the billing demand is 100 kW or more. This rate is not available for street lighting service or for resale purposes.

**Nature of Service:**

Alternating current, 60 hertz, single phase or three phase, the particular nature of the voltage in each case to be determined by the Department.

Where service is supplied at a nominal voltage of 15,000 volts or less, the customer shall furnish, install and maintain all necessary transforming, controlling and protective equipment.

Beginning July 1, 2014 any new customers must purchase and retain ownership of all necessary transforming, controlling and protective equipment, and, install and maintain this equipment at their expense. The customer is responsible for all costs and liability associated with the transforming, controlling and protective equipment.

Where the Department elects to measure the service at a nominal voltage of less than 2,400 volts, 3% will be added for billing purposes to the demand and energy measurements thus made.

**Monthly Rate:**

- Customer Charge: \$200.00 per meter per month, plus
- Capacity Charge: \$14.05 per kW of on-peak billing demand
- Energy Charge: 6.26¢ per kWh for all kWh consumed during the on-peak period.  
5.06¢ per kWh for all kWh consumed during the off-peak period.

**Power Service Cost Recovery:**

This rate is subject to the Department's Power Service Cost Recovery.

**High Load Factor Credit:**

Monthly credits will be given to high load factor customers as follows:

| <u>Load Factor</u> | <u>% Credit on Total Billed Amount</u> |
|--------------------|--|
| 90% - 100%         | 5%                                     |
| 80% - 89%          | 4%                                     |
| 70% - 79%          | 3%                                     |

**Schedule of On-Peak and Off-Peak Hours**

The following schedule shall apply Monday through Friday (except holidays designated by the Department). Weekends and holidays are off-peak.

|                 |            |    |            |
|-----------------|------------|----|------------|
| On-Peak Hours:  | 10:00 a.m. | to | 5:00 p.m.  |
| Off-Peak Hours: | 5:00 p.m.  | to | 10:00 a.m. |

Fig. 2. Primary Service-High Load Factor, Rate I1

The I1 rate has a high monthly fixed fee (\$200/mo), a peak period monthly demand charge of \$14.05, an off-peak energy charge of 5.06 cents, and an on-peak charge of 6.26 cents per kWh. Customers with load factors over 90% receive a 5% credit on the total amount billed; load factors over 70% and 80% receive a 3% and 4% credit respectively. The monthly fixed fee is typical for primary-rate industrial customers with

large transformers. If the monthly capacity charge of US \$14.05 per kW of on-peak demand can be offset with smart controls, demand management, and solar PV, average retail electric prices can approximate 5 to 6 cents per kWh. Off-peak periods include all weekends (65 hours), holidays, and all but seven hours each weekday. In fact, 80% of the hours in a typical week are off-peak.

#### Building Characteristics

- School campus property: 90 acres (36 ha)
- Building roof: 210,000 ft<sup>2</sup> (19,520 m<sup>2</sup>) (or 5 acres)
- Annual energy expense: \$284,849
- Present annual kWh/year: 1,521,120
- Natural (fossil) gas kWh/year: 2,582,611 (based on 117,526 ccf gas)
- Total building annual energy kWh: 4,103,731
- Estimated school bus EV kWh/year: 60,300.
- Total kWh/year w/buses: 4,146,031
- Present peak kW demand: 346 kW

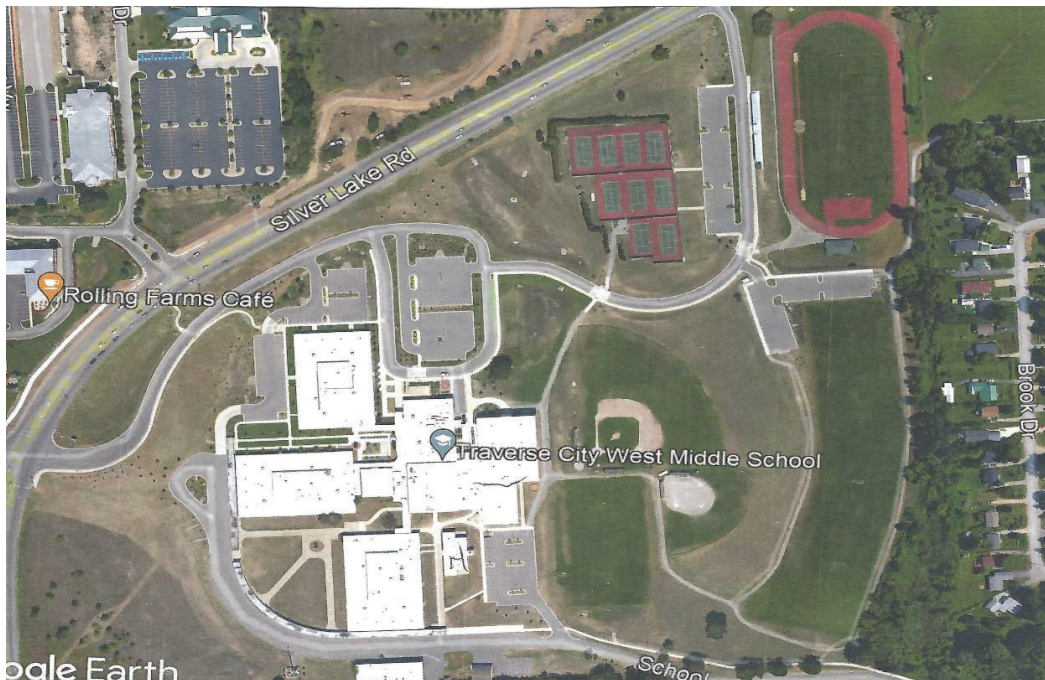


Fig. 3. School Area

Presently, the cost of fossil methane gas for heating is between US 4 and 5 cents per kWh, varying with the system efficiency (70% – 90%) and the delivered price of gas (US \$1.00 +/- per CCF or therm). This cost comparison is for direct electric resistance heating, domestic hot water tanks, baseboard electric heating, and all other internal electric sources. With these low prices, off-peak thermal and electric energy storage can be cost-competitive. With the application of heat pumps for space heating and domestic

hot water (DHW), the value of electricity for heating is cut 50% or more with a comparison thermal value of 2.5 to 3 cents/kWh. During on-peak periods (10 a.m. – 5 p.m. weekdays) solar energy will directly offset higher-cost electricity, avoiding demand charges and reducing overall electric prices.

This facility has two large boilers totaling 3.2 MWt (10.9 million BTU). To electrify the thermal system variable-controlled electric boilers and heaters with associated storage (hot water, salts, or hot bricks) in the range of 3 MWt can be pre-fed into the existing systems with little change. Such electric boilers and heaters can also be used for power quality management.

Project characteristics of this solar CHP system (see Figure 4):

- Solar PV for 100% net kWh: 3,400 KWac (23 acres of 90 acres – 25% of the property)
- 3 MWt electric boiler/heater (10 million BTU) with variable output controls.
- Thermal storage: Electric hot bricks and/or hot water.
- Electric battery storage: stationary Li-ion, EV buses, and service vehicles.

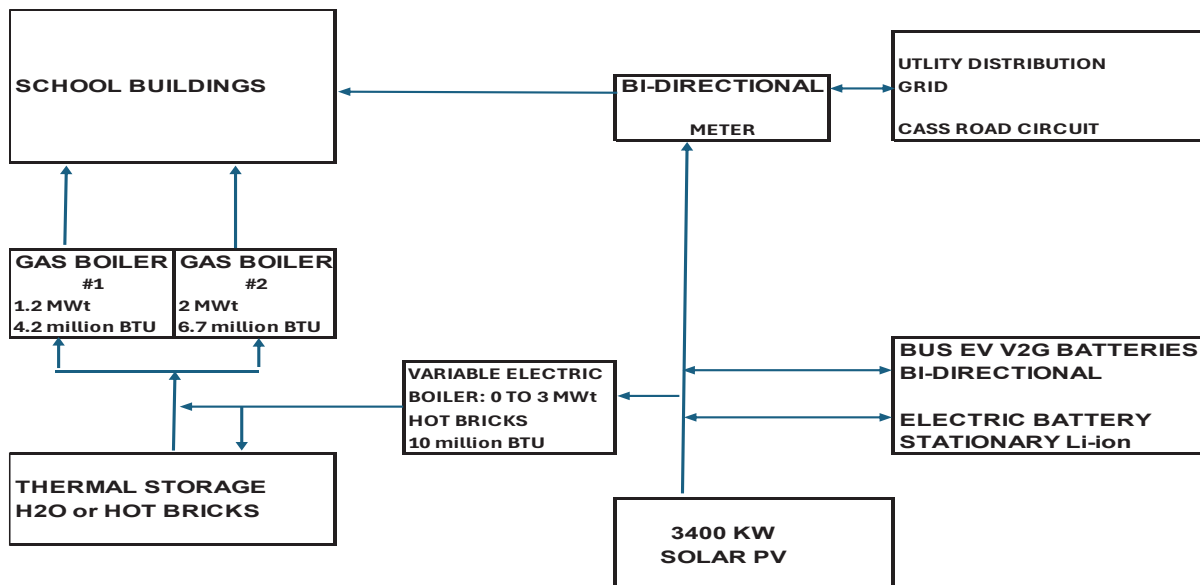


Fig. 4. Project System Components and Flows

To achieve 100% solar PV generation the proposed 3,400 kWac peak solar arrays on the building and grounds must have interconnection capacity on the distribution circuit. Preliminary examination, based on recent distribution grid analysis, indicates this is feasible without significant modifications to the distribution circuit shown in Figure 5, circuit CD 31 on the Cass Road substation.



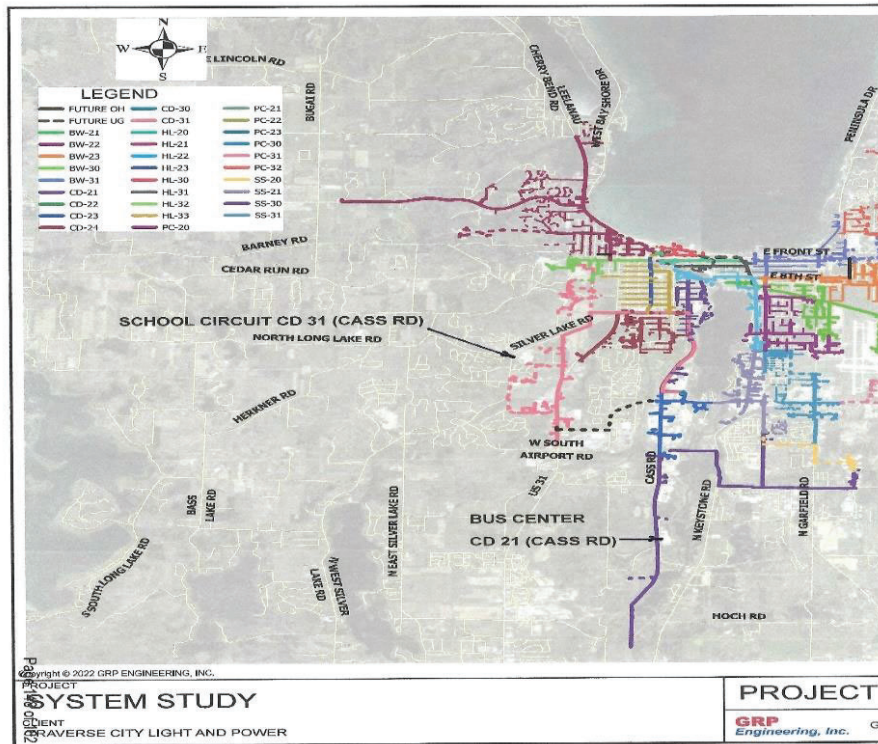


Fig. 5. Distribution Circuits

The transformer loads on the circuit are shown in the following Table 1 where column (f) indicates the Cass #2 transformer is presently loaded on average at <30%, 6.52 MVA of the 22.4 MVA rating, columns (a), (e), and (f).

| LOAD STUDY DATA FROM ENGINEERING REPORT |       |                |                           |       | SMILEY EXTRAPOLATION OF DATA |                             |       |                            |                    |                           |
|---|-------|----------------|---------------------------|-------|------------------------------|-----------------------------|-------|----------------------------|--------------------|---------------------------|
|   |       | (a)            | (b)                       | (c)   | (d)                          | (e)                         | (f)   | (g)                        | (h)                | (i)                       |
|   |       |                | Summer Peak Loading (MVA) | % Max | Net of 100% (MVA)            | Avg Loading at 40/70 (MVA)* | % Avg | Net of 45% Safety Factor** | 45% Avg Load (MVA) | Avg Net Load at 45% (MVA) |
| Substation                              | Trans | Rating (MVA)   |                           |       |                              |                             |       |                            |                    |                           |
| Barlow                                  | #1    | 13.4/17.9/22.4 | 6.95                      | 31.0% | 15.45                        | 3.97                        | 17.7% | 27.3%                      | 10.08              | 6.11                      |
| Barlow                                  | #2    | 13.4/17.9/22.4 | 7.54                      | 33.7% | 14.86                        | 4.31                        | 19.2% | 25.8%                      | 10.08              | 5.77                      |
| Cass                                    | #1    | 13.4/17.9      | 7.57                      | 42.3% | 10.33                        | 4.33                        | 24.2% | 20.8%                      | 8.055              | 3.73                      |
| Cass                                    | #2    | 13.4/17.9/22.4 | 11.41                     | 50.9% | 10.99                        | 6.52                        | 29.1% | 15.9%                      | 10.08              | 3.56                      |
| Parsons                                 | #1    | 13.4/17.9      | 7.00                      | 39.1% | 10.90                        | 4.00                        | 22.3% | 22.7%                      | 8.055              | 4.06                      |
| Parsons                                 | #2    | 13.4/17.9/22.4 | 11.58                     | 51.7% | 10.82                        | 6.62                        | 29.5% | 15.5%                      | 10.08              | 3.46                      |
| Hall                                    | #1    | 22.4/29.9/37.3 | 9.57                      | 25.7% | 27.73                        | 5.47                        | 14.7% | 30.3%                      | 16.785             | 11.32                     |
| Hall                                    | #2    | 22.4/29.9/37.3 | 11.03                     | 29.6% | 26.27                        | 6.30                        | 16.9% | 28.1%                      | 16.785             | 10.48                     |
| South                                   | #1    | 13.4/17.9/22.4 | 3.63                      | 16.2% | 18.77                        | 2.07                        | 9.3%  | 35.7%                      | 10.08              | 8.01                      |
| South                                   | #2    | 13.4/17.9/22.4 | 4.77                      | 21.3% | 17.63                        | 2.73                        | 12.2% | 32.8%                      | 10.08              | 7.35                      |
|   |       | 244.8          | 81.05                     |       | 163.75                       | 46.31                       | 19.5% | 25.5%                      | 110.16             | 63.85                     |

Table 1. Transformer loading – peak summer and average

The box on the left in Table 1 is data provided from the engineering study “2012 System Load Study and Analysis” (GRP Engineering, Inc. 2021). It contains transformer ratings and summer peak loading, with a percentage of full load capacity, column (c). Column (d) results from subtracting the summer peak, for example, Cass #2 of 11.41 MVA (b), from the rated 22.4 MVA transformer (a), resulting in a net of 10.99 MVA, or 50.9% of the full load rating. The box on the right in Table 1 is an extrapolation by the author from the system load study. Column (e) is the average load compared to the peak load, assuming 40 MW (MVA) is the annual average, and 70 MW (MVA) is the annual peak. While the actual annual average is roughly 35 MW, 40 MW is assumed for a margin of safety.

For example, the Cass #2 transformer summer peak of 11.41 MVA (b), multiplied times  $(40/70)$ , results in an average loading of 6.52 MVA shown in column (e) and an average percentage load of 29.1% shown in column (f). This is well under the 45% safety limit, a limit set to provide transformer circuit emergency backup. Column (h) shows the Cass #2 transformer maximum 45% target capacity of 10.08 MVA, which is 3.56 MVA (i) over the average of 6.52 MVA (e). This provides an average excess capacity of 3.56 or 15.9%, while meeting the 45% safety target.

Summarizing the solar PV solution:

- The solar PV should generate 100% annual kWh – 4,103,731.
- A 3,400 kWac peak solar array is projected assuming local solar resources derived from the National Renewable Energy Laboratory “PV Watts” methodology.
- The solar array plan includes installations on parking lots, fields, and building roofs totaling 23 acres (9.2 ha) of the 90-acre (36 ha) property.
- A peak period (10 a.m. to 5 p.m. weekdays) “peak shaving” program will be implemented to eliminate demand charges weekdays, totaling 35 hours per week. Even at 10% of solar PV output, or 340 kW (cloudy/snow days), peak demand fees can be negated — eliminating the \$14.05 kW/mo. demand charge, providing an energy only cost of 5 to 6 cents/kWh.
- Peak shave and distribute excess summer solar at high value demand periods.
- This solar PV system peak capacity represents 10% of the entire utility average 35 MW load and 5% of the peak summer load!

The following Figure 6 shows the monthly energy consumption, including combined thermal and electric loads (blue line) and monthly projected solar PV generation (orange line). Beginning in mid-March, monthly solar PV exceeds the building energy use until October, when heating loads increase. During the period when solar PV exceeds energy consumption, the value of solar should be set at a fair price such as a minimum of 9 to 10 cents/kWh.

The solar PV system must always be dispatched to eliminate any peak demand charges during the 10 a.m. to 5 p.m. weekday peak period. Historically, electric-only demand at the school had a peak of roughly 346 kW. With solar PV output of only 10% of the 3,400 kWac, the solar output of 340 kWac approximates the historic annual peak. During the winter months, when snow cover can impact fixed solar arrays that are inaccessible, the proposed ground mount, roof top, and single axis tilting arrays can be cleared of snow.

During off-peak periods, with or without solar PV, excess energy required (not from storage) can be purchased at the low off-peak price of 5 to 6 cents per kWh. The spread between selling solar high, for example 9 to 10 cents/kWh and exchanging energy at a low price of 5 to 6 cents/kWh, provides for additional net revenues. With additional net revenues from the solar and storage system, the total energy costs of operation will be reduced.

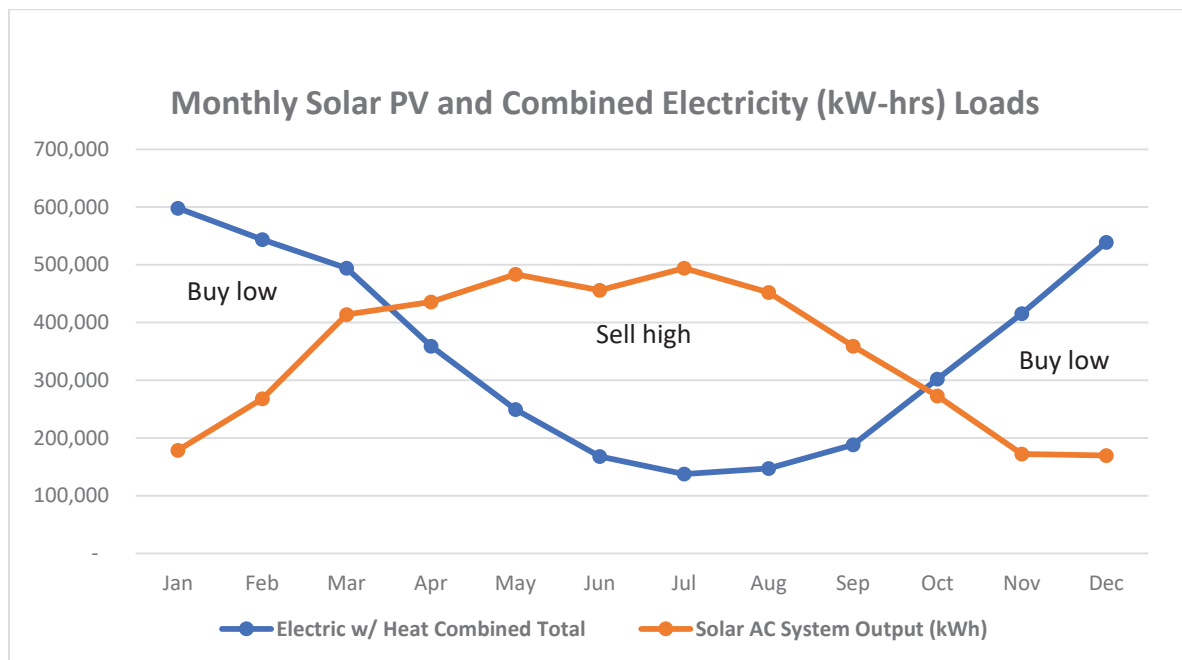


Fig. 6

Four types of battery storage systems are considered:

- EV V2G vehicles
- Stationary lithium-ion
- Hot water
- Advanced hot bricks

The value of EV V2G school buses and service vehicles cannot be overstated. With off-peak electricity priced between 5 and 6 cents per kWh, the comparative cost of fuel is between \$0.56 and \$0.67 per gallon (\$0.15 to \$0.18 per liter) petroleum equivalent for buses. For EV service and staff vehicles with higher efficiency than buses with 3 to 3.5

miles (5 to 5.75 km) per kWh, the comparative fuel cost is \$0.43 to \$0.50 per gasoline gallon (\$.11 to \$.13 per liter).

Six of the buses analyzed, each with a 60-kW dispatch capability to the grid and net 218-kWh capacity, can provide a 360-kW peak and 1,308 kWh per day exceeding the average seven-hour load of 1,214 kWh. This roughly matches a stationary battery system, with no added cost. In addition to peak and cost shaving, energy discharged into the grid with the V2G school buses provides additional revenues, and these EV buses and service vehicles, with much lower fuel and maintenance costs, pay for themselves.

In addition, local rebates and federal incentives are available and are highly justified as the external health and climate benefits are significant. A recent study by the U.S. National Academy of Sciences, “Adopting electric school buses in the United States: Health and climate benefits” calculated the average diesel bus would generate a benefit of US \$84,000 per bus and cut 181 metric tons of carbon dioxide emissions and reduce childhood deaths and asthma cases (Choma, Robinson & Nadeau, 2024). Under the recent U.S. Environmental Protection Agency Clean School Bus Program, US \$5 billion in funds have been designated to support public school districts and tribal organizations.

With V2G EVs, stationary electric battery storage can be eliminated. However, for security reasons and to eliminate the expense of a fossil fuel standby generator, some minimum fixed storage can be installed. For stationary battery storage, a typical 20-foot container consisting of a 250-kW peak output inverter with 1300 kWh stated energy, priced under \$400/kWh can be considered. With no sun and demand management, the school can operate without the grid for an extended period.

Charging thermal storage is accomplished either with an electric boiler (for hot water) or direct electric resistance with hot bricks (for steam) during off-peak periods. The hot water or hot brick storage should have the capacity to heat the building during the weekday seven-hour peak period. Hot brick systems store energy at high temperatures (1,000°C/1,832°F) and can provide either steam, hot water, or hot air. Importantly, no significant mechanical HVAC (heating, ventilation, air conditioning) changes will be required inside the school. When hot water or steam is supplied, the *fossil gas will never fire in the boilers*.

### 3. Conclusion

The school should implement a system to manage loads with solar PV, electric heating, and storage making the school a “high load factor” consumer (90% +/-) qualifying for low-cost electricity of 5 to 6 cents/kWh under the “Primary Service-High Load Factor Rate I1, competitive with fossil methane gas. The solar, storage, and demand management system must never allow positive kW demand during the peak periods. The school should install electric heating with thermal storage, both hot water and hot

rocks, and directly feed hot water or steam into the existing fossil gas boilers, shutting the gas off, with this simple retrofit. The building mechanical heating system components will remain the same, whether hot water or steam distribution, thermostats and zone controls, boiler circuit valves, and pumps.

The school should only draw high electric load heating off-peak (80% of hours) and put any excess solar energy in storage. When storage is full, solar can be sold into the grid. 3,400 KWac peak solar will benefit the entire distribution circuit, not just the school, providing high-value peak period solar for other utility consumers, off-loading circuit transformers, reducing transmission deliveries, costs, and efficiency losses, while providing improved grid voltage control.

Working inside the utility “distribution” system avoids ISOs, the independent system operators, with their structural, financial, market, and institutional barriers. The school and utility will create direct competition between cheap solar electricity and fossil “natural” gas, petroleum, gasoline, diesel, LP gas, and fuel oil. This keeps energy savings and solar income local with economic multiplier and environmental benefits.

With school projects like this the community and electric utility can implement and apply their own local policies including GHG fees, renewable energy credits, TOU rates, rebates, on-bill financing, and net metering. With school and green bonds, these policies can be used to incentivize local projects, community solar, fuel switching, smart grids with broadband, energy efficiency, and infrastructure upgrades.

Construction inside the local distribution grid boosts local employment opportunities for utility technicians, solar installers; and electric, mechanical, and general contractors. School projects such as this with a focus on local ownership versus PPA's enhance democracy and justice putting energy, money, and power into local citizens' hands.

Schools can be the catalyst for accelerating renewable energy.

### **Conflict of Interest**

There are no conflicts of interest to disclose.



## References

- Choma, E. F., Robinson, L. A., and Nadeau, K. C. (2024). *Adopting electric school buses in the United States: health and climate benefits*. PNAS National Academy of Science. <https://doi.org/10.1073/pnas.2320338121>
- GRP Engineering, Inc. (2012). *Traverse City Light and Power, Traverse City, Michigan: Petoskey, Michigan, 2012 system load study*.
- Smiley, S. (2023). *Accelerating 100% renewable energy plans*. Proceedings of the American Solar Energy Society, National Conference 2023. <https://www.springerprofessional.de/en/proceedings-of-the-52nd-american-solar-energy-society-national-s/25871118>

**Comparative Analysis of Building Envelope Performance across Income Levels  
for Enhancing Thermal Resilience during Heatwaves**

<sup>a</sup>Suman Paneru

<sup>a</sup>Yuqing Hu

<sup>b</sup>Guangqing Chi

<sup>a</sup>Julian Wang\*

<sup>a</sup>Department of Architectural Engineering, Penn State University, University Park, PA

<sup>b</sup>Department of Rural Sociology, Penn State University, University Park, PA

\* Corresponding Author: [julian.wang@psu.edu](mailto:julian.wang@psu.edu)

## Abstract

The increased occurrence of extreme heatwaves in communities can have disproportionate impacts on vulnerable low-income communities. The study of building envelopes and their role in reducing thermal vulnerability lacks a specific focus on low-income groups, which indicates that there is a research gap. This research explores the performance of the envelope in reducing thermal vulnerability across different community income levels. A Department of Energy (DOE) prototype building was selected and Atlanta was chosen as a case study to explore thermal resilience across three different income groups: low-income, middle-income, and high-income. The Energyplus simulation indicate that the peak cooling load is significantly higher for low-income groups compared to high-income groups (8.4 kW vs. 14.2 kW). Additionally, the energy usage during extreme heatwaves in low-income community groups compared to medium and high-income community groups is larger (3804.29 MJ vs. 3000.07 MJ). This suggests that with an improved and tailored building envelope the thermal vulnerability can be reduced.

Keywords: building envelope, thermal resilience, decarbonization, low-income communities

## 1.0 Introduction

The rising global temperatures and frequent extreme heatwaves highlight the critical role of building envelopes in mitigating the impact of climate change and improving resilience, particularly within vulnerable communities such as low-income ones (Flores-Larsen & Filippín, 2021). The increased frequency of these extreme events has demanded a resilience plan to mitigate climate change and extreme weather events (Sharifi & Yamagata, 2015). Climate-induced extreme events and weather variations will not only affect energy demand but also put extra strain on the resiliency of urban systems (Nik et al., 2021). As low-income communities often bear a disproportionate burden of heat stress, safeguarding them from heatwaves demands tailored solutions that address thermal resilience (Liu et al., 2023). Furthermore, acute or prolonged exposure to heat can have various adverse effects on human health and quality of life (Hatvani-Kovacs et al., 2016). In extreme cases, excessive exposure to heat can lead to mortality (Shindell et al., 2020). Although it is widely acknowledged that buildings in low-income communities exhibit less thermal resilience to heatwaves, putting occupants at a greater risk of health issues, there is a noticeable lack of quantitative analysis on how housing in these areas responds to heatwaves compared to those in middle- and high-income communities. During heatwaves or similar extreme weather stressors, building-envelope properties become the most crucial factor mediating the indoor environment and affecting passive habitability (Kesik et.al., 2019). In regions experiencing heatwaves, the between minimum use of the mechanical system with the high-performance envelope/enclosures can help to reduce thermal vulnerability.

**Accordingly, this study seeks to assess the thermal resilience of building envelopes within low-income communities during periods of heatwaves, in comparison to middle- and high-income communities.** Specifically, the study first

## Analysis of Building Performance across Income Levels during Heatwaves

statistically identified the properties of the building envelope, including walls, roofs, windows, and infiltration aspects across different household income levels. Subsequently, we integrated these envelope properties into prototypical models as defined by the Department of Energy and conducted energy simulations under specific heatwave conditions. The analysis of energy use and peak energy demands allowed us to compare the resilience of these communities and discuss the potential vulnerabilities of low-income communities in the face of extreme heat.

### 2.0 Method

The methodology for this study consists of two parts: i) selection of envelope properties and ii) energy performance simulation as shown in Figure 1. For the selection of building envelope thermal properties, ResStock data for Atlanta, GA was used. We categorized the income brackets defined in this dataset into three levels: low (<\$60K), middle (\$60K-\$150K), and high (>\$150K), representing low, middle, and high-income community groups, respectively. Following this categorization, we computed the corresponding probabilities for various envelope components and properties. The envelope properties with the highest probabilities in each income cluster were considered. When the probabilities were similar, properties with lower thermally insulating levels were selected, assuming a worst-case scenario for each income cluster. Once the envelope properties for different community groups were established, energy simulations of the DOE prototypical buildings (single-family houses with a floor area of 4,754.19 square feet each) were carried out for each income group. A representative heatwave weather condition from July 23rd to July 29th, 2012, in Atlanta, GA, was employed in this specific simulation analysis. One-week energy use and peak demand are obtained through the simulations and then compared across different household income clusters.

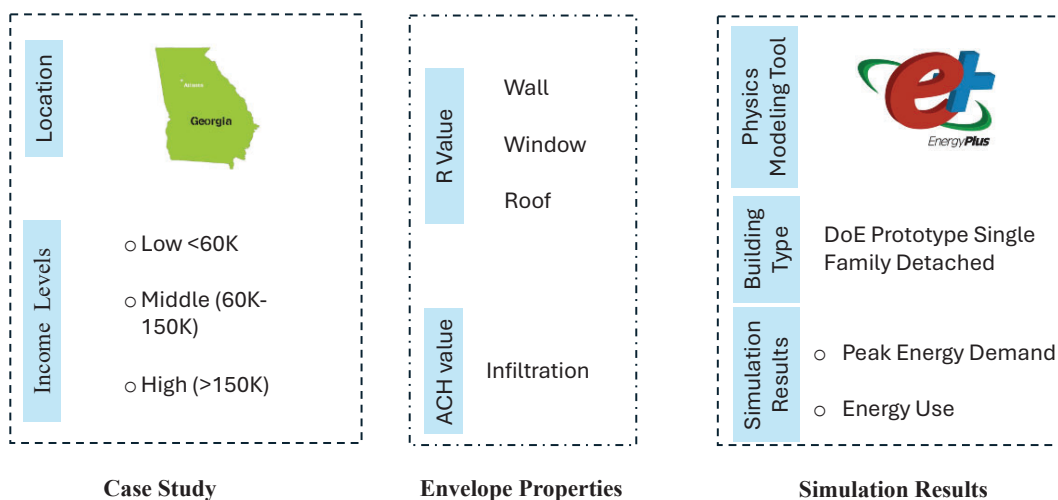


Fig. 1. Methodology used in this study

### 3.0 Results

This results section discusses the selection of building envelope properties across different communities and the simulated cooling load demand and energy use during the selected heatwave week.

#### *3.1 Selection of Envelope Properties across Different Community Levels*

The envelope properties with the highest probability within each cluster were selected as representative. Using the Restock dataset, a Dirichlet distribution was obtained for each income cluster (<\$60K, \$60-150K, >\$150K) individually, with probability density frequencies of each envelope property depicted in Figs. 2-5. In particular, regarding the wall insulation conditions shown in Figure 2, for the low-income group (<\$60K), uninsulated and R- 11 are both dominant wall insulation properties. As indicated above in the methodology section, the relatively lower thermal condition, uninsulated, was selected. For the middle-income group and the high-income group, the predominant R-value of the wall is R-11. As depicted in Figure 3, the Dirichlet distribution illustrates the window preferences across varying income levels. The following selections were identified based on the income levels: for incomes <\$60K, single-clear windows with metal frames were chosen; for incomes between \$60-150K, double-clear windows with metal frames were selected; and for incomes >\$150K, double low-e windows with non-metal frames and m-gain were chosen. For roof, uninsulated (R-0) roofing thermal properties across all three household income levels, as depicted in Figure 4. Additionally, we analyzed the features of the whole home infiltration at the different income levels. The probability distribution in Figure 5 shows that the 15 ACH50 of infiltration dominates across all income clusters. This is also consistent with building codes and standards.

# Analysis of Building Performance across Income Levels during Heatwaves

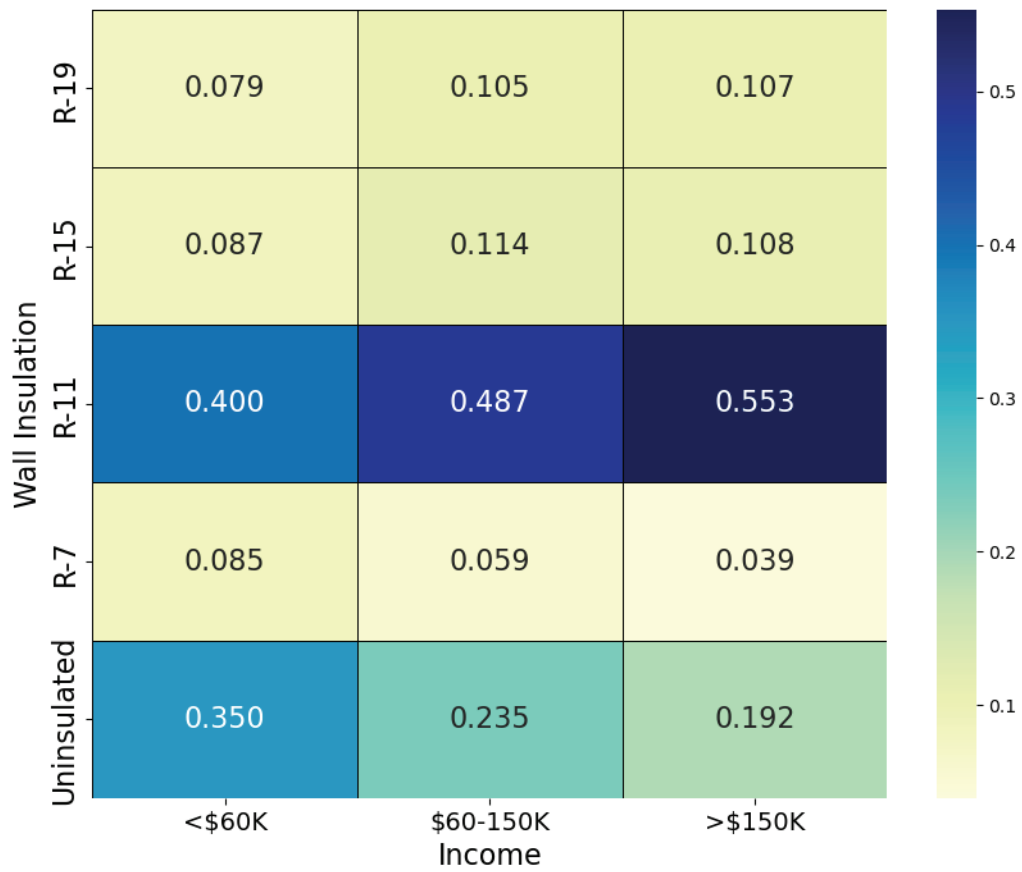


Fig. 2. Dirichlet Distribution of Insulation of wall for differing income levels

## Analysis of Building Performance across Income Levels during Heatwaves

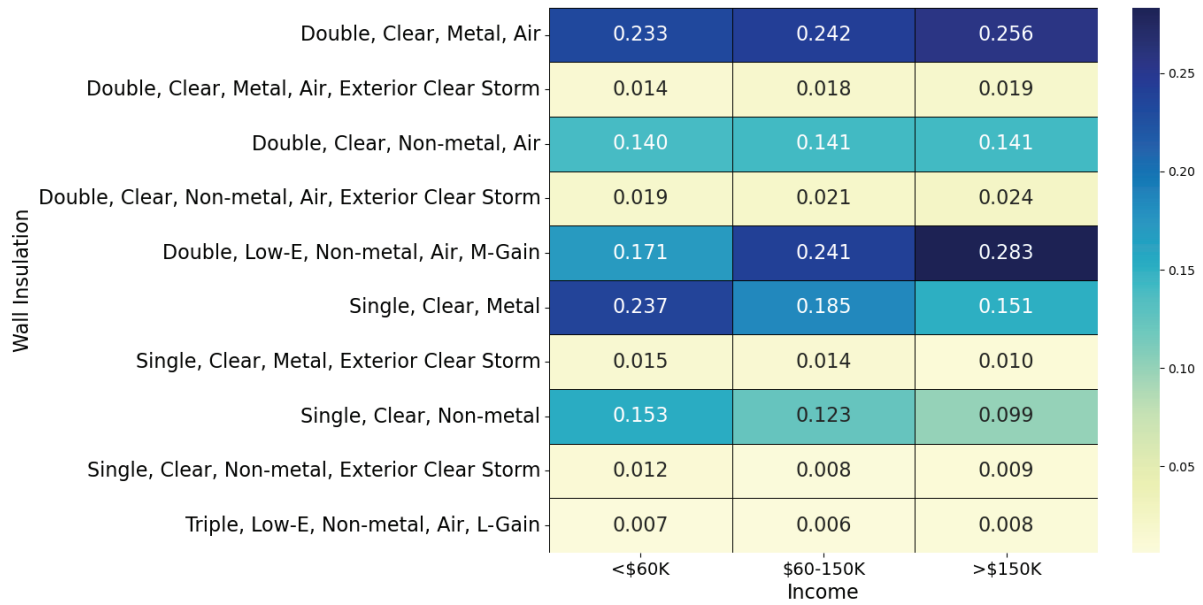
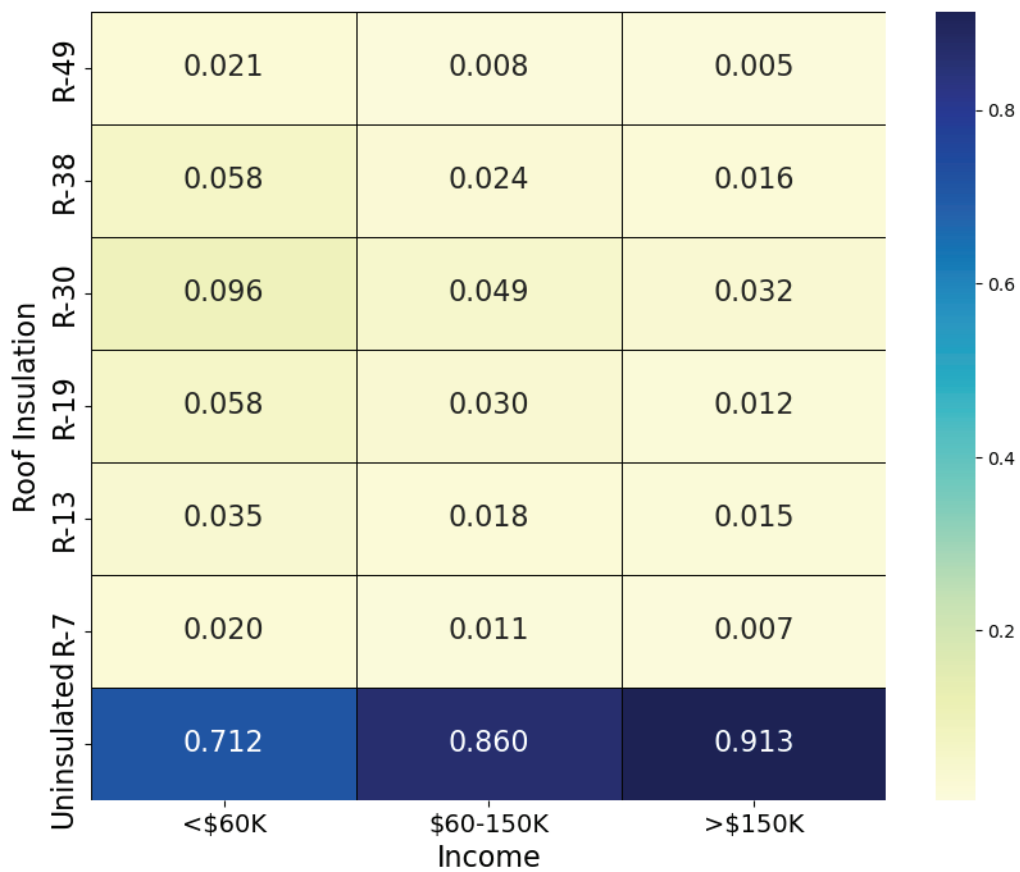


Fig. 3. Dirichlet Distribution of a window for differing income levels





## Analysis of Building Performance across Income Levels during Heatwaves

Fig. 4. Dirichlet Distribution of roof insulation for differing income levels

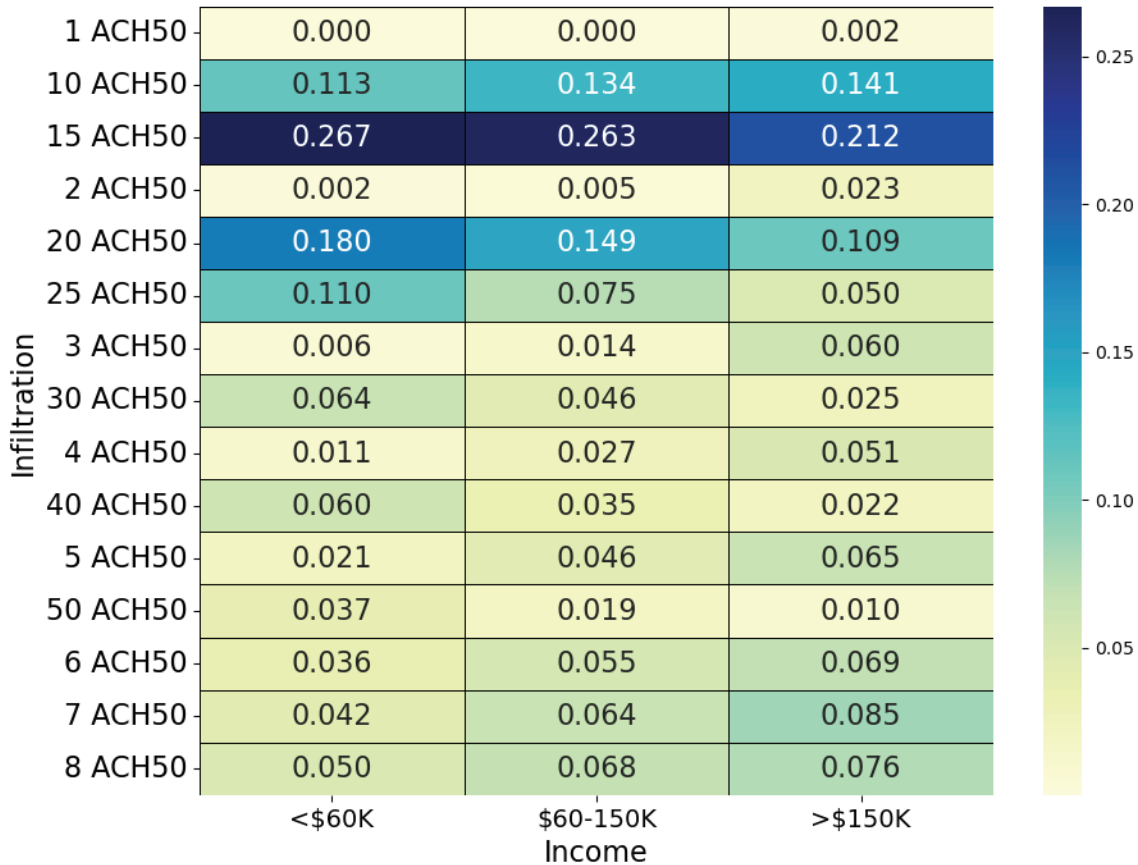


Fig. 5. Distribution of infiltration for differing income levels

Based on the above probability distributions across three different income-community levels, the findings are summarized in Table 1. The specific window properties for each window typology were determined based on the actual window product database and parametric relationship found in our prior studies (Wang, Caldas, Huo, et al., 2016). These data were then used to simulate the peak energy demand and energy use at the whole building level during heatwaves.

Table 1: Building Envelope Selection Based on Income

| Income Level | Low (<\$60K)                               | Middle (\$60-150K)                         | High (>\$150K)   |
|--------------|--|--|--|
| Wall         | Uninsulated                                | R-11                                       | R-11   |
| Window       | Single-clear, metal frame<br>U-factor=1.12 | Double clear, metal frame<br>U-factor=0.68 | Double low-e, non-metal, m-gain<br>U-factor=0.57 (e=0.1) |

## Analysis of Building Performance across Income Levels during Heatwaves

|              |                      |                      |                      |
|--------------|----------------------|----------------------|----------------------|
|              | SHGC=0.79<br>VT=0.76 | SHGC=0.64<br>VT=0.69 | SHGC=0.51<br>VT=0.64 |
| Infiltration | 15 ACH50             | 15 ACH50             | 15 ACH50             |
| Roof         | Uninsulated          | Uninsulated          | Uninsulated          |

Table 1 illustrates variations in envelope characteristics among low, medium, and high-income levels. These differences are evident in the R-values for walls and the U-values and solar heat gain coefficients (SHGC) for windows. For instance, there is a contrast between uninsulated and R-11 for the walls, between U values of 1.12 and 0.57, and between SHGC of 0.79 and 0.51 for windows. Relatively higher U-factors of building walls and windows in low-income community houses may not insulate the buildings well during extreme weather conditions, and the higher SHGC may further worsen the indoor heat gains from solar radiation. In brief, this reveals that the differences in income levels among communities influence the prioritization of specific envelope characteristics. Low-income communities may prioritize cost-effective options that still offer adequate thermal protection, while higher-income communities may opt for premium materials with superior insulation properties.

### *3.2 Heatwave Period-Specific Cooling Load Demand*

The simulation was set up for a week from 07/23 to 07/29 for the year 2012. The envelope properties as depicted in Table 1 were used for simulation for three different communities: low-, middle-, and high-income groups. Understanding the peak cooling demand is crucial for sizing air conditioning systems appropriately. A higher peak demand necessitates a larger unit and it also puts more strain on the power grid. Thus, having insight into peak load demand in communities is vital for ensuring thermal resilience and reducing thermal vulnerability.

## Analysis of Building Performance across Income Levels during Heatwaves

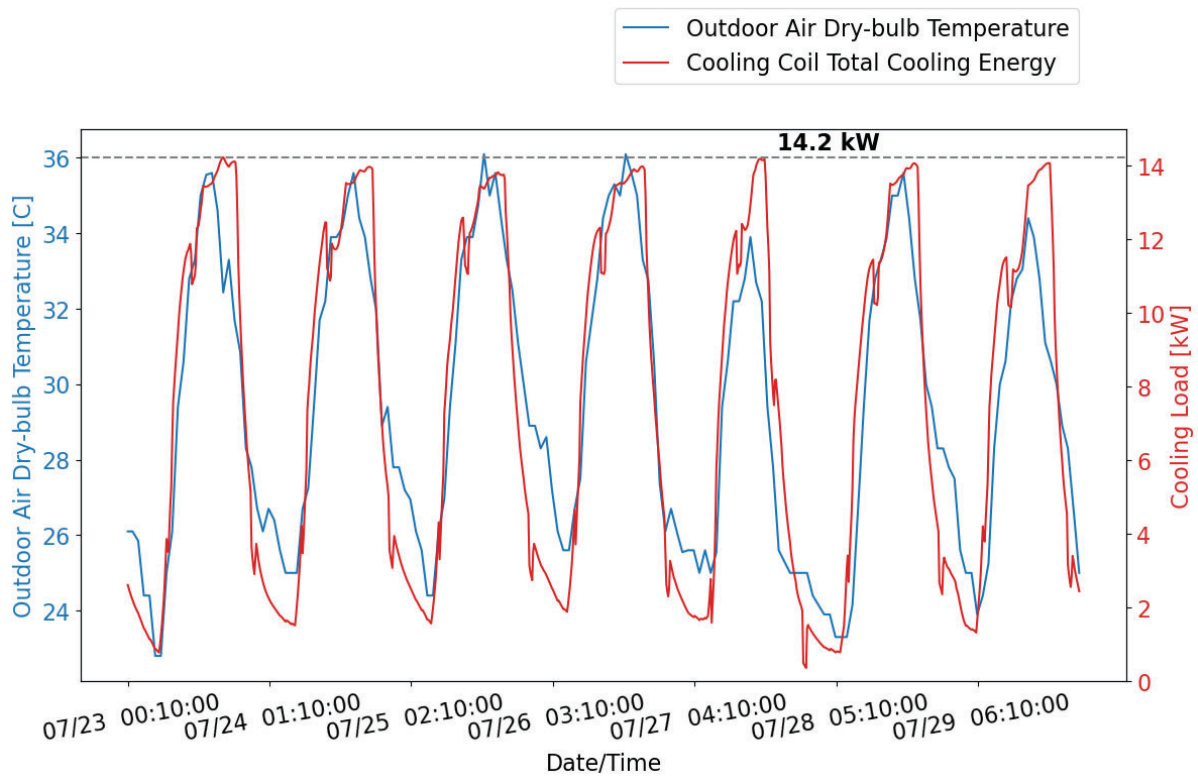


Fig. 6. Cooling load vs outdoor air-dry bulb temperature for low-income communities

## Analysis of Building Performance across Income Levels during Heatwaves

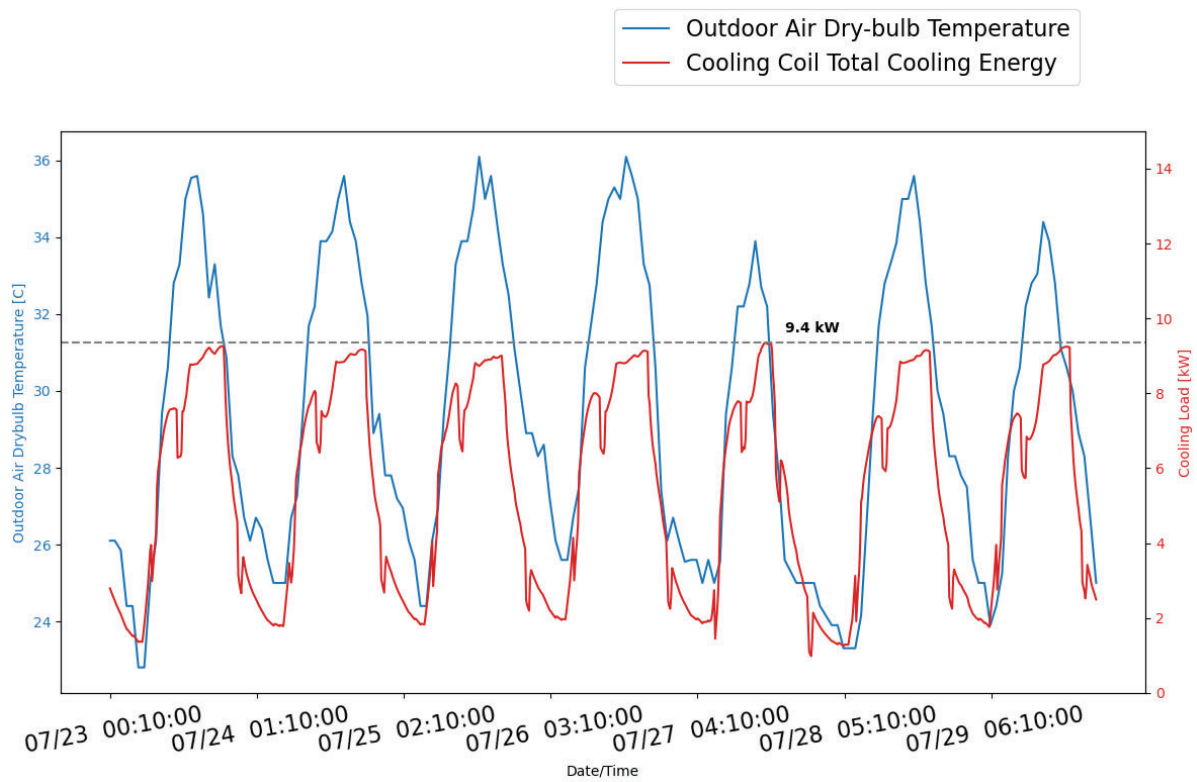


Fig. 7. Cooling load vs outdoor air-dry bulb temperature for middle-income communities

## Analysis of Building Performance across Income Levels during Heatwaves

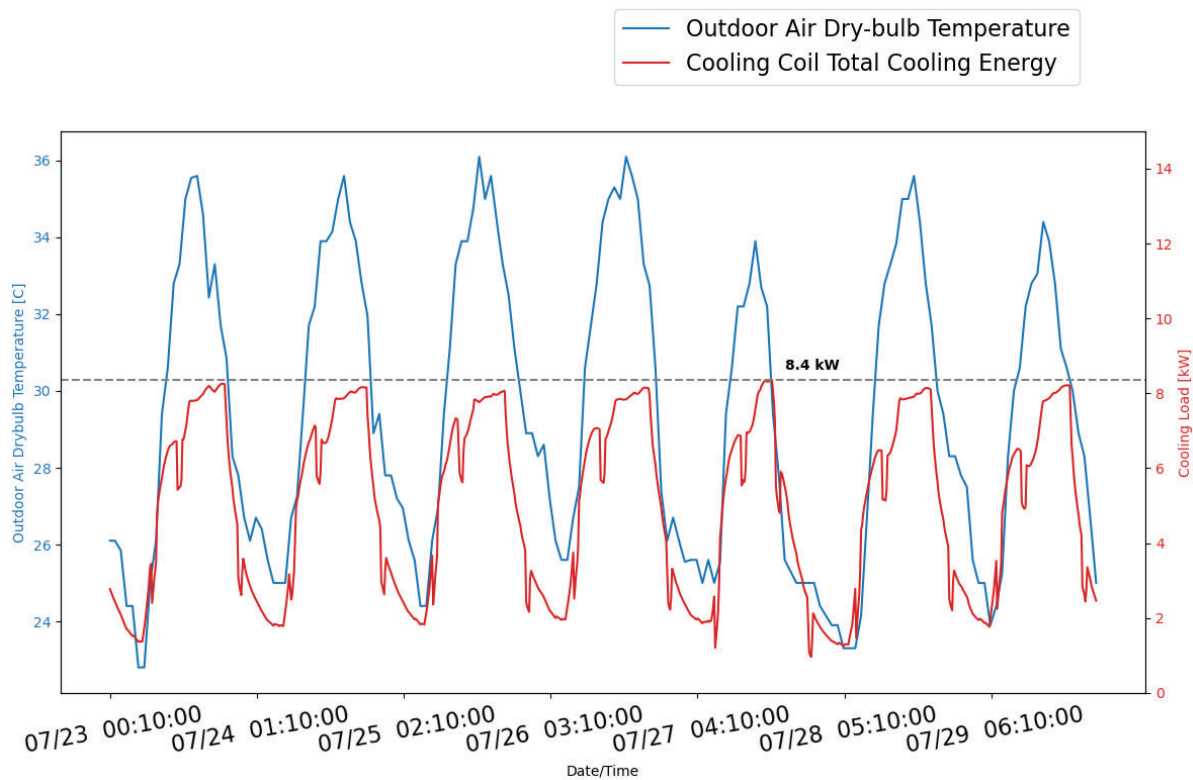


Fig. 8. Cooling load vs. outdoor air-dry bulb temperature for high-income communities

For the low-income community, the peak cooling load demand was 14.2 kW, as shown in Figure 6. As the temperature outside increased, the cooling load also increased subsequently. For the medium-income community, the peak cooling load demand was 9.4 kW, as shown in Figure 7. Though the pattern resembled the temperature profile, the overall cooling load demand was reduced significantly compared to the low-income groups. For the high-income community group, the peak cooling load demand was 8.4 kW, as shown in Figure 8. The highly insulated envelope helped to reduce the peak cooling demand significantly compared to the low-income groups; additionally, the peak demand was also lower than the medium-income community. The cooling load ratio between low and high-income groups is about 1.7.

During heatwaves, the cooling load is of utmost importance. The peak cooling load represents the maximum amount of cooling capacity required to maintain indoor comfort levels during these extreme conditions. It is evident from the simulations that the cooling load demand varies significantly across different income groups. Low-income communities typically experience higher cooling load demands due to factors such as inadequate insulation, lower-quality building materials, and limited access to energy-efficient cooling systems.

### 3.3 Heatwave Period-Specific Cooling Energy Use

## Analysis of Building Performance across Income Levels during Heatwaves

The total cooling energy during the selected heatwave period in these three income community groups shown in Table 2. It presents that the energy consumption for the low-income groups is significantly higher than for the other two community groups. As residents increase their use of cooling systems to combat the heat, the demand for electricity rises, potentially straining the power grid and leading to higher energy consumption across the community.

Table 2: Energy use for various income groups

| <b>Community groups</b> | <b>Total Energy Use (MJ)</b> |
|-------------------------|------------------------------|
| Low-income              | 3804.29                      |
| Medium-income           | 3286.84                      |
| High-income             | 3000.07                      |

The comparison of cooling energy use during heatwave periods across the three income groups not only applies to those extreme conditions but also informs the understanding of energy use patterns under typical weather conditions throughout the year. Increased energy consumption can lead to higher utility costs, which could pose a financial burden for low-income people who are already struggling to make ends meet. This could potentially expose them to thermal vulnerability. If they opt not to condition their homes to maintain a certain indoor temperature, it could exacerbate existing adverse effects.

### 4.0 Conclusion

The study reveals a significant disparity in peak cooling load between low-income and high-income groups, with low-income households experiencing higher peak cooling demand (8.4 kW vs. 14.2 kW). Additionally, during the heatwaves, energy usage in low-income communities surpassed that of high-income groups (3,804.29 MJ vs. 3,000.07 MJ). These discrepancies exacerbate thermal vulnerability, especially for low-income households, due to costlier mechanical units and increased energy consumption, leading to higher utility expenses. Higher peak demands may exacerbate thermal vulnerability, especially for low-income groups. Effective mechanical systems and insulation significantly influence thermal resilience, with higher insulation levels correlating with reduced cooling energy demands. During heatwaves, cooling load demand peaks, particularly in low-income communities, which shows the importance of sufficient insulation in walls and windows. Ensuring equitable access to resources and solutions is essential for enhancing thermal comfort across communities. Enhancing the thermal characteristics of building envelopes through improved insulation and efficiency measures can mitigate these disparities. Prioritizing equitable access to resources and implementing targeted strategies is crucial for enhancing thermal comfort and resilience across all communities, irrespective of income levels.

There are limitations in our study. Firstly, we assumed that all income levels have the same building size, but in reality, this may not be the case. Future research will consider

## Analysis of Building Performance across Income Levels during Heatwaves

varying building area sizes in thermal modeling. Secondly, we assumed that the representative DOE building prototype represented the households in Atlanta, GA.

### **Conflict of Interest**

This research work is supported by the NSF Award # 2215421 CAS-Climate: An Integrated Framework to Investigate Thermal Resilience of Sustainable Buildings and Living Environments for Greater Preparedness to Extreme Temperature Events.

## References

- Flores-Larsen, S., & Filippín, C. (2021). Energy efficiency, thermal resilience, and health during extreme heat events in low-income housing in Argentina. *Energy and Buildings*, 231, 110576. <https://doi.org/10.1016/j.enbuild.2020.110576>
- Hatvani-Kovacs, G., Belusko, M., Skinner, N., Pockett, J., & Boland, J. (2016). Heat stress risk and resilience in the urban environment. *Sustainable Cities and Society*, 26, 278–288. Scopus. <https://doi.org/10.1016/j.scs.2016.06.019>
- Liu, L., Brossman, J., & Lou, Y. (2023). *ResStock communities LEAP Pilot residential housing analysis—detailed methodology* (NREL/TP--5500-88058, 2274781, MainId:88833; p. NREL/TP--5500-88058, 2274781, MainId:88833). <https://doi.org/10.2172/2274781>
- Nik, V. M., Perera, A. T. D., & Chen, D. (2021). Towards climate resilient urban energy systems: A review. *National Science Review*, 8(3), nwa134. <https://doi.org/10.1093/nsr/nwaa134>
- Sharifi, A., & Yamagata, Y. (2015). A conceptual framework for assessment of urban energy resilience. *Energy Procedia*, 75, 2904–2909. <https://doi.org/10.1016/j.egypro.2015.07.586>
- Shindell, D., Zhang, Y., Scott, M., Ru, M., Stark, K., & Ebi, K. L. (2020). The effects of heat exposure on human mortality throughout the United States. *GeoHealth*, 4(4), e2019GH000234. <https://doi.org/10.1029/2019GH000234>
- Thermal-Resilience-Guide-v1.0-May2019.pdf*. (n.d.). Retrieved March 18, 2024, from [https://pbs.daniels.utoronto.ca/faculty/kesik\\_t/PBS/Kesik-Resources/Thermal-Resilience-Guide-v1.0-May2019.pdf](https://pbs.daniels.utoronto.ca/faculty/kesik_t/PBS/Kesik-Resources/Thermal-Resilience-Guide-v1.0-May2019.pdf)



Analysis of Building Performance across Income Levels during Heatwaves

Wang, J., Caldas, L., Huo, L., & Song, Y. (2016). *Simulation-based optimization of window properties based on existing products*. Retrieved March 18, 2024, from [https://publications.ibpsa.org/proceedings/bs0/2016/papers/bs02016\\_1054.pdf](https://publications.ibpsa.org/proceedings/bs0/2016/papers/bs02016_1054.pdf)

**This page intentionally left blank.**

**Review of Sustainable Urban Planning and Design Policy Interventions for  
Heatwave Management in Urban Environments**

Huijin Zhang<sup>a,b</sup>

Nan Wang<sup>a</sup>

Qian Shi<sup>b</sup>

Chao Xiao<sup>b</sup>

Julian Wang<sup>a,\*</sup>

<sup>a</sup> Pennsylvania State University, University Park PA 16801, USA

<sup>b</sup> Tongji University, 1239 Siping Road, Shanghai 200092, China

Corresponding author: Julian Wang

[julian.wang@psu.edu](mailto:julian.wang@psu.edu)

## Abstract

Climate change leads to frequent extreme temperature events, making cities vulnerable to severe heatwaves. Therefore, this study aims to provide a systematic and overarching review of the urban planning and design policy interventions for heatwave management. This study used a series of key terms to search for relevant studies in three databases, including Web of Science, ScienceDirect, and Wiley and then identified 28 articles published between 2007 and 2023 after several inclusion and exclusion criteria. After a systematic review, 15 policy interventions for heatwave management were summarized from the built environment level and building level. Cooling mechanisms and scope of application were discussed. The results of this study provide policymakers with comprehensive guidance on sustainable urban design and planning for heatwave management.

Keywords: Heatwave management, Sustainable urban planning and design, Policy interventions, Adaptation strategies, Urban environment

## 1 Introduction

Increasing global temperatures and frequent heatwave events have significantly driven up cooling energy demand, particularly in the residential sector, which comprises an average of 14.7% of annual home energy use in the U.S. (Feng et al., 2021). Heatwaves usually refer to events with extremely high air temperatures that last for several days, causing huge losses to urban systems, (Lau & Nath, 2012). To mitigate the negative impacts of heatwaves, a series of policy interventions and related adaptation strategies from the behavior perspective has been adopted (Kiarsi et al., 2023). Long-term strategies consisting of urban planning and infrastructure, including climate-responsive housing, have not yet been incorporated into existing mainstream heatwave management plans (Pathak, Shukla, Garg, & Dholakia, 2015). However, with urbanization and urban renewal, it is difficult to simply consider adaptive behaviors to achieve the goal of improving urban thermal resilience. From a positive perspective of leveraging urbanization, sustainable urban planning and design strategies that incorporate green spaces have been called for to minimize the adverse effects associated with heatwaves (Kabisch, Strohbach, Haase, & Kronenberg, 2016).

Although increasing studies have begun to focus on policy interventions or adaptation strategies for sustainable urban planning and design, these existing interventions for heatwave management are still fragmented and unsystematic (Yadav, Rajendra, Awasthi, & Singh, 2023). Specifically, these interventions target different groups, scopes, and implementation objects, but are released in a

disorganized and mixed manner, which may lead to confusion and hinder their effectiveness as guidance. For example, the cooling strategies proposed by the U.S. Environmental Protection Agency (EPA) include measures for individual buildings, such as installing green roofs, and measures for the urban built environment, such as using cool pavements (U.S. Environmental Protection Agency, 2023). A mix of released urban planning and design policy interventions will not be conducive to guiding urban managers at all levels and the public to participate in sustainable urban planning, design, and renewal in response to heatwaves. Therefore, it is necessary to extract and systematically sort out policy interventions to provide policymakers with comprehensive sustainable urban planning and design guidelines for heatwave management.

This study aims to provide a systematic and overarching review of sustainable urban planning and design policy interventions for heatwave management in urban environments. For this purpose, related papers were reviewed to extract effective planning and design policy interventions and classified from the perspectives of urban built environments and buildings.

## **2 Methodology**

This study compiles and examines peer-reviewed papers related to policy interventions for heatwaves. The publications were selected from three databases, including Web of Science, ScienceDirect, and Wiley. Referring to the research of Kotharkar & Ghosh (2021), several key terms are used, including “heatwave”, “adaption policies”, “cooling strategies”, etc. Through the initial search and quick screening, this study obtained 69 records. We reviewed the full texts of these potentially relevant studies and screened them for inclusion according to three criteria: research content, article type, and language. After screening, this study identified 28 articles published between 2007 and 2023. The flowchart of the selection of literature is shown in Figure 1.

## Urban Planning and Design Policy Interventions for Heatwave Management

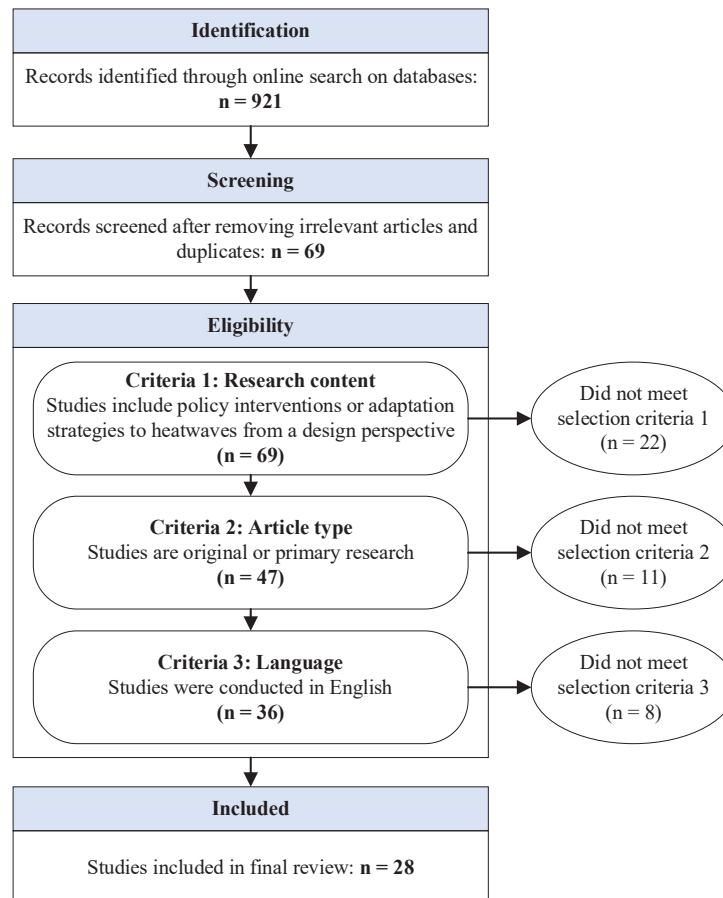


Fig.1 Flowchart of the selection of literature

### 3 Policy Interventions for Heatwave Management

After a systematic review, existing urban planning and design policy interventions can be divided into two categories according to their scope: those that improve the urban built environment outside the building and those that improve buildings inside, as shown in Table 1. Further, different policy interventions use different cooling mechanisms, which can be divided into five main types: *evaporation*, *reflection*, *insulation*, *cooling*, and *shade*.

## Urban Planning and Design Policy Interventions for Heatwave Management

Table 1. Summary of existing design policy interventions

| Scope                          | Specific measures  | Mechanism   | Source  |
|--------------------------------|--|-------------|---|
| <b>Urban built environment</b> | Use of green and blue space  | Evaporation | (Cui, Yin, Cheng, Tang, & He, 2024; Eum, Kim, Jung, & Rho, 2018; Gunawardena, Wells, & Kershaw, 2017)                           |
|                                | Urban greening: roadside planting                                  | Evaporation | (Badura, Krkoška Lorencová, Ferrini, & Vačkářová, 2021; Zanocco & Sousa-Silva, 2023; Ziter, Pedersen, Kucharik, & Turner, 2019) |
|                                | Restoration of urban ecosystems, including biotope creation        | Evaporation | (Eum et al., 2018)  |
|                                | Ecological river restoration                                       | Evaporation | (Eum et al., 2018)  |
|                                | Use of permeable surfaces  | Evaporation | (Badura et al., 2021; Wang et al., 2019)  |
|                                | Outdoor shade spaces and shade screens                             | Shade       | (Hong, Min, Lee, & Choi, 2022)  |
|                                | Use of cool/reflective material materials on urban surfaces        | Reflection  | (Zanocco & Sousa-Silva, 2023)   |
| <b>Building</b>                | Green roofs  | Evaporation | (Badura et al., 2021; Cui et al., 2024; Eum et al., 2018; Liu, Tian, Feng, Hou, & Ma, 2022)                                     |
|                                | Green walls  | Evaporation | (Badura et al., 2021; Cui et al., 2024; Eum et al., 2018)   |
|                                | Cool roofs   | Reflection  | (Burlotos, Dresser, & Shandas, 2023; Liu et al., 2022; Santamouris, Synnefa, & Karlessi, 2011)                                  |
|                                | Cool/reflective material   | Reflection  | (Cui et al., 2024; Santamouris et al., 2011; Zanocco & Sousa-Silva, 2023)   |
|                                | Attic and cavity-wall insulation retrofits (additional insulation) | Insulation  | (Jahani & Cetin, 2022; Porritt, Cropper, Shao, & Goodier, 2013)   |
|                                | Cooling system efficiency improvement                              | Cooling     | (Jahani & Cetin, 2022)  |
|                                | Cool loop installation   | Cooling     | (Eum et al., 2018)  |
|                                | Installing shutters  | Shade       | (Porritt et al., 2013)  |

## 4 Discussion

### 4.1 Policy Interventions at the Urban Built-Environment Level

As shown in Table 1, the existing policy interventions or adaptation strategies for heatwave management at the urban built-environment level mainly include seven pathways: use of green and blue space, urban greening, restoration of urban ecosystems, ecological river restoration, use of permeable surfaces, expanding outdoor shade spaces and shade screens, and use of cool or reflective material materials on urban surfaces. The cooling mechanisms of these policy interventions mainly include *evaporation*, *reflection*, and *shade*, the majority of which are nature-based strategies.

Use of green and blue space mainly refers to the evaporation of water through plants, transferring urban surface heat to the atmosphere to cool the city (Badura et al., 2021). This strategy has a significant cooling effect during heatwaves. For example, green spaces can reduce the average temperatures of their surroundings by 1.1°K in summer and up to 4°K at night (Gunawardena et al., 2017). Based on these fundamental strategies, the thermal-environment improvement policies presented by South Korea in the First Implementation Plan for Climate Change Adaptation Measures (2012–2016) also included the restoration of urban ecosystems and the ecological river restoration (Eum et al., 2018).

However, these interventions are often restricted by the urban original ecological characteristics. Therefore, increasing studies focus on small-scale urban greening, i.e. increasing vegetative cover in urban built environments. In particular, planting street trees has been widely supported by the public (Zanocco & Sousa-Silva, 2023). According to Ziter et al. (2019), the temperature decreases nonlinearly with the increase of canopy coverage of street trees and the cooling effect is best when the canopy coverage exceeds 40%. This intervention combines two cooling mechanisms, *evaporation* and *shade*, which can effectively reduce the temperature while limiting the increase in economic costs. Similar shading interventions include expanding outdoor shade spaces and shade screens (Hong et al., 2022).

In addition, urban surfaces that are difficult to cover with vegetation, such as pavements, also need to be considered to increase adaptability to heatwaves. Given the principle of *evaporation*, permeable pavement with high water absorption capacity is also conducive to enhancing evaporation and reducing surface temperatures, which was considered to be one of the effective strategies for dealing with high temperatures (Wang et al., 2019).



## Urban Planning and Design Policy Interventions for Heatwave Management

However, effective permeable pavement materials are still in the experimental exploration stage and have not been widely promoted. Therefore, instead of using *evaporation*, many studies explored the use of highly reflective materials on urban surfaces (called 'cool surfaces'), such as cool pavements formed by applying reflective coatings on the surfaces (Zanocco & Sousa-Silva, 2023). This type of material enables urban surfaces to have high solar reflectance (or albedo) and high thermal emittance characteristics that might leave them cooler than surfaces constructed with traditional building materials (Maggiotto, Miani, Rizzo, Castellone, & Piscitelli, 2021).

### *4.2 Policy Interventions at the Building Level*

As many existing residences can no longer meet the needs of dealing with heatwaves, the majority of existing urban planning and design policy interventions or adaptation strategies for heatwave management focus on the retrofits of buildings. After a systematic review, policy interventions at the building level include eight pathways: green roofs, green walls, cool roofs, use of cool or reflective material, attic and cavity-wall insulation retrofits, cooling system efficiency improvement, cool loop installation, and installing shutters.

As representative adaptation strategies at the building level, green and cool roofs have been proven to have good cooling effects during heatwaves. For example, during heatwaves, the absolute cooling intensities of cool and green roofs were 0.06°C and 0.03°C respectively (Liu et al., 2022).

It is worth noting that the effectiveness of a green roof depends largely on the moisture level of the soil (Krayenhoff et al., 2021). This also means that the cooling effectiveness of green roofs and green walls will be limited by the growing environment of the plants used and are only suitable for cities or regions with high precipitation or high humidity, such as Singapore.

Therefore, for buildings where green roofs cannot be installed, we consider cool roofs to be an alternative effective intervention to deal with heatwaves. Cool roofs were also proposed to increase the surface albedo by using advanced materials or coatings to reduce the building roof-surface capture of solar radiation (Liu et al., 2022). In addition to such cool-roof interventions, the application of advanced cool materials to other building coatings and structures has also been widely explored (Santamouris et al., 2011). These materials are specifically developed to respond to the solar infrared portion, which has been identified as the most impactful component for building energy efficiency and indoor thermal conditions (Song et al., 2020).

In theory, attic and cavity-wall insulation retrofits can reduce the rise in indoor temperatures due to heatwaves by blocking or reducing heat transfer, which is also

regarded as an important policy intervention for housing retrofit projects to deal with heatwaves (Jahani & Cetin, 2022). However, this intervention is not suitable for all house types. For example, cavity-wall insulation is not suitable for old solid wall terraced houses. It is also difficult for modern, well-insulated houses to benefit from upgraded insulation (Porritt et al., 2013). Therefore, compared with attic and cavity-wall insulation retrofits, installing shutters has been widely adopted as an easy-to-operate alternative intervention that can reduce the increase in indoor temperature due to heatwaves by reducing direct solar radiation (Porritt et al., 2013).

Unlike the above slow and indirect cooling mechanisms, optimization of the cooling system can often directly and quickly achieve cooling, including cooling-system efficiency improvement (Jahani & Cetin, 2022) and cool loop installation (Eum et al., 2018). However, these types of design policy interventions have high economic costs that may limit their adoption and promotion (Porritt et al., 2013), especially for low-income groups.

### **5 Conclusion, implications, and Limitations**

This study systematically summarizes 15 policy interventions for heatwave management from the perspectives of urban built environments and buildings that are categorized into five types according to their cooling mechanisms. The applicability, scope, and constraints of these interventions were discussed, providing valuable insights and guidelines for policymakers on formal policy implementation that can effectively coordinate relevant organizations to carry out cross-departmental efforts while increasing public participation to develop sustainable cities.

However, sustainable urban planning and design policy interventions for heatwave management may conflict with other policies. For example, green walls may conflict with building regulations for wall appearance. Therefore, future research is expected to consider coordination between policies. In addition, with the development of technology and the update of materials, more design strategies that can contribute to resisting heatwaves and saving energy will be implemented. For example, the reversible photothermal windows proposed by Jahid et al. (2022) were expected to dynamically adjust solar heat according to weather conditions. It is worth noting that since policy interventions increase the economic cost to the public, future research is expected to further explore how to effectively attract the public to implement these measures.

## References

- Anwar Jahid, M., Wang, J., Zhang, E., Duan, Q., & Feng, Y. (2022). Energy savings potential of reversible photothermal windows with near infrared-selective plasmonic nanofilms. *Energy Conversion and Management*, 263(May), 115705. <https://doi.org/10.1016/j.enconman.2022.115705>
- Badura, T., Krkoška Lorencová, E., Ferrini, S., & Vačkářová, D. (2021). Public support for urban climate adaptation policy through nature-based solutions in Prague. *Landscape and Urban Planning*, 215. <https://doi.org/10.1016/j.landurbplan.2021.104215>
- Burlotos, A., Dresser, C., & Shandas, V. (2023). Portland's response to the western North American heatwave: a brief report. *Disaster Medicine and Public Health Preparedness*, 17(10145), 2021–2024. <https://doi.org/10.1017/dmp.2023.184>
- Cui, Y., Yin, M., Cheng, X., Tang, J., & He, B. J. (2024). Towards cool cities and communities: Preparing for an increasingly hot future by the development of heat-resilient infrastructure and urban heat management plan. *Environmental Technology and Innovation*, 34(January), 103568. <https://doi.org/10.1016/j.eti.2024.103568>
- Eum, J. H., Kim, K., Jung, E. H., & Rho, P. (2018). Evaluation and utilization of thermal environment associated with policy: A case study of Daegu Metropolitan

- Urban Planning and Design Policy Interventions for Heatwave Management  
City in South Korea. *Sustainability (Switzerland)*, 10(4).  
<https://doi.org/10.3390/su10041179>
- Feng, Y., Duan, Q., Chen, X., Yakkali, S. S., & Wang, J. (2021). Space cooling  
energy usage prediction based on utility data for residential buildings using  
machine learning methods. *Applied Energy*, 291, 116814.  
<https://doi.org/10.1016/j.apenergy.2021.116814>
- Gunawardena, K. R., Wells, M. J., & Kershaw, T. (2017). Utilising green and  
bluespace to mitigate urban heat island intensity. *Science of the Total  
Environment*, 584–585, 1040–1055.  
<https://doi.org/10.1016/j.scitotenv.2017.01.158>
- Hong, Y. J., Min, Y. K., Lee, S., & Choi, S. (2022). Expanded orientation of urban  
public health policy in the climate change era: response to and prevention of  
heat wave in Paris and Seoul: a brief review. *Iranian Journal of Public Health*,  
51(7), 1461–1468. <https://doi.org/10.18502/ijph.v51i7.10080>
- Jahani, E., & Cetin, K. (2022). Energy savings and retrofit assessment for city-scale  
residential building stock during extreme heatwave events using genetic  
algorithm-numerical moment matching. *Clean Technologies and Environmental  
Policy*, 24(7), 2081–2098. <https://doi.org/10.1007/s10098-022-02299-w>
- Kabisch, N., Strohbach, M., Haase, D., & Kronenberg, J. (2016). Urban green space  
availability in European cities. *Ecological Indicators*, 70, 586–596.  
<https://doi.org/10.1016/j.ecolind.2016.02.029>

## Urban Planning and Design Policy Interventions for Heatwave Management

- Kiarsi, M., Amiresmaili, M., Mahmoodi, M. R., Farahmandnia, H., Nakhaee, N., Zareiyan, A., & Aghababaeian, H. (2023). Heat waves and adaptation: A global systematic review. *Journal of Thermal Biology*, 116(July), 103588.  
<https://doi.org/10.1016/j.jtherbio.2023.103588>
- Kotharkar, R., & Ghosh, A. (2021). Review of heat wave studies and related urban policies in South Asia. *Urban Climate*, 36(April 2020), 100777.  
<https://doi.org/10.1016/j.uclim.2021.100777>
- Krayenhoff, E. S., Broadbent, A. M., Zhao, L., Georgescu, M., Middel, A., Voogt, J. A., Martilli, A., Sailor, D. J., & Erell, E. (2021). Cooling hot cities: a systematic and critical review of the numerical modelling literature. *Environmental Research Letters*, 16(5), 053007. <https://doi.org/10.1088/1748-9326/abdcb1>
- Lau, N.-C., & Nath, M. J. (2012). A model study of heat waves over North America: meteorological aspects and projections for the twenty-first century. *Journal of Climate*, 25(14), 4761–4784. <https://doi.org/10.1175/JCLI-D-11-00575.1>
- Liu, X., Tian, G., Feng, J., Hou, H., & Ma, B. (2022). Adaptation strategies for urban warming: Assessing the impacts of heat waves on cooling capabilities in Chongqing, China. *Urban Climate*, 45(June 2021), 101269.  
<https://doi.org/10.1016/j.uclim.2022.101269>
- Maggiotto, G., Miani, A., Rizzo, E., Castellone, M. D., & Piscitelli, P. (2021). Heat waves and adaptation strategies in a mediterranean urban context.

- Urban Planning and Design Policy Interventions for Heatwave Management  
*Environmental Research*, 197(March), 111066.  
<https://doi.org/10.1016/j.envres.2021.111066>
- Pathak, M., Shukla, P. R., Garg, A., & Dholakia, H. (2015). *Integrating climate change in city planning: framework and case studies*.  
[https://doi.org/10.1007/978-81-322-2310-8\\_8](https://doi.org/10.1007/978-81-322-2310-8_8)
- Porritt, S. M., Cropper, P. C., Shao, li, & Goodier, C. I. (2013). Heat wave adaptations for UK dwellings and development of a retrofit toolkit. *International Journal of Disaster Resilience in the Built Environment*, 4(3), 269–286.  
<https://doi.org/10.1108/IJDRBE-08-2012-0026>
- Santamouris, M., Synnefa, A., & Karlessi, T. (2011). Using advanced cool materials in the urban built environment to mitigate heat islands and improve thermal comfort conditions. *Solar Energy*, 85(12), 3085–3102.  
<https://doi.org/10.1016/j.solener.2010.12.023>
- Song, Y., Duan, Q., Feng, Y., Zhang, E., Wang, J., & Niu, S. (2020). Solar infrared radiation towards building energy efficiency: measurement, data, and modeling. *Environmental Reviews*, 28(4), 457–465. <https://doi.org/10.1139/er-2019-0067>
- U.S. Environmental Protection Agency. (2023). *Heat island cooling strategies*. Retrieved September 21, 2024, from <https://www.epa.gov/heatislands/heat-island-cooling-strategies>
- Wang, J., Meng, Q., Zhang, L., Zhang, Y., He, B.-J., Zheng, S., & Santamouris, M. (2019). Impacts of the water absorption capability on the evaporative cooling

Urban Planning and Design Policy Interventions for Heatwave Management  
effect of pervious paving materials. *Building and Environment*, 151, 187–197.

<https://doi.org/10.1016/j.buildenv.2019.01.033>

Yadav, N., Rajendra, K., Awasthi, A., & Singh, C. (2023). Systematic exploration of  
heat wave impact on mortality and urban heat island: A review from 2000 to  
2022. *Urban Climate*, 51(September 2022), 101622.

<https://doi.org/10.1016/j.uclim.2023.101622>

Zanocco, C., & Sousa-Silva, R. (2023). Extreme heat experience influences public  
support for local climate adaptation policies in Germany. *Urban Climate*,  
52(August), 101759. <https://doi.org/10.1016/j.uclim.2023.101759>

Ziter, C. D., Pedersen, E. J., Kucharik, C. J., & Turner, M. G. (2019). Scale-  
dependent interactions between tree canopy cover and impervious surfaces  
reduce daytime urban heat during summer. *Proceedings of the National  
Academy of Sciences*, 116(15), 7575–7580.

<https://doi.org/10.1073/pnas.1817561116>

**Navigating South Africa's Energy Crisis: Advancing Toward a Solar-Powered Future**

Akua Debrah<sup>1</sup>  
Monica Cudjoe<sup>2</sup>

<sup>1</sup>Sustainable Development Strategies Group and the University of Houston

<sup>2</sup> University of Johannesburg, Department of Mining, Engineering and Mine Survey

Email: [aadebrah@gmail.com](mailto:aadebrah@gmail.com)



## Abstract

In South Africa, daily losses of US \$51M – \$237M, attributed to power shortages and inadequate national grid management, underscore the urgent need for a more comprehensive energy reform. The economic costs, coupled with severe social impacts, are further compounded by the country's significant environmental footprint. With 85% of electricity derived from coal, South Africa ranks as the 14th-largest global emitter of greenhouse gases, jeopardizing its climate commitments under the Paris Accord. Despite government pledges, achieving net-zero emissions and aligning with climate targets remains uncertain. This paper discusses some of the root causes of South Africa's energy crisis, investigating barriers to optimal energy resource usage. It emphasizes the imperative for strategic government initiatives to attract investments and enhance existing energy infrastructure. Additionally, a significant move toward practical solar possibilities, specifically, rooftop solar PV, may be required as the foundation for energy independence and a long-term resolution to South Africa's energy challenges.

Keywords: Energy crisis, South Africa, renewable energy, solar power, energy security

## Introduction

Despite South Africa (SA) having the largest and most advanced economy in Africa, it has been plagued by a persistent energy crisis since 2008. The Central Bank of South Africa estimates that the economic impact of these frequent blackouts costs the nation almost US \$51M daily, sometimes reaching between US\$87M – \$237M, depending on the stage of load shedding (Gbadamosi, 2024; Naidoo, 2023). Although the government recognizes the problem of energy supply deficits, attempts to address these have been inadequate.

The Electricity Supply Commission (Eskom), the state regulatory body that manages all three aspects of electricity supply, generation, transmission, and distribution, produces about 95% of the country's power. The challenges faced by Eskom have led to a massive accumulation of debt coupled with the mismanagement of the country's aging coal infrastructure. Besides these constraints, dependence on coal also heightens CO<sub>2</sub> emissions, affecting commitments from the Paris Agreement that involve scaling back and decommissioning of some coal-fired power plants in favor of renewable energy sources.<sup>3</sup>

Pragmatically, the scale of the current energy crisis has forced the government to further scale back on many of its climate-related commitments. However, this may not be the optimal solution to the pressures facing the economy, as global efforts toward a lower-carbon future intensify. This paper aims to dissect some of the root causes of SA's energy crisis, investigating barriers to optimal energy resource use. The study makes the case that given the severity of the crisis, solar energy presents the best potential for mass uptake and a guarantee for energy security in the short to medium term.

<sup>3</sup> The country has committed under the Paris Climate Agreement to cut emissions by decommissioning eight of its fourteen coal-fired power plants by 2030.

1.1 South Africa's Energy Profile

South Africa is endowed with abundant energy resources including coal, uranium, some natural gas, and oil; and renewable energy, notably solar, wind, and hydro. Primarily, coal accounts for 77% of the energy supply, followed by crude oil at roughly 14%. Renewable technologies saw a recent increase from 5.5% in 2020 to 8% in 2022. In terms of the ratio of total energy production to supply, the country remains energy self-sufficient (Figure 1). While coal has provided a reliable source of electricity for decades, it has also exacted a toll on the environment, contributing to air pollution and greenhouse gas emissions (Ncube, 2021).

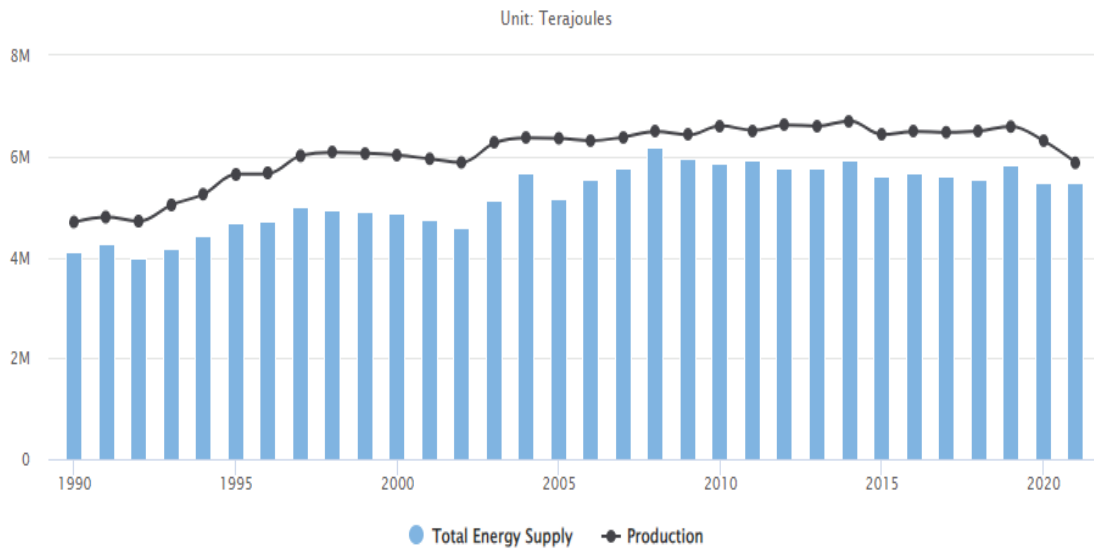


Figure. 1. Total Energy Production and Energy Supply 1990-2020 (UNSD, 2024)

In terms of the electricity sector, 14 large coal plants account for 85% of the utility's installed capacity, followed by hydroelectric capacity at 6%, 5% of electricity generated by open-cycle gas, and 4% generated by Koeberg nuclear power. Figure 2 puts into perspective the plant mix for electricity generation managed by Eskom.

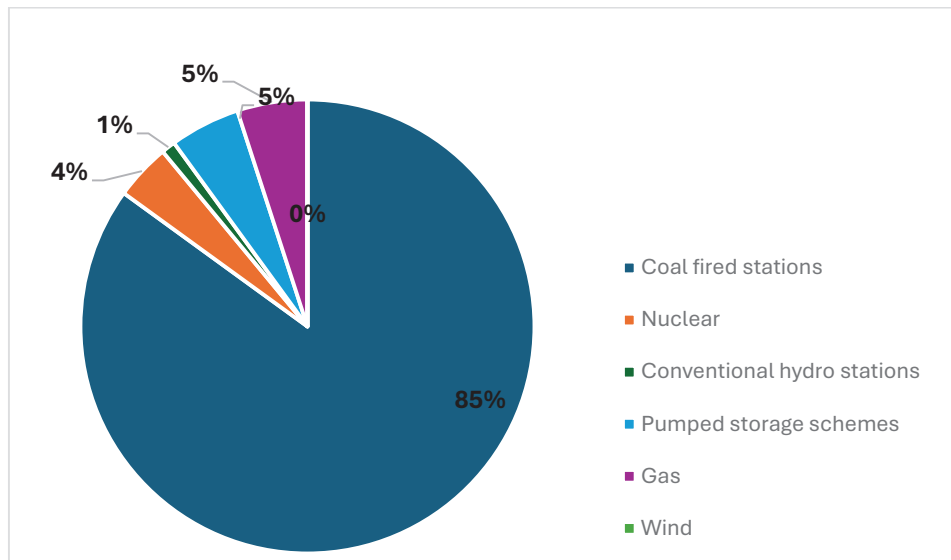


Fig. 2. Plant Mix for Electricity Generation by South Africa's Utility Provider Eskom (Eskom, 2022)

From Figure 2, it can be observed that coal remains the dominant energy source in electricity generation. The country's natural comparative advantage in coal has become a key fixture in its energy makeup. This overdependence on coal has led to national energy intensity per capita being high at (92.33 GJ/person) compared to most developing countries and in the African region.

South Africa exports coal power to neighboring countries through the Southern African Power Pool founded in 1995. Much of this sale is at the expense of domestic demand, since only 70% and 80% of produced and consumed coal respectively go towards domestic electricity production (African Energy Chamber, 2023). Even during times of severe load-shedding crisis (stages 4-6) between 2018- 2022,<sup>4</sup> the country has maintained net exports of coal power to Botswana and Namibia at the expense of local demand. Beyond coal, Eskom also manages seven hydropower plants with an energy capacity of 3,484 megawatts and gas-fired power plants that often serve as backup or supplemental energy. Currently, renewable energy plays a small role in the total energy supply in the country with installed capacity gradually increasing (see Figure. 3).

<sup>4</sup> Load-shedding is an electricity-supply tool used to reduce excessive demand for electricity on the grid. It consists of (1-8) stages, where at each stage 1000 MW of power is unavailable. The schedule was developed ensure that power rationing is conducted in an equitable manner.

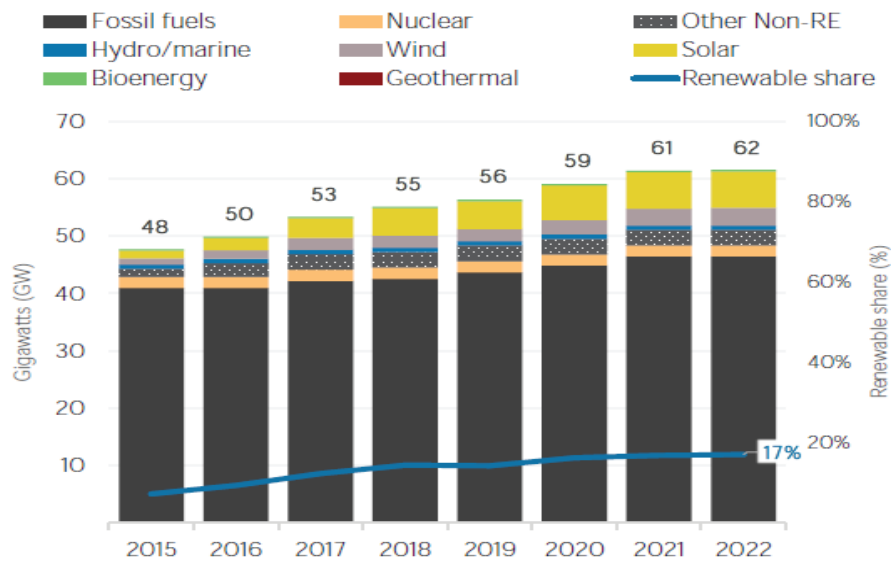


Fig. 3. Installed Capacity Trends 2015- 2022 (IRENA, 2023)

To help manage its debts, Eskom recently increased electricity tariffs to stay profitable as production of primary coal reduced in 2021. Overall, the utility's systemic challenges, mismanagement, and a rapidly evolving global energy landscape have resulted in supply unable to meet the power needs of the nation. The rate of expansion of renewable energy is not increasing quickly enough to meet rising demand.

### 1.2 The Energy Crisis in South Africa

The building of new coal power plants managed by Eskom increased when the country's need for electricity started to rise in the early 2000s. Because the utility has a monopoly over energy transmission and distribution, internal strife naturally affects the overall national energy situation. This aside, there are diverse factors that have led to the current energy crisis. A few are discussed below.

Firstly, a major element of the crisis has been Eskom's debt burden, which hampered the utility's efforts in managing its portfolio. Nkosi's (2020) assessment of Eskom's financials showed that a bailout from the government and increasing tariffs have kept the utility afloat from 1985-2017, rather than sales contributing to profitability. The utility's poor management led to the massive accumulation of debt, to the tune of 450 billion rands (about US \$31 billion) (Nguyen, 2023). These financial constraints have hindered needed infrastructure upgrades and maintenance, perpetuating the cycle of energy shortages.

Also, political interference in Eskom's management has affected the stability and effective functioning of the agency. Wentink (2023) and Naidoo (2023) note that corruption and state capture have led to the government often using the utility as a vehicle for scoring

political points.<sup>5</sup> Some of these fraudulent dealings are part of the reason for Eskom's mounting debt and mismanagement. Hence, although the crisis may be self-inflicted, as noted by Wentink (2023), the impact has been extensive, resulting in decreased industry productivity, job losses, and reduced investor confidence in the country.

Moreover, despite rich coal reserves, rapid expansion to address the current crises may be cost-prohibitive. The current financial climate makes obtaining financing for new coal plant development an impossibility. This may lead to a renewed focus on expanding nuclear energy options. However, detractors of this choice also argue that the environmental implications and costs of the potential expansion of the Koeberg nuclear plant may not be commensurate with the benefits. This is because nuclear energy's risks are negatively wide-reaching, such as those that occurred in the cases of Fukushima and Chernobyl (Steve, 2015).

Another notable element of the crisis has been the inconsistent policies and regulatory frameworks that have previously limited the diversification of the sector and investments in renewables. Commitments were made in 2018 to scale back coal. However, increasing energy insecurity led to the government renegeing on some of its climate commitments (Mukherjee, 2023). Also, initial limitations that were set for renewable generation under the Electricity Regulation Act (ERA) of 2006 limited generation capacity for renewables. This caused delays in uptake due to bureaucratic challenges in the issuing of these licenses. This led to the World Energy Council recommending that SA adjust its policy proposals to foster public-private partnerships in favor of the energy transition (Todd & McCauley, 2021).

Overall, the current crisis cannot be pinpointed to one source, but rather is due to a hodgepodge of policy indecision, political agendas, mismanagement on the part of Eskom, and the inability to plan and adequately forecast energy demand to meet supply. Together with climate-centered improvements to its aging coal fleets, the country needs to smartly upgrade its national energy systems and expand renewable energy generation.<sup>6</sup>

### *1.3 Expanding Renewable Energy Supply in SA's Energy Mix*

Regarding the production of energy from renewable sources, SA released a white paper in 2003 that set a goal of producing 10 TWh of power from biomass, wind, solar, and small-scale hydro. This was followed by the Integrated Resource Plan, which introduced the Renewable Energy Independent Power Producer's Programme (REIPPP) in 2011,

<sup>5</sup> 'State capture' is a phrase used to refer to corrupt government machinery that siphons state resources in favor of personal interest over the public interest.

<sup>6</sup> The expectation is for coal to decline in the long term. This has been problematic, as recently, almost 20,000 MW of coal power went offline resulting in Stage 6 load-shedding of more than 37% of the population without power.

setting a target of an additional 17,800 MW of renewable energy generation by 2030. Thus far, it has increased renewable installed capacity by over 6280 MW from different technologies, mostly from wind and solar. Although, this has not been enough to diversify the energy mix sufficiently to accomplish its climate goals.

Moreover, because of renewables' non-dispatchability issues and the grid's limitation in absorbing large renewably sourced power, the REIPPP planned a phase-wise scaleup. The REIPPP has had six bidding procurement windows for independent power producers (IPP). The current 7<sup>th</sup> window seeks to procure 14,771 MW of new generation capacity – 3,940 MW of PV, 9, 600 MW of wind, and 1,231 MW of battery energy storage capacity (IPP Renewables, 2024). The IPPs are expected to develop 5,000 MW of new generation – 1,800 MW from solar PV and 3,200 MW of wind power.

Another challenge beyond the phase-wise additions to the grid was the generation-capacity license for IPPs. This required producers to apply for a license of 1 MW of solar generation. The threshold was later extended to 100 MW and was finally scrapped under amendments to section 3 of the ERA, Act 4 of 2006 in 2022. This currently allows the generation of renewable power without limitations in so far as IPPs have an agreement with municipalities to access their point of connection for the transmission and distribution of solar power. Currently, the IPPs generate and use third-party transmission of generated power to municipalities who then distribute power to customers. Locally, this is referred to as third wheeling. This policy directive is the single most influential directive that has transformed and liberalized the generation, transmission, and distribution of power in SA.

Physically, SA's atmospheric characteristics are ideal for solar and wind, with the annual solar radiation average at 220 W/m<sup>2</sup> of direct normal irradiance. Many areas average annual sunshine of more than 2,500 hours per day in the range of between 4.5 and 6.5 kWh/m<sup>2</sup> which are also ideal conditions for solar (Soly, 2023). Currently, renewable energy's levelized cost of electricity (LCOE), which measures the net present value of building, generating, and operating an energy system, divided by the total electricity generation over the entire lifetime of the system, shows that renewables are comparable and cheaper to build than coal, the dominant power system (see Figure. 4).

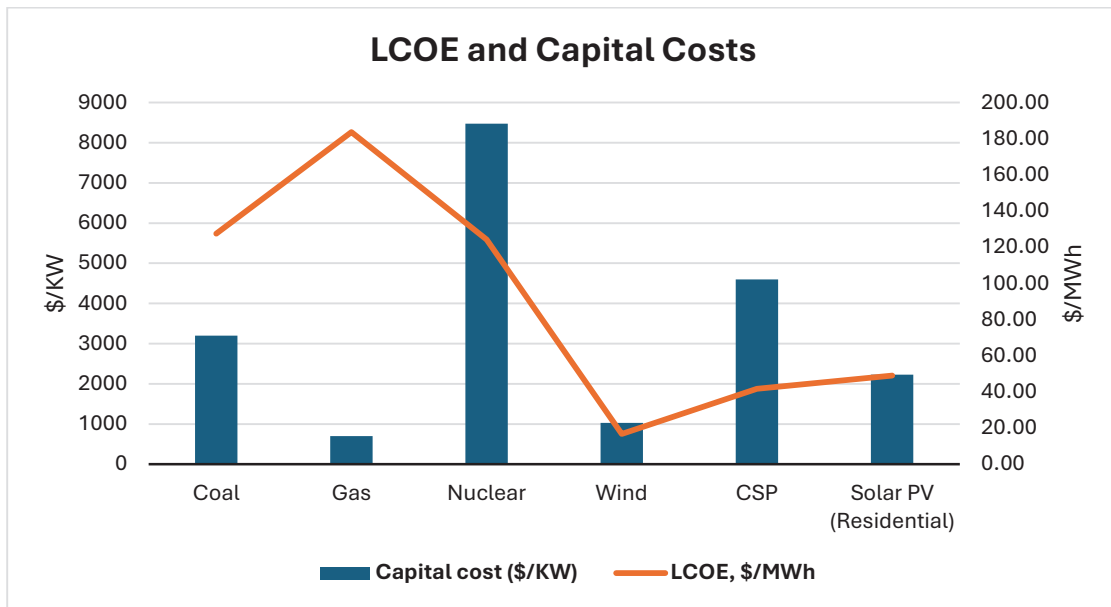


Fig. 4. Comparing Levelized Costs of Electricity and Capital Costs by Energy Technology (Data sources: Lazard, 2023; Mulongo & Kholopane, 2018)

Our updated calculations for LCOE from Mulongo and Kholopane’s (2018) study show the LCOE for wind (\$16.72/MWh) and solar PV (Residential) (\$41.68/MWh) are cheapest compared to building a new coal and natural gas plant or a nuclear plant. Capital costs for natural gas (\$700/KW), wind (\$1,025/KW), and solar PV (residential) (\$2,230/KW) are lower compared to coal, nuclear, and concentrated solar power. Although the LCOE assessment shows lower costs for wind compared to solar, expanding rooftop solar PV access may have a wider ameliorating effect of relieving the pressures on the grid and providing energy security for households. Current estimates of solar PV (rooftop) additions to the energy mix show more than a quadrupling of solar generation since 2022 (see Figure. 5).



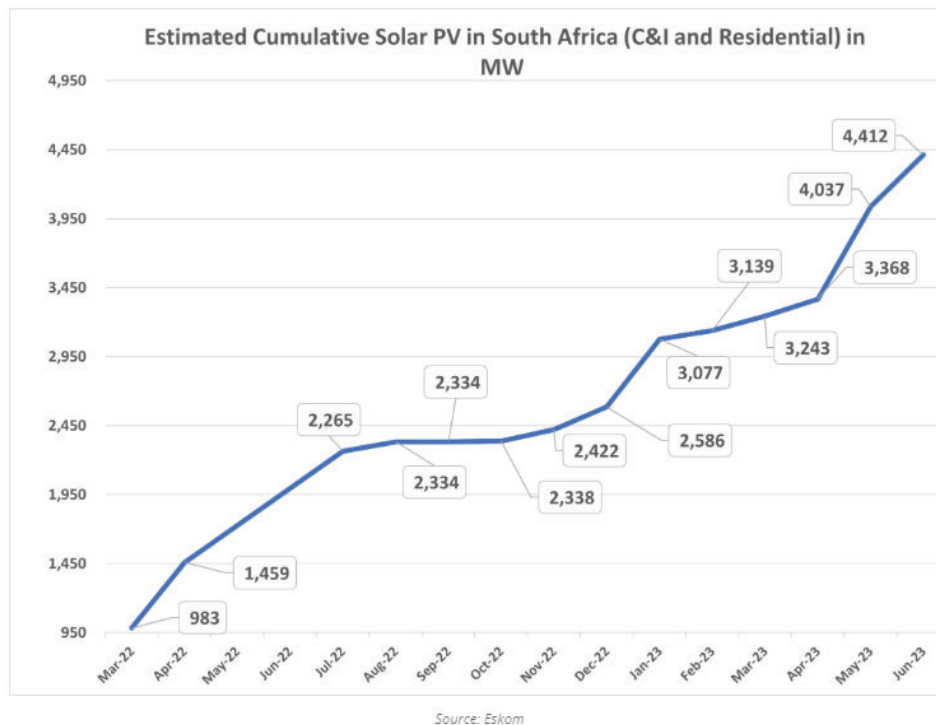


Figure 5. Solar PV Capacity Additions (Kuhudzai, 2023)

From 2022 to 2023, there were over 3000 MW of solar rooftop systems added for commercial and industrial (C&I) users and the residential sector combined, reaching 4,412 MW as of June 2023 (Kuhudzai, 2023).

#### 1.4 Conclusion: Toward a Solar-Powered Future and the Goal of Net-Zero by 2050

The current energy crisis has negatively impacted the economy and its dependence on coal has caused untold environmental damage to mining communities and the broader biosphere. According to the Climate Action Tracker (CAT) (2023), SA is unlikely to meet its climate commitments. CAT, the tracking agency that models scenarios of national climate commitments rated the country's current efforts as 'insufficient' in meeting its net-zero commitments by 2050. Although its targets are aimed at maintaining the range of 350-420 MtCO<sub>2e</sub>, the severity of the crisis has led to a scaling back of goals.

To tackle the energy crisis, a comprehensive strategy consisting of diversifying the nation's energy sources toward renewable energy sources such as solar, wind, and hydroelectric power will be needed. Solar presents the biggest potential since the country's atmospheric conditions and current LCOE indicate a viable alternative to help reduce the burden on the grid and foster energy security.

A lack of infrastructure investments and smart upgrades to the national grid and liberalization of the power system were the optimal barriers to renewable solar energy



expansion. With the amendments of Schedule 3 under the ERA 4, opportunities for liberalization have commenced. Also, enhancing public-private partnerships can further mobilize more capital and expertise to accelerate infrastructure development. Since the limitation on the license system for generation has been removed, 'wheeling' will be one of the best options to enhance utility-scale solar for municipalities in terms of relieving the grid's load burden.

Moreover, a policy focus on subsidies in the form of incentives to encourage rooftop solar PV uptake for the residential and C&I sectors would have to be amplified through credit schemes, tax breaks, and rebates. The rebate consideration should be higher than the current 25% of the cost of the panels and establishing a net metering system nationwide would be beneficial. The rapid adoption of distributed solar systems can reduce the demands on the grid. Lastly, to boost solar potential, supply-side promotion through government-driven awareness programs and retrofitting of government buildings with solar can increase interest. This must be done in concert with energy efficiency and conservation measures to reduce the grid's load. Finally, solar energy can be strategically positioned, with other renewables and natural gas, to address the intermittency issues, and help close the energy deficit gap. This will improve national energy efficiency targets in line with the Paris Accords.

### **Conflict of Interest**

The authors declare that we have no known competing financial interests or personal relationships that could have appeared to influence the work reported in this paper.

## References

African Energy Chamber. (2023). *The state of South African energy 2023*.

<https://energychamber.org/report/the-state-of-south-african-energy-2023/>

Climate Action Tracker. (2023). *South Africa*.

<https://climateactiontracker.org/countries/south-africa/>

Cocks, T. (2021, November 4). Insight: The cost of coal in South Africa: Dirty skies, sick kids. *Reuters*. Retrieved on 10<sup>th</sup> October 2023.

<https://www.reuters.com/business/cop/cost-coal-south-africa-dirty-skies-sick-kids-2021-11-04/>.

Centre for Scientific and Industrial Research (CSIR). (2023). CSIR releases statistics on power generation in South Africa for 2022 | CSIR. *CSIR*.

<https://www.csir.co.za/csir-releases-statistics-on-power-generation-south-africa-2022>

Electricity Supply Commission (Eskom) (2021.) *Coal in South Africa, Eskom fact sheet*,

<https://www.eskom.co.za/wp-content/uploads/2021/08/CO-0007-Coal-in-SA-Rev-16.pdf>

Eskom. (2022). *Fact sheet: generation plant mix*. [https://www.eskom.co.za/wp-](https://www.eskom.co.za/wp-content/uploads/2022/06/GX-0001-Generation-PlantMix-Rev-26.pdf)

[content/uploads/2022/06/GX-0001-Generation-PlantMix-Rev-26.pdf](https://www.eskom.co.za/wp-content/uploads/2022/06/GX-0001-Generation-PlantMix-Rev-26.pdf)

Gbadamosi, N. (2024, June 13). How South Africa's energy crisis became an economic crisis. *Foreign Policy*. Retrieved on 20<sup>th</sup> November 2023.

<https://foreignpolicy.com/2023/01/25/south-africa-energy-crisis-corruption-anc/>

IPP Renewables. (2024). *IPP Renewables*. <https://www.ipp-renewables.co.za/>

International Renewable Energy Agency (IRENA). (2020). *Renewable Energy*

*Prospects: South Africa*, <https://www.irena.org/->

[/media/Files/IRENA/Agency/Publication/2020/Jun/IRENA\\_REmap\\_South\\_Africa\\_report\\_2020.pdf?rev=4c91c220ae4b441dbbfaf1ce36c2d3ec](https://www.irena.org/-/media/Files/IRENA/Agency/Publication/2020/Jun/IRENA_REmap_South_Africa_report_2020.pdf?rev=4c91c220ae4b441dbbfaf1ce36c2d3ec)

IRENA. (2023). Energy Profile: South Africa. *International Renewable Energy Agency*.

<https://www.irena.org/->

[/media/Files/IRENA/Agency/Statistics/Statistical\\_Profiles/Africa/South-](https://www.irena.org/-/media/Files/IRENA/Agency/Statistics/Statistical_Profiles/Africa/South-Africa_Africa_RE_SP.pdf?rev=9851ed405064418e94d8ddd8b24893e9)

[Africa\\_Africa\\_RE\\_SP.pdf?rev=9851ed405064418e94d8ddd8b24893e9](https://www.irena.org/-/media/Files/IRENA/Agency/Statistics/Statistical_Profiles/Africa/South-Africa_Africa_RE_SP.pdf?rev=9851ed405064418e94d8ddd8b24893e9)

Kruger, A. (2022, October 9). New data reveals ugly truth about load shedding in South

Africa. *Economy24*. Retrieved on 10<sup>th</sup> January 2024.

<https://economy24.co.za/2022/10/new-data-reveals-ugly-truth-about-load-shedding-in-south-africa/>

Kuhudzai, R. J. (2023, August 3). South Africa now has over 10 GW of wind & solar generation capacity | REVE News of the wind sector in Spain and in the world.

Reve. <https://www.evwind.es/2023/08/03/south-africa-now-has-over-10-gw-of-wind-solar-generation-capacity/93237>

Lazard. (2023). 2023 Levelized Cost of Energy+. <https://www.lazard.com/research-insights/2023-levelized-cost-of-energyplus/>

Moneyweb. (2023, April 21). Eskom rushes back to Stage 6 as breakdowns hit the fleet.

*Moneyweb*. Retrieved on 5<sup>th</sup> December 2023.

<https://www.moneyweb.co.za/news/south-africa/eskom-rushes-back-to-stage-6-as-breakdowns-hit-fleet/>

Mukherjee, P. (2023). Exclusive: South Africa to miss 2030 emissions goal as it keeps coal plants burning | Reuters. *Reuters*.

<https://www.reuters.com/sustainability/south-africa-miss-2030-emissions-goal-it-keeps-coal-plants-burning-2023-11-09/>

Mulongo, N. Y., & Kholopane, P. (2018). An economic competitiveness analysis of power generation plants. *2018 5th International Conference on Industrial Engineering and Applications (ICIEA)*, 543–547.

<https://doi.org/10.1109/IEA.2018.8387160>

Naidoo, P. (2023). Eskom load shedding may cost South Africa \$51 Million a day, central bank says — Bloomberg. *Bloomberg*. 18<sup>th</sup> August 2023.

<https://www.bloomberg.com/news/articles/2023-02-06/blackouts-may-cost-south-africa-51-million-day-central-bank-says?embedded-checkout=true>

Ncube, V. (2021, May 14). South Africa's 'Deadly Air' case highlights health risks from coal. *Human Rights Watch*. <https://www.hrw.org/news/2021/05/14/south-africas-deadly-air-case-highlights-health-risks-coal>

Nguyen, L. (2023, June 14). Understanding the Energy Crisis in South Africa. *Earth.Org*.

<https://earth.org/energy-crisis-south-africa/>

Soly. (2023). South African Region's Year-Round Sunshine. *Soly.Co.Za*.

<https://soly.co.za/knowledge-base/south-african-regions-year-round-sunshine/>

Steve, T. (2015, June 15). Why nuclear power would be a bad option for South Africa. *World Economic Forum*. <https://www.weforum.org/agenda/2015/06/why-nuclear-power-would-be-a-bad-option-for-south-africa/>

Todd, I., & McCauley, D. (2021). Assessing policy barriers to the energy transition in South Africa. *Energy Policy*, 158, 112529. <https://doi.org/10.1016/j.enpol.2021.112529>

United Nations Statistics Division (UNSD). (2024). *UNSD – Energy Balance (South Africa)*. <https://unstats.un.org/unsd/energystats/dataPortal/>

Wentink, G. J. (2023). A disaster of politics: The energy supply crisis in South Africa. *Jàmbá. Journal of Disaster Risk Studies*, 15(1), 1492. <https://doi.org/10.4102/jamba.v15i1.1492>

## AUTHOR INDEX

|                       |          |
|-----------------------|----------|
| Ayankojo, Bolu.....   | 271      |
| Bass, Moses.....      | 285      |
| Birturk, Asli.....    | 100      |
| Budagyan, Boris.....  | 4        |
| Clark, Stephen.....   | 294      |
| Clayton, Phillip..... | 112      |
| Cliburn, Jill.....    | 258      |
| Debrah, Akua.....     | 371      |
| Demissie, Tariku..... | 88       |
| Field, Kristin.....   | 255      |
| Foster, Robert.....   | 20       |
| Ghaeili, Neda.....    | 167      |
| Ho, Clifford.....     | 308      |
| Khan, Ali.....        | 179      |
| Khoie, Rahim.....     | 61, 75   |
| Krakauer, Nir.....    | 118      |
| Maloo, Nea.....       | 191      |
| Mueller, David.....   | 93       |
| Olson, Gaylord.....   | 34       |
| Paneru, Suman.....    | 342      |
| Perez, Marc.....      | 319      |
| Renné, Dave.....      | 203      |
| Sharma, Prabhat.....  | 244      |
| Si, Xiuhua.....       | 127      |
| Smallen, Martin.....  | 216      |
| Smiley, Steven.....   | 329      |
| Subnom, R.....        | 49       |
| Taheri, Roya.....     | 228      |
| Yang, Yizhou.....     | 142, 154 |
| Zhang, Huijin.....    | 358      |

